COMPARATIVE ANATOMY AND HISTOCHEMISTRY OF THE ASSOCIATION OF *PUCCINIA POARUM* WITH ITS ALTERNATE HOSTS

By

TALIB OWAID AL-KHESRAJI

Department of Botany, University of Sheffield

Thesis for the degree of Doctor of Philosophy

JUNE 1981

Vol 2

Figure 3.1

Early pycnial stage of *P. poarum* in *Tussilago* leaf. Intercellular hyphae are seen extending between palisade cells. Scale lines = 20 µm.

a - Transverse section of epon-embedded tissue. Note intracellular hypha (arrowhead) and chloroplasts in mesophyll cell.

b - Tangential section (cut by freezing microtome) through upper mesophyll of *Tussilago* leaf.

c - Tangential section (from epon-embedded tissue) through upper mesophyll of *Tussilago* leaf.

See Fig. 3.1a, b and c for methodology.

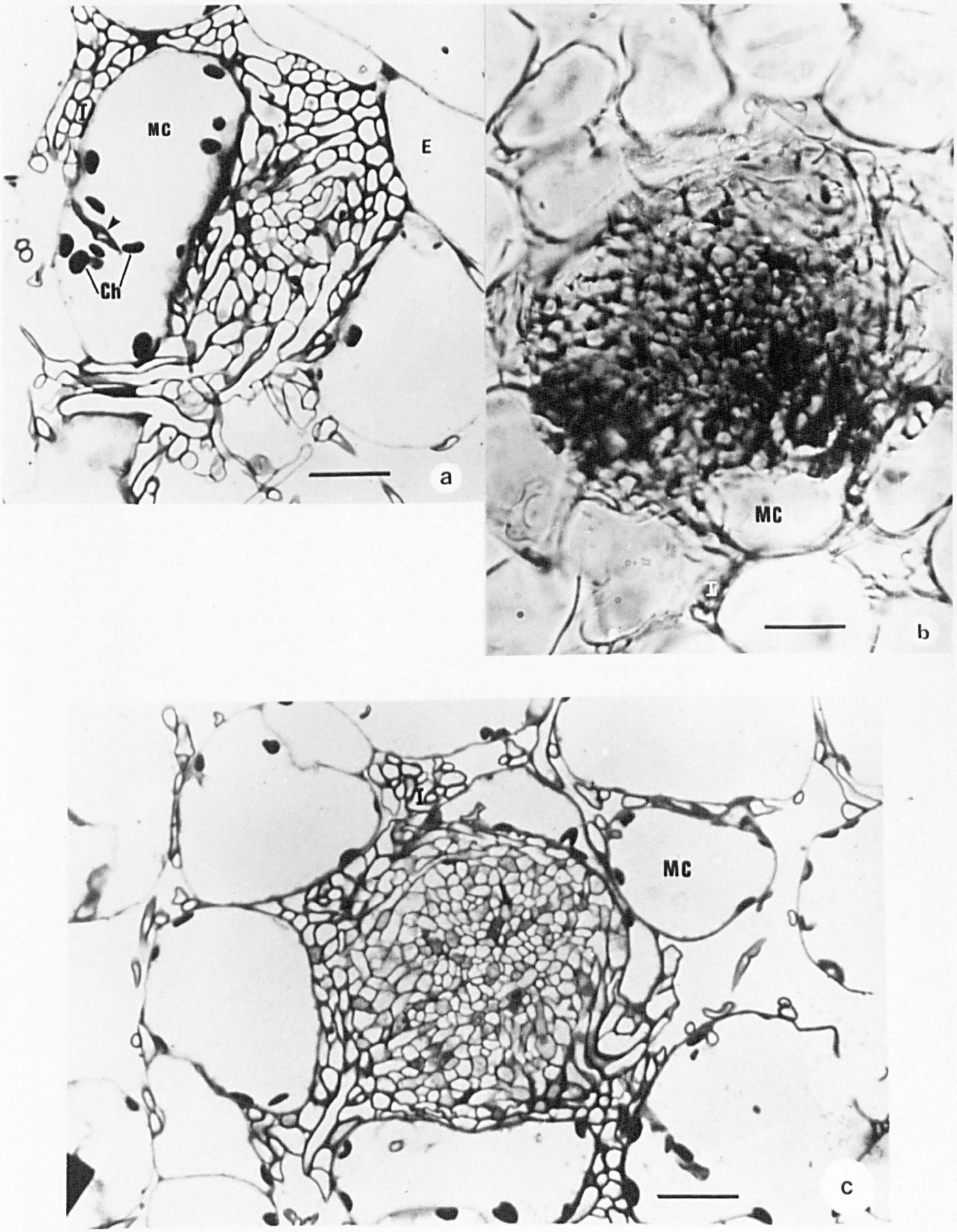
T
MC
E
Ch
a
MC
T
b
T
MC
c

Figures 3.2-3.6

Pycnium and pycniospores of *P. poarum*. Scales lines = 10 µm

Figures 3.2 and 3.3

Transverse sections through pycnium showing pycniosporophores and densely packed hyphae (arrows).

Figure 3.2

Semi-thin section of epon-embedded tissue. Note immature pycniospores at the apices of sporophores (arrowheads). Note also mature pycniospores in the pycnial cavity.

Figure 3.3

Cryostat section. Pycniospores appear to be released from the pycnial cavity.

Figure 3.4

Immature pycniospores are still attached to the sporophores (arrowheads). The formation of pycniospore is marked by a swelling of the sporophore apex.

Figure 3.5

Mature pycniospores on the host surface. Note pycniospores are smooth and pear-shaped.

Figure 3.6

Mature pycnium with pointed periphyses surrounded by numerous pycniospores.

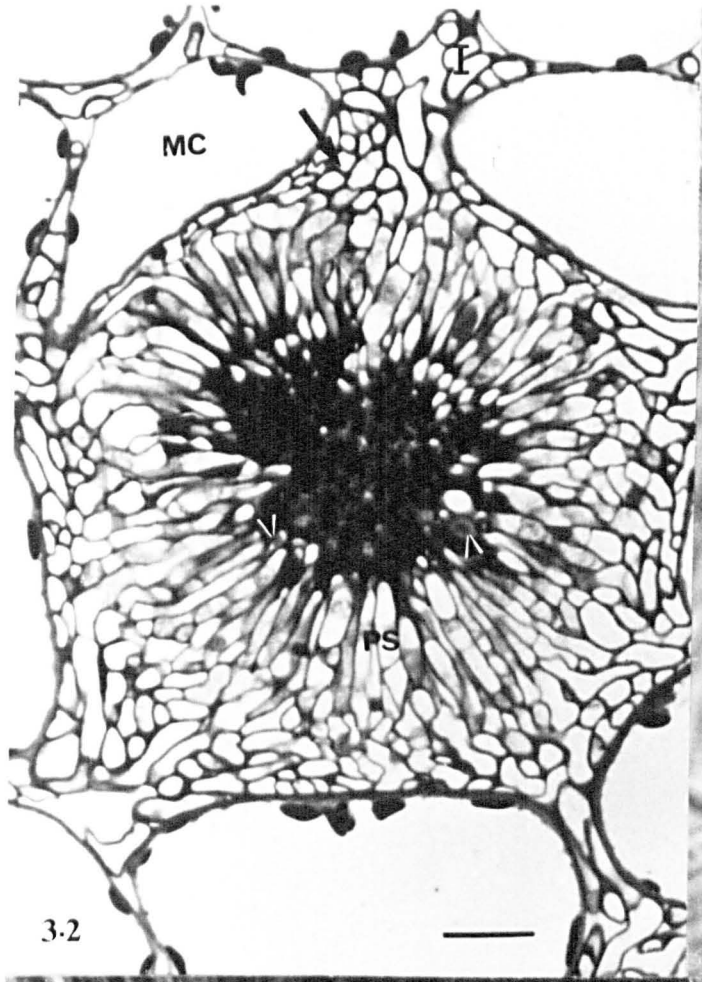

3·2

3·5

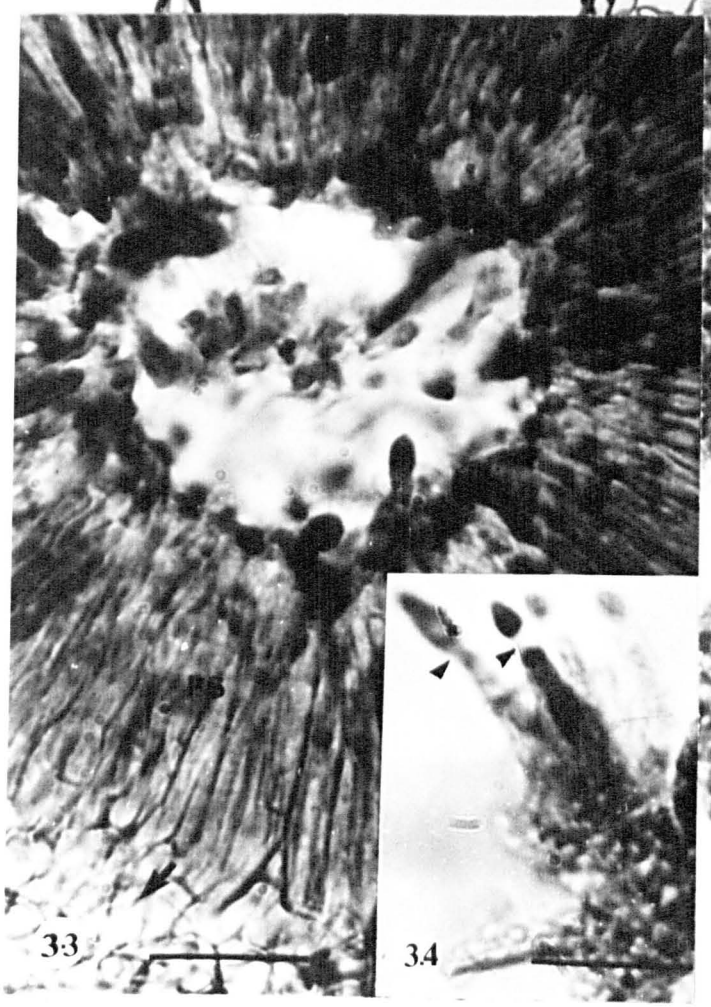

3·3

3·4

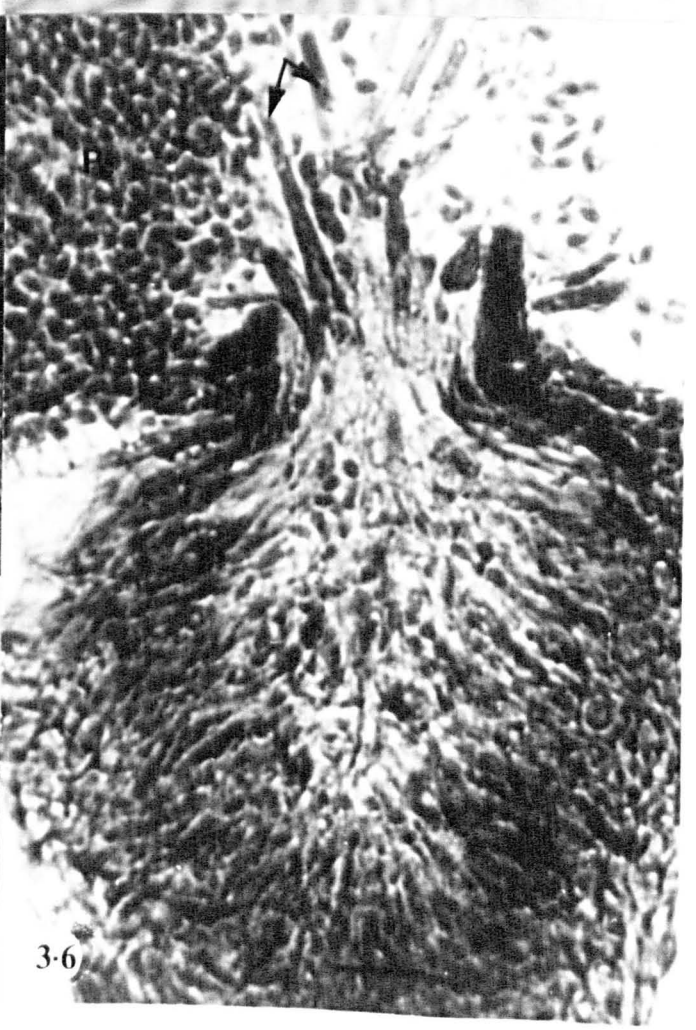

3·6

Figures 3.7 and 3.8

Mature pycnium of *P. poarum* on the host epidermis. Scale lines = 10 µm

Figure 3.7

S.E.M. micrograph showing pycniospores and pointed periphyses (arrows).

Figure 3.8

S.E.M. micrograph showing numerous pycniospores, periphyses (arrows) and flexuous hyphae.

3·7

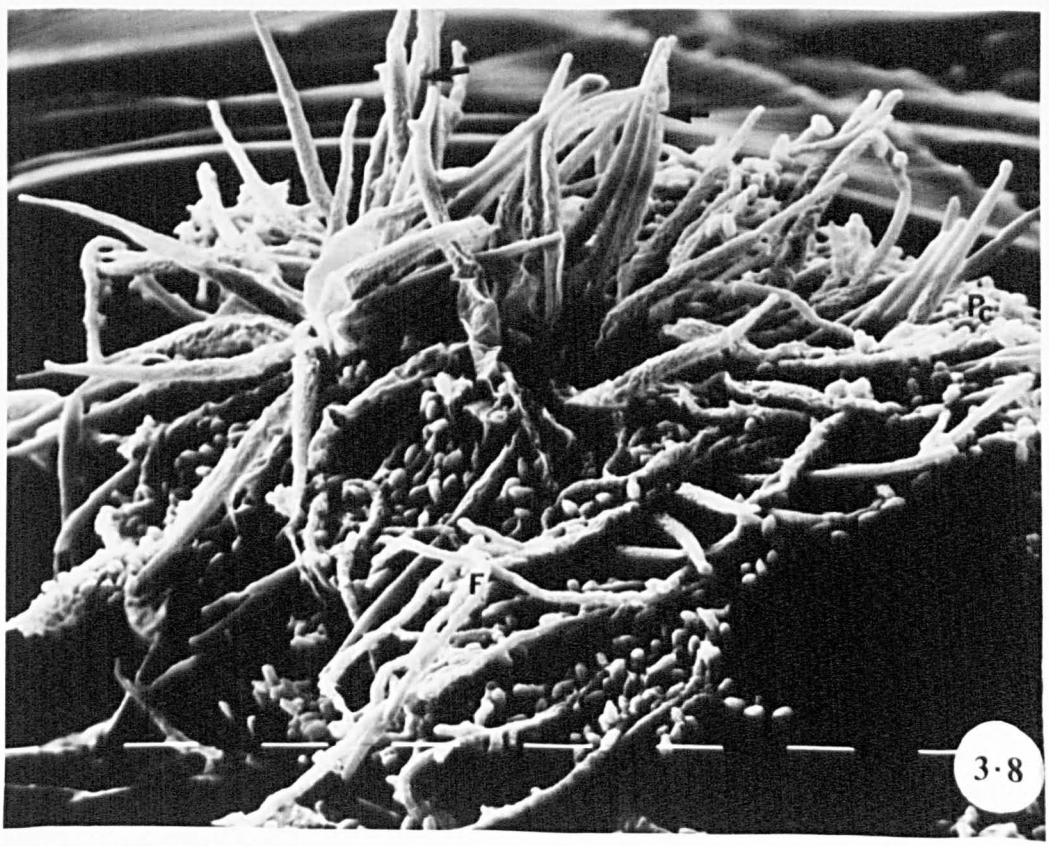

3·8

Figures 3.9-3.12

Mature pycnium of *P. poarum*. Scale lines = 20 μm (except in Figure 3.10 = 10 μm)

Figure 3.9

A young pycnium on the host epidermis. The periphyses and flexuous hyphae are covered by a sticky matrix. Note stoma (arrow).

Figure 3.10

Vertical section of pycnium. Note free pycniospores in the pycnial cavity, pycniosporophores and dense fungal tissue (small arrow) surrounding the pycnium. Note also periphyses and flexuous hyphae (large arrow) extending through the pycnial ostiole.

Figure 3.11

A young pycnium showing pointed, unbranched periphyses (arrow) and branched flexuous hyphae. Note the flexuous hyphae are shorter than the periphyses.

Figure 3.12

Old pycnium showing flexuous hyphae longer than periphyses (arrow).

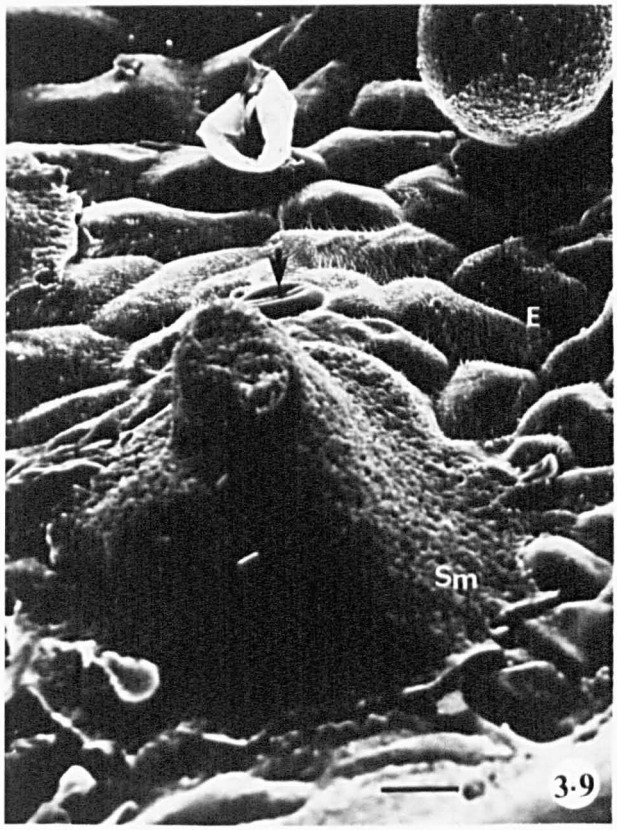
E
Sm
3·9

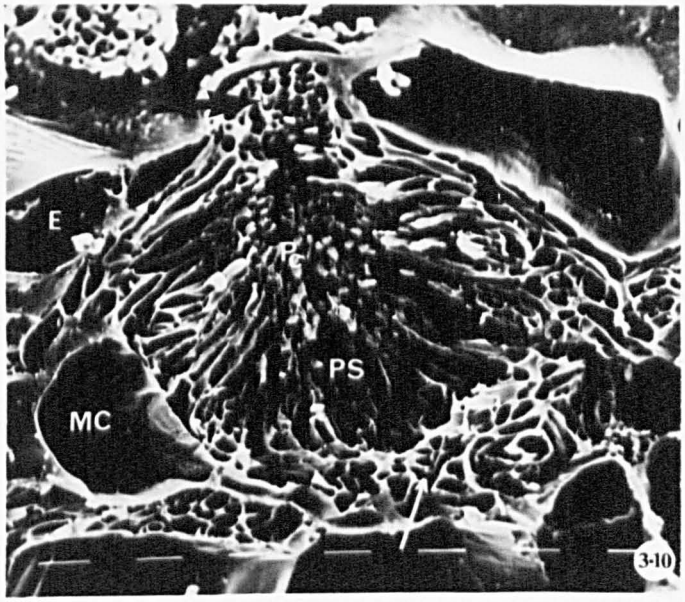
E
PS
MC
3·10

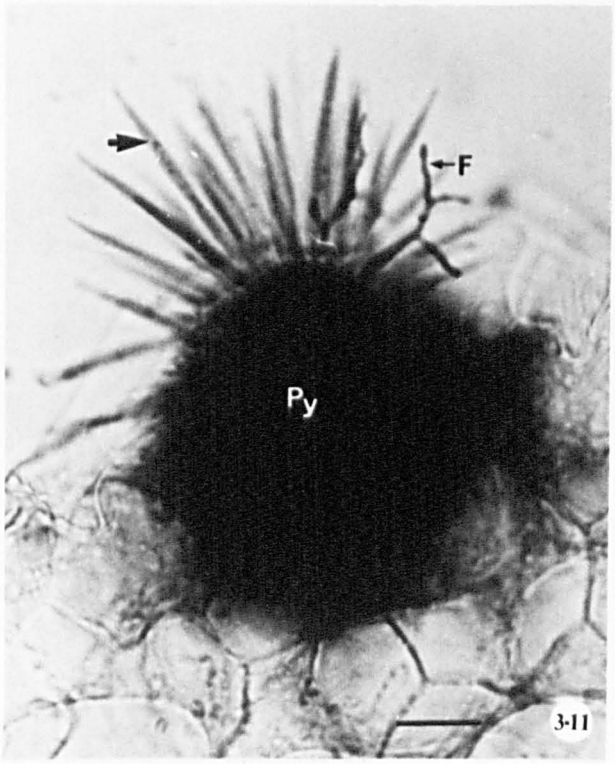
F
Py
3·11

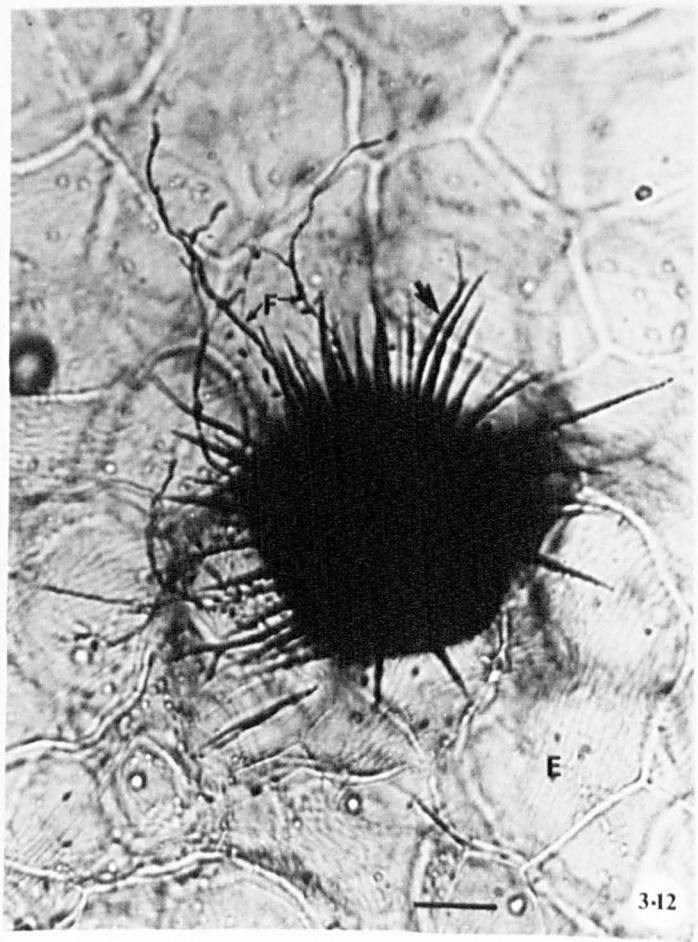
F
E
3·12

Figures 3.13-3.14

Transformation of periphyses into flexuous hyphae in *P. poarum*.

Scale lines = 20 μm

Figure 3.13

Surface view of mature pycnium showing periphyses transformed into flexuous hyphae (arrowheads).

Figure 3.14

S.E.M. of mature pycnium showing pycniospores in a sticky matrix and periphyses (small arrows). Flexuous hyphae are forming at the apices of periphyses (large arrows). Compare transformed and untransformed periphyses.

Figures 3.15 and 3.16

Protoaecium of *P. poarum*. Scale lines = 20 μm

Figure 3.15

In semi-thin section from Epon-embedded tissue. No dikaryotic cells are seen. Note dense hyphal growth below protoaecium.

Figure 3.16

Vertical section of protoaecium, showing dense basal prosenchyma (arrow), developing hymenial region and larger-celled, thin-walled pseudoparenchyma (arrowhead).

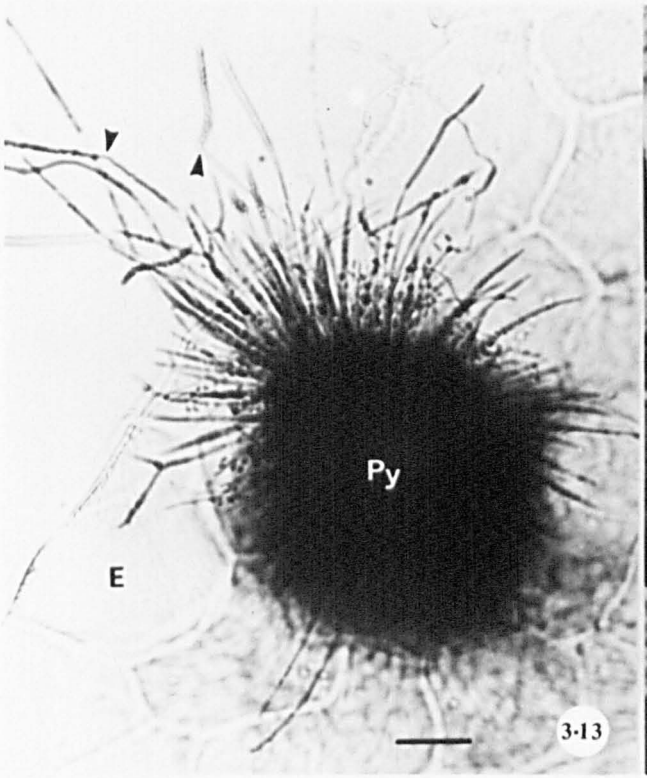

3·13

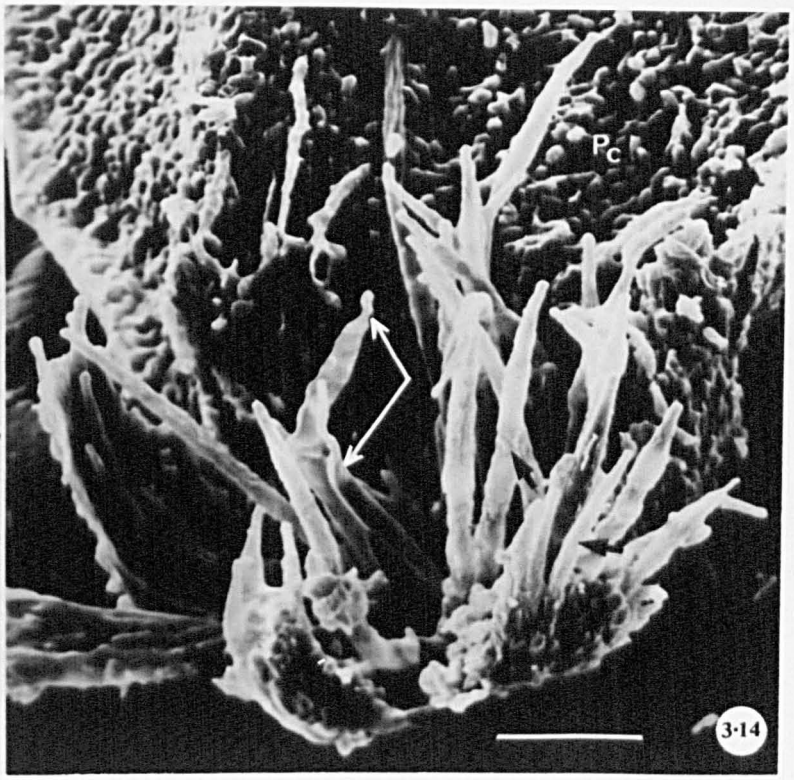

3·14

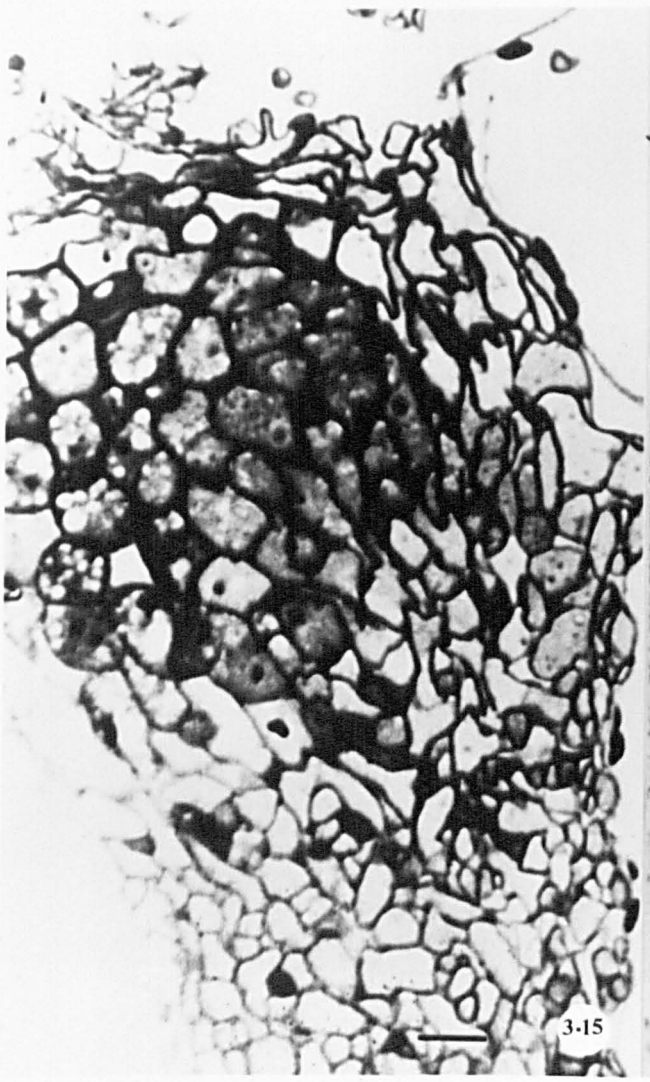

3·15

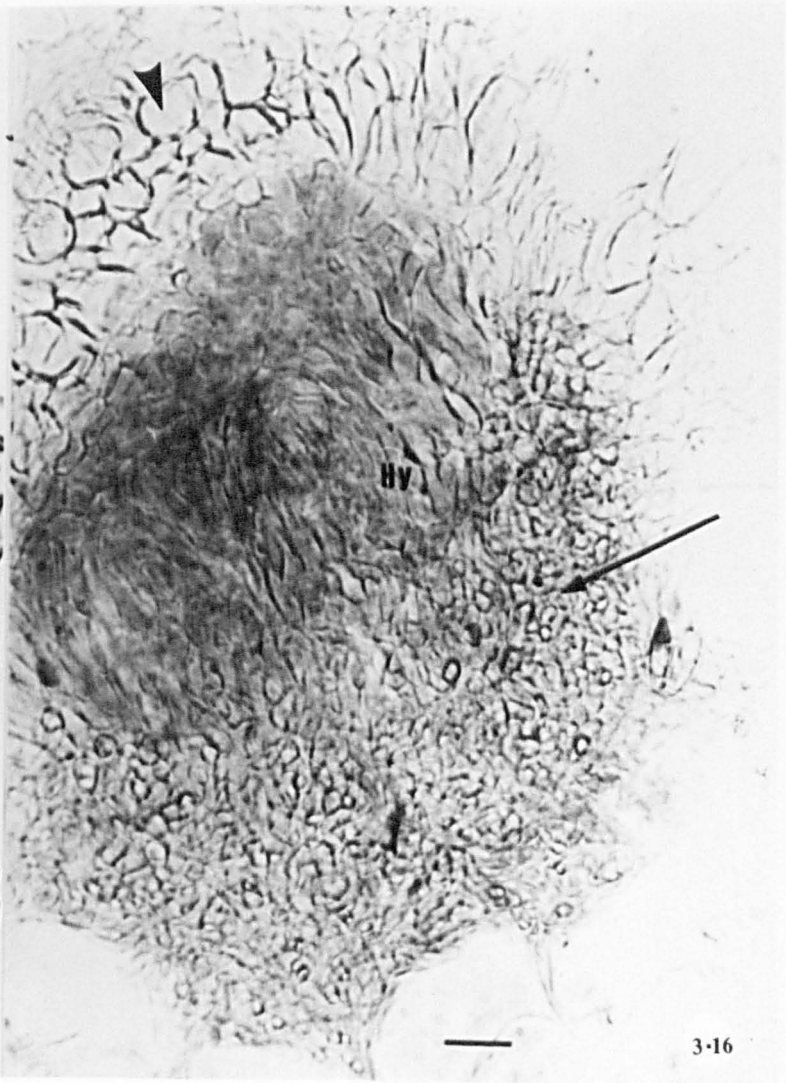

3·16

Figure 3.17

Aceium of *P. poarum*. Scale lines = 15 µm

a - Semi-thin section showing aeciosporophores, intercalary cells (arrow) and aeciospores. Note the basal stroma.

b - Part of aecium showing aeciosporophores giving rise to aeciospore initials which cleave into mature aeciospores and intercalary cells (arrowheads). Note thickening of the wall at the distal end of aeciosporophores (arrow).

Figure 3.18

Semi-thin section through an aecial stroma showing large, elongated aeciosporophores, aeciospore initials, and thickening of the wall at the distal end of sporophores (arrows). Note septum separating sporophore from aeciospore initial. Note also the cell fusion (arrowheads) in the aecial stroma.

Scale line = 15 µm

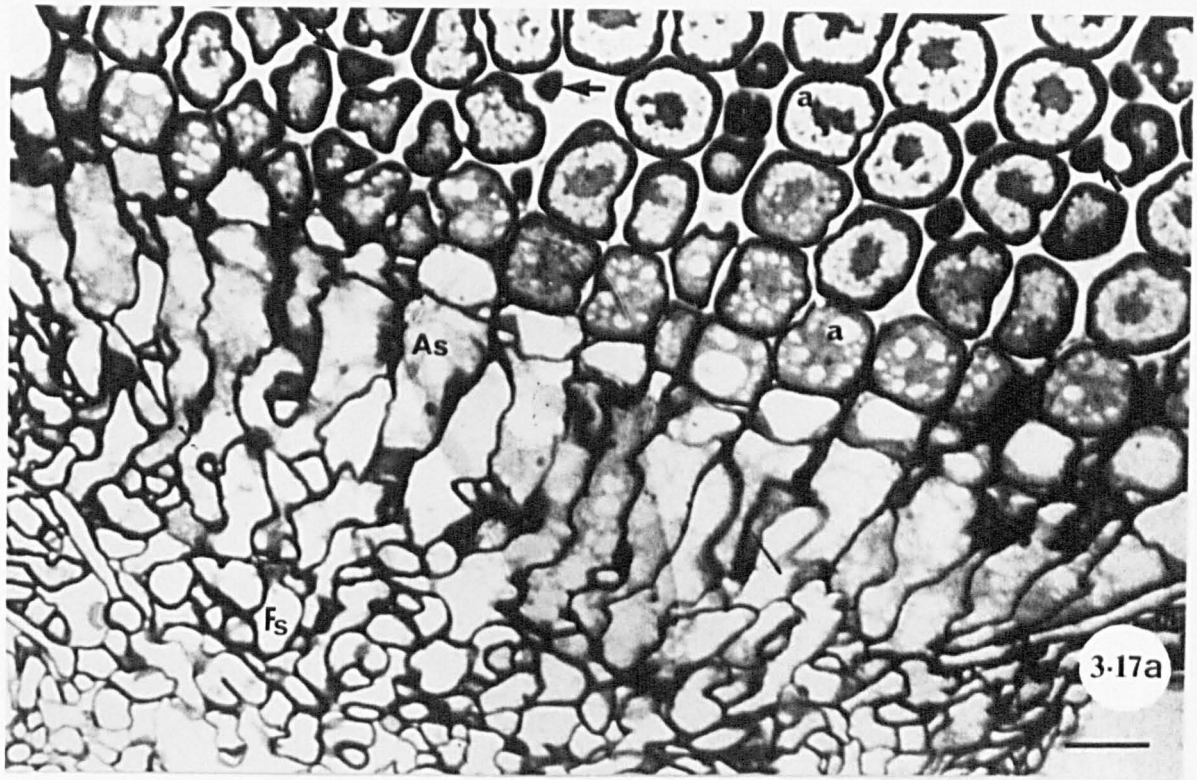

3·17a

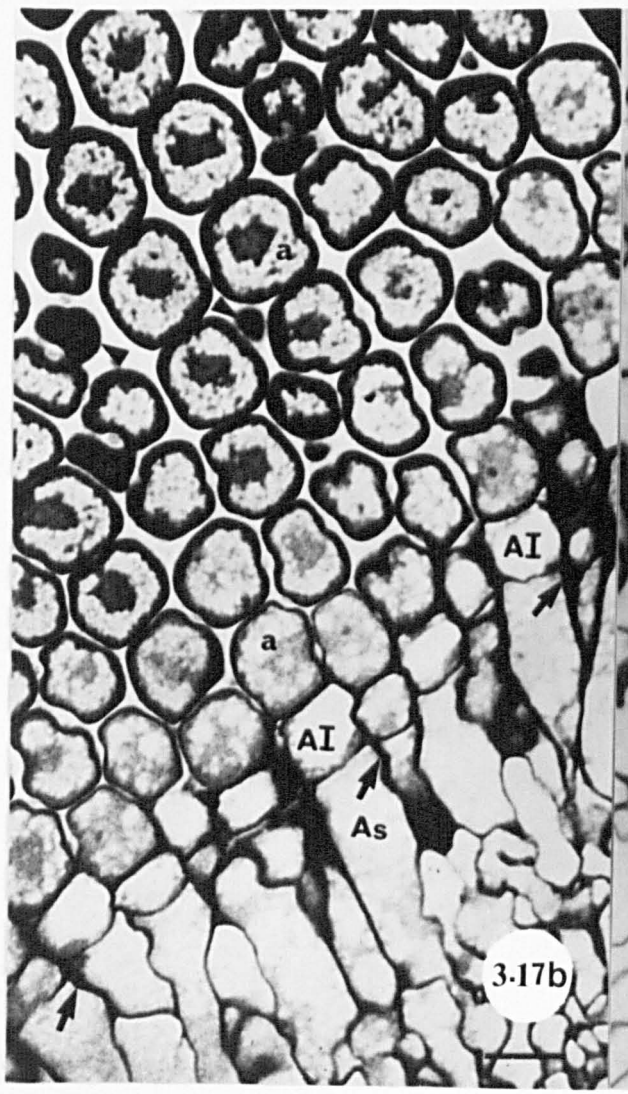

3·17b

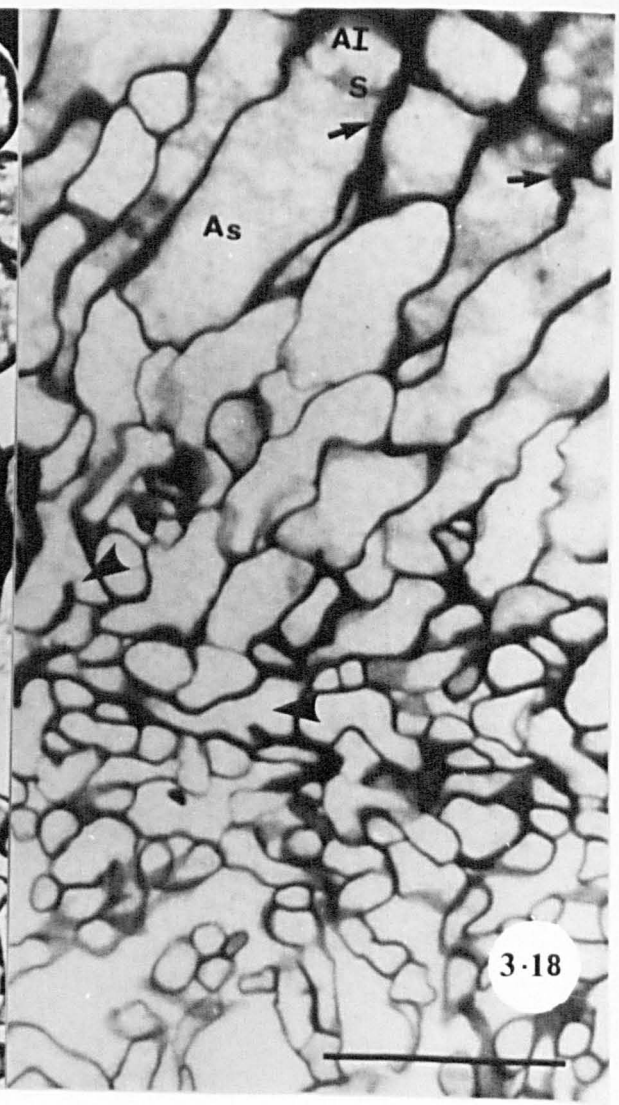

3·18

Figure 3.19

Part of fungal tissue below aecium of *P. poarum*. Hyphae appear highly vacuolated. Note nucleus, septum and lipid drops. Note also unilateral partial septum (arrow).

x6250

Figures 3.20 and 3.21

Aeciospores of *P. poarum*. Scale line = 10 μm

Figure 3.20

Freezing microtome section of aecium showing aeciospores with dense cytoplasm and small intercalary cells (arrows).
Compare with Figure 3.17 for methodology.

Figure 3.21

Aeciospore with germ pores (arrow).
Note germ tube.

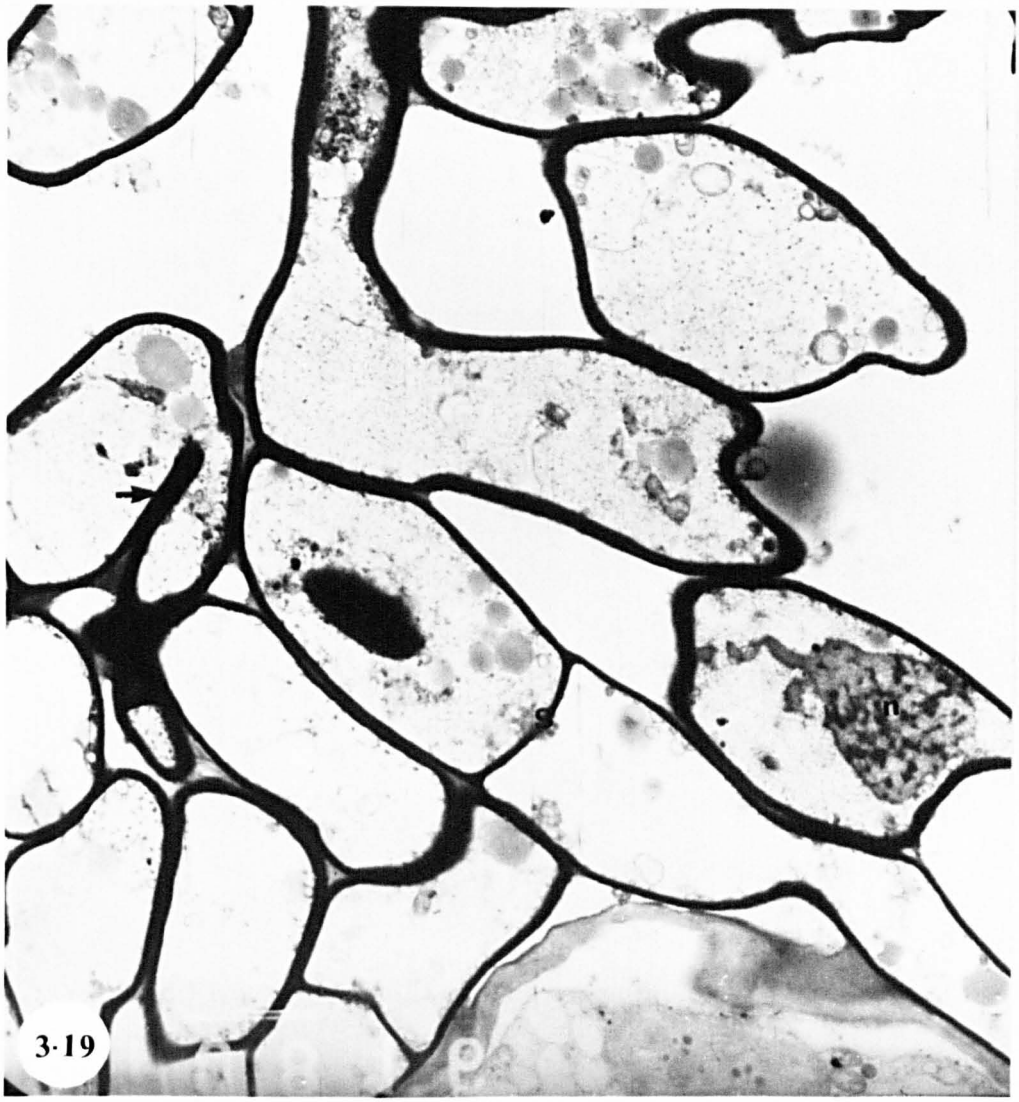
3·19

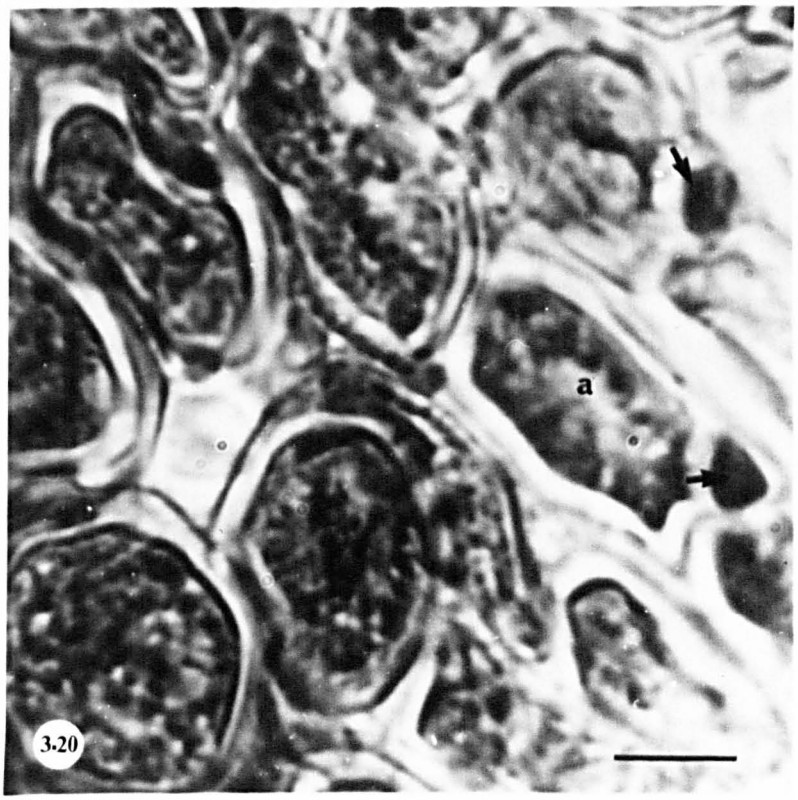
a
3·20


3·21

Figures 3.22 and 3.23

Aecium of *P. poarum*. Scale lines = 50 µm

Figure 3.22

Light microscope micrograph of closed aecium showing chains of aeciospores enclosed by peridium. Aeciospores in the distal end of the chains are larger than those near to aeciosporophores.

Figure 3.23

Light microscope micrograph of opened aecium (from epon-embedded material) showing chains of aeciospores and peridial cells (open arrow). Intercalary cells are also seen.

Figures 3.24 and 3.25

Stages in emergence and dehiscence of aecia of *P. poarum*.

Scale lines = 80 µm

Figure 3.24

S.E.M. micrograph showing early stage in emergence and dehiscence of aecia (arrows).

Figure 3.25

Enlarged S.E.M. micrograph of aecium. Note aeciospores in the aecium cavity and the ruptured host epidermis.

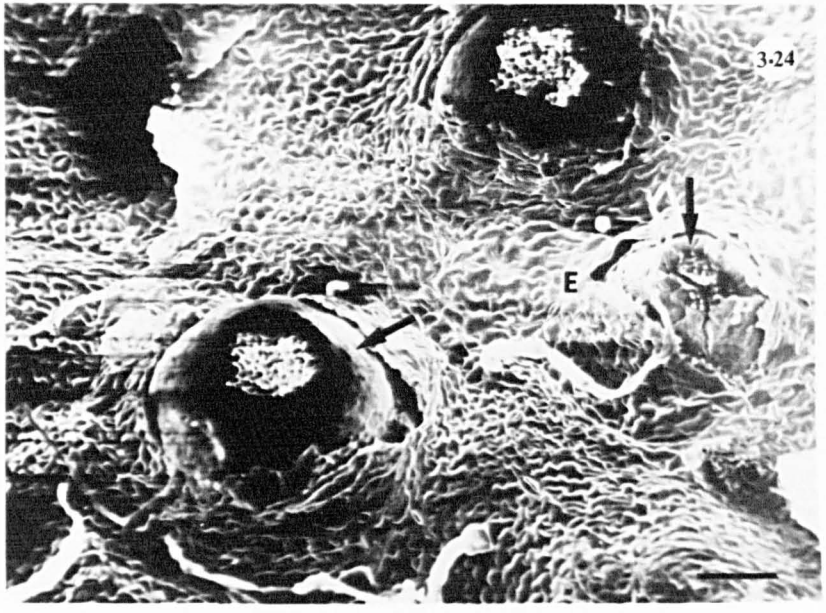
3-24
E

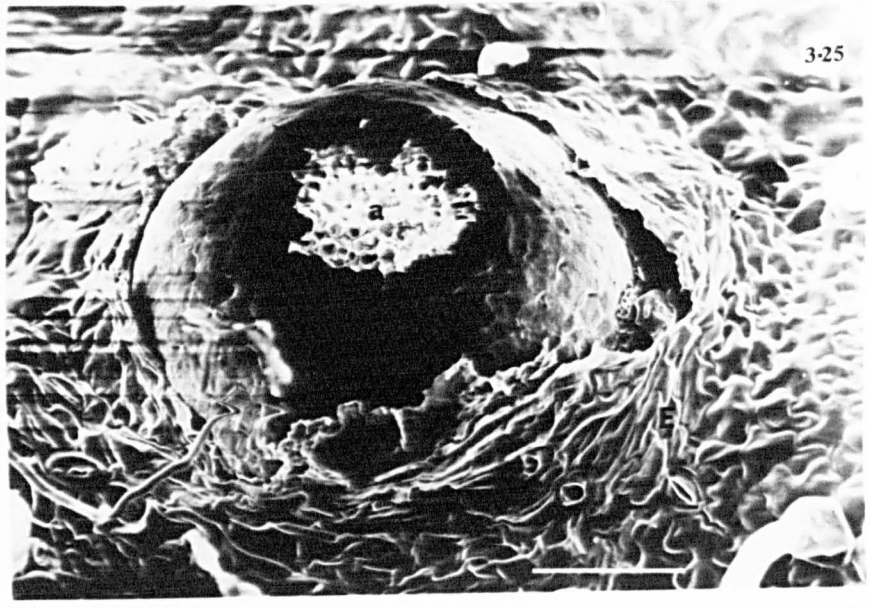
3-25
a
E

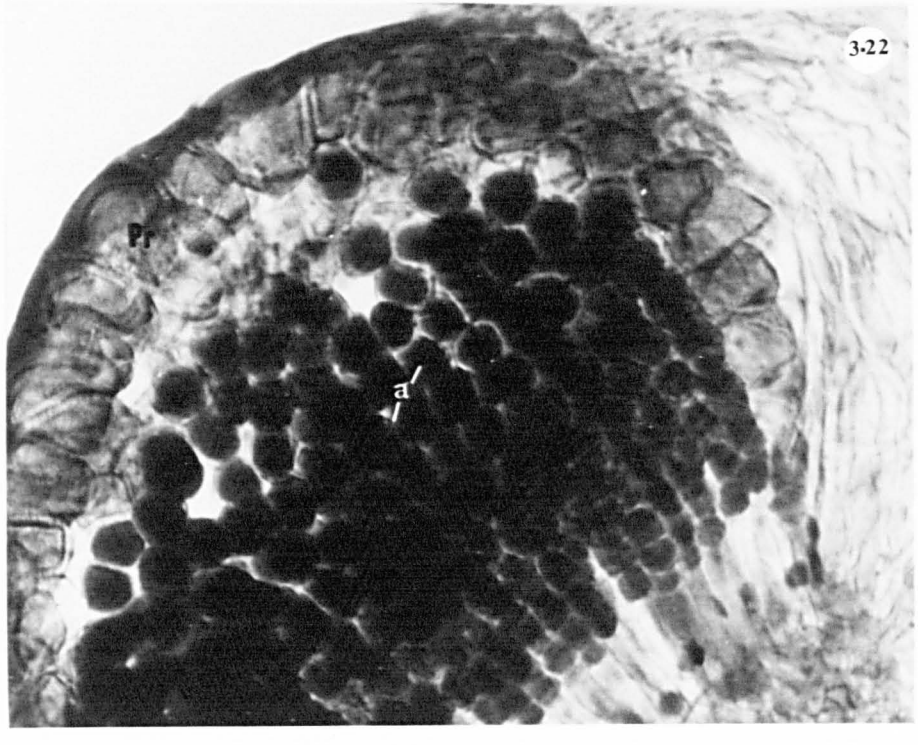
3-22
Pr
a

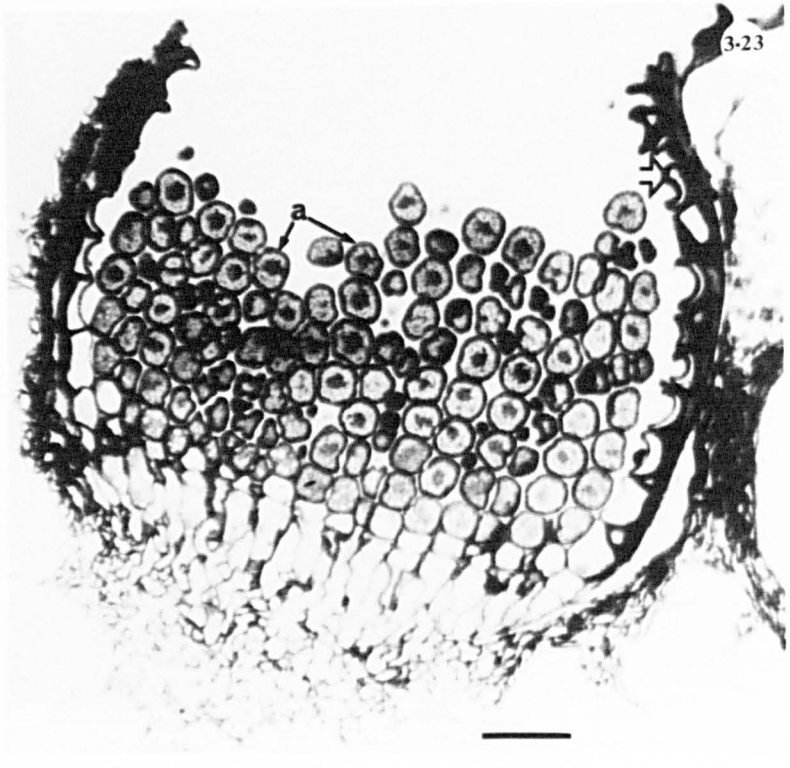
3-23
a

Figure 3.26

S.E.M. micrograph of aecium showing ruptured peridium which shows several teeth. Scale line = 100 µm

Figure 3.27

S.E.M. micrograph of mature aeciospore. The outer surface shows coglike ornamentations. Scale line = 1 µm

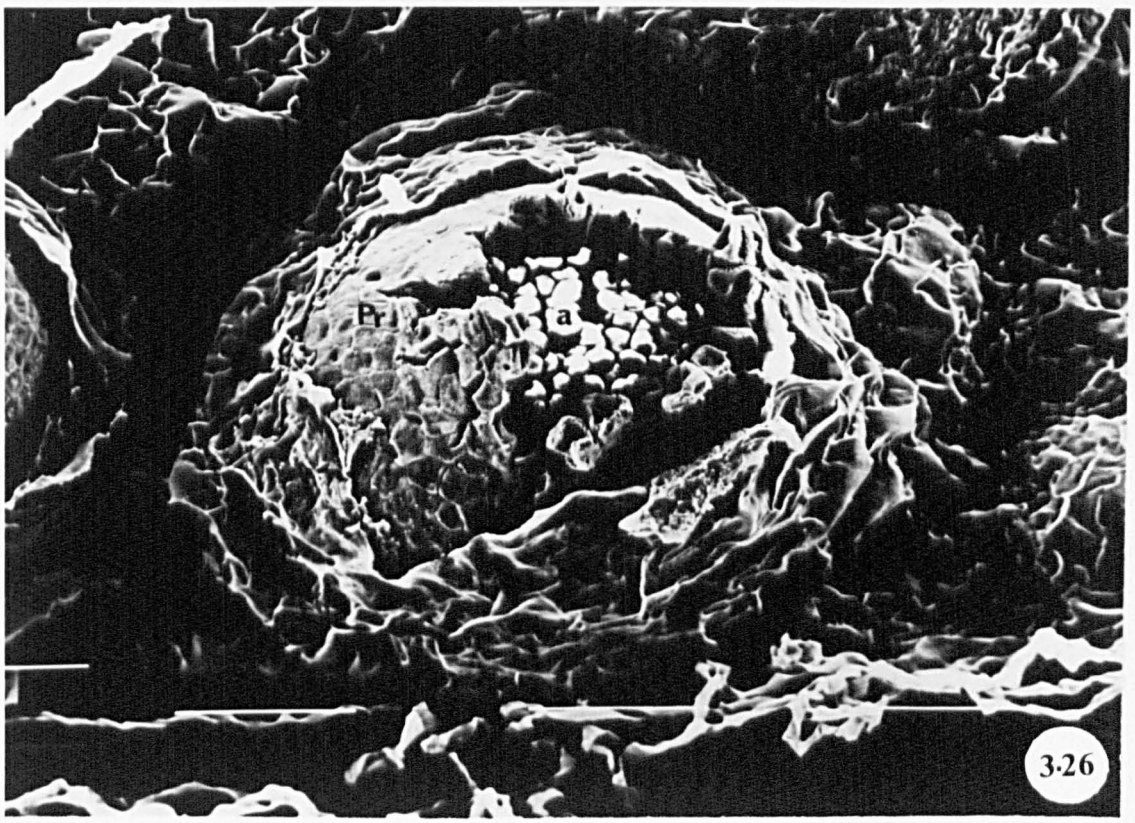

3·26

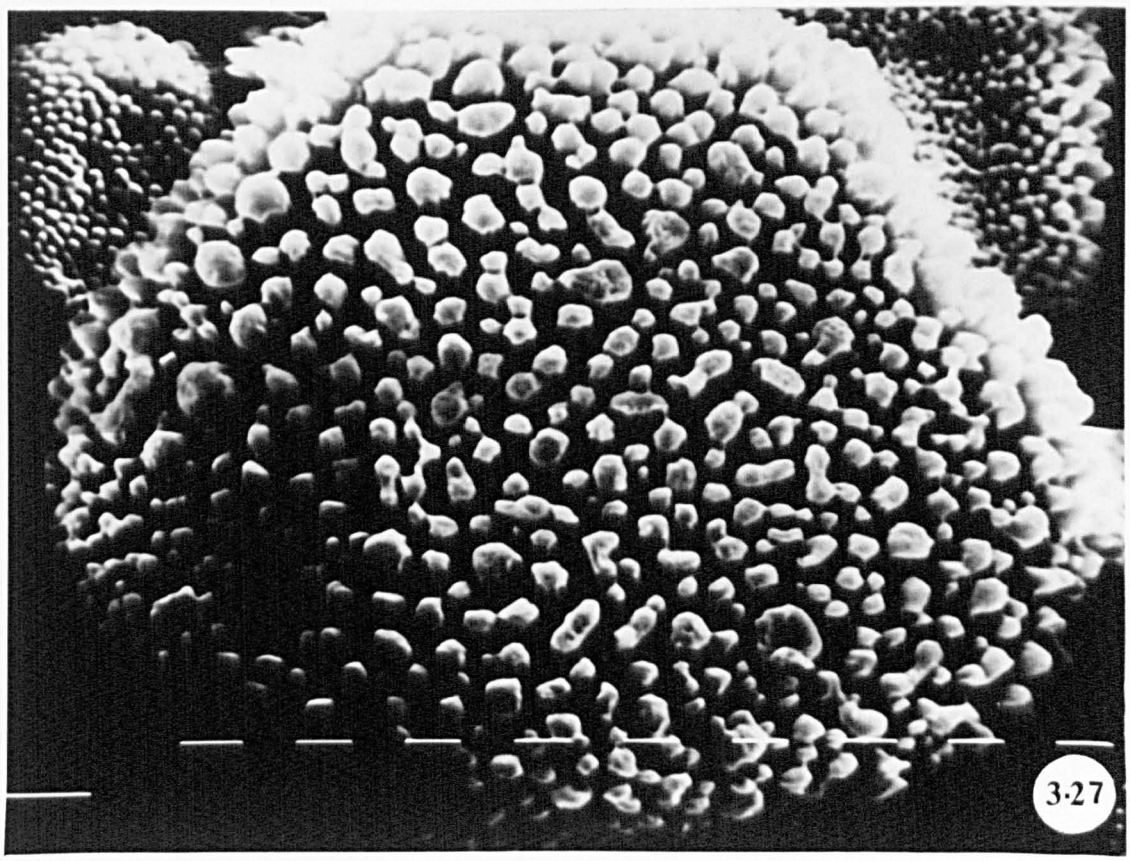

3·27

Figures 3.28 and 3.29

Aeciospores of *P. poarum*. Scale lines = 10 μm

Figure 3.28

S.E.M. micrograph of aeciospores showing surface ornamentations (arrows) and refractive granule.

Figure 3.29

S.E.M. micrograph of aeciospores on the upper surface of *Poa* leaf. Several germ pores (unlabelled arrows) are seen on aeciospore. The refractive granules appear to assist the spores and germ tubes to stick to the leaf surface of the host. Note those at some distance from the spore appear to be carried there by the growing germ tubes. Note also germ tubes (arrowheads).

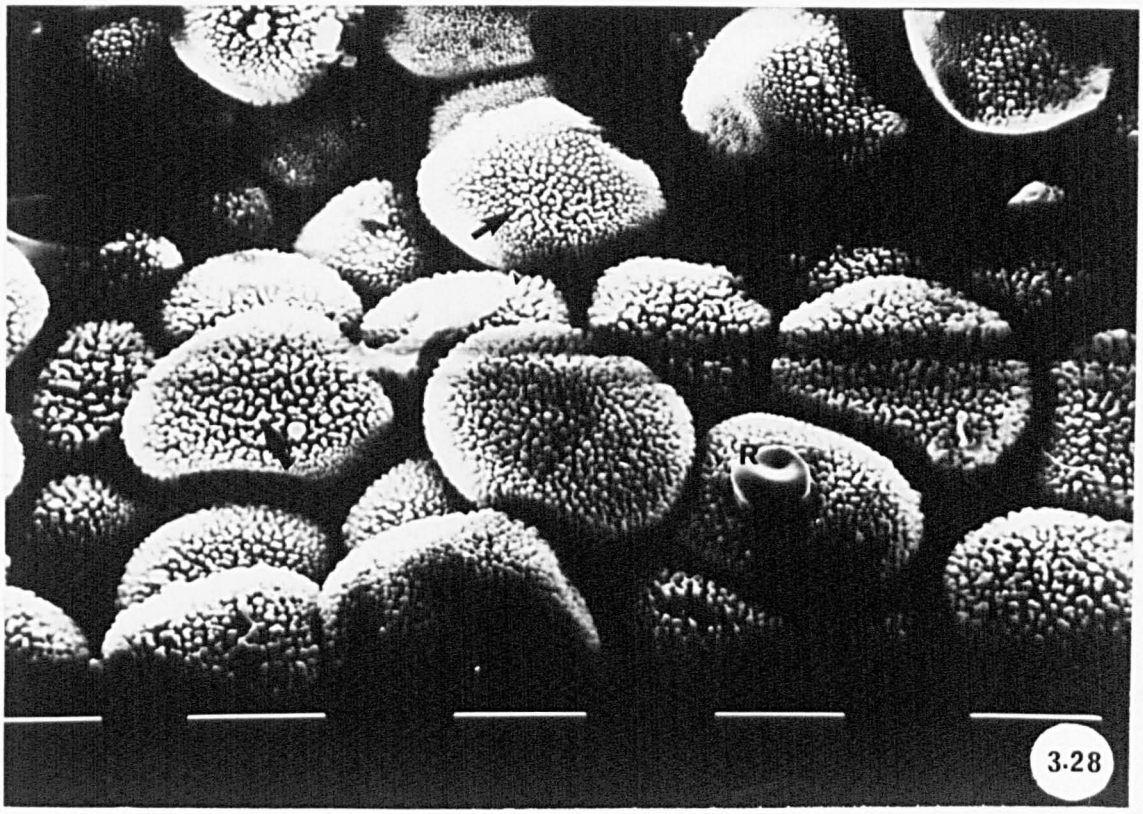
R
3.28

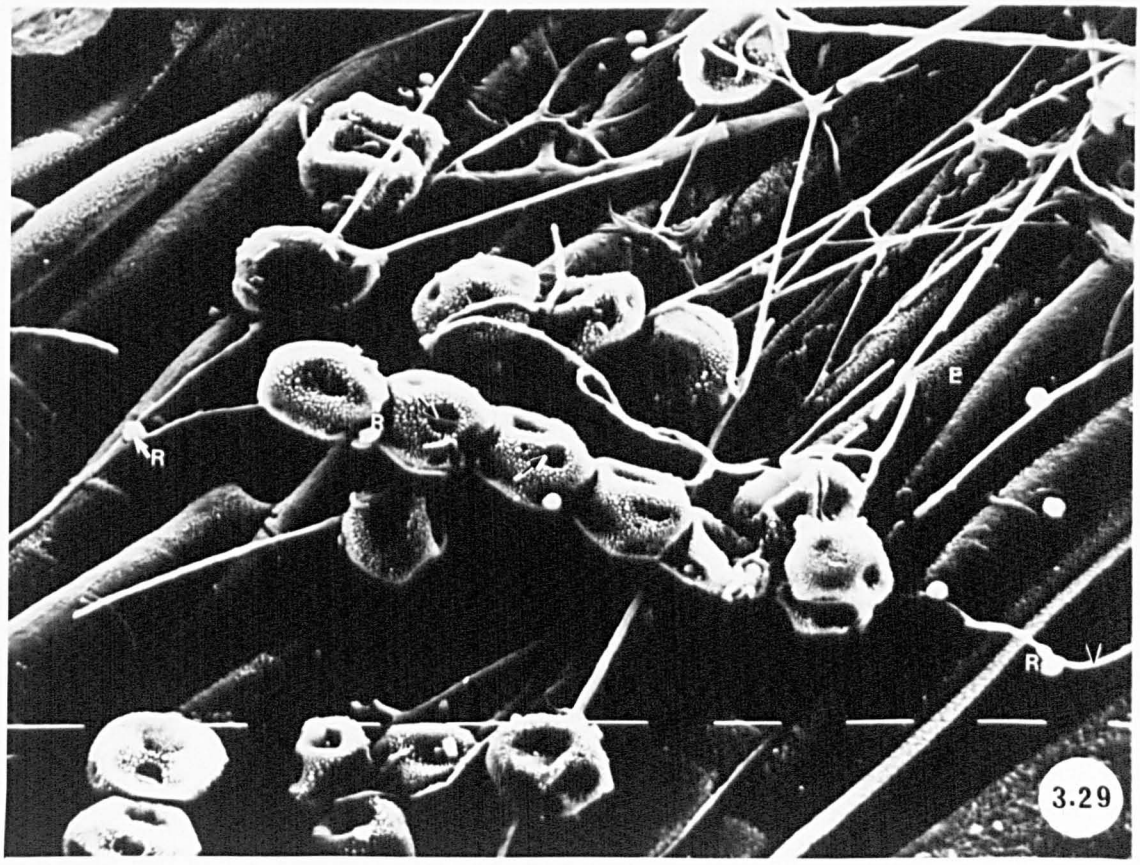
R
R
R
3.29

Figures 3.30-3.32

Aeciospores of *P. poarum*. Scale lines = 10 m

Figure 3.30

S.E.M. micrograph showing chains of aeciospores on the lower surface of *Poa* leaf. Note germ pores and refractive granules which may enable the germ tubes to stick to the host leaf surface.

Figure 3.31

S.E.M. micrograph of aeciospores. The germ pores appear to be filled to varying extents by material (arrows) which may represent stages in the development of refractive granules while other pores appear to have lost their plug material.

Figure 3.32

S.E.M. micrograph of mature aecium showing aeciospores with several refractive granules (arrows). The peridium has opened, exposing the aeciospores and the margin appears as five teeth, bending outwards (cf. Figures 3.23 and 3.26). Note ornamented surface of peridial cells (arrowheads).

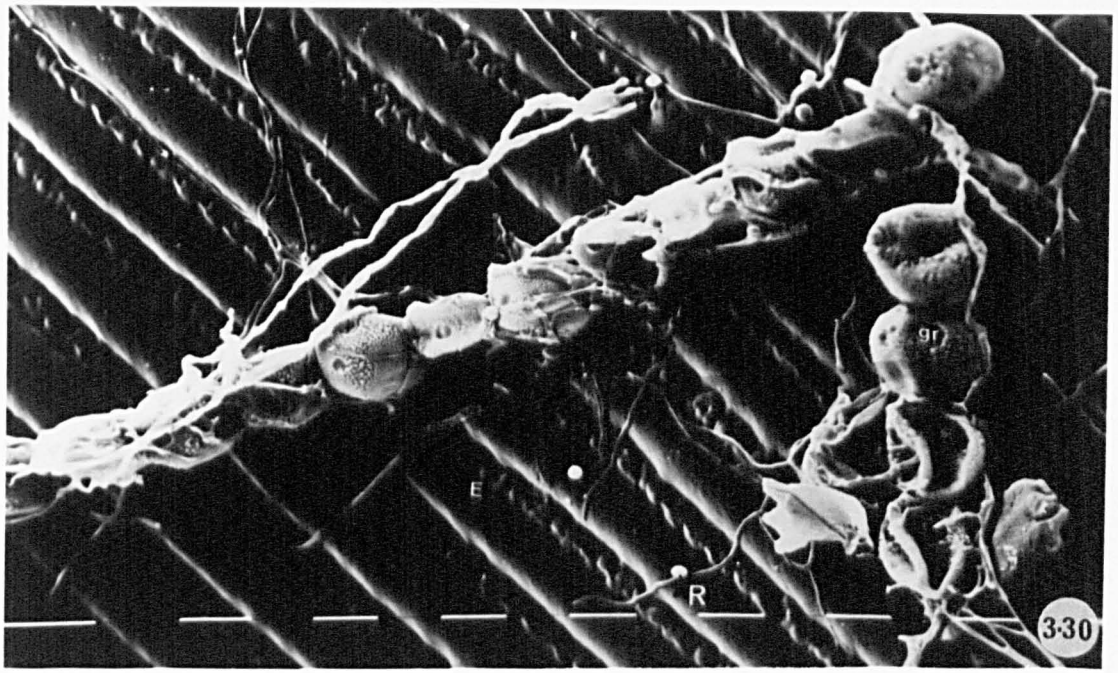

3·30

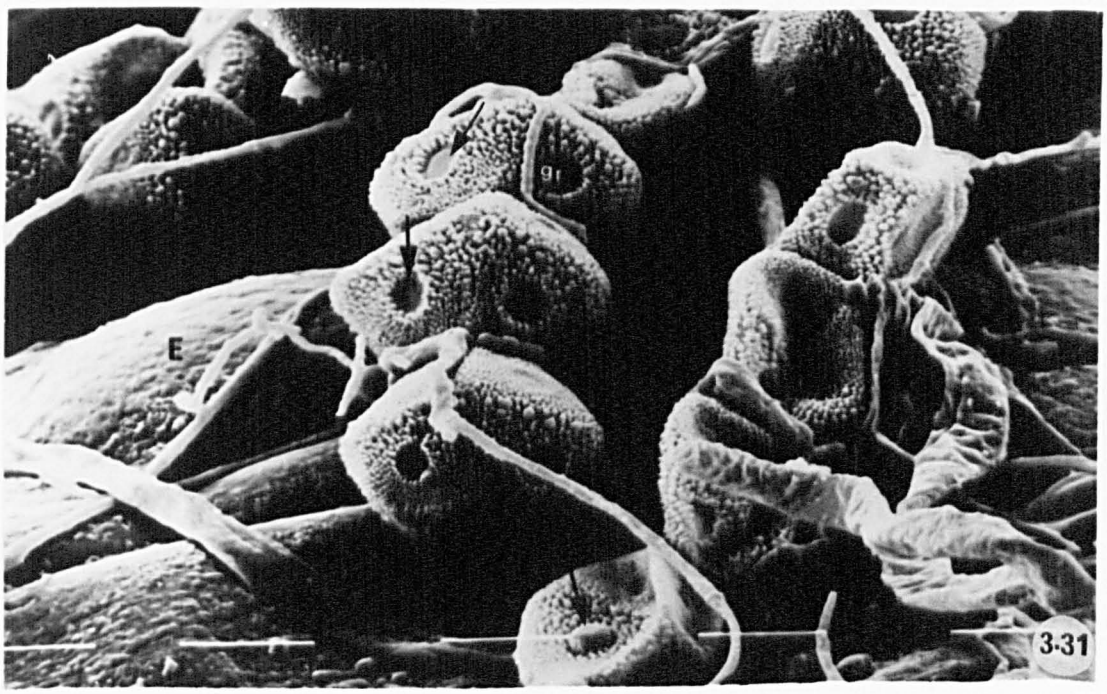

3·31

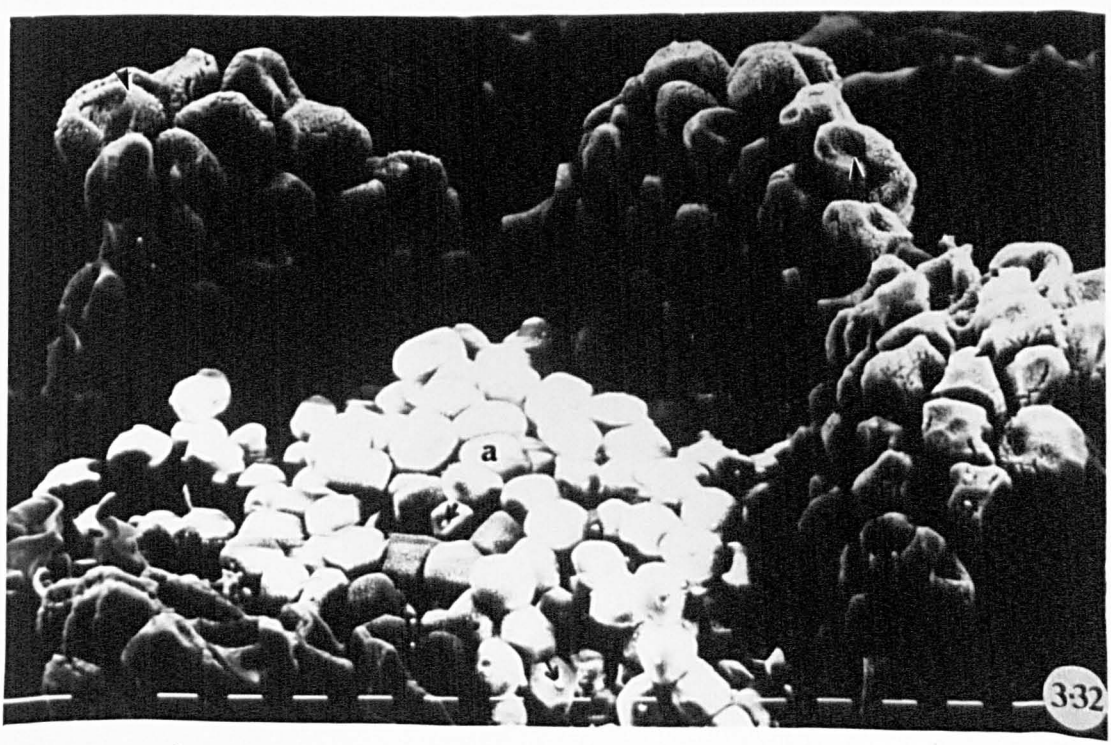

3·32

Figure 3.33

Part of aecium showing chains of aeciospores. Note germ pores (unlabelled arrow) and refractive granules (arrowheads). Scale line = 20 μm

Figure 3.34

Light micrograph of isodiametric peridial cells. Ornamentation of the surface of peridial cell is seen. Scale line = 20 μm

Figure 3.35

Light micrograph showing dense layer of fungal cells around aecium (arrow). Note peridium. Scale line = 20 μm

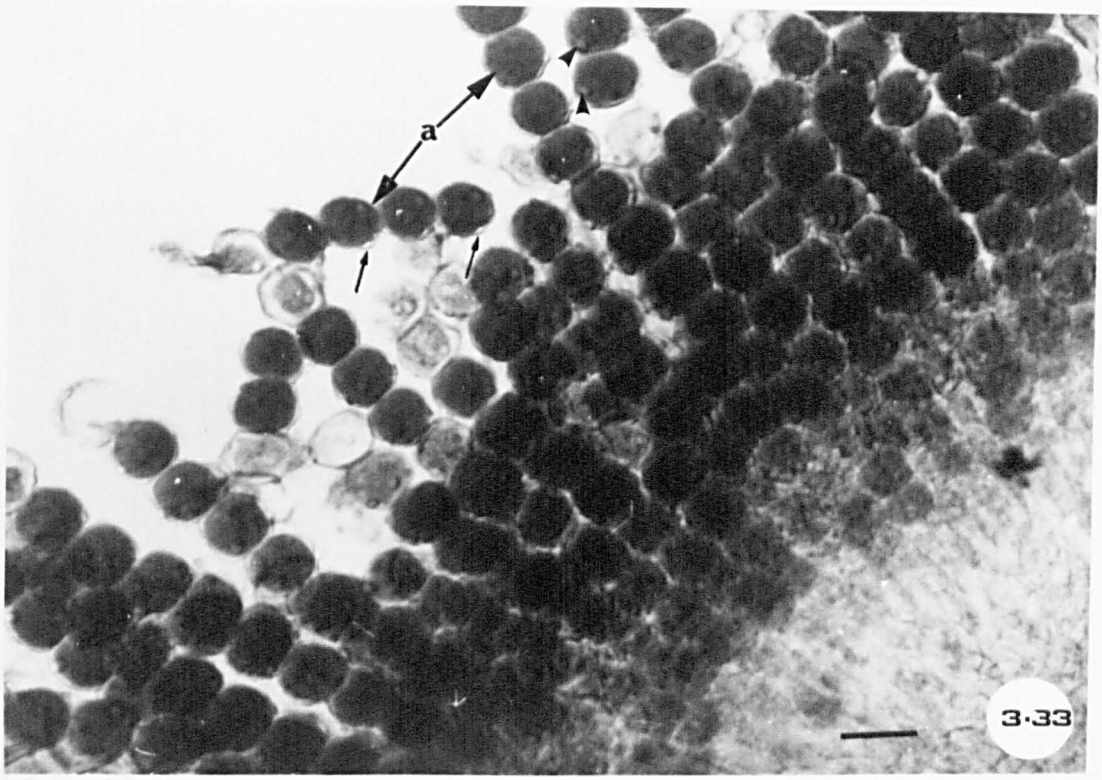
a
3·33

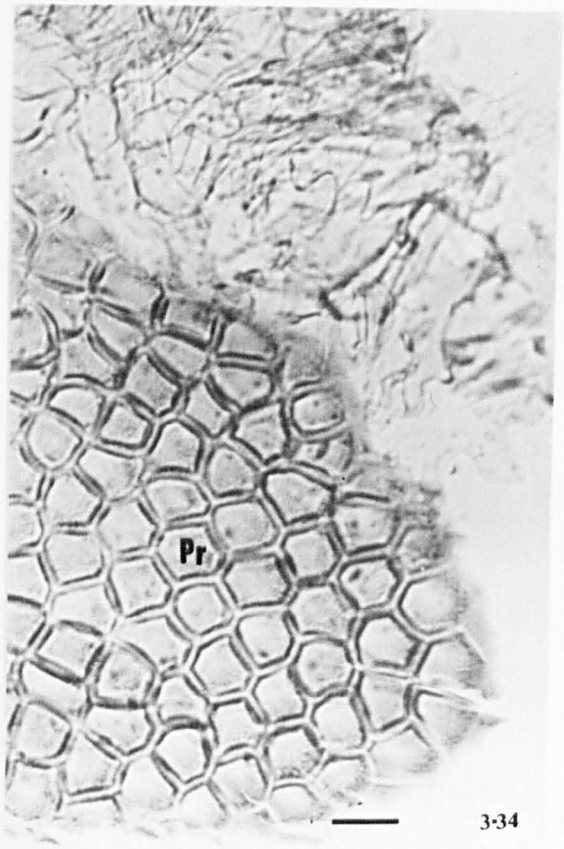
Pr
3·34

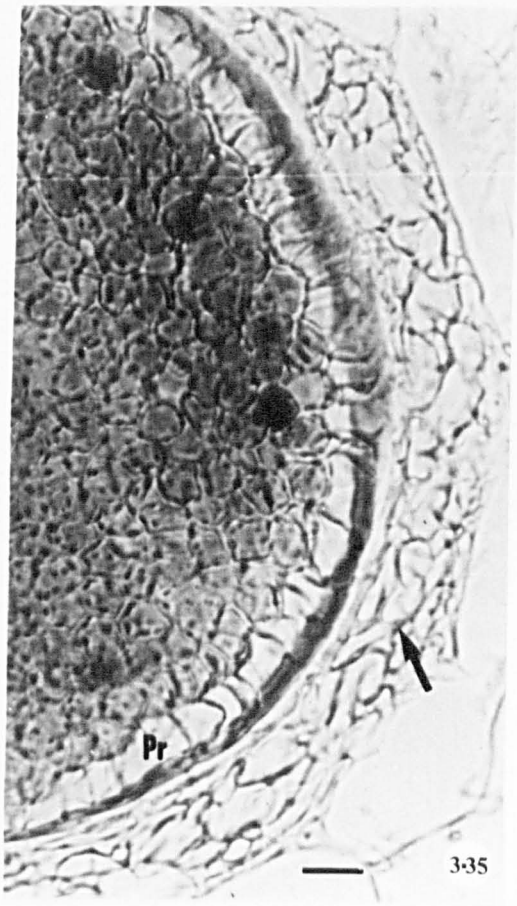
Pr
3·35

Figure 3.36

Transverse section, light micrograph of mature uredium of *P.poarum*. The uredium is surrounded by the ruptured upper epidermis. Note several germ pores occur in each urediospore (arrows). Scale line = 20 μm

Figure 3.37

Tangential section, light micrograph of uredium in *Poa* leaf showing a mass of pseudoparenchymatous tissue (arrow) which is formed under the host epidermis. Note urediospores. Scale line = 20 μm

Figure 3.38

T.E.M. micrograph of pseudoparenchyma of uredial primordium. Two nuclei can be seen in one dikaryotic cell, and at another point one nucleus appears to have migrated through a partial septum. Note the thickened fungal cell wall (arrowheads). x6250

Figure 3.39

Stalked urediospore of *P. poarum*. Scale line = 20 μm

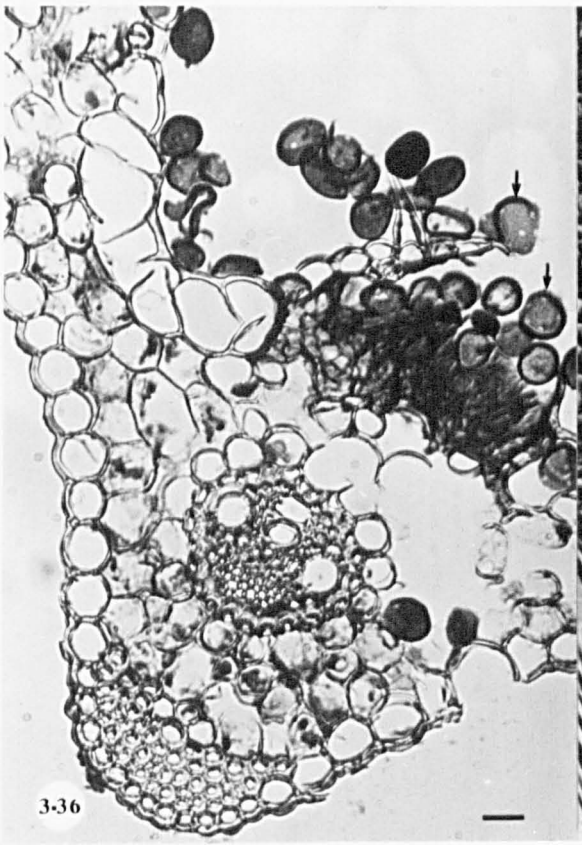

3·36

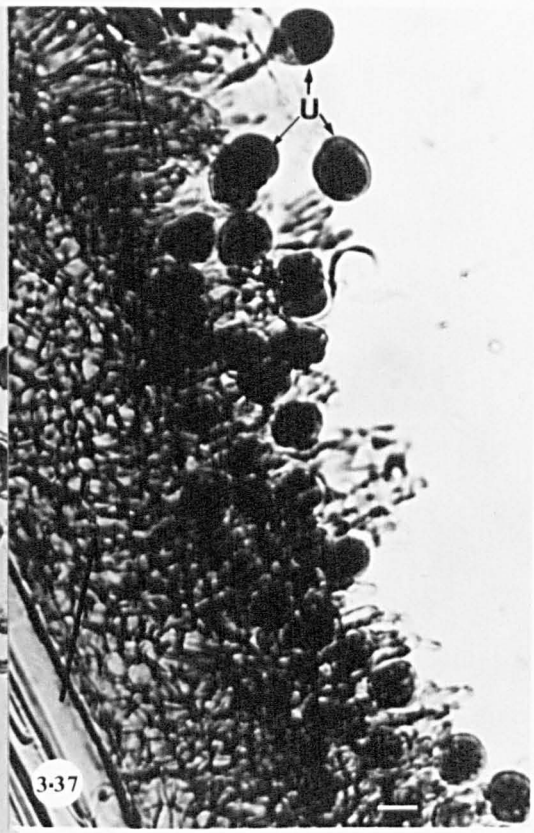

3·37

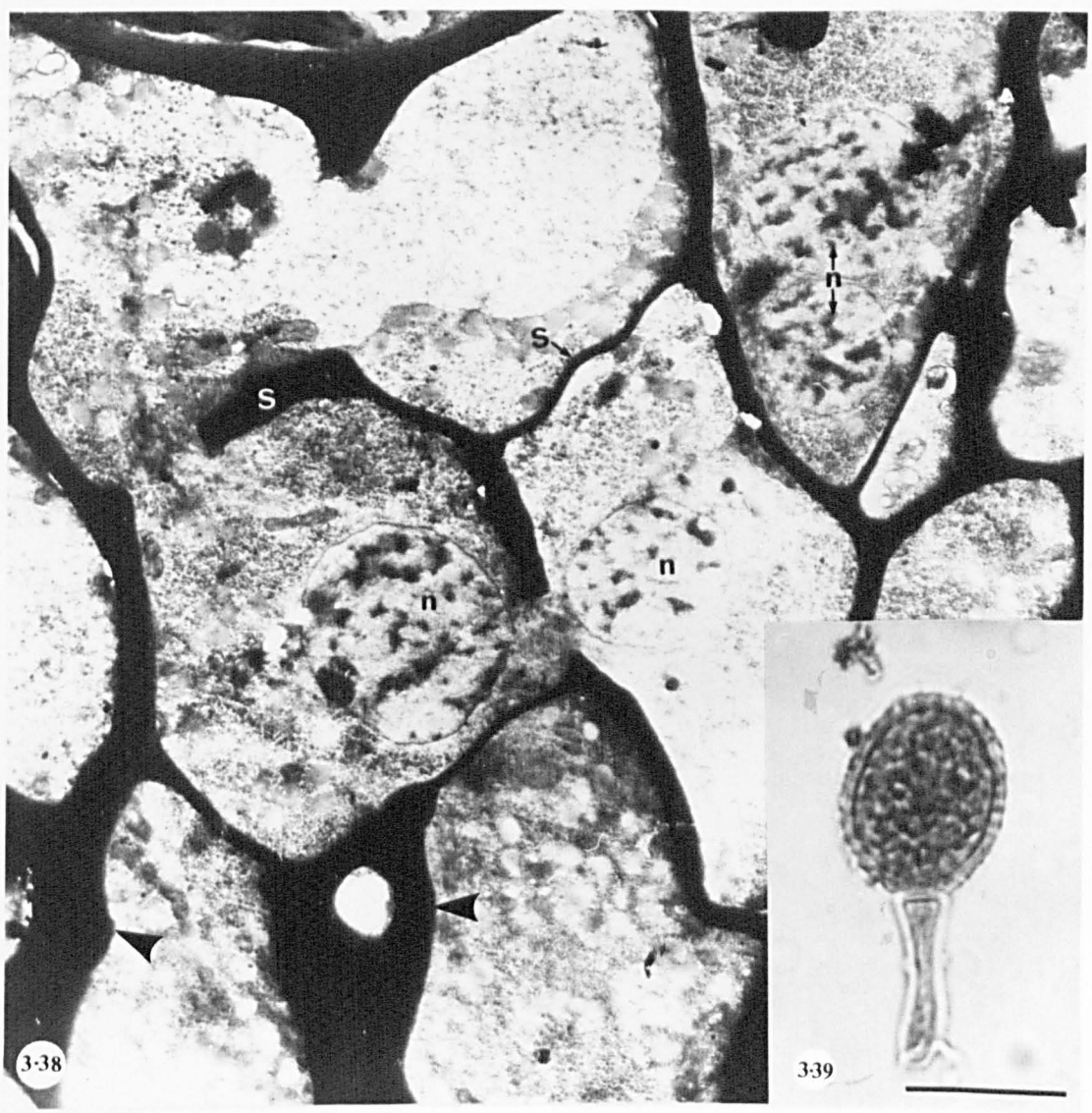

3·38

3·39

Figures 3.40 and 3.41

Urediospores and urediosori of *P. poarum*. Scale line = 10 μm

Figure 3.40

S.E.M. micrograph of urediosorus just breaking through the host epidermis. Note ornamented surface of urediospores and depression indicating covered germ pore (arrowhead).

Figure 3.41

S.E.M. micrograph of urediosorus showing urediospores with ornamented surface. The base of the urediospore is detached from the apex of the stalk (open arrow). Note scar on the base of urediospore and thickened rim (arrow), also depression over germ pore (arrowhead).

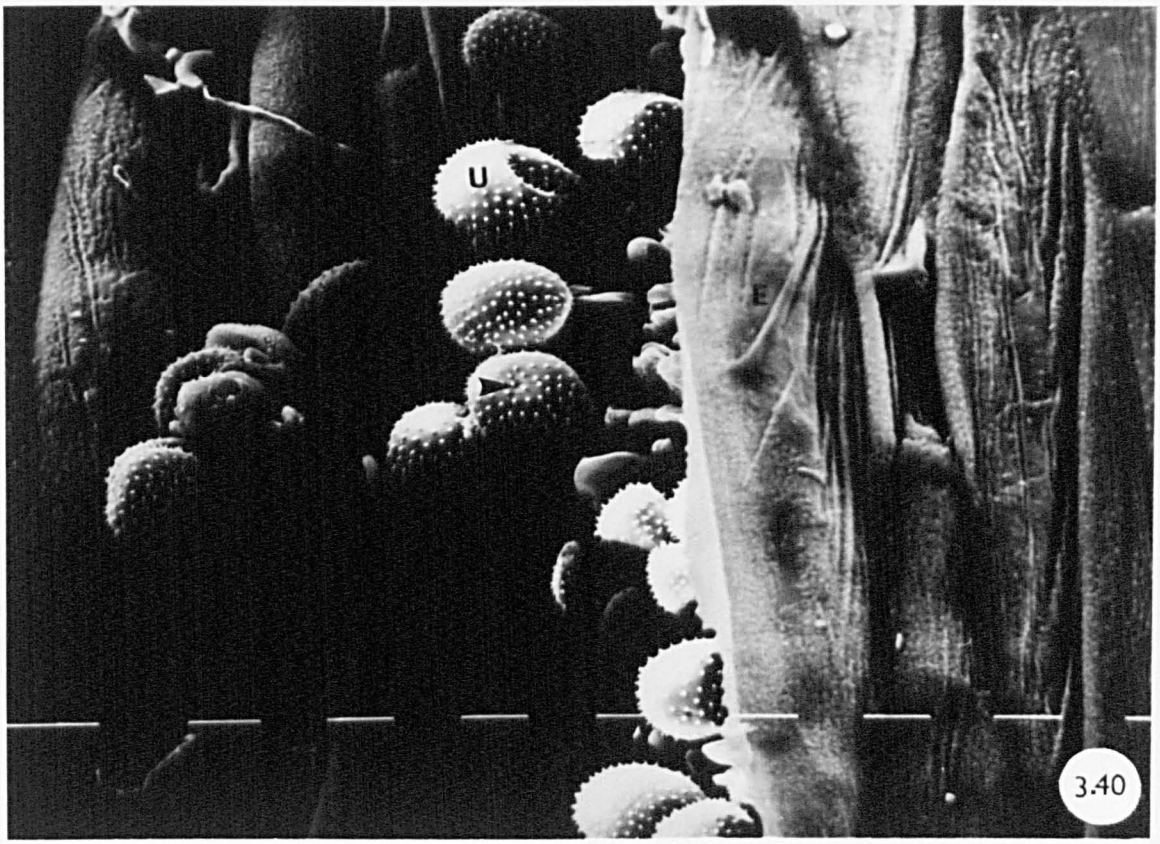

3.40

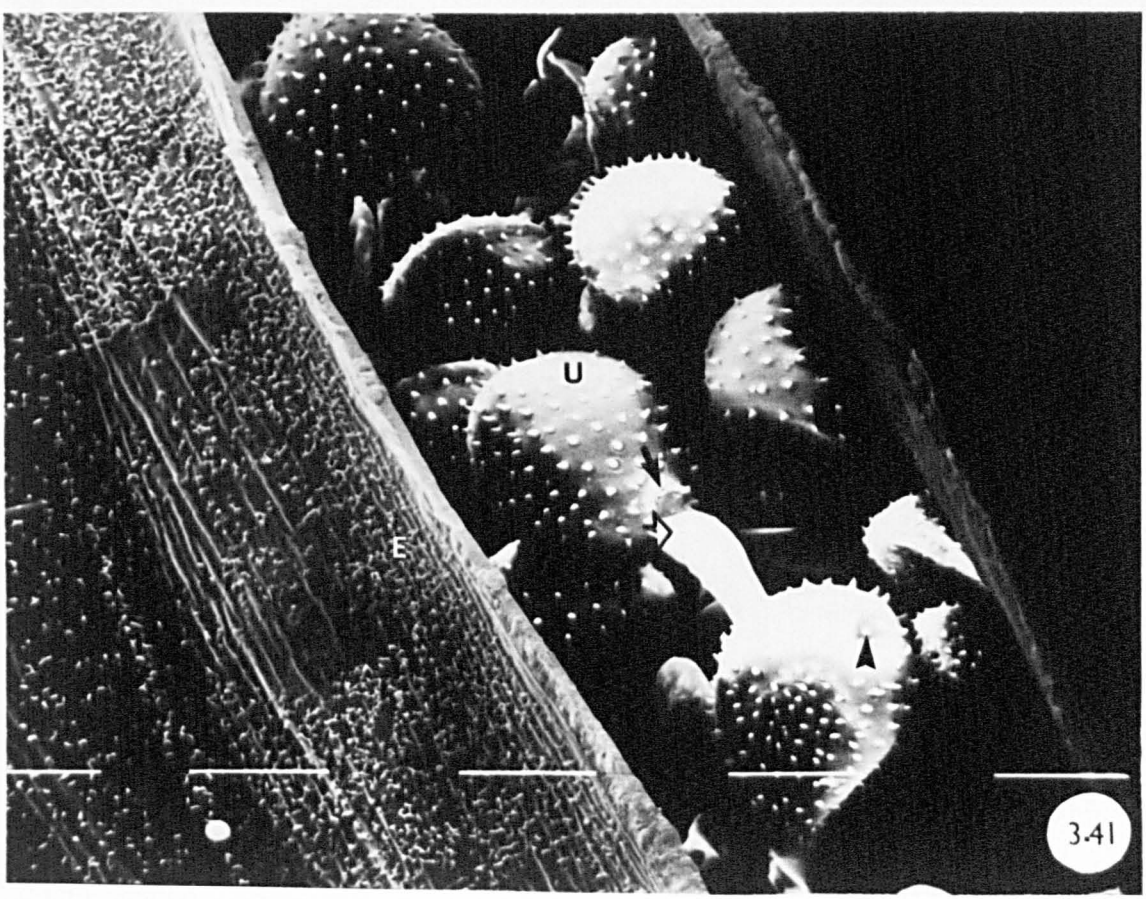

3.41

Figures 3.42-3.46

Urediospores of *P. poarum*. Scale line = 10 μm

Figure 3.42

Light micrograph of urediospore showing five germ pores.

Figure 3.43

Light micrograph of germinated urediospores.

a - Urediospore with one germ tube (arrow). Note large lipid drop in urediospore and dense cytoplasm in germ tubes.

b - Urediospore with two germ tubes (arrows). The proximal regions of the germ tubes become highly vacuolated. Note also large lipid drop in urediospore.

Figure 3.44

Light micrograph of urediospore with three germ tubes.

Figure 3.45

Mature urediospore with large lipid drop.

Figure 3.46

Section of uredium from resin-embedded tissue showing stalked urediospores, lipid droplets and germ pores (unlabelled arrows).

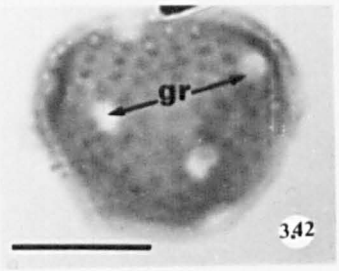

3.42

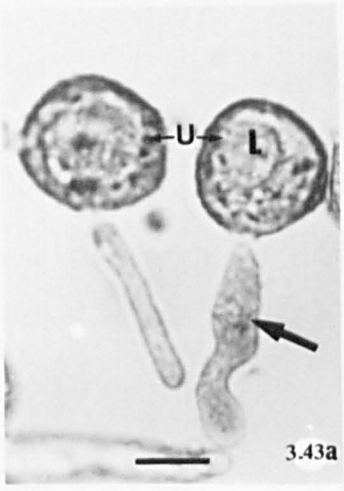

3.43a

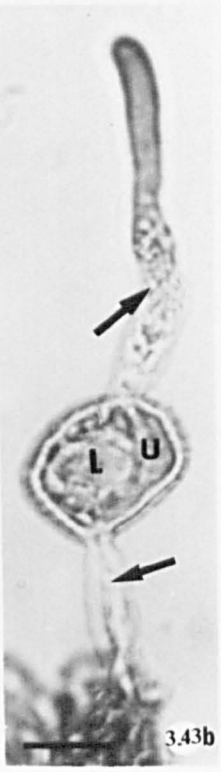

3.43b

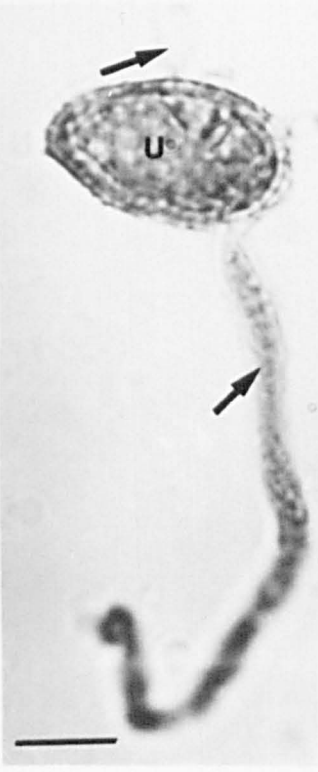

3.44

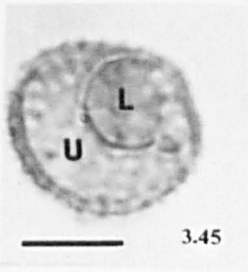

3.45

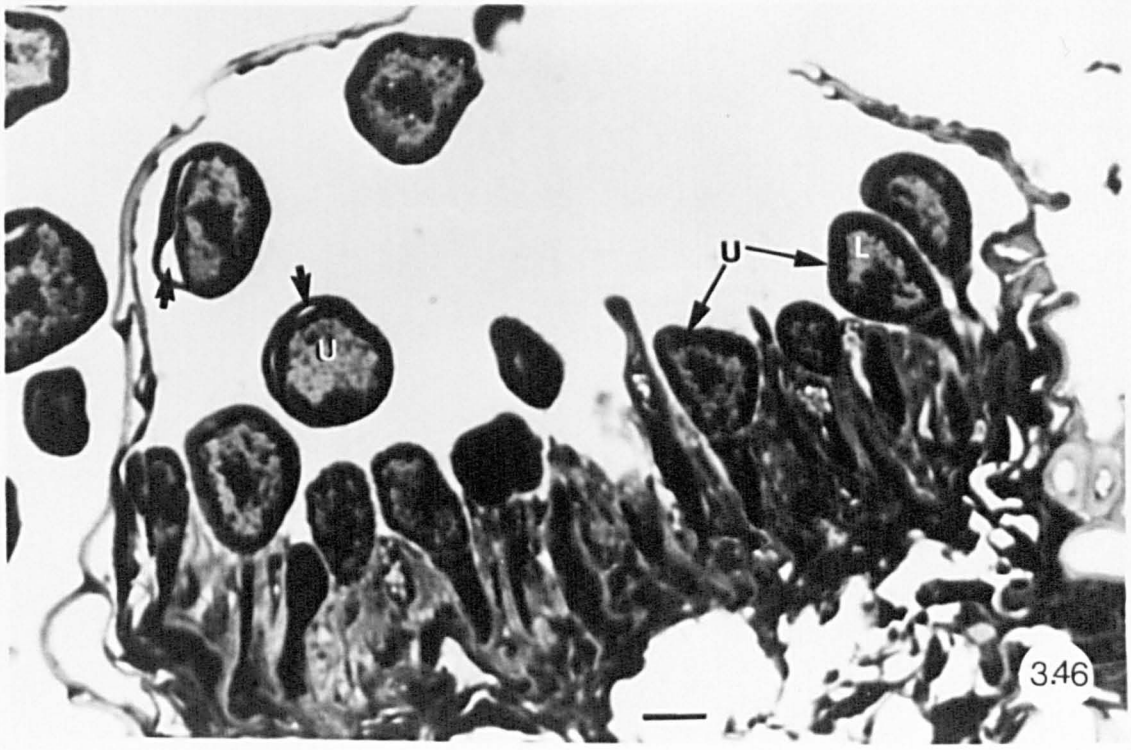

3.46

Figures 3.47-3.50

Uredia and urediospores of *P. poarum*. Scale line = 20 µm

Figure 3.47

Cryostat section, light micrograph of immature uredium. The host epidermis is still intact. Note fungal peridium (arrow), urediospores and lipid drops. Ornamentations can be seen on the surface of urediospores.

Figure 3.48

Light micrograph of mature uredium showing urediospores and colourless, capitate uredial paraphyses.

Figure 3.49

Light micrograph showing elongated, colourless, capitate uredial paraphyses adjacent to urediospore (from macerated tissue).

Figure 3.50

Light micrograph of semi-thin section showing urediospores and uredial paraphyses. Note lipid droplets (unlabelled arrow) in urediospore.

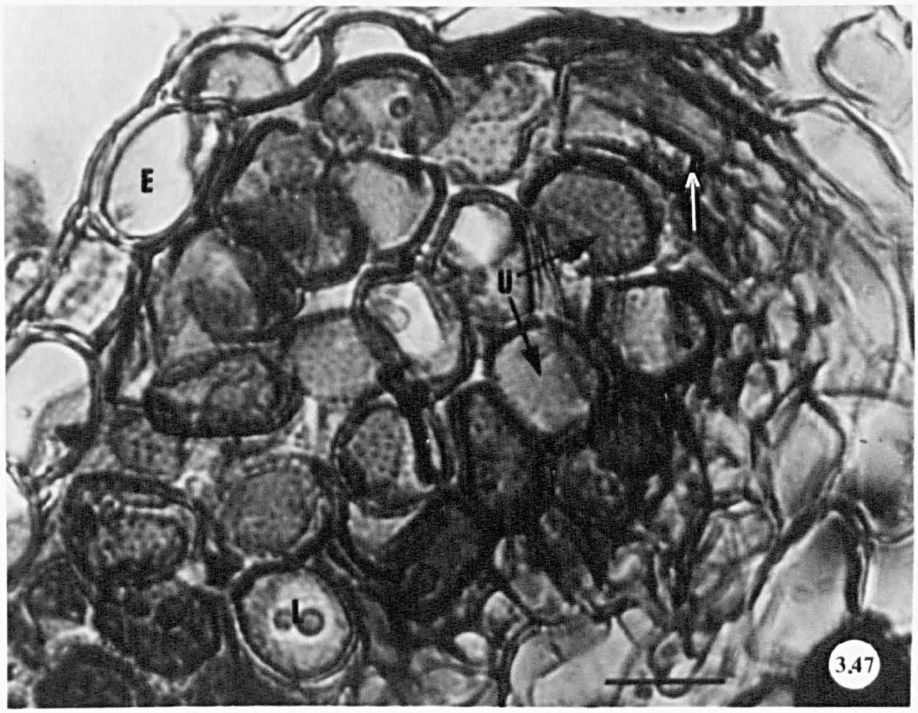
E
U
3.47

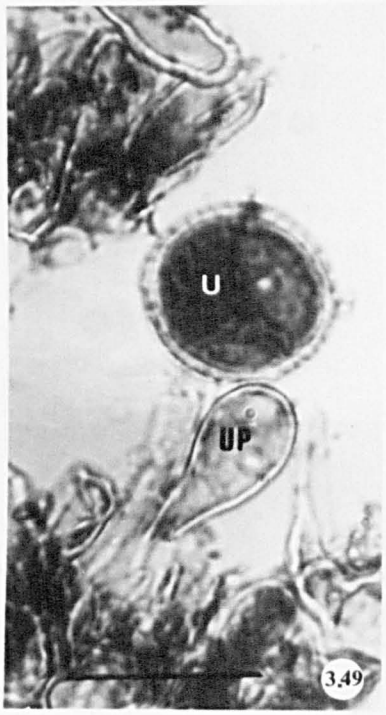
U
UP
3.49

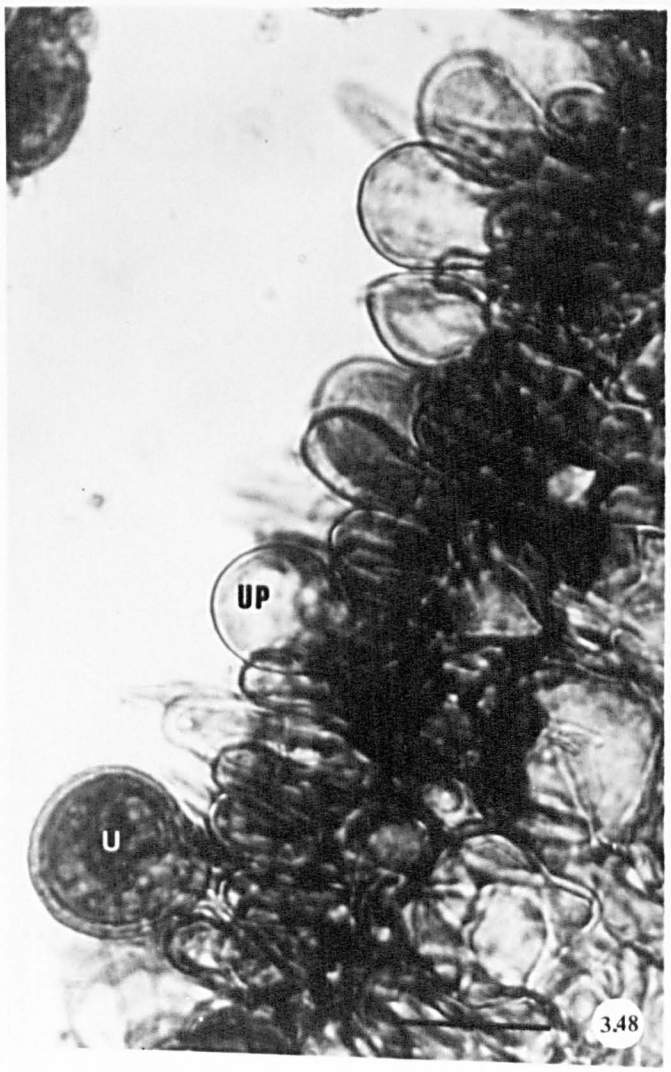
UP
U
3.48

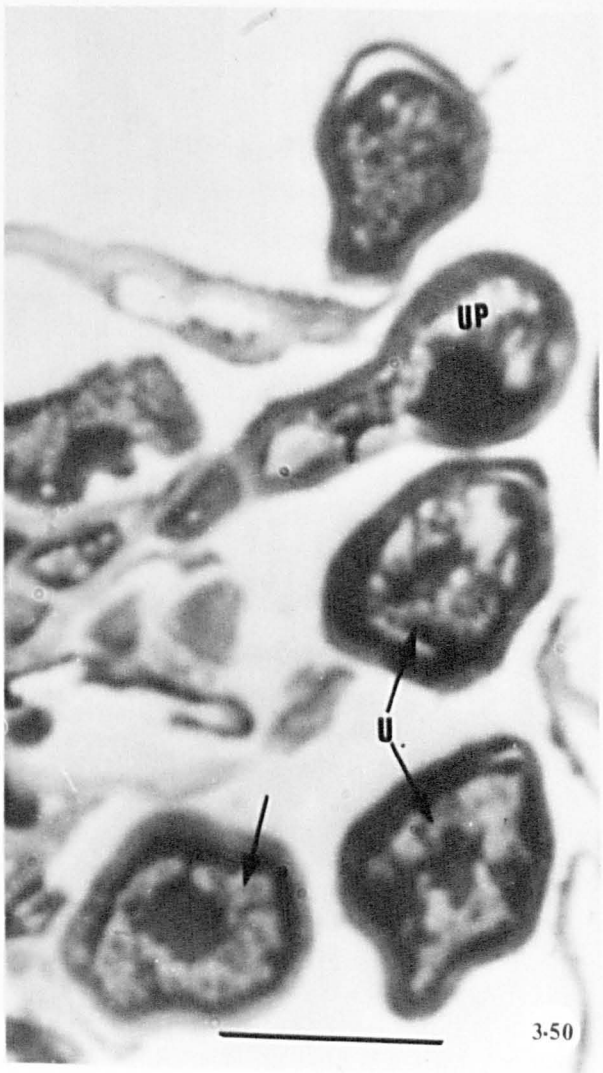
UP
U
3·50

Figures 3.51 and 3.52

Uredium of *P. poarum*. Scale lines = 10 µm

Figure 3.51

S.E.M. micrograph of mature uredium showing large urediospores with ornamented surface and smaller, capitate uredial paraphyses with smooth surface.

Figure 3.52

S.E.M. micrograph of mature uredium showing ornamented urediospores and smooth-surfaced paraphyses. Some paraphyses appear similar in size to urediospores. Note a scar on the base of urediospore (open arrow) corresponding exactly in appearance and size with the exposed ends of urediospore stalks which have lost their spores (arrowheads). Note also central pore in the base of urediospore (arrow).

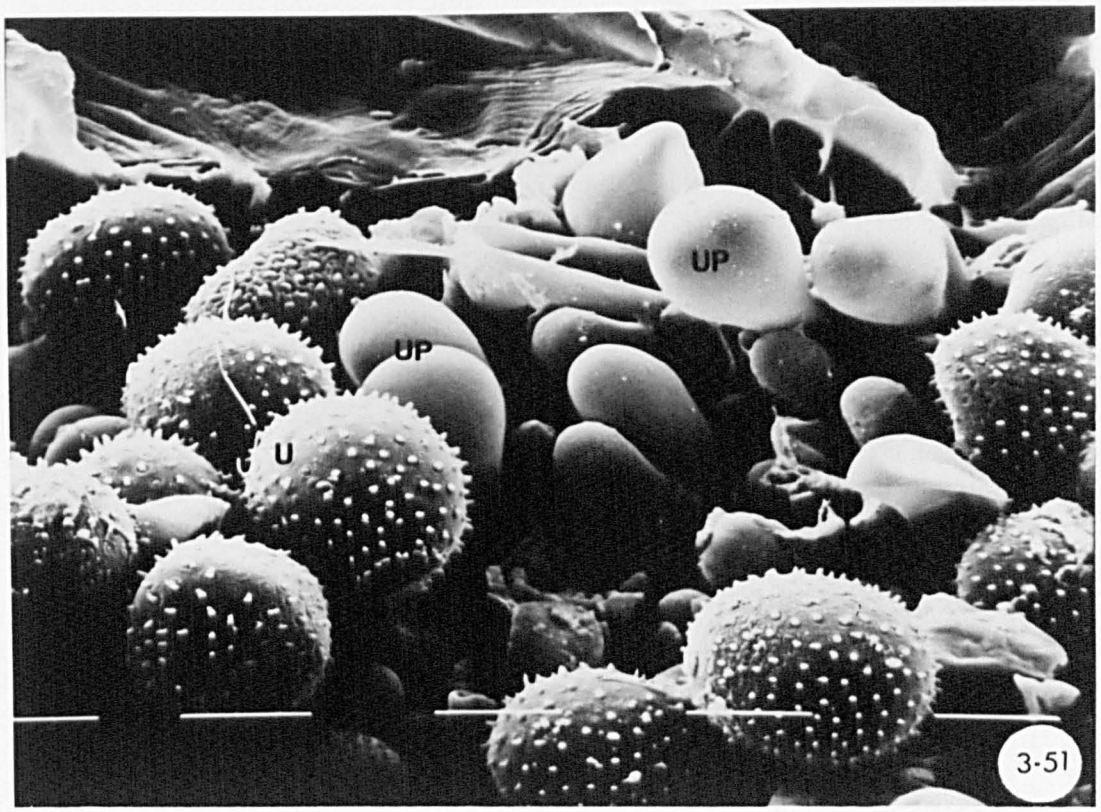
UP
UP
U
3-51

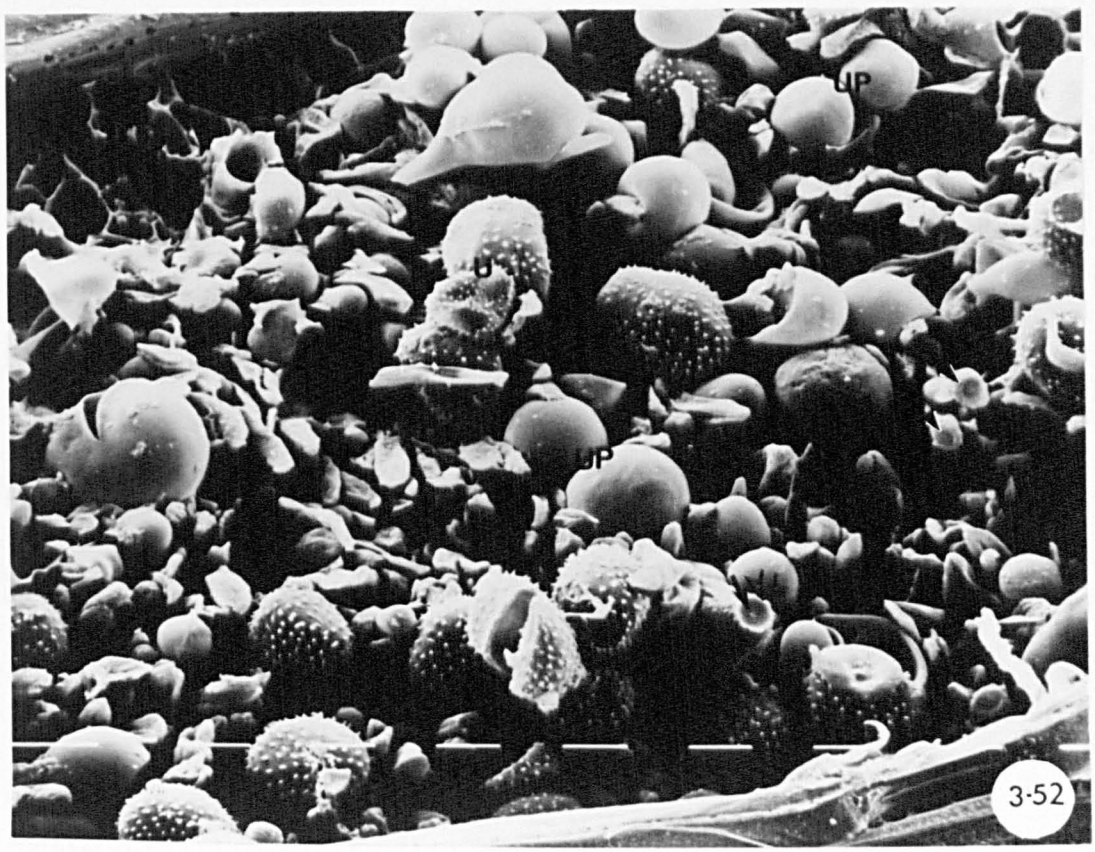
UP
U
UP
3-52

Figures 3.53-3.56

Urediospores and uredial paraphyses of *P. poarum*.

Scale lines in Figures 3.53 and 3.54 = 15 μm
Scale lines in Figures 3.55 and 3.56 = 10 μm

Figure 3.53

S.E.M. micrograph of small urediospores and larger uredial paraphyses. Note ornamentations on the surface of urediospores.

Figure 3.54

Light micrograph of urediospores and uredial paraphyses. Note difference in size of spores and paraphyses.

Figure 3.55

S.E.M. micrograph of urediospore showing spines (arrows), each situated in a circular depression encircled by an annulus (arrowheads). Note paraphyses.

Figure 3.56

S.E.M. micrograph of urediospores showing ornamentations in the form of spines (arrows). Each spine resides in a circular depression. Note annuli (arrowheads) and urediospore stalk.

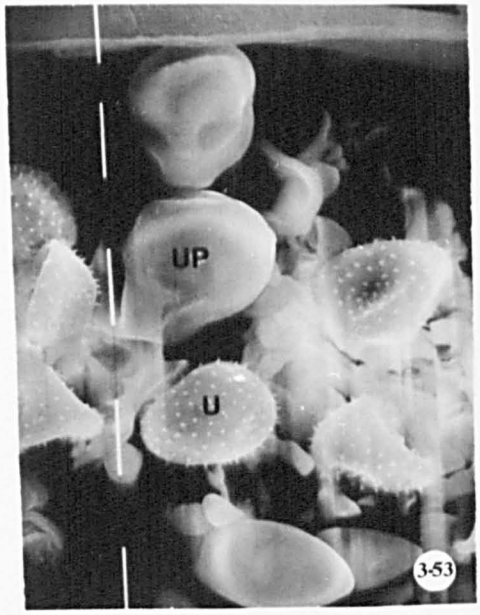
UP
U
3-53

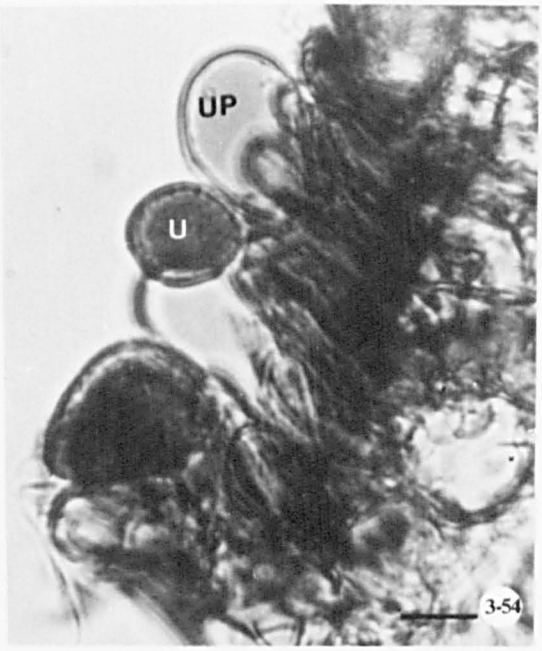
UP
U
3-54

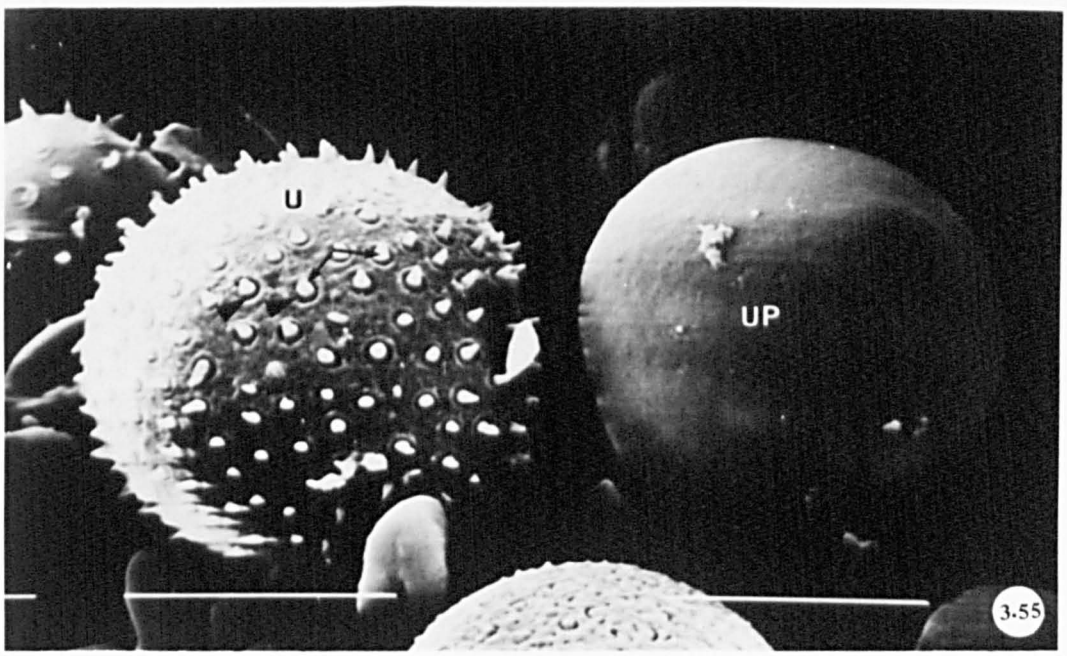
U
UP
3-55

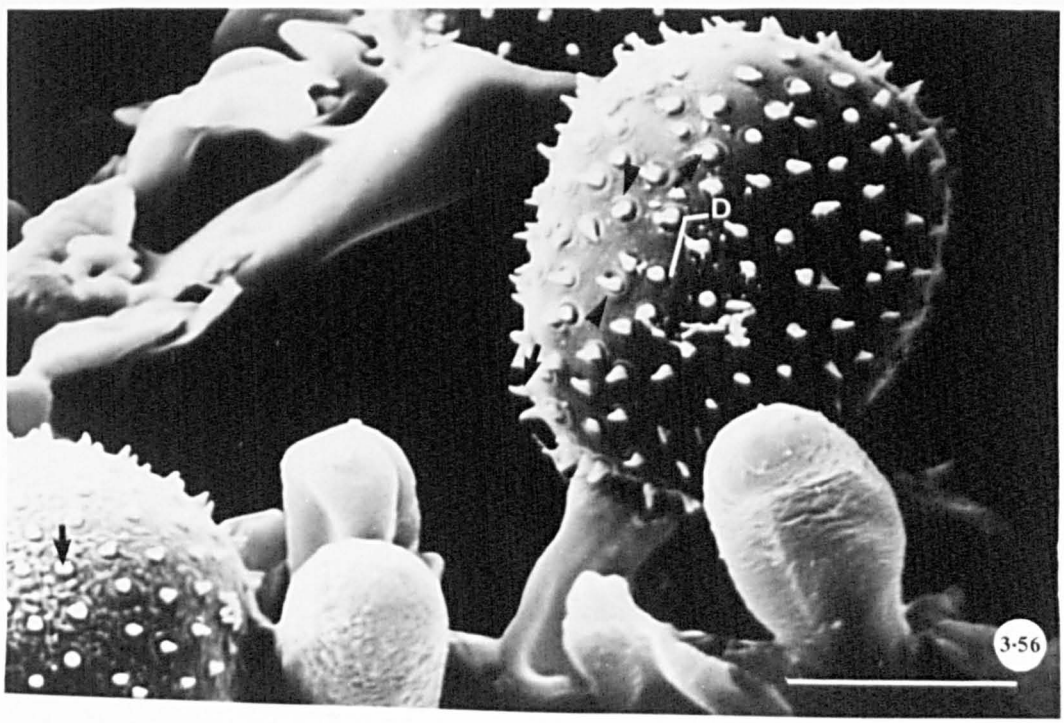
D
3-56

Figures 3.57 and 3.58

Uredium of *P. poarum*. Scale lines = 10 µm

Figure 3.57

Light micrograph of uredium showing teliospore and urediospore arising from the same sorus.

Figure 3.58

S.E.M. micrograph of uredium showing teliospore arising among urediospores.

3·57

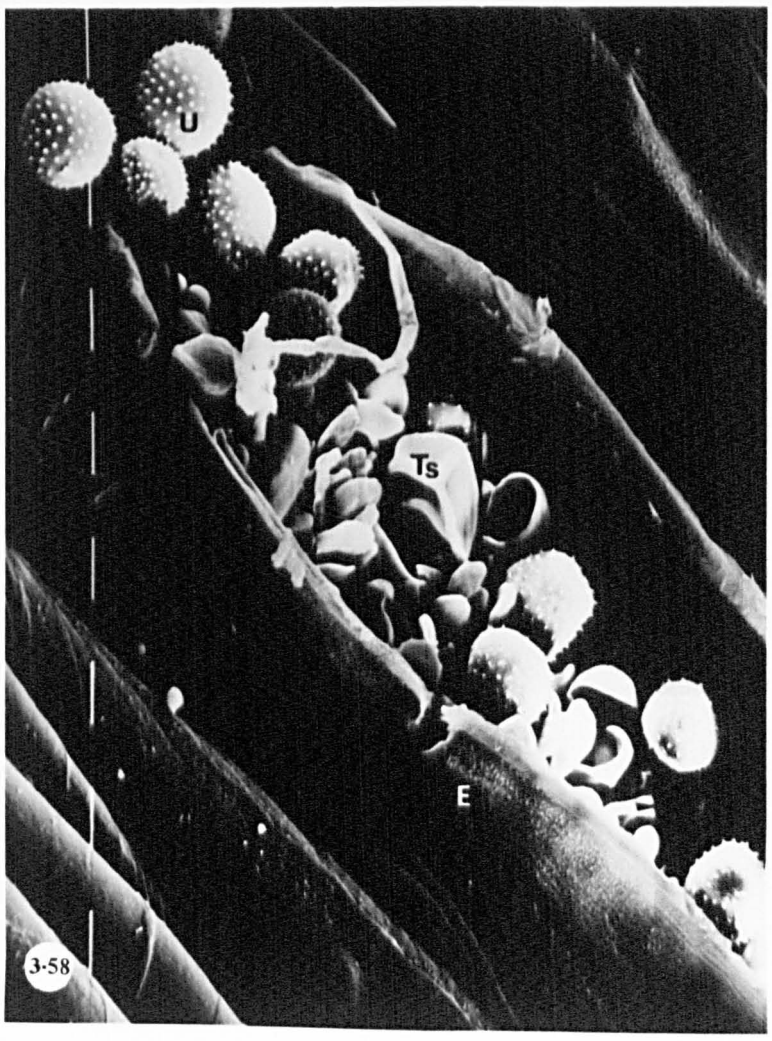

3·58

Figures 3.59 and 3.60

Uredium of *P. poarum*. Scale lines = 20 µm

Figure 3.59

Light micrograph of immature uredium showing urediospores and a layer of fungal cells (peridium) (arrows) covering the urediospores. Note intact host epidermis

Figure 3.60

Light micrograph of mature uredium showing urediospores (arrowheads) and fungal peridium (arrows). Note ruptured host epidermis.

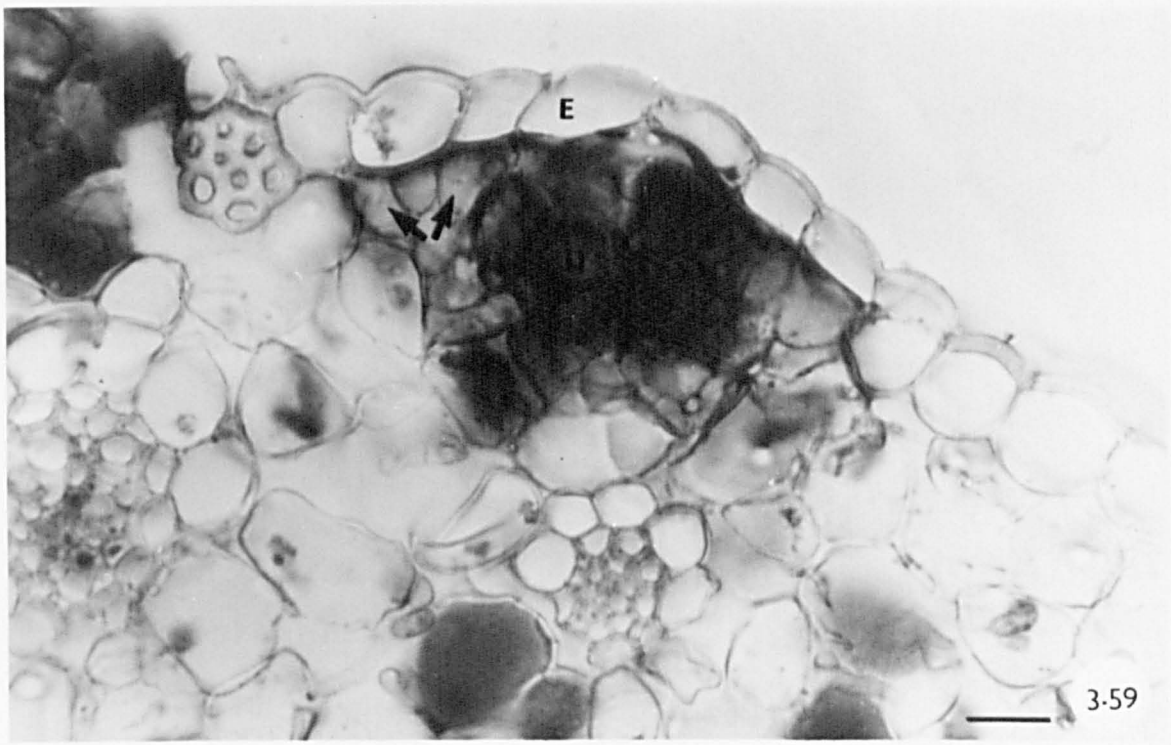

3·59

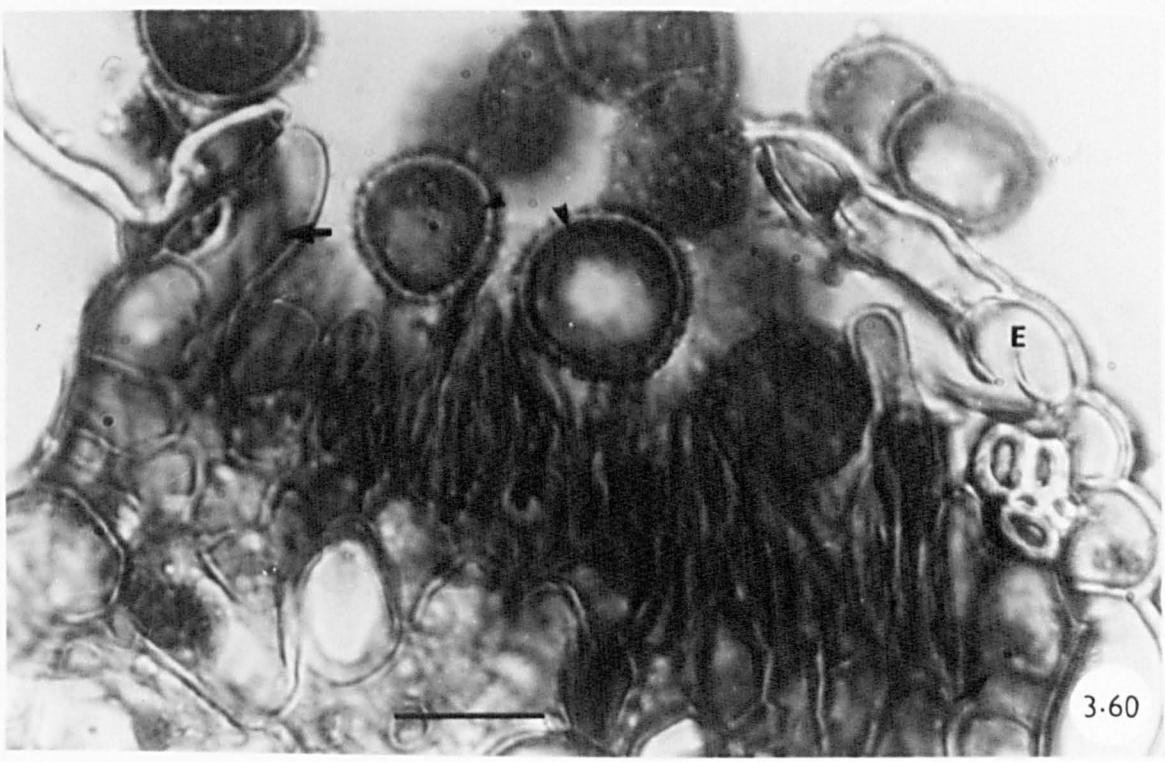

3·60

Figures 3.61 and 3.62

Uredial peridium of *P. poarum*. Scale lines = 20 µm

Figure 3.61

Surface view of infected *Poa* leaf showing urediospores covered by peridium. Note the outline of the walls (arrows) of the peridial cells.

Figure 3.62

Low-power light micrograph of infected *Poa* leaf after pressure has been applied to release the urediospores from the uredium. Note fungal peridium still intact covering the urediospores (arrows).

Figures 3.63 and 3.64

Telia of *P. poarum*. Scale lines = 20 µm

Figure 3.63

Light micrograph of telia on lower epidermis of *Poa* leaf. Note intact host epidermis, two-celled teliospores, and telial paraphyses.

Figure 3.64

S.E.M. micrograph of telia covered by host epidermis. Note fungal intercellular hyphae (arrows) and telial paraphyses (arrowhead).

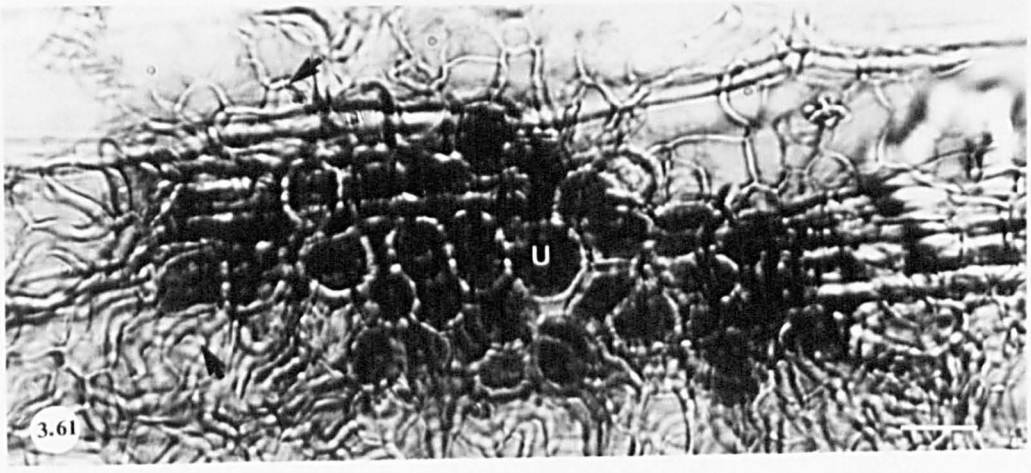

3.61

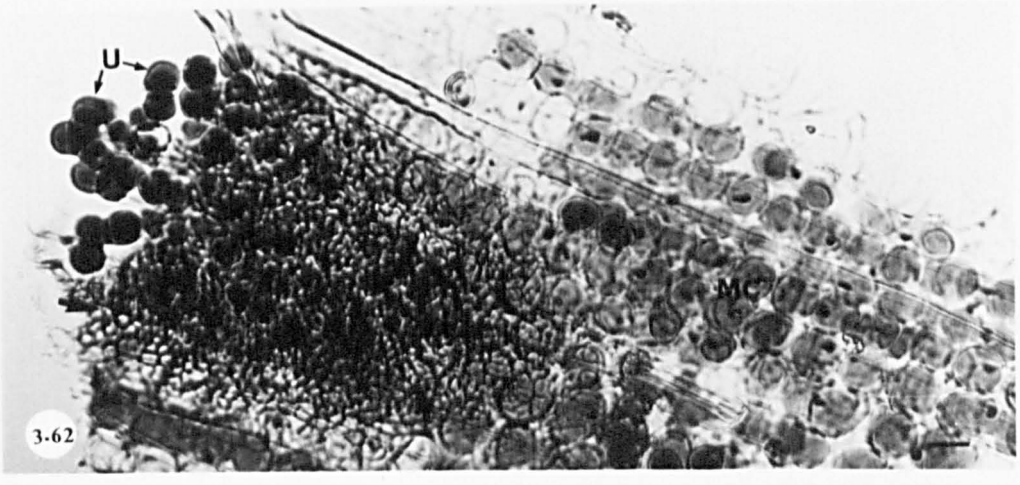

3.62

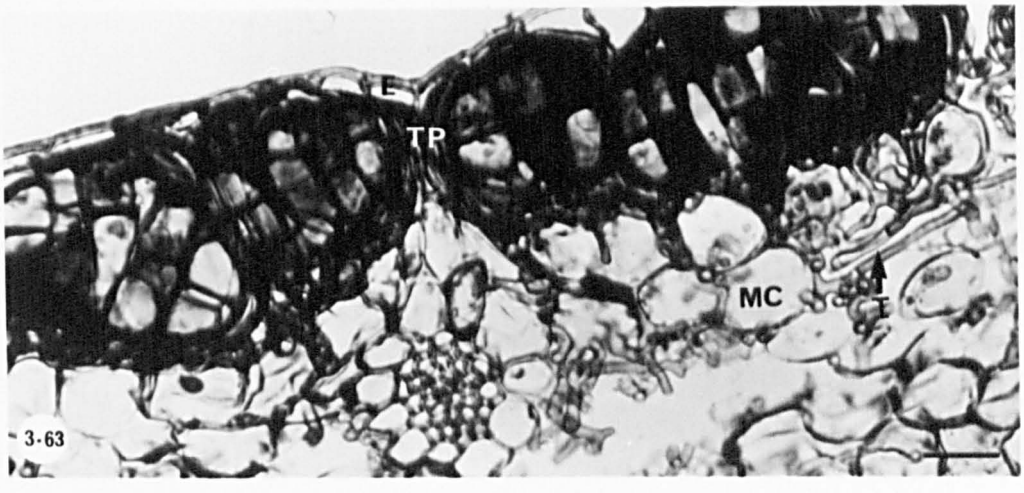

3.63

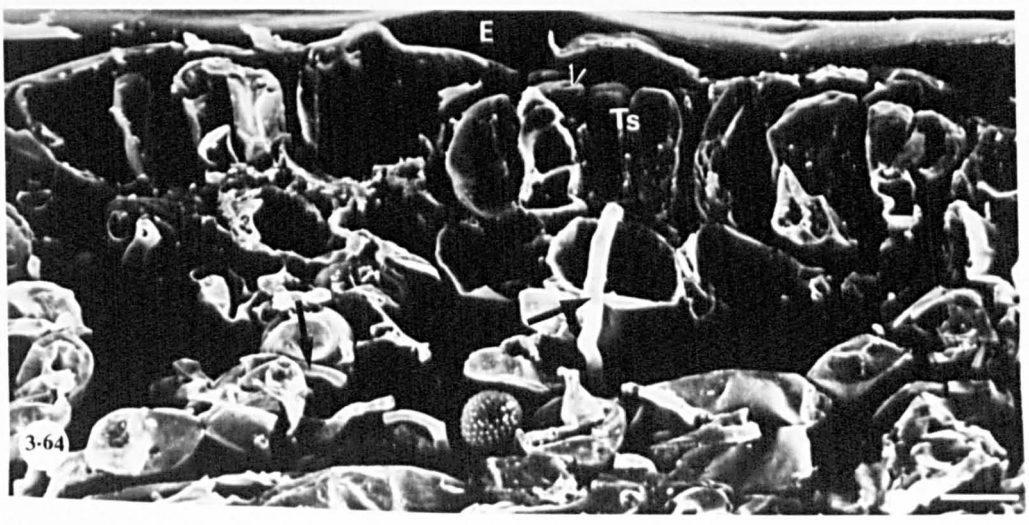

3.64

Figure 3.65

T.E.M. micrograph of teliospore of *P. poarum*. The spore is separated from its pedicel by a septum. Note the dikaryotic sporogenous tissue and lipid drops.
x10000

Figures 3.66 and 3.67

Teliospores of *P. poarum*. Scale lines = 15 μm

Figure 3.66

Light micrograph of two-celled, elongated, oblong-clavate or obovoid teliospores. Note the rounded or truncate apices of the spores and pedicels (arrow).

Figure 3.67

Light micrograph of teliospore showing septum separating the two cells of the spore. Note the continuity of material between these cells through a septal pore (arrow). Note also lipid drop.

3.65

3.66

3.67

Figures 3.68 and 3.69a

Telial paraphyses of *P. poarum*. Scale lines = 10 µm

Figure 3.68

S.E.M. micrograph of telium showing elongated capitate telial paraphyses and teliospores with shallow rugulose ornamentations.

Figure 3.69a

Light micrograph of telial paraphyses enclosing groups of teliospores. Note host epidermis.

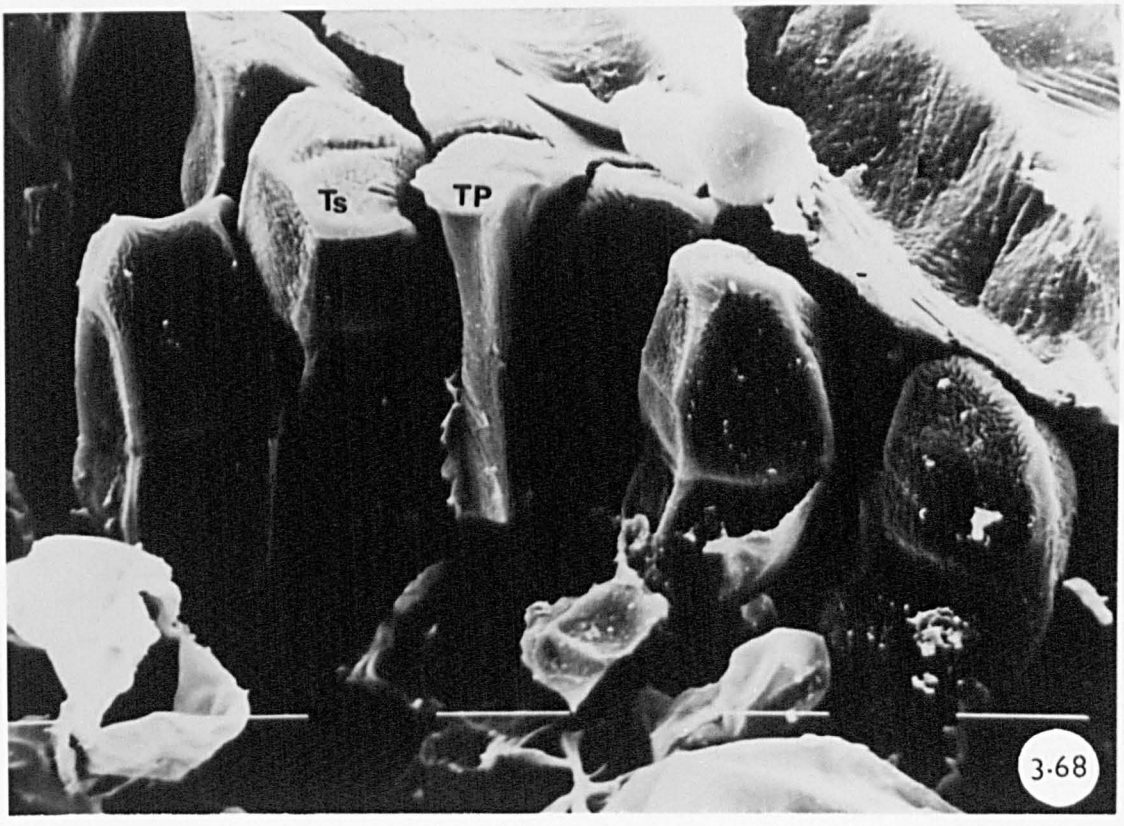
Ts
TP
3·68

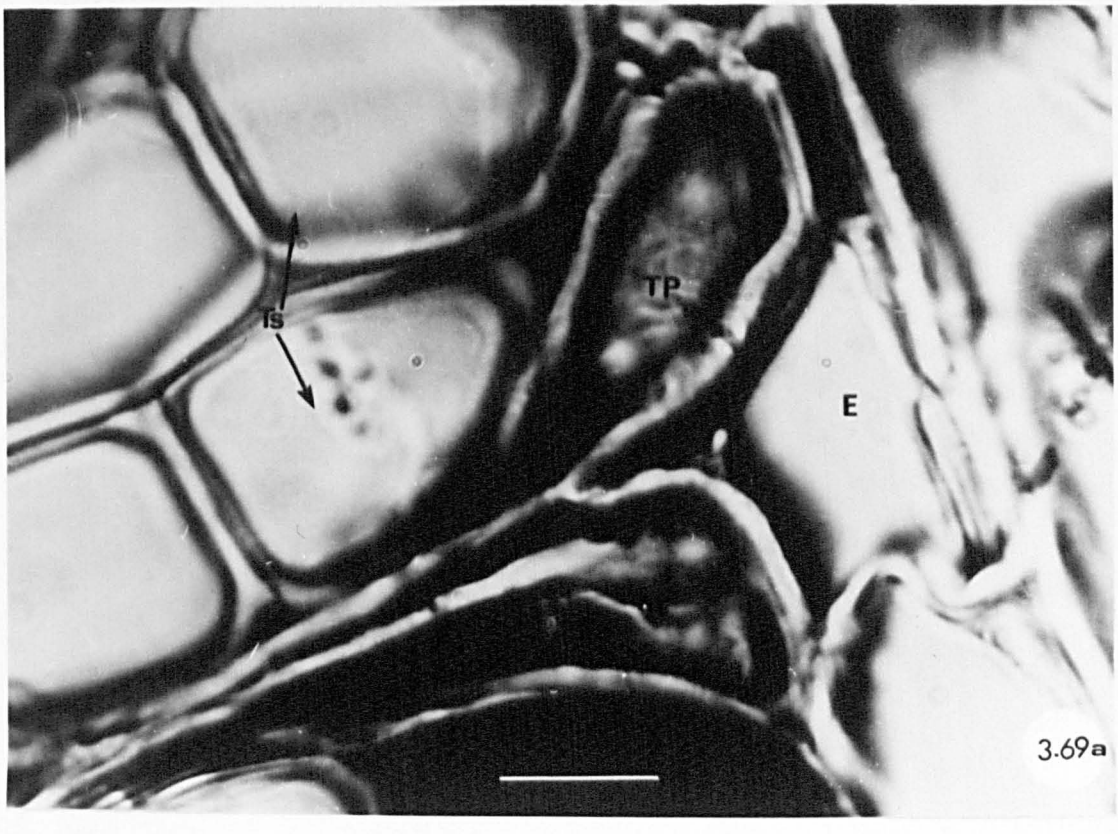
Ts
TP
E
3·69a

Figure 3.69b

Light micrograph of telial paraphyses, between two groups of teliospores. Note intact host epidermis and fungal intercellular hyphae.

Scale line = 15 µm

Figure 3.70

S.E.M. micrograph of a smooth, ovate to pyriform basidiospore of *P. poarum*. Note the spore is attached to a conical apiculus.

Scale line = 4 µm

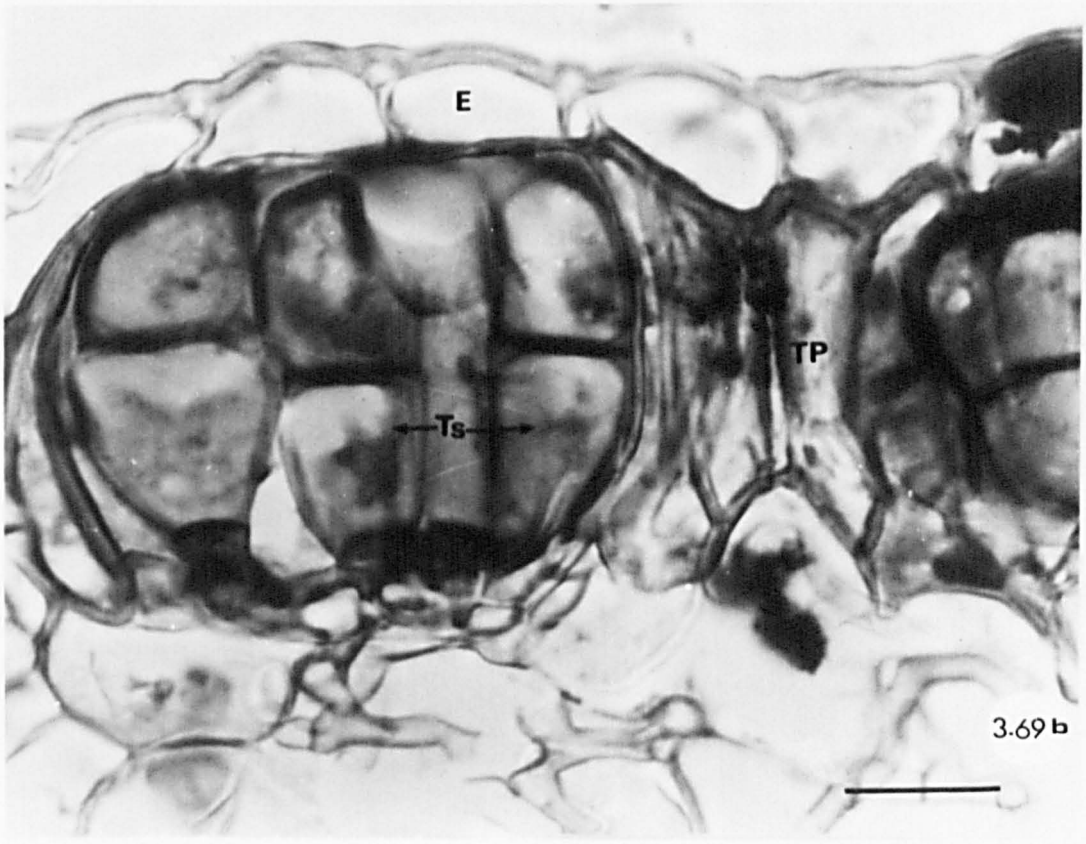
E
TP
Ts
3.69b

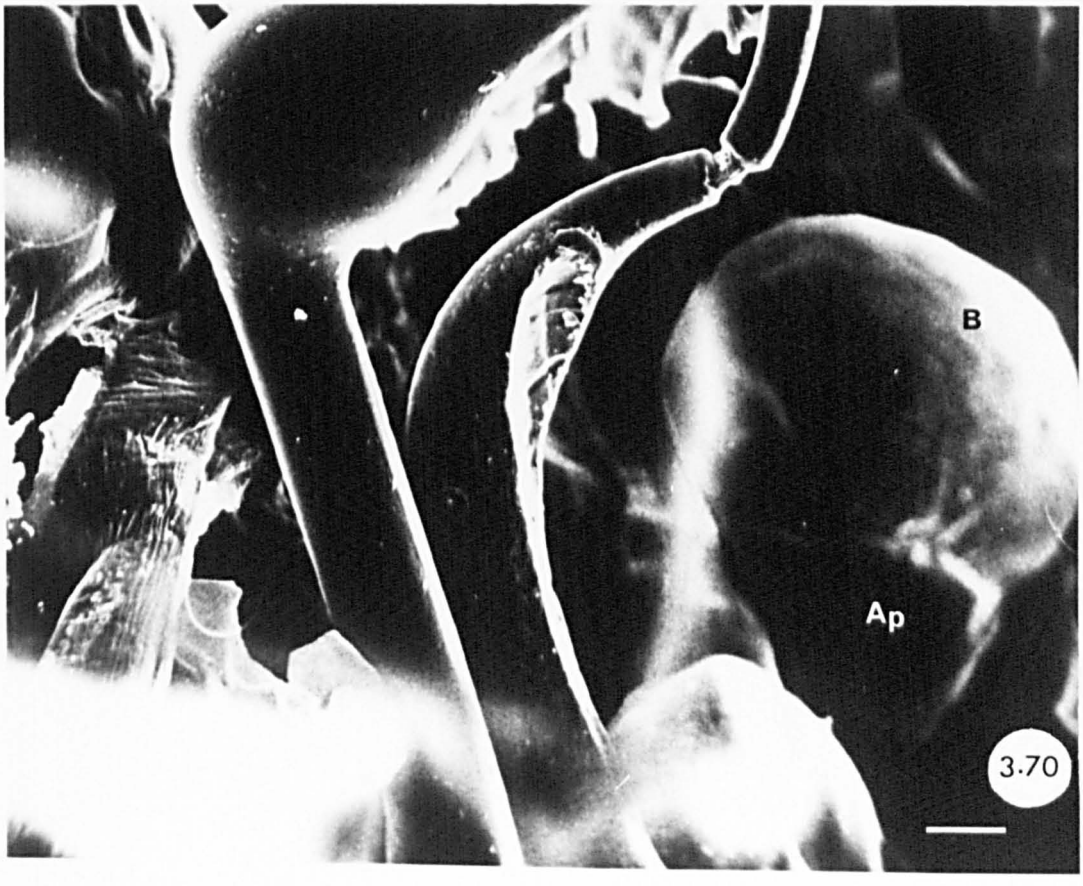
B
Ap
3.70

Figures 4.1-4.3

P. poarum infection on *T. farfara* leaf. Scale lines = 15 μm

Figure 4.1

Tangential section of upper mesophyll of *Tussilago* leaf through margin of pycnial colony, showing intercellular (arrows) and intracellular (arrowheads) hyphae, mesophyll cells and upper epidermis.

Figure 4.2

Intercellular hyphae bearing type X intracellular hypha, near margin of monokaryotic colony. Note constricted region at point of entry into upper mesophyll cell (arrow). Note also intercellular hyphae.

Figure 4.3

Type Y intracellular hypha near centre of pycnial region, showing no constriction at point of entry. Note lipid drops (arrows) and intercellular hyphae.

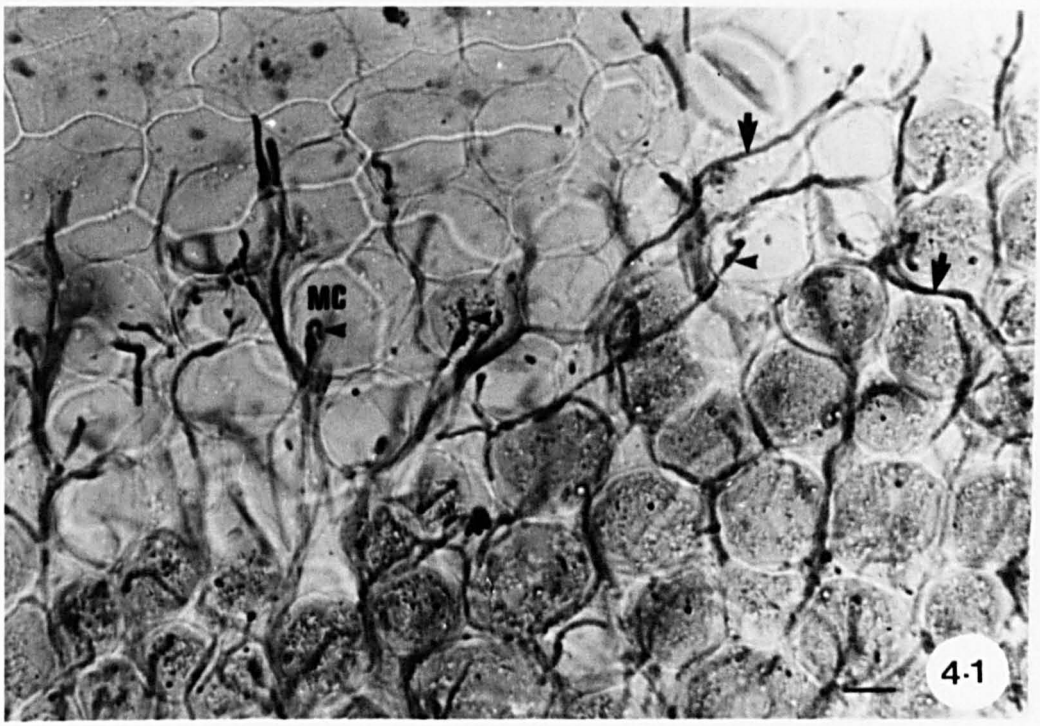
MC
4·1

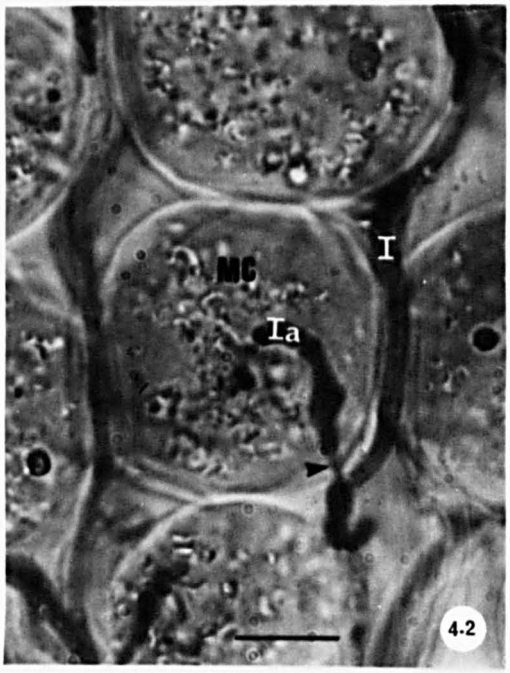
MC
I
Ia
4·2

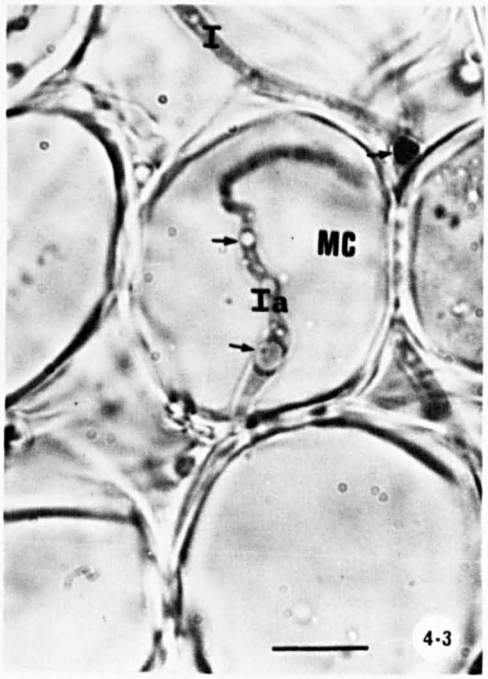
I
MC
Ia
4·3

Figures 4.4-4.6

P. poarum infection in tangential section of *T. farfara* leaf.

Scale lines = 15 µm

Figure 4.4

L.S. *Tussilago* leaf (from epon-embedded material) tangential to minor vein showing septate intracellular hyphae. Septum (arrow) is located away from the site of penetration. Note intercellular hyphae.

Figure 4.5

Intracellular hyphae in mesophyll cells. Note lipid drops in intracellular hyphae (arrowheads) and in host cells.

Figure 4.6

Intracellular hyphae (arrows) in cells of upper epidermis.

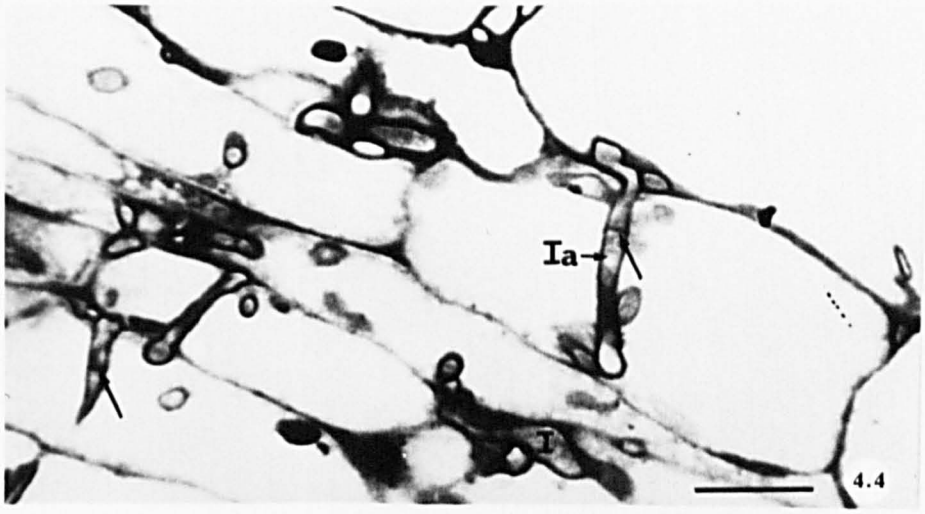

4.4

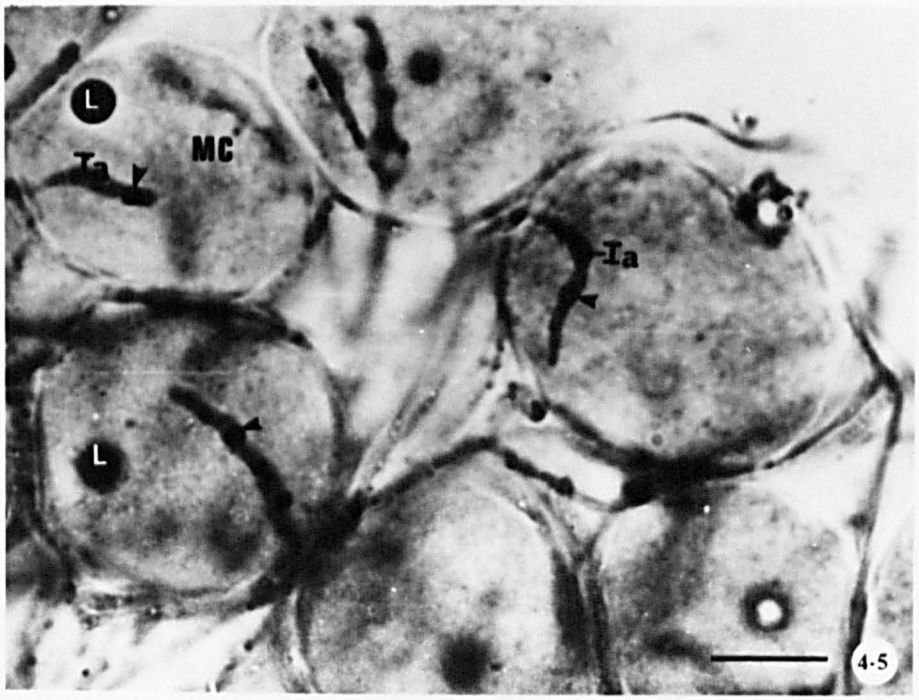

4·5

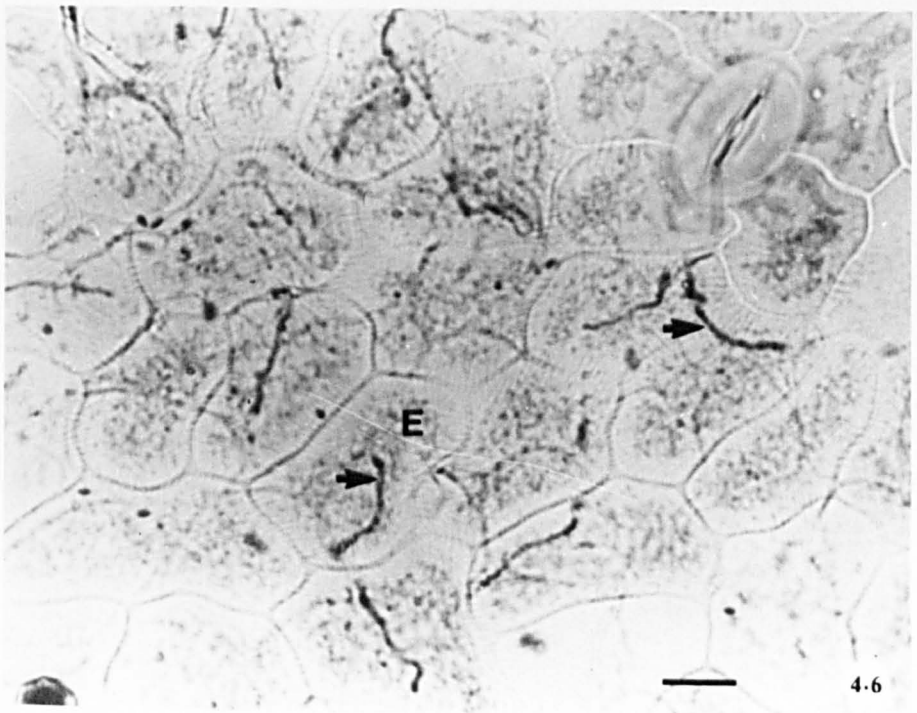

4·6

Figure 4.7

P. poarum infection on *T. farfara* leaf. Scale lines = 15 μm

a - Mesophyll cell penetrated by two intracellular hyphae. Note intercellular hyphae.

b - Mesophyll cell penetrated by several hyphae. Darkly-stained lipid drops are present in host cells. Note intercellular hyphae.

Figure 4.8

P. poarum infection on *Poa pratensis* leaf. Note dense growth of brown-pigmented hyphae in intercellular space of mesophyll.

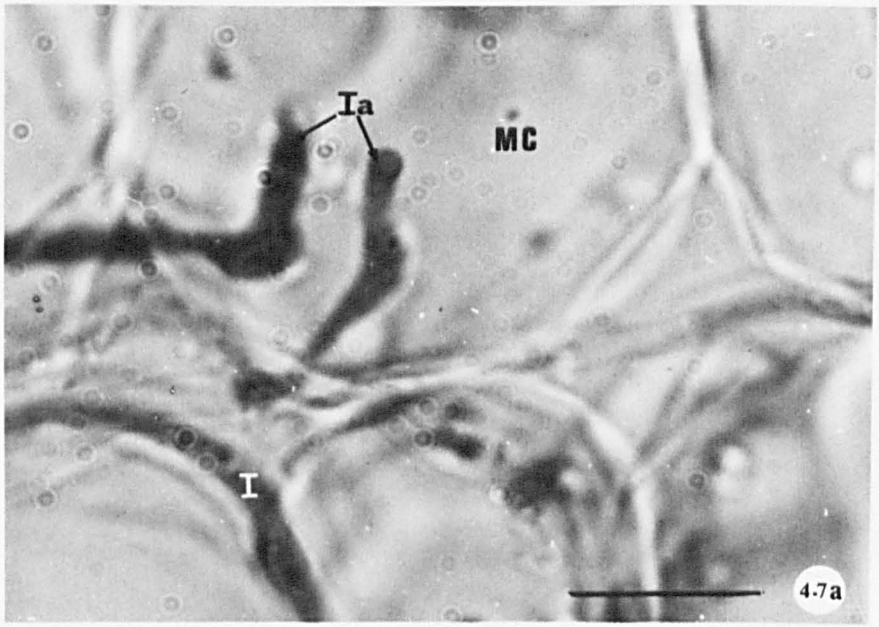

4·7a

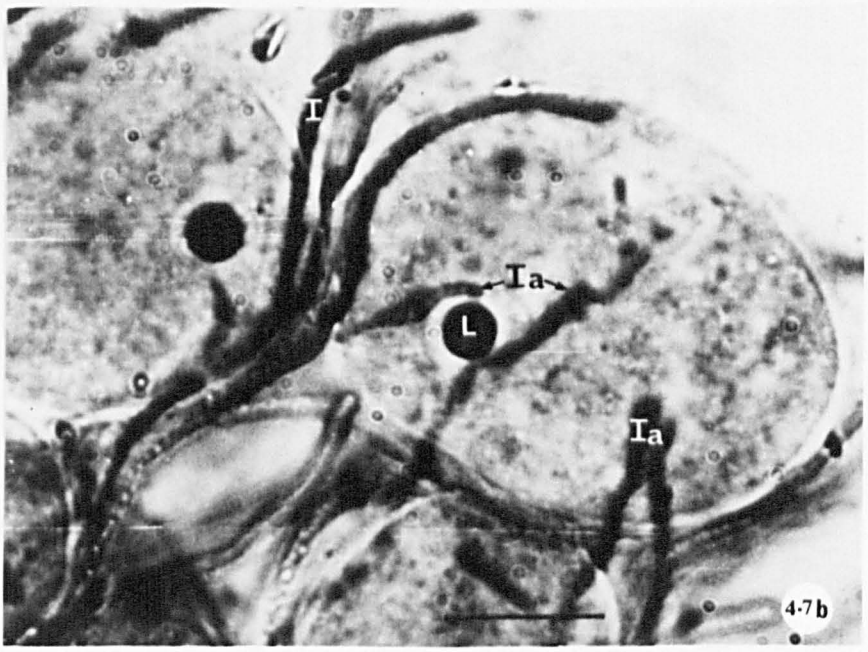

4·7b

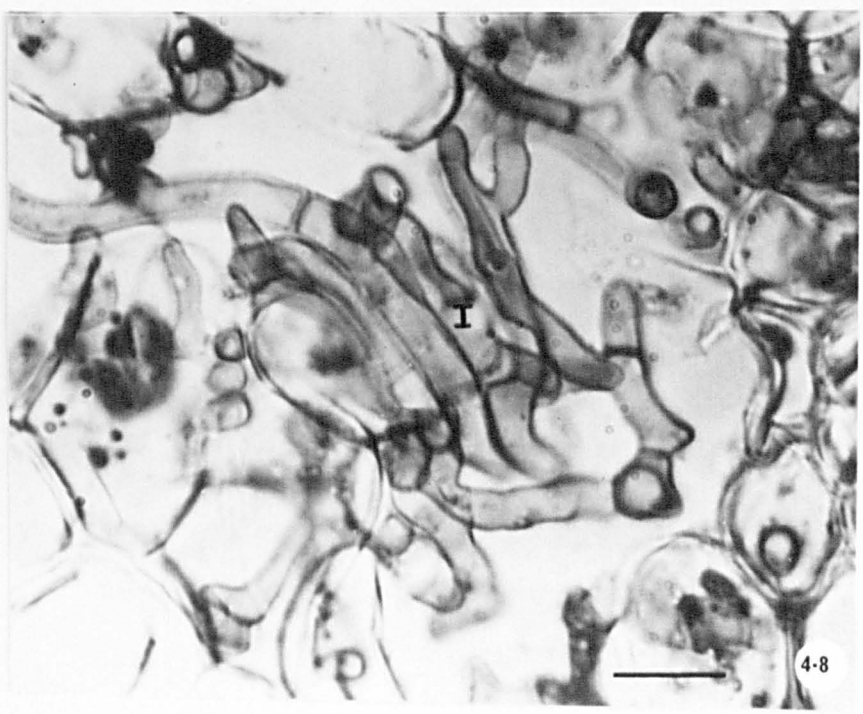

4·8

Figures 4.9-4.11

P. poarum infection of *P. pratensis* leaf. Scale lines = 10 μm

Figure 4.9

Haustoria in mesophyll cell. Note the matrix region around haustorium and haustorial neck (arrow).

Figure 4.10

Haustorium-mother cell from which haustorium has entered host mesophyll cell. Note the haustorial neck (arrowhead) and septum (arrow) between haustorium-mother cell and intercellular hypha. Note also haustoria in the adjacent mesophyll cell.

Figure 4.11

Epidermal cell of *Poa*, penetrated by several haustoria.

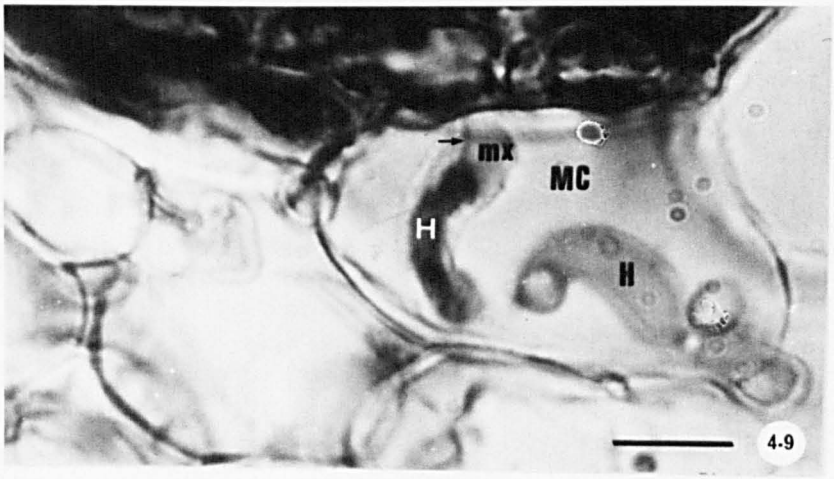

4-9

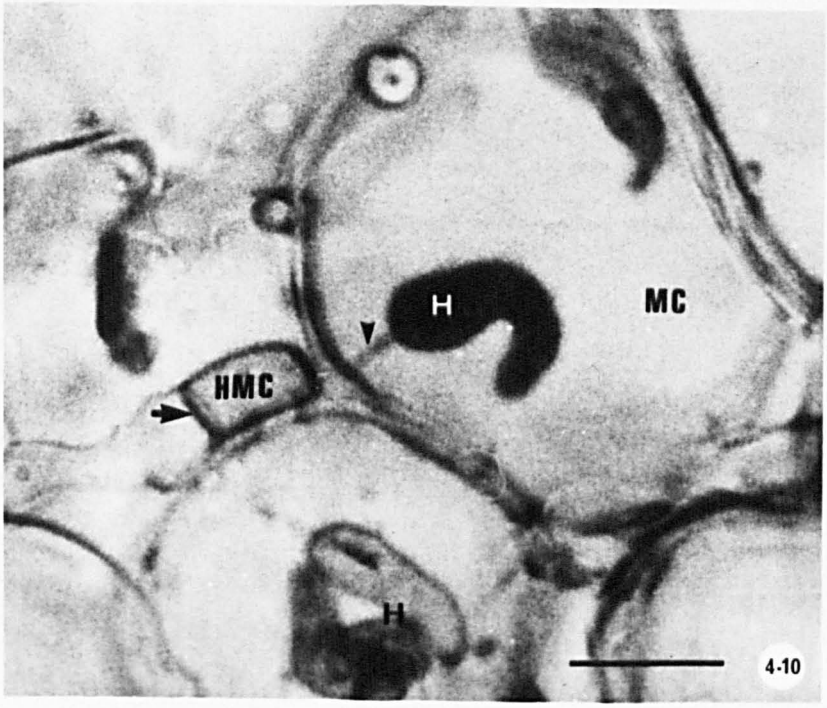

4-10

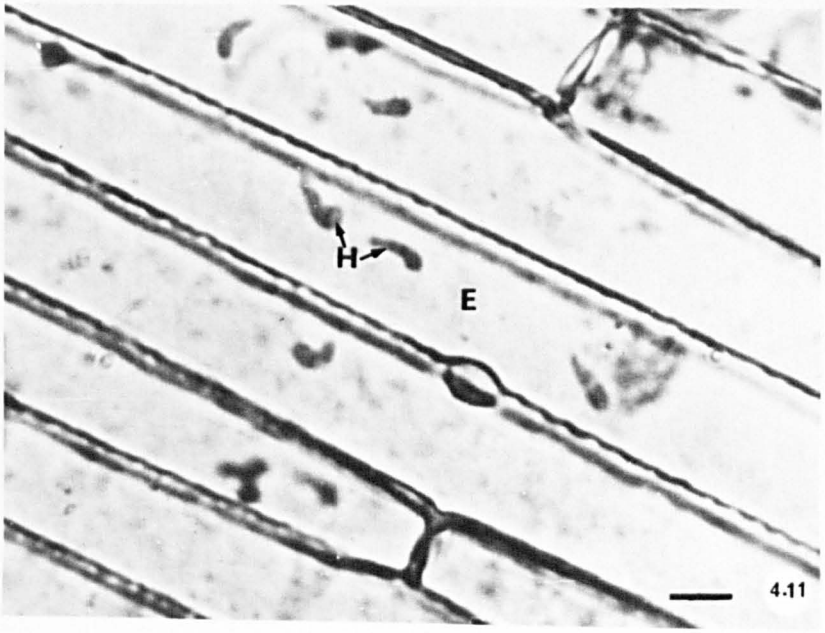

4-11

Figures 4.12-4.15

P. poarum infection on *P. pratensis* leaf. Scale lines = 10 μm

Figure 4.12

Haustorium in epidermal cell showing constricted neck (arrow).

Figure 4.13

Mesophyll cell containing two haustoria, in one of which the fungal nucleus is visible.

Figure 4.14

Mesophyll cell pentrated by several haustoria. Note matrix (arrow) around haustorium in the lower cell.

Figure 4.15a,b and c

Principal forms of haustorium:

a - rod-shaped
b - L-shaped with haustorium-mother cell
c - C-shaped. Note host chloroplasts

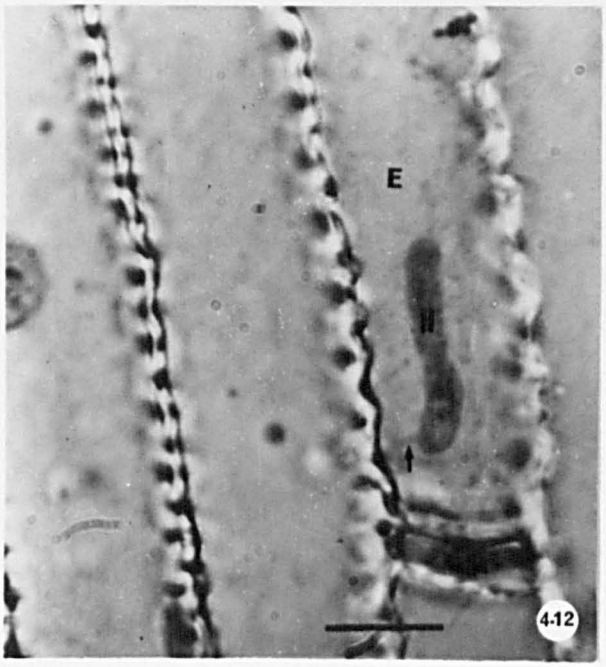

4.12

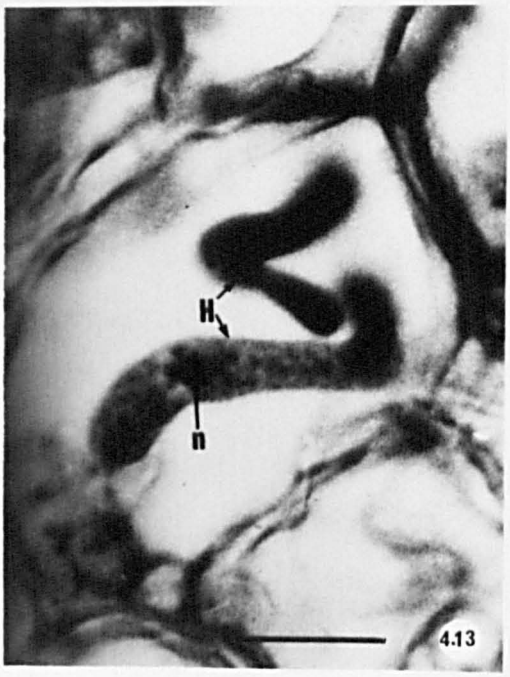

4.13

4.14

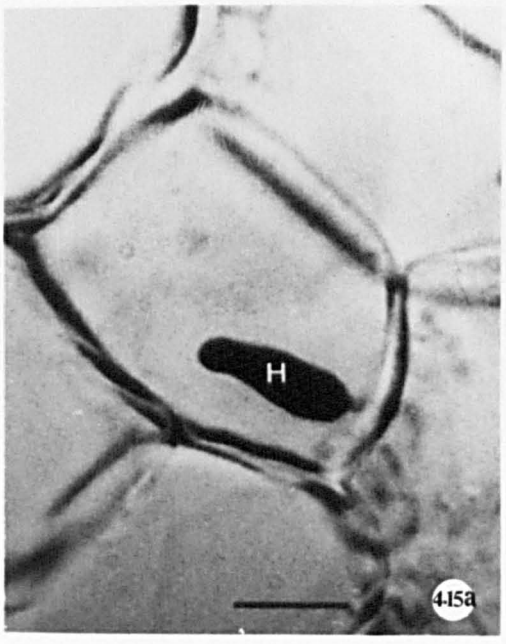

4.15a

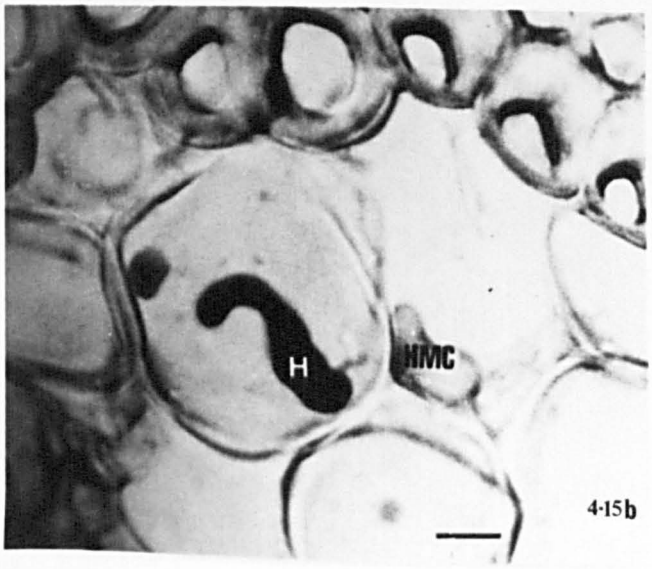

4.15b

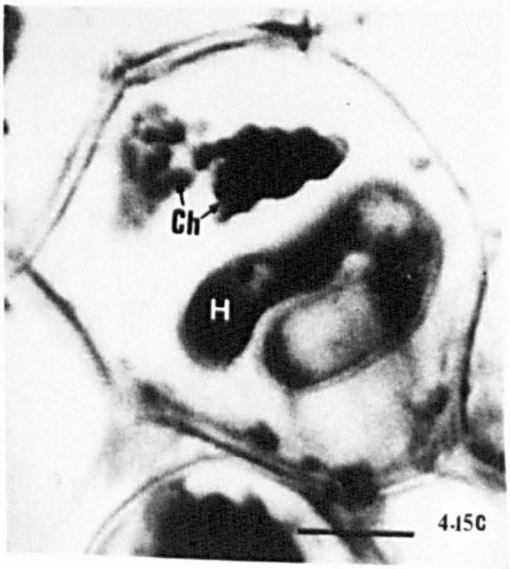

4.15c

Note: Figures 5.1, 5.24, 5.25, 5.28b, 5.3, 5.31 and 5.5 show scanning electron micrographs and all other plates transmission electron micrographs of *Puccinia poarum* in host tissue.

Figure 5.1

Monokaryotic thallus in mesophyll tissue of *Tussilago*.
x640

Figure 5.2

Monokaryotic hyphae in mesophyll of *Tussilago* growing in intercellular space and middle lamella region as well as parietally (arrowhead) inside the host cell, encased in wall material. Note host chloroplasts (arrows) and intracellular hypha.
x3750

Figure 5.3

Dikaryotic thallus in mesophyll of *Poa*.
x640

Figure 5.4

Dikaryotic hyphae growing in intercellular space of *Poa* mesophyll tissue. There is little adhesive material deposited between the fungal and host walls and hyphae are less closely attached to the host wall than those of the monokaryon. Note the lipid drops and septum. Host chloroplast (arrow) is also seen.
x4500

Figure 5.5

Dikaryotic hyphae growing between mesophyll cells of *Poa*. No close contact is seen between fungal hyphae and host cells.
x1280

Figure 5.6

Adhesive material deposited between fungal and host walls in *Tussilago*.
x30000


I
5.1

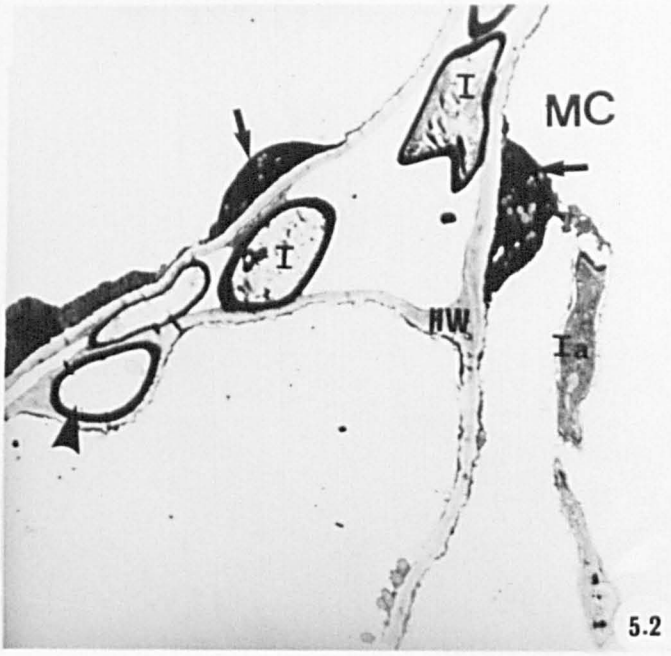
I
MC
I
HW
Ia
5.2

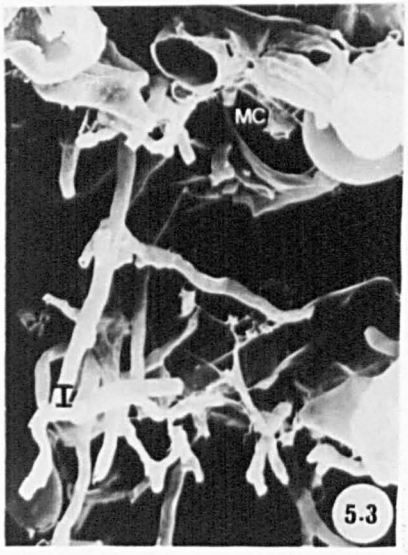
MC
I
5.3

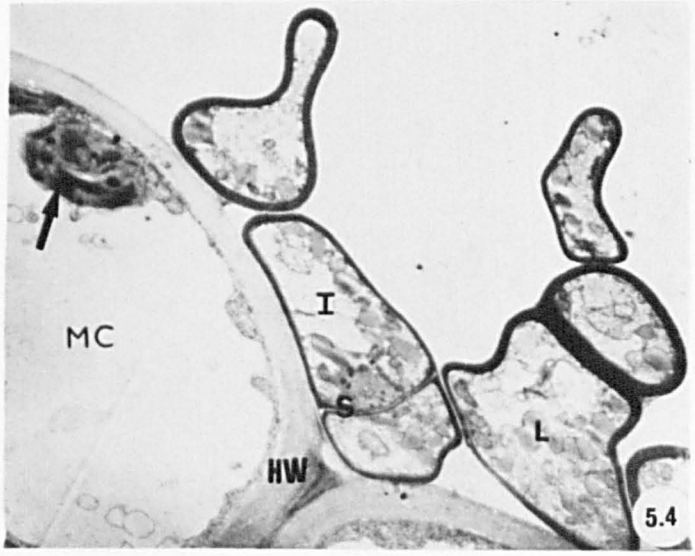
MC
I
S
L
HW
5.4

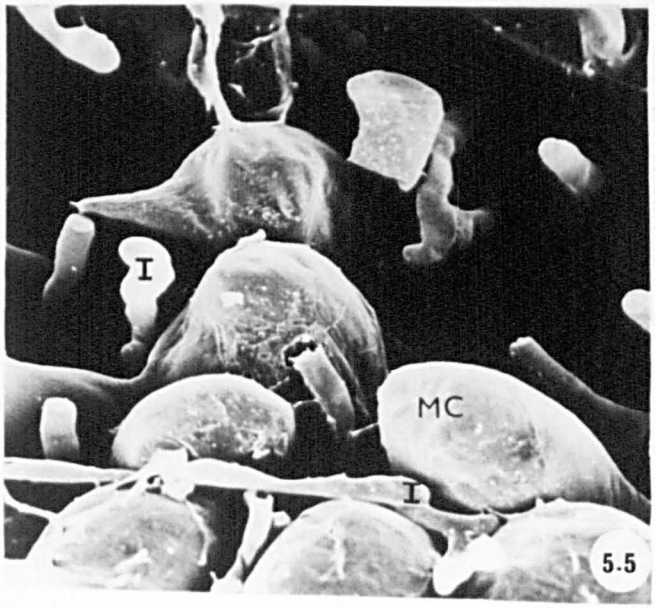
I
MC
I
5.5

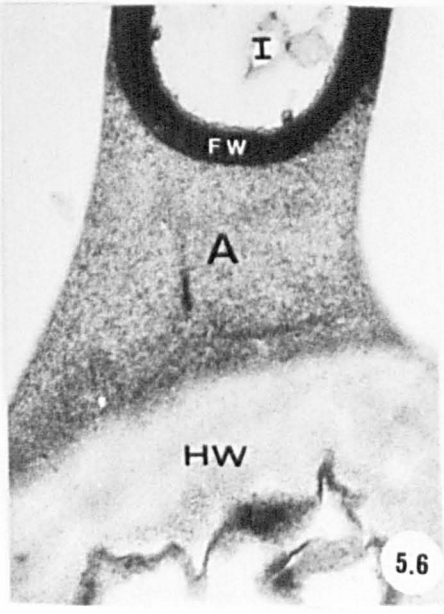
I
FW
A
HW
5.6

Figure 5.7

Transverse section of monokaryotic hyphae embedded in wall of bundle sheath cell of *Tussilago* showing dense fungal wall, nucleus, mitochondria, lipid drops and vacuole. Note vesicle with membranous material (arrowhead).

x20000

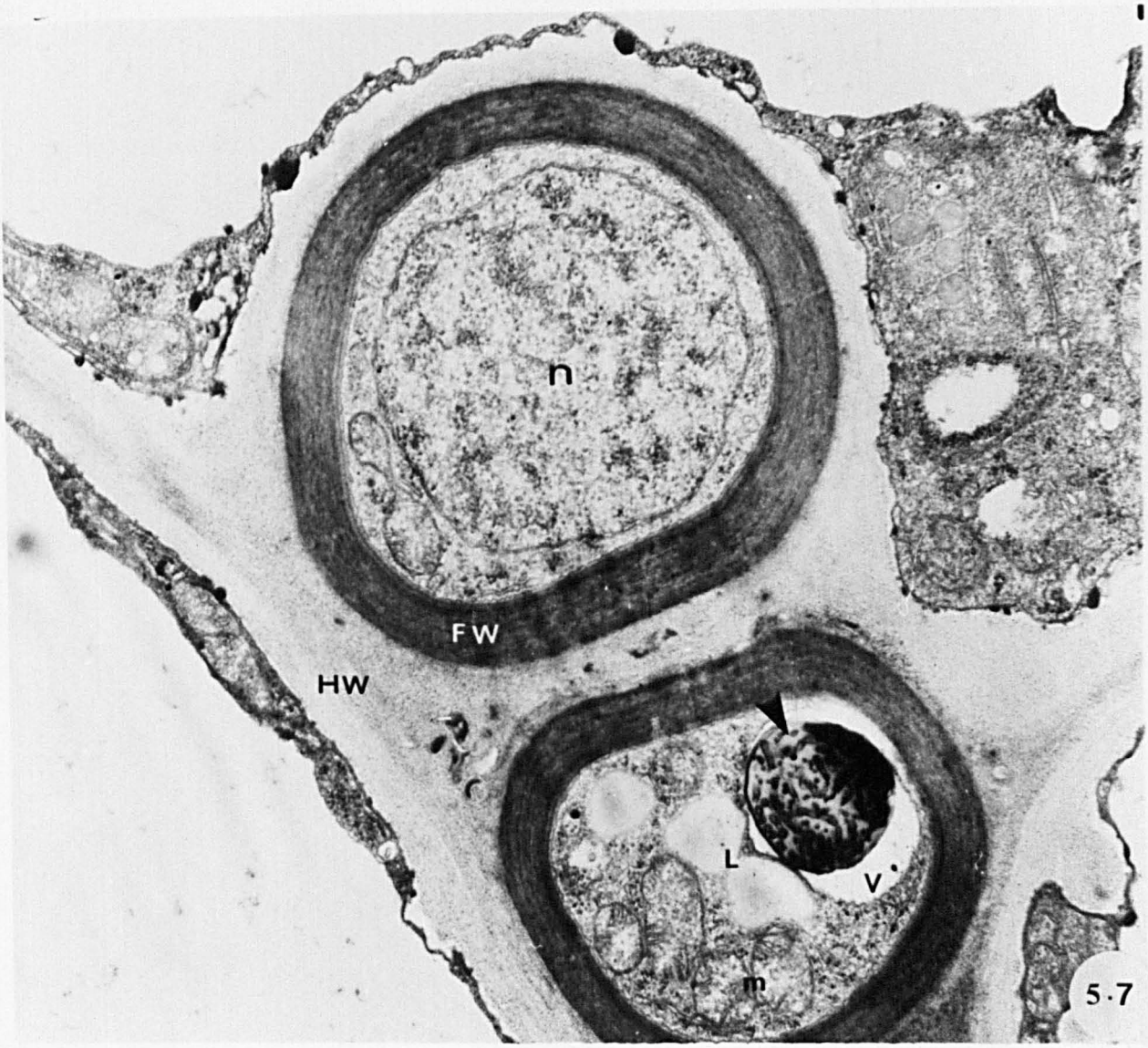
n
FW
HW
L
V
m
5·7

Figure 5.8

Dikaryotic intercellular hypha from mesophyll of *Poa*, containing two nuclei, mitochondria, endoplasmic reticulum and lipid droplets. Note the nucleolus and heterochromatin (arrowheads).
x15000

Figure 5.9

Part of monokaryotic intercellular hypha showing aggregates of electron-lucent areas (arrowhead) of granular appearance, unlike that of either lipid drops or vesicles, which suggest the presence of glycogen. Black rosette particles, which may also be glycogen, are seen (arrow). Note large lipid drops.
x43750


n
L
m
er
nu
n
5.8

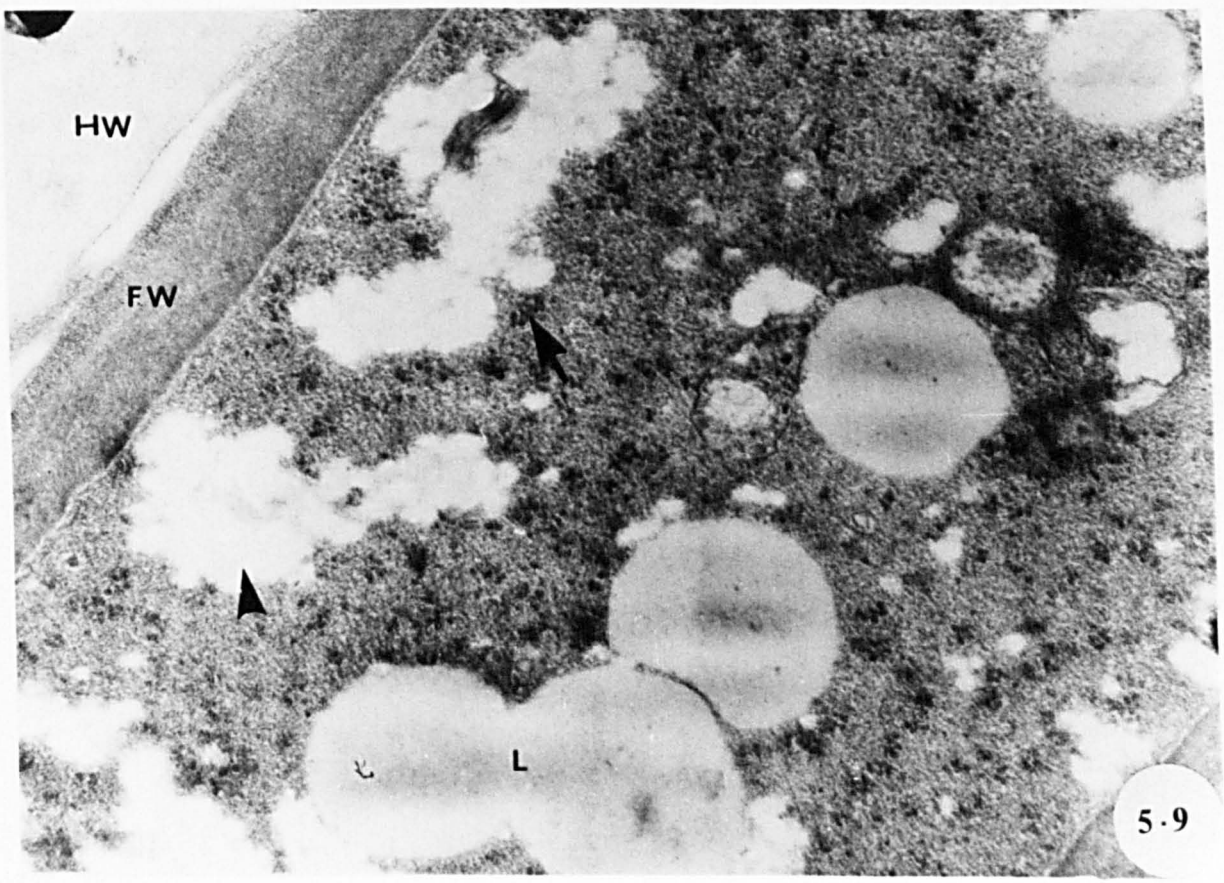
HW
FW
L
5.9

Figure 5.10

Section of monokaryotic intercellular hypha showing nucleus, mitochondria, endoplasmic reticulum (arrowhead) and glycogen-like aggregates (open arrow).

x30000

Figure 5.11

Dikaryotic hypha containing two nuclei, nucleolus, lipid drops and microbody. Note euchromatin and heterochromatin (open arrow).

x20000

Figure 5.12

Section of dikaryotic hypha showing mitochondria, lipid drops, and microbodies dispersed in the fungal cytoplasm.

x25000

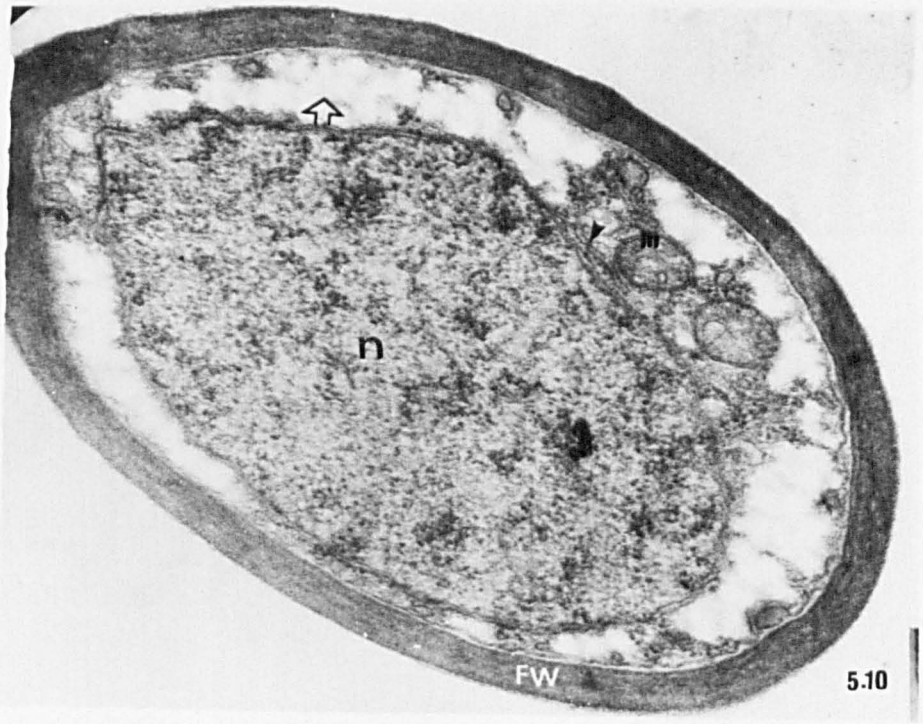

5.10

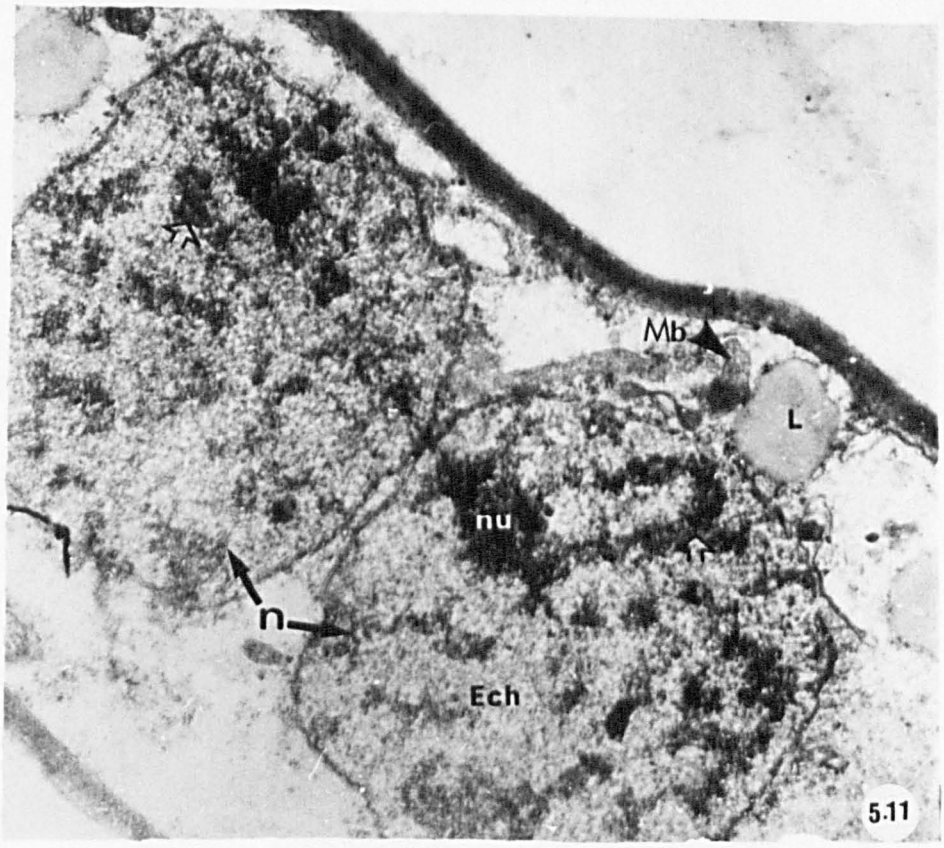

5.11

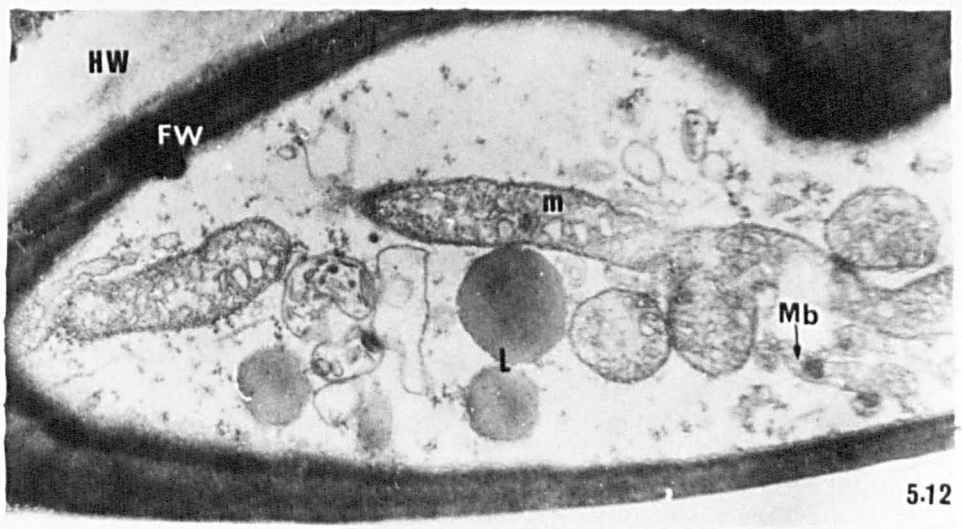

5.12

Figure 5.13

Perforate septum in intercellular hypha of pycnial-aecial stage showing cross-walls consisting of two, electron-dense layers separated by an electron-lucent lamella (arrow), tapering towards the central pore (open arrow). Note the organelle-free pore apparatus and the fungal plasmalemma over the septum (large arrow).
x37500

Figure 5.14

Perforate septum (pycnial-aecial stage), showing a plugged pore (arrow). Note the pore apparatus which appears distinct from the surrounding cytoplasm and the crystal-containing microbody (arrowhead) in its periphery. Adhesive material can be seen between the fungal cell walls. Note also mitochondria and lipid drops.
x25000

Figure 5.15a

Non-medium section of a perforate septum showing vesicles with dense material and crystal-containing microbodies surrounding the pore apparatus.
x90000

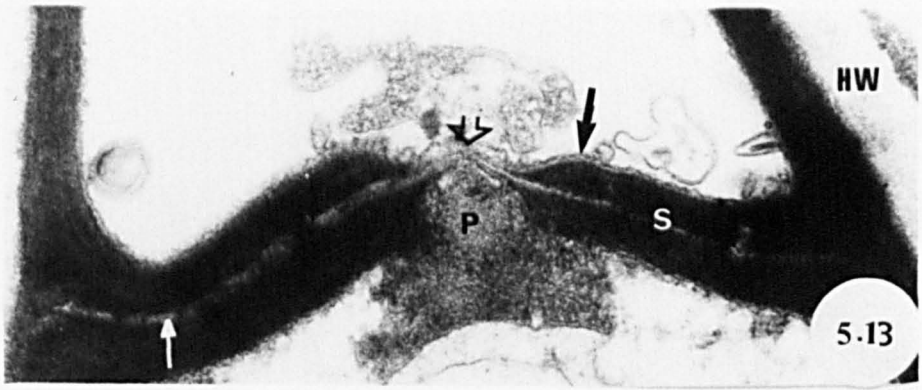
HW
P
S
5.13

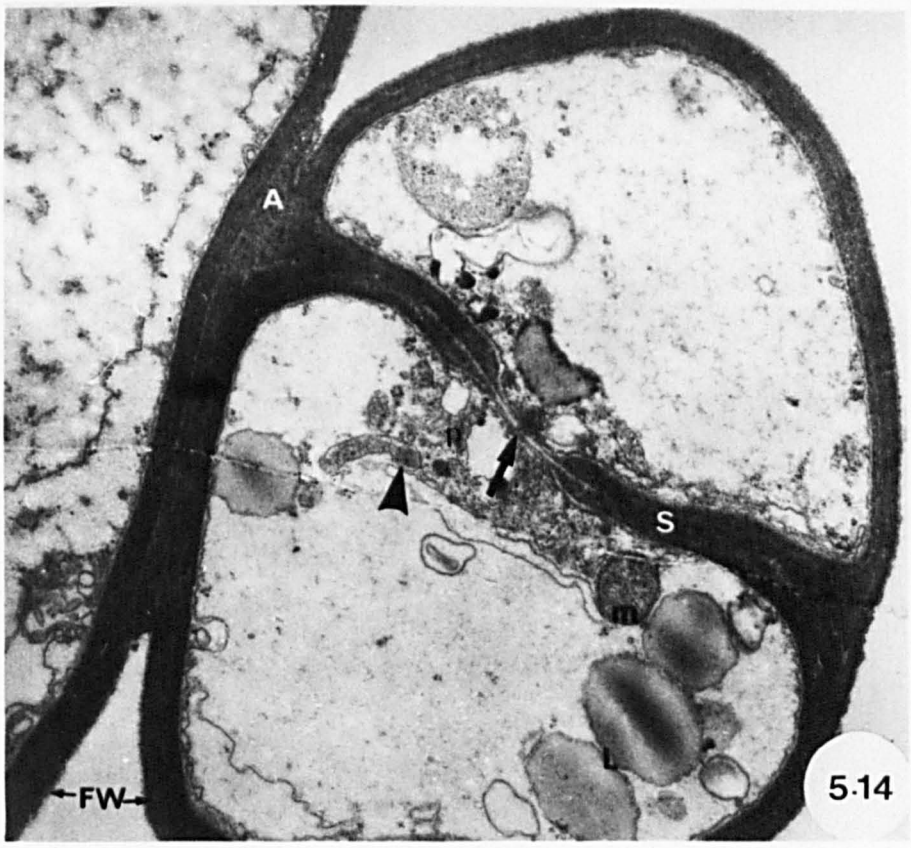
A
S
m
L
FW
5.14

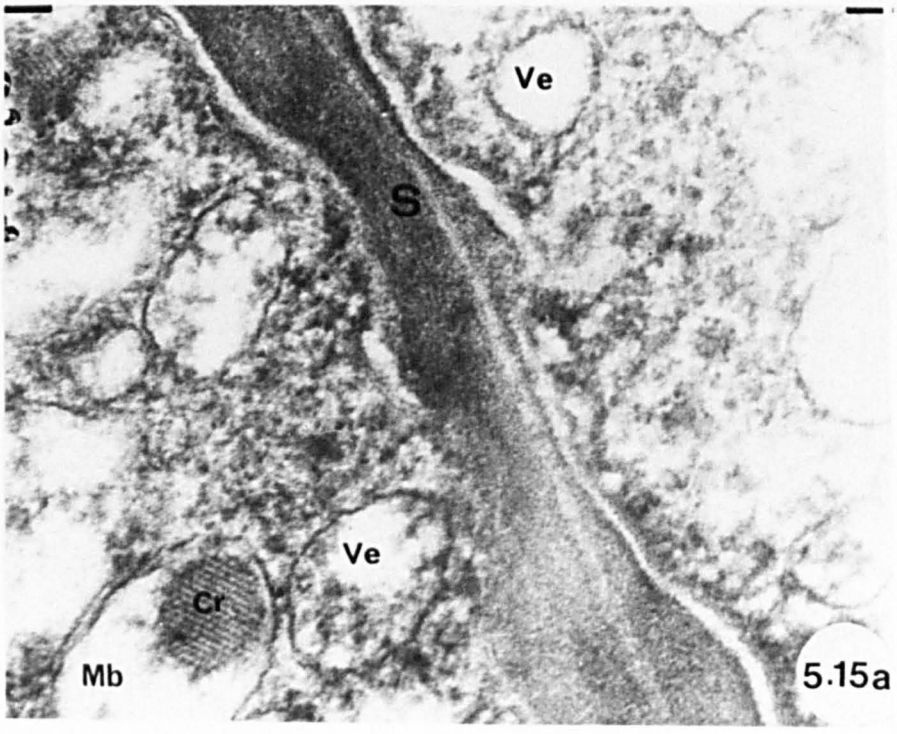
Ve
S
Ve
Cr
Mb
5.15a

Figure 5.15b

Non-median section of perforate septum (pycnial-aecial stage) showing crystal-containing microbody, empty vesicles and electron-dense vesicles at the periphery of the pore apparatus. Note the lomasome-like structure between fungal plasmalemma and the septum (arrow), the large, electron-dense vesicle near the septal pore (arrowhead) and a lipid drop.

x50000

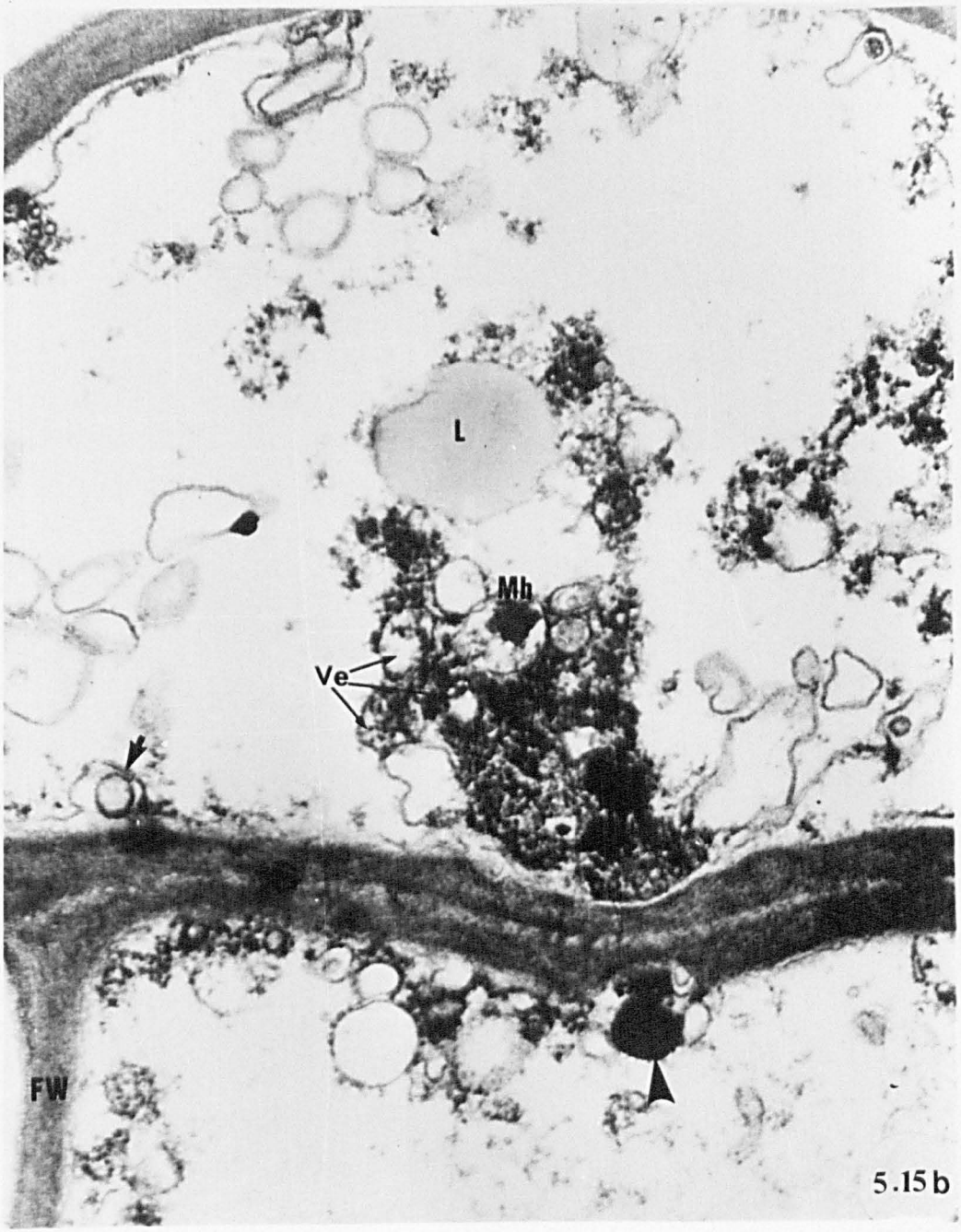

5.15b

Figure 5.16

Perforate septum (pycnial-aecial stage) showing three crystal-containing microbodies bordering the pore apparatus. The section is non-median and does not show the septal pore.

x100000

Figure 5.17

Perforate septum (pycnial-aecial stage) showing two crystal-containing microbodies at the periphery of the septal pore apparatus. Note the continuity of fungal plasmalemma over the septum (arrowheads). Note mitochondria and large lipid drops.

x75000

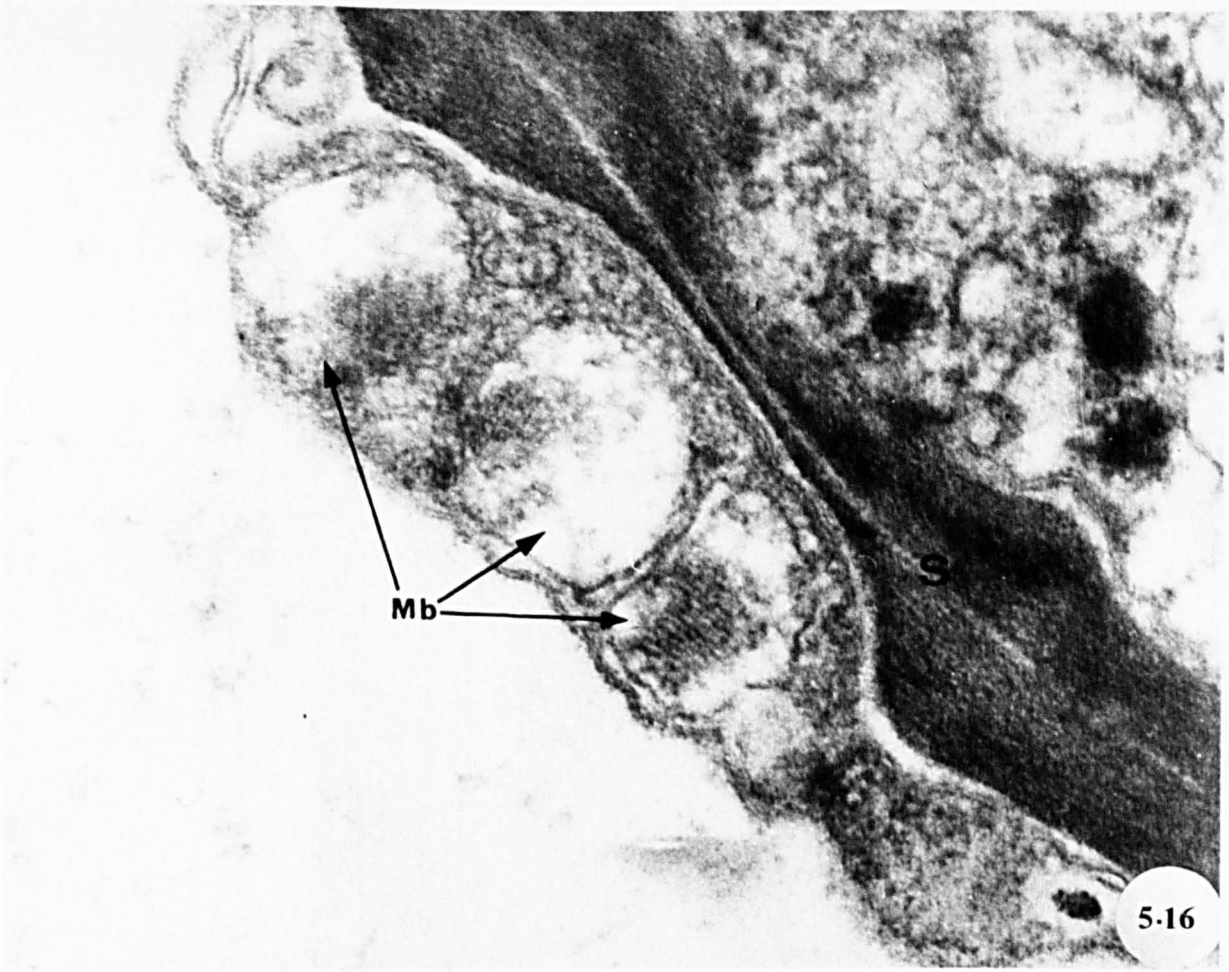

5·16

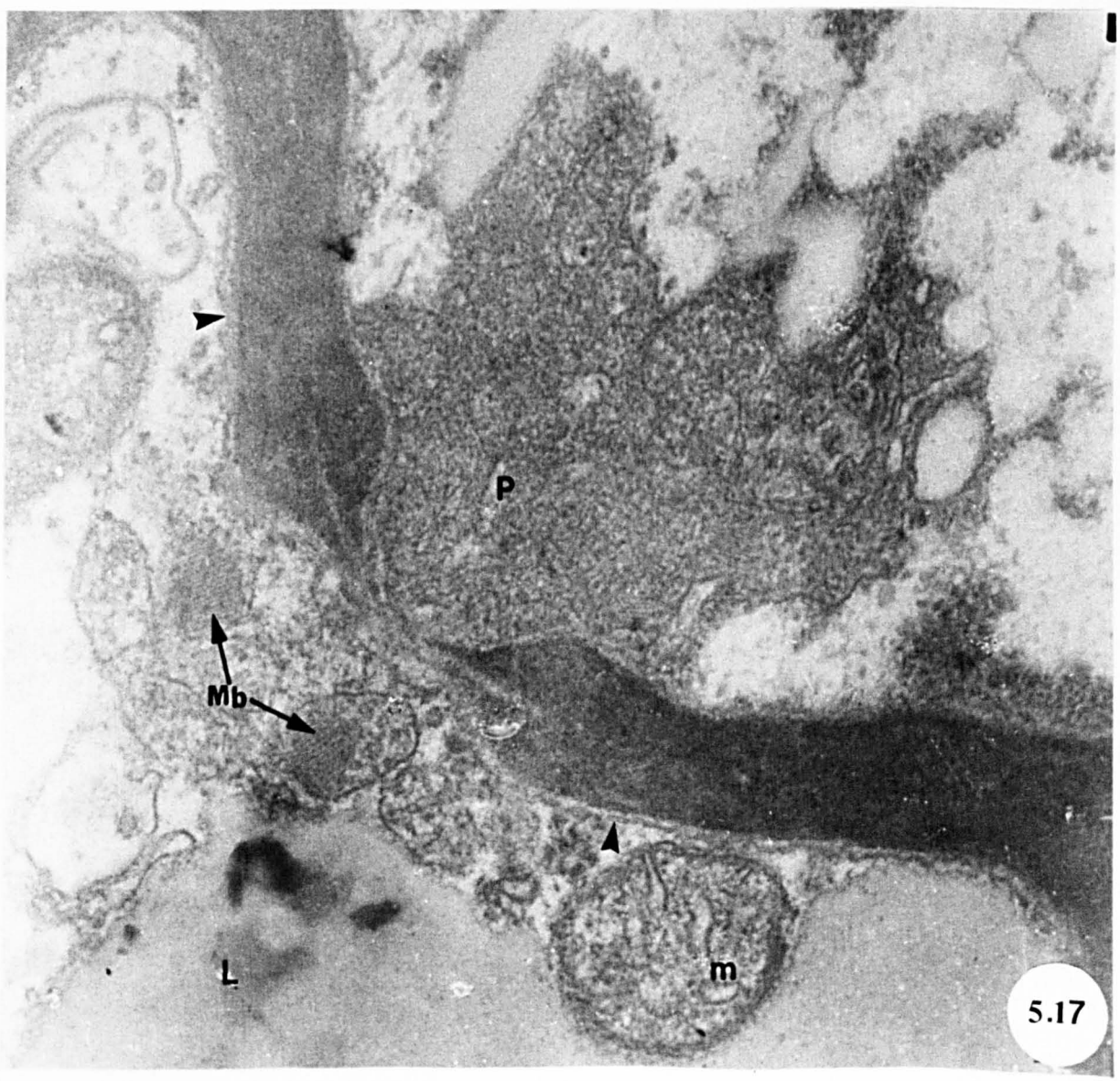

5.17

Figure 5.18

Perforate septum (pycnial-aecial stage) showing lomasomes associated with the fungal plasmalemma. Note the pore plug (arrowhead) and the pore apparatus, lipid drops, vesicle with membranes and fungal plasmalemma (open arrow) near the pore margin.
x30000

Figure 5.19

Unilaterial partial septum in an intercellular hypha of the monokaryon. The large pore and absence of a pore apparatus allow free passage of materials between the compartments.
x20000

Figure 5.20

Bilateral partial septum in dikaryotic intercellular hypha. Both sides of the hypha are infolded centripetally leaving a large pore. Note lipid drops.
x30000

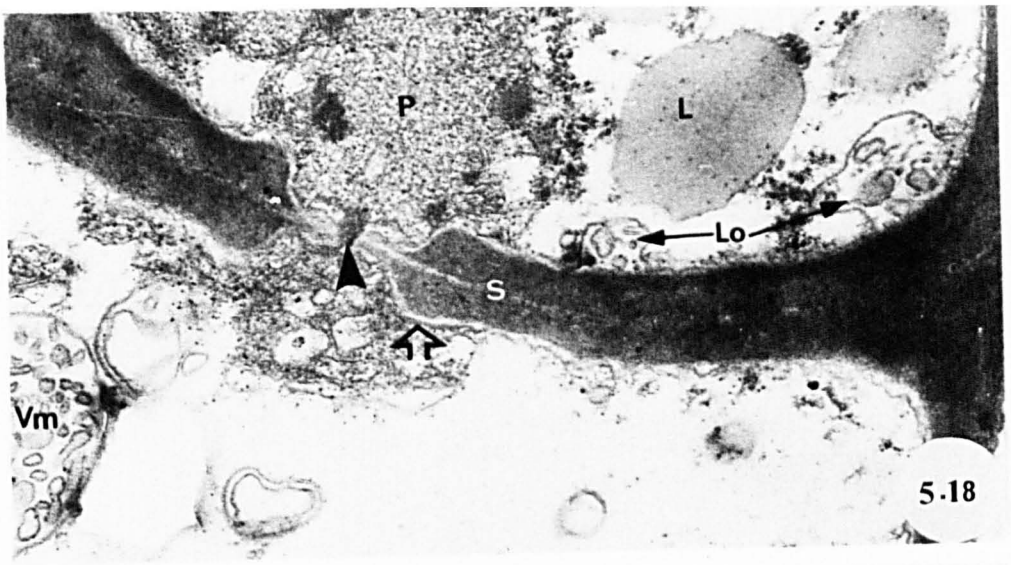

5.18

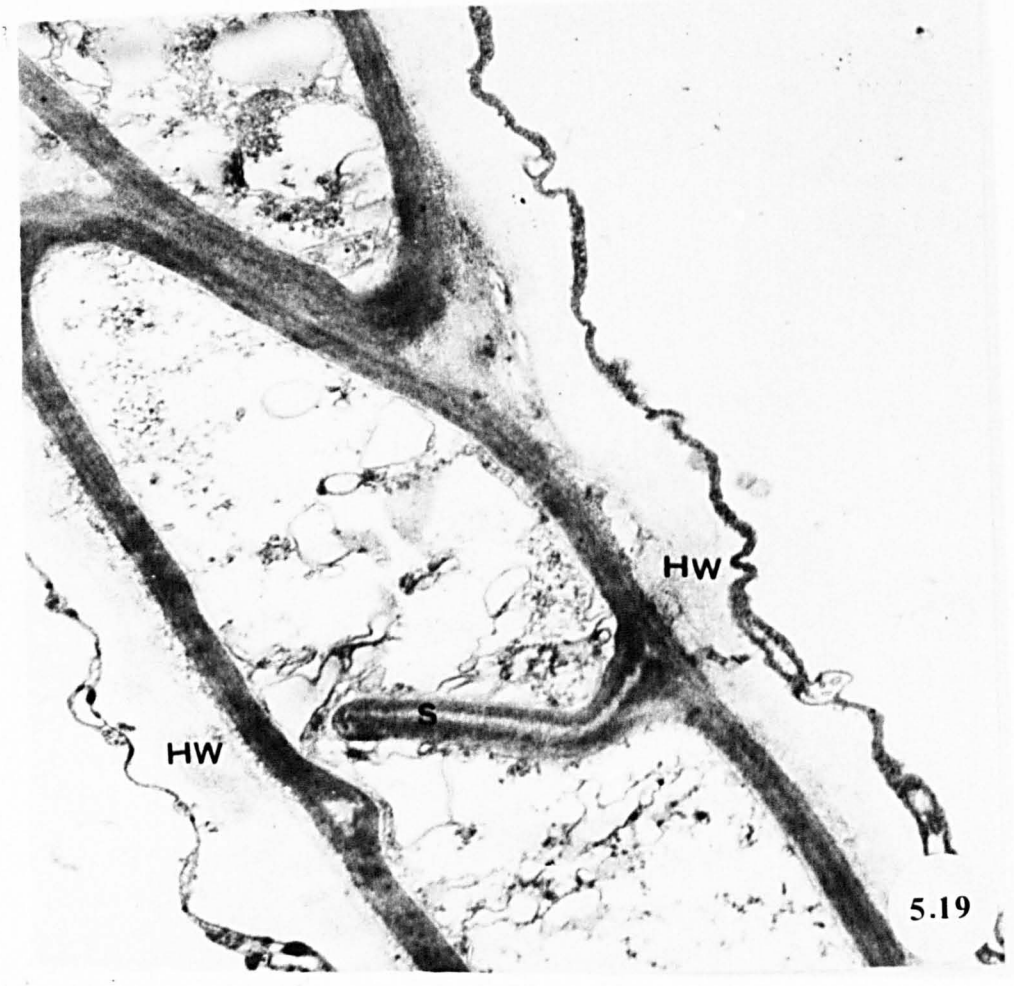

5.19

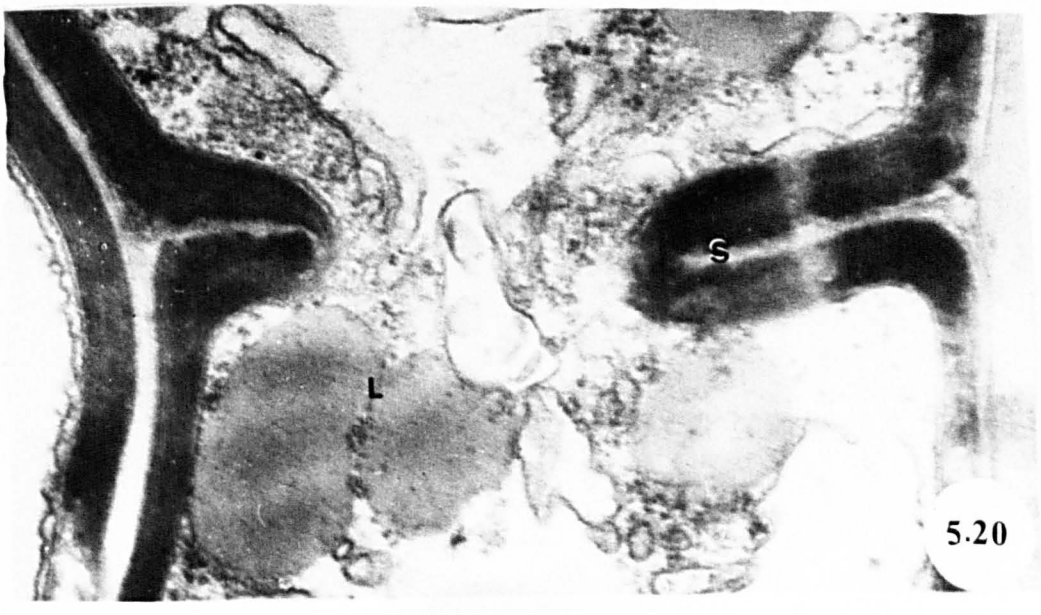

5.20

Figure 5.21

Unilateral partial septum (uredial stage) showing crystal-containing microbodies near the inner margin of the septum. Note lipid drops and mitochondria.

x75000

Figure 5.22

Electron micrograph showing a complete septum (arrowhead) in dikaryotic hypha. Note the absence of the pore and pore apparatus and the uniform thickness of the septum. Note also fungal nuclei and lipid drops.

x15000

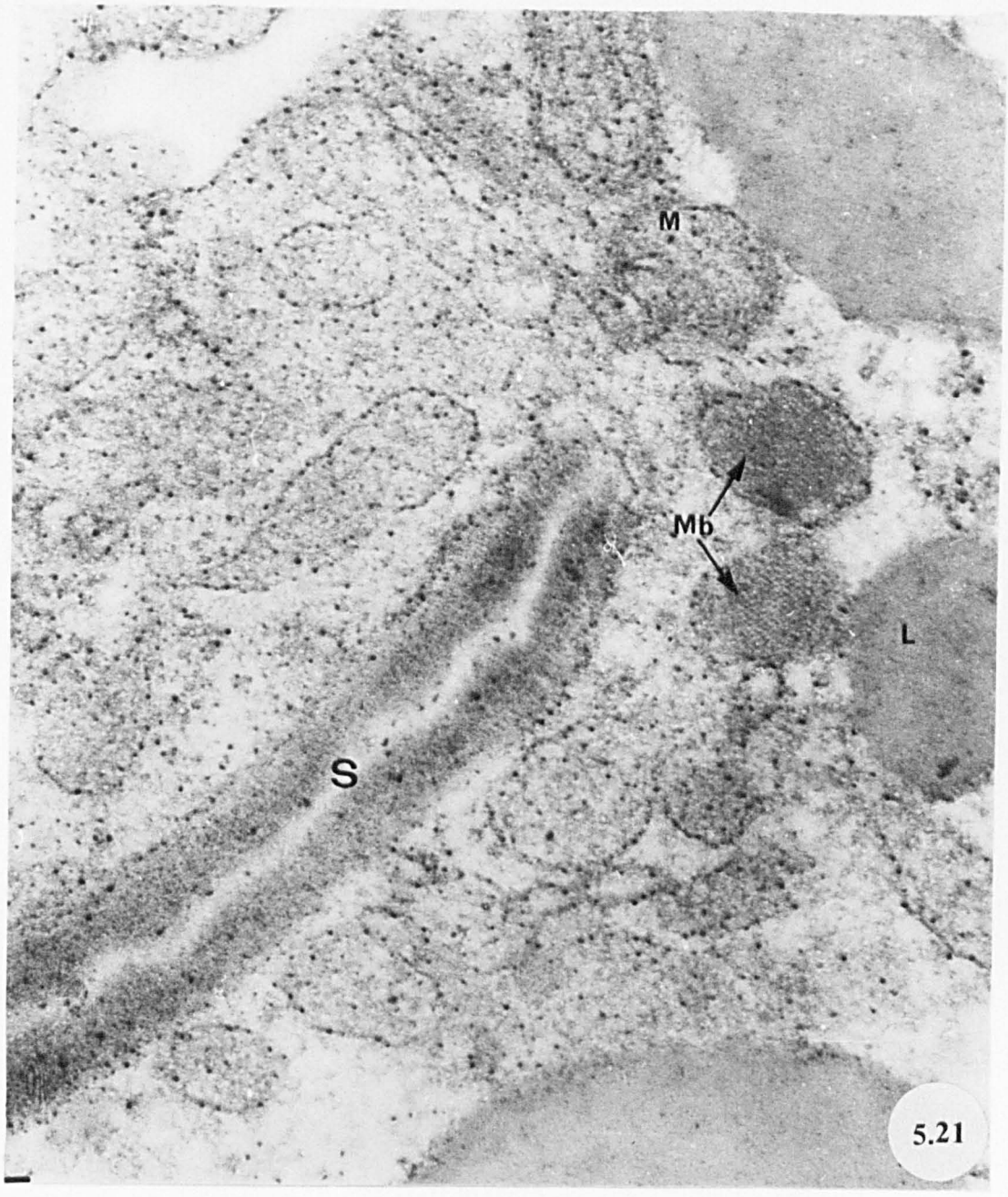

5.21

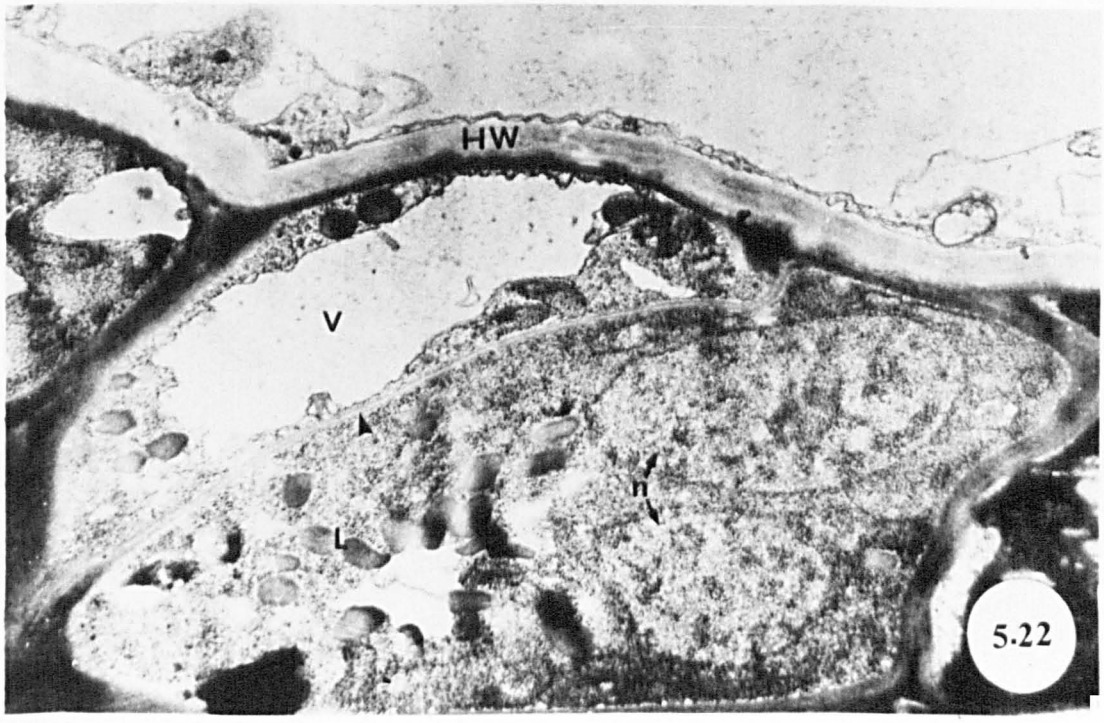

5.22

Figure 5.23

Intracellular hypha in mesophyll cell of *Tussilago* showing irregular shape. Note intercellular hyphae closely attached to the host cell wall.

x2500

Figure 5.24

Finger-like monokaryotic intracellular hyphae in mesophyll cells of *Tussilago*. Note the intracellular hyphae are not differentiated into body and neck regions. Intercellular hyphae and host chloroplasts (arrows) are seen.

x1600

Figure 5.25

Twisted and coiled intracellular hyphae in mesophyll cells. Note intercellular hyphae.

x2500

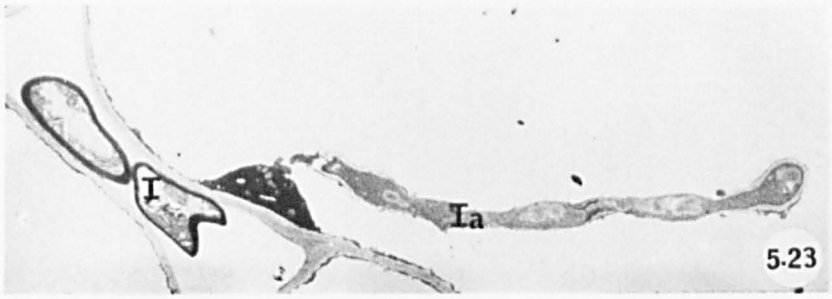
I
Ia
5.23

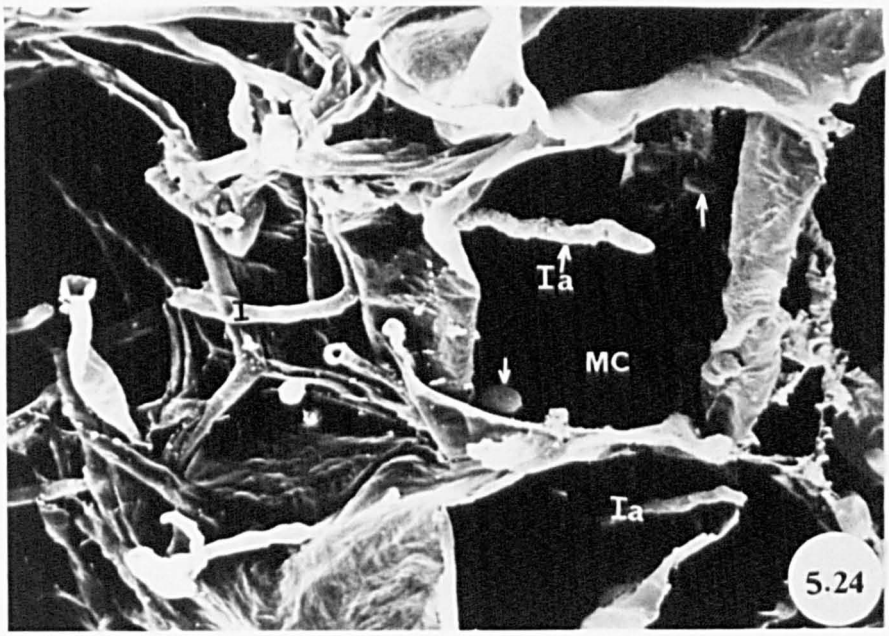
Ia
I
MC
Ia
5.24

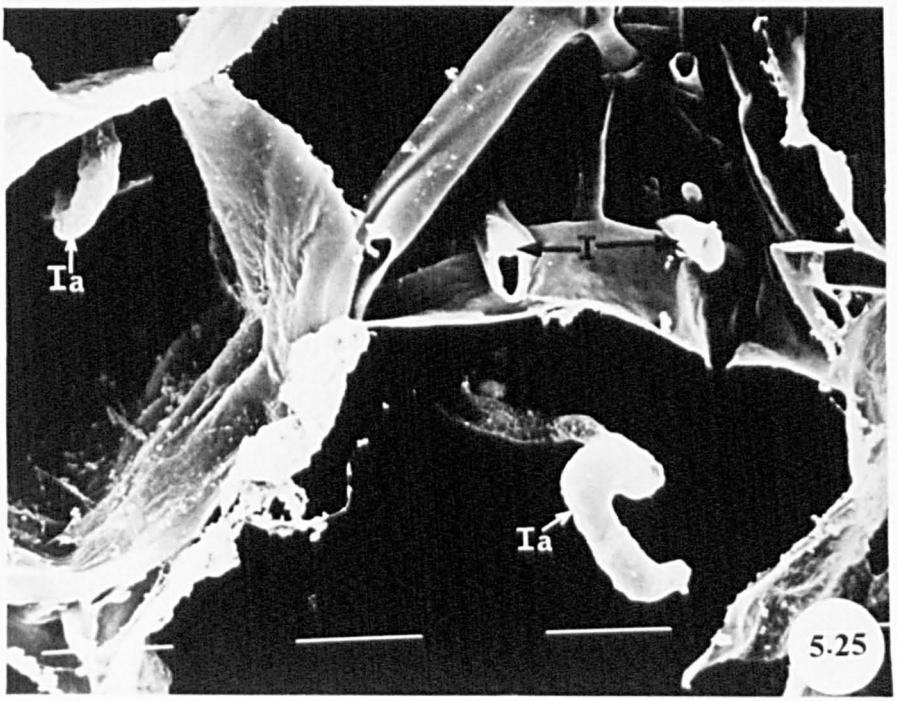
Ia
I
Ia
5.25

Figure 5.26a

Section through penetration point of intracellular hypha in mesophyll cell of *Tussilago*, showing ingrowth of host cell wall and plasmalemma around the penetrating hypha. A septum cuts off the mother cell from the rest of the hypha. Note glycogen-like particles (open arrows) and lipid droplets in intercellular hypha and penetrating peg and the adhesive layer surrounding the intercellular hyphal walls. The fungal wall (unlabelled solid arrow) is continuous between the mother cell and the penetration peg.
x12500

Figure 5.26b

Penetration into *Tussilago* mesophyll cell. The intracellular hypha is relatively little constricted where it penetrates the host cell wall (arrow). Note nucleus in the penetrating hypha. Note intercellular hyphae and lipid droplets.
x6250

5.26a

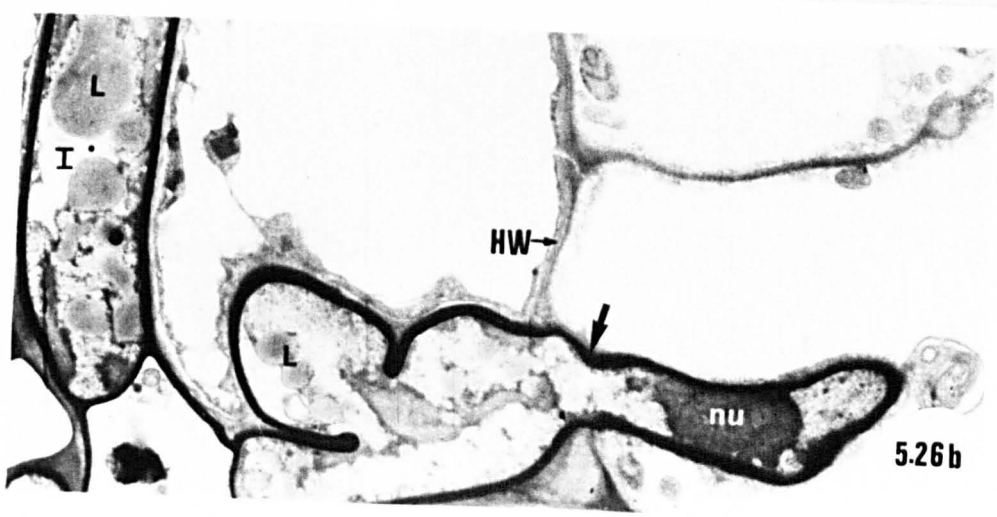

5.26b

Figure 5.27

Penetration site of a haustorium showing localized thickening of the haustorium-mother cell wall at the point of entry, part of the neck region, the invaginated host plasmalemma, and a nucleus which appears to be migrating from the highly vacuolated haustorium-mother cell to the haustorium. Note the interruption of the fungal wall where it penetrates the host wall. Note also lipid drop in host cell and adhesive material (arrow).
x62500

Figure 5.28a

Near-median longitudinal section of haustorium in *Poa* showing neck-band. Note lipid droplets in haustorial body.
x18750

Figure 5.28b

Scanning electron micrograph of haustorium showing neck with neck-band (arrow) and part of the expanded body region.
x20000

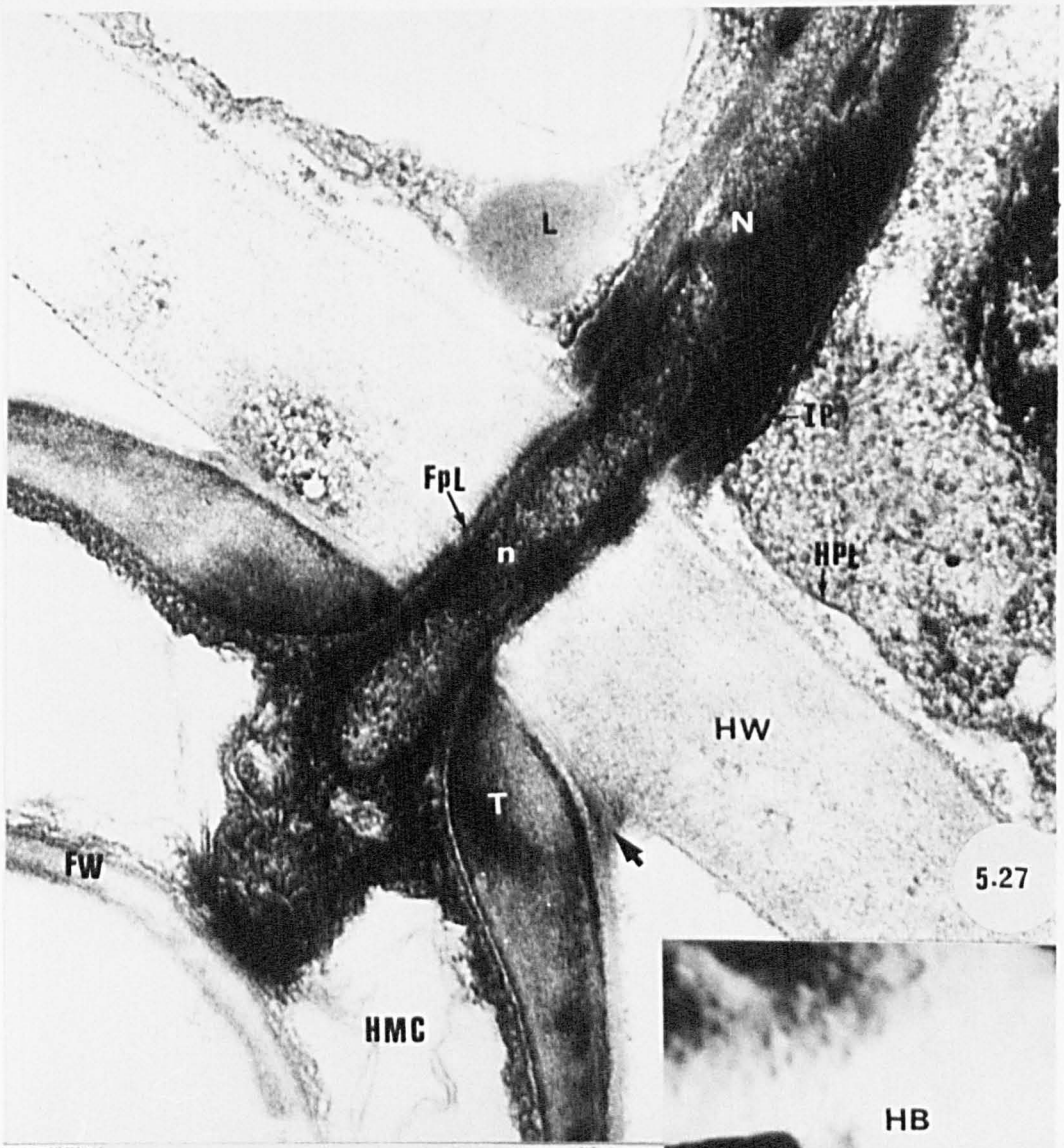

5.27

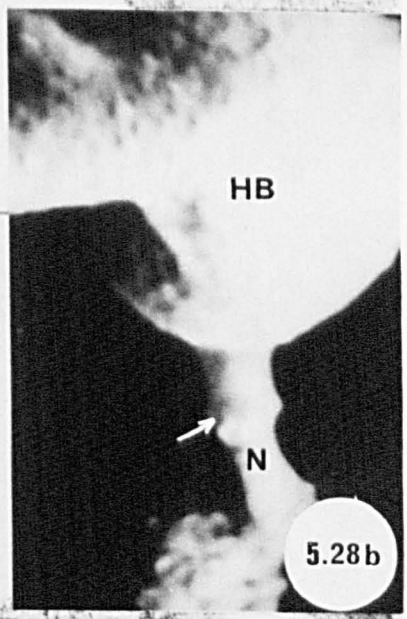

5.28b

5.28a

Figure 5.29

Oblique section of a septate intracellular hypha. No difference is seen in the thickness of the invaginated (arrow) and non-invaginated parts of the host plasma membrane. Note lipid bodies and intercellular hypha closely attached to host wall.

x7500

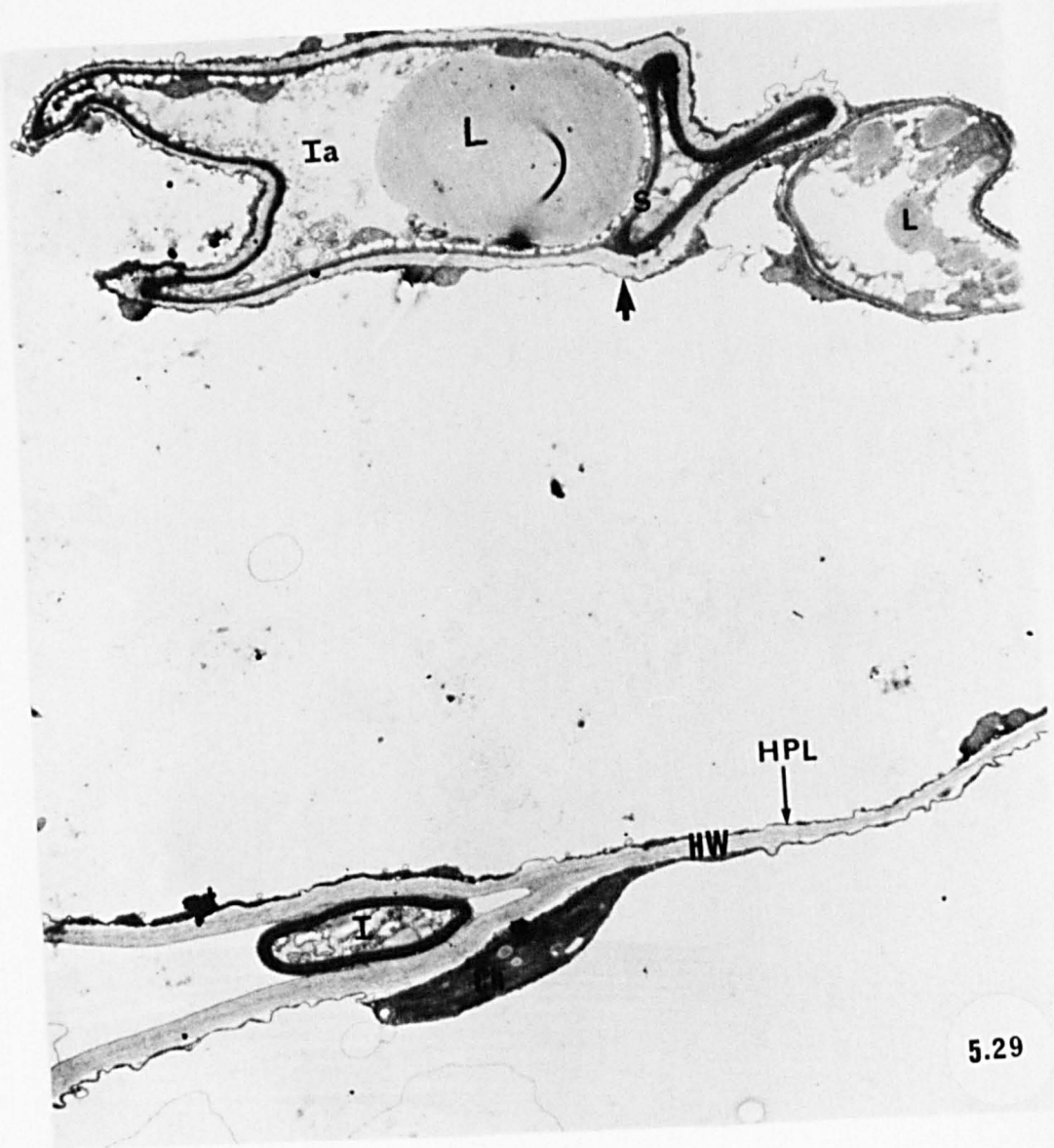

5.29

Figure 5.30a

Transverse sections of intracellular hyphae showing nucleus, mitochondria vesicles (arrowhead), fungal plasmalemma and concentric aggregations of endoplasmic reticulum. The matrix region of each hyphae is surrounded by portions of host plasmalemma, which lie very close together between the two hyphae. Fibrillar material (open arrow) in the matrix region may indicate early stages in the deposition of host wall material. Note rosette arrangement of glycogen-like black particles (solid arrows) and host endoplasmic reticulum.
x34750

Figure 5.30b

Monokaryotic intracellular hypha showing several mitochondria, lipid droplets, glycogen-like particles (solid arrows), vacuoles, endoplasmic reticulum and vesicles containing membranous materials (open arrow). Note the invaginated host plasma membrane (arrowhead) and host mitochondria adjacent to intracellular hyphae.
x12500

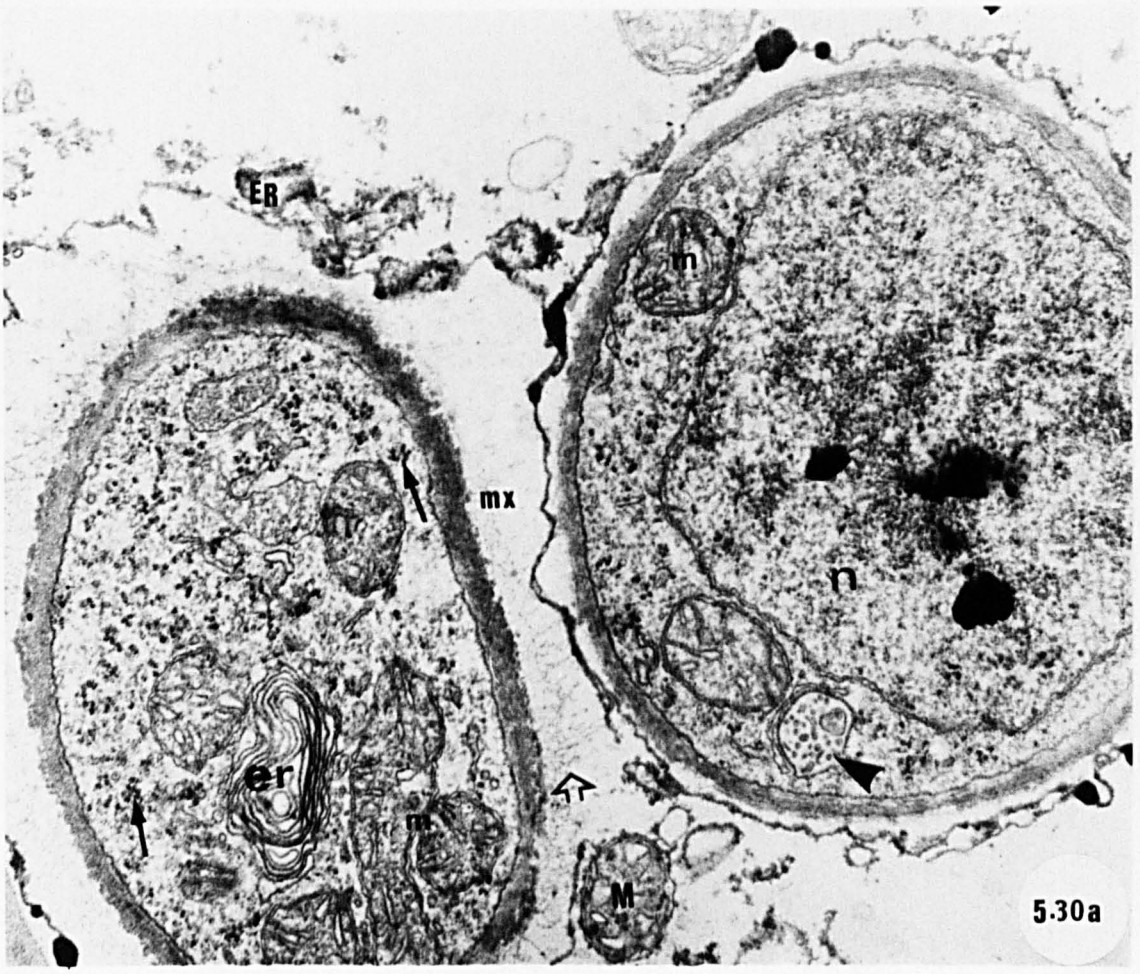

5.30a

5.30b

Figure 5.31

A haustorium-mother cell is seen attached to a mesophyll cell of *Poa*. A septum (arrowhead) separates the mother cell from the rest of the hypha. Note other septum between two fungal cells.

x2500

Figure 5.32a

Haustorium body in transverse section showing several mitochondria and endoplasmic reticulum adjacent to lipid drop. Fungal plasmalemma (arrowhead) and invaginated host plasmalemma are shown (open arrow). Note host mitochondria and nucleus.

x 25000

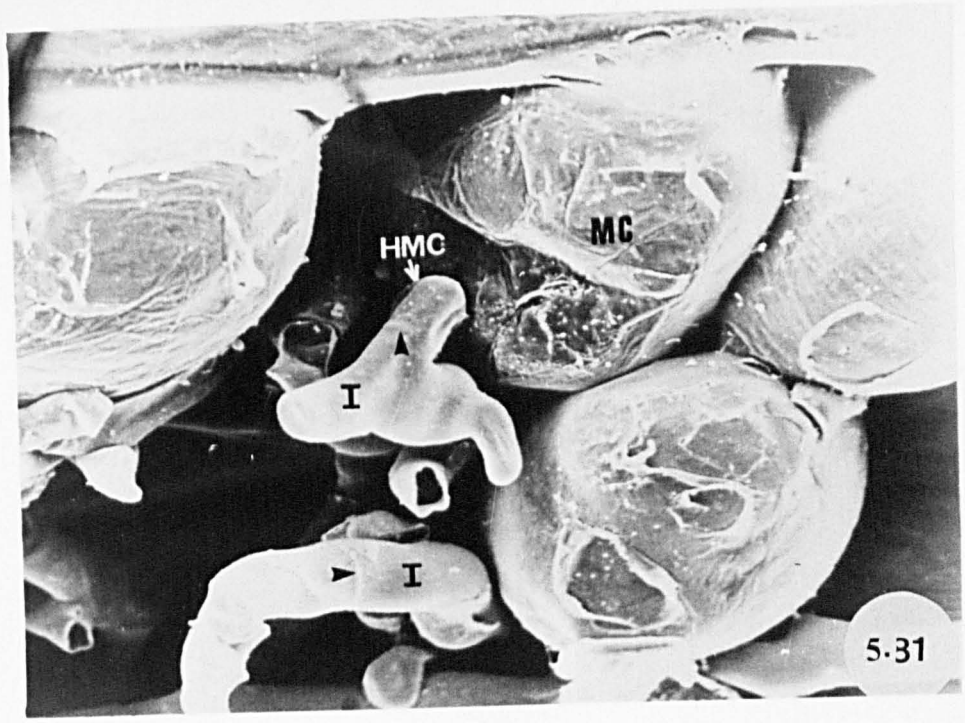

5.31

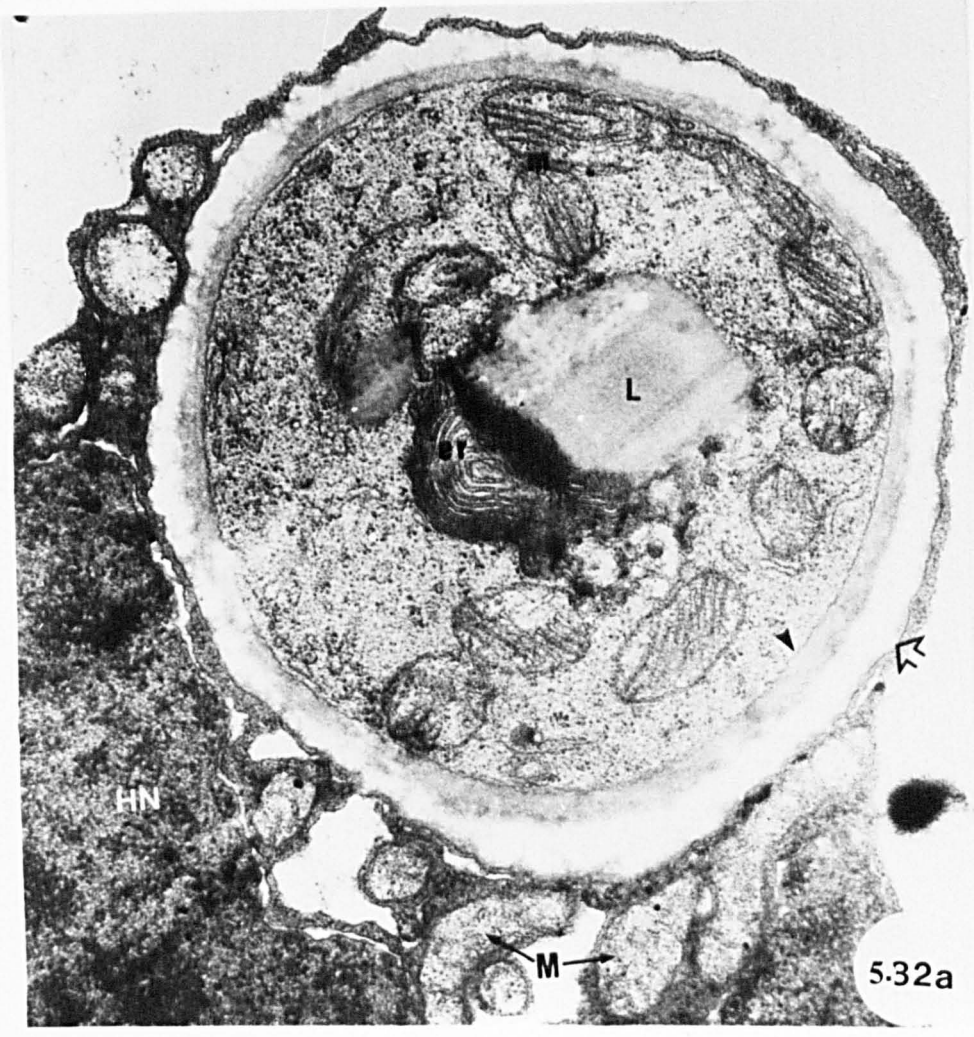

5.32a

Figure 5.32b

Haustorium showing nucleus, mitochondria, vacuole with membranous material and few lipid drops. Note host endoplasmic reticulum around haustorium.

x28000

Figure 5.32c

Haustorium showing single nucleus. More heterochromatin material is seen in the nucleus of the haustorium than that in the nucleus of the intracellular hypha in Figure 5.30a.

x28000

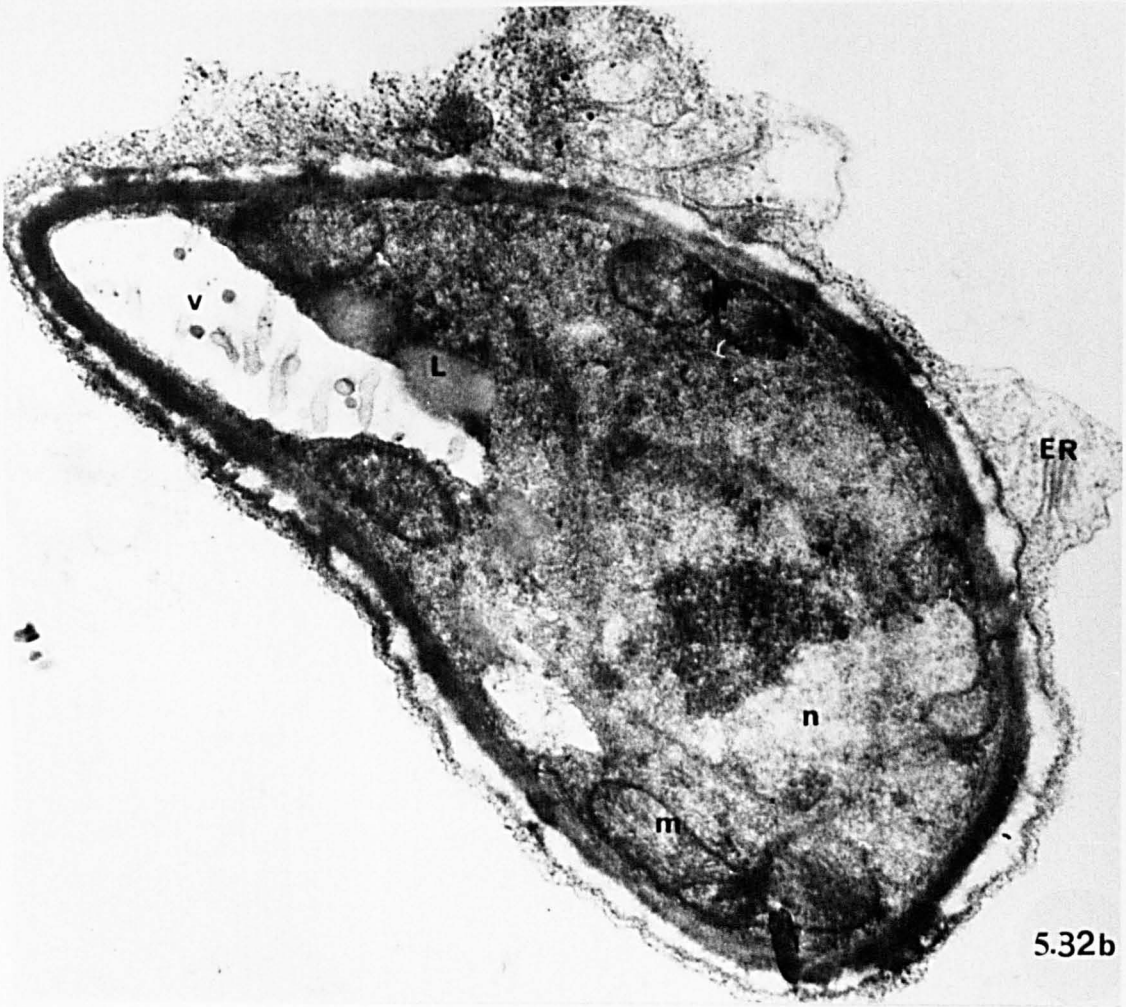

5.32b

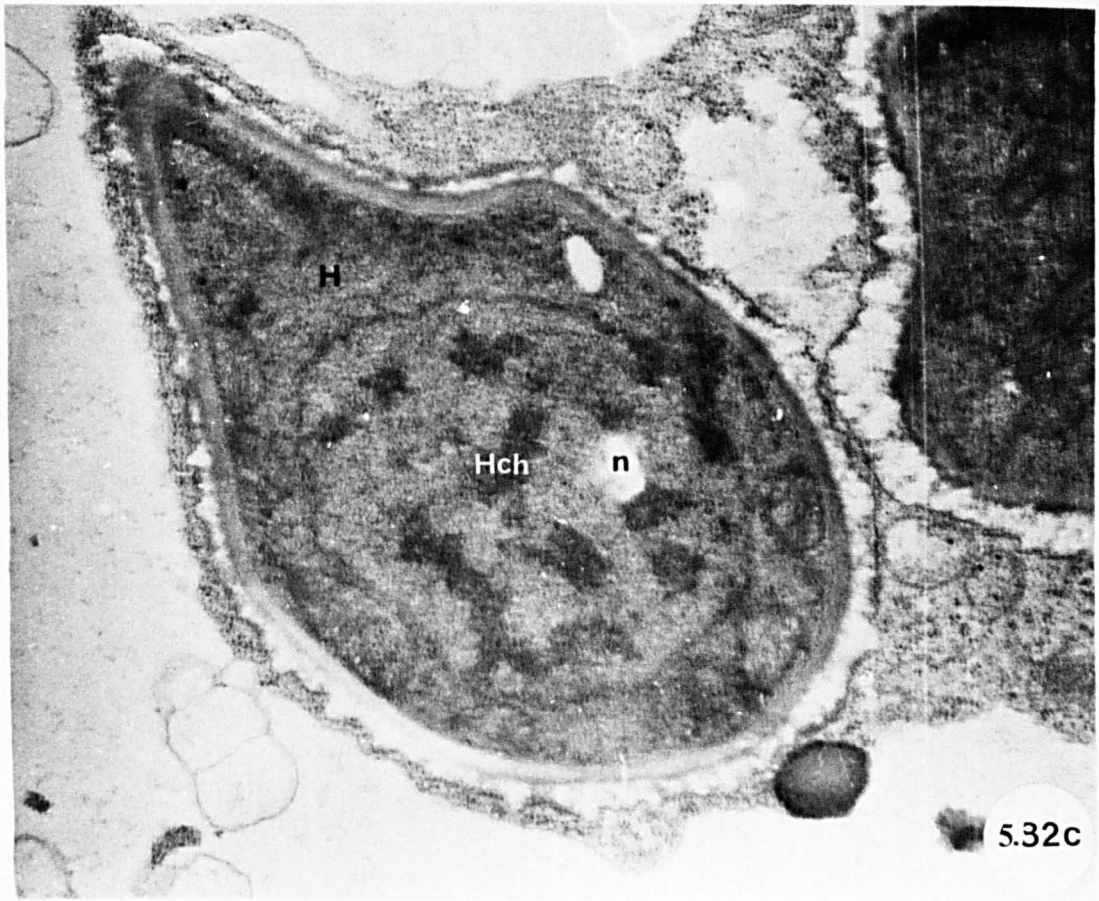

5.32c

Figure 5.33

Haustorium showing lomasomes associated with plasmalemma (arrowheads). Note electron-dense material in the matrix region and fungal mitochondria.

x35000

Figure 5.34

Longitudinal section of intracellular hypha passing near the point of penetration into mesophyll cell. Note the invaginated host plasmalemma (arrowheads), the collar of host wall material around the very slightly constricted neck-like region, and traces of host wall-like material (arrows) deposited on the fungal wall within the matrix surrounding distal regions.

x10000


H
m
mx
5.33

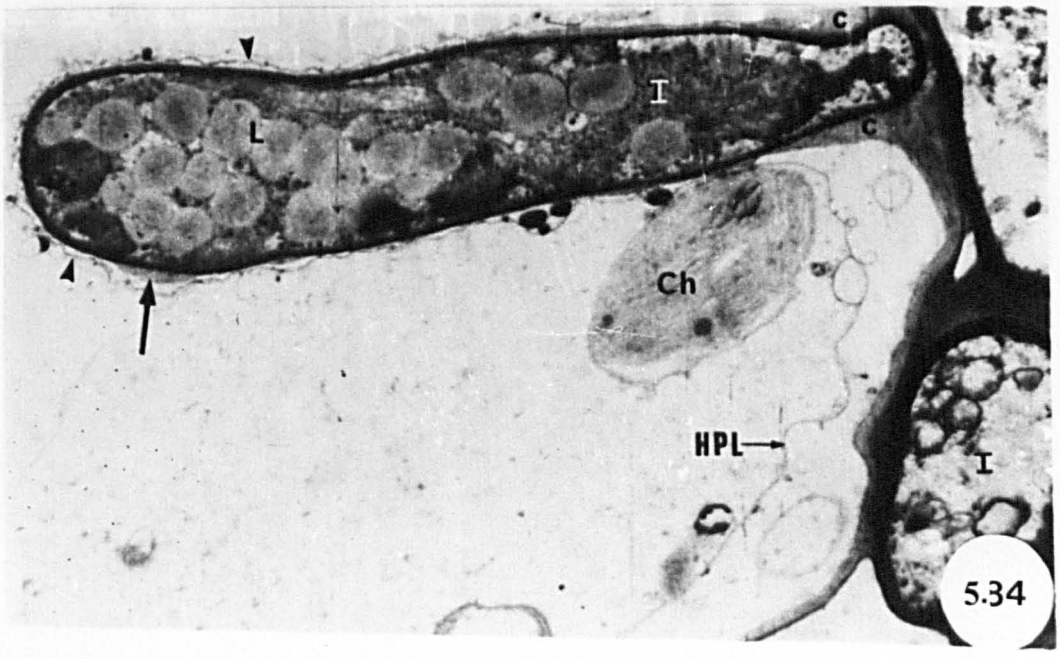
C
I
L
C
Ch
HPL
I
5.34

Figure 5.35

Part of haustorium body showing fungal wall and matrix region bounded by the host plasmalemma. Electron-dense fibrils (arrowheads) in the matrix appear to be contributing to the haustorium wall. Note mitocondria.

x100000

Figure 5.36

Transverse section of intracellular hypha showing matrix region composed of material resembling the host cell wall, deposited directly on the more electron-dense fungal wall (arrow) and enclosed by host plasmalemma and a thin layer of cytoplasma (arrowhead). Note intercellular hypha closely attached to host cell wall.

x25000

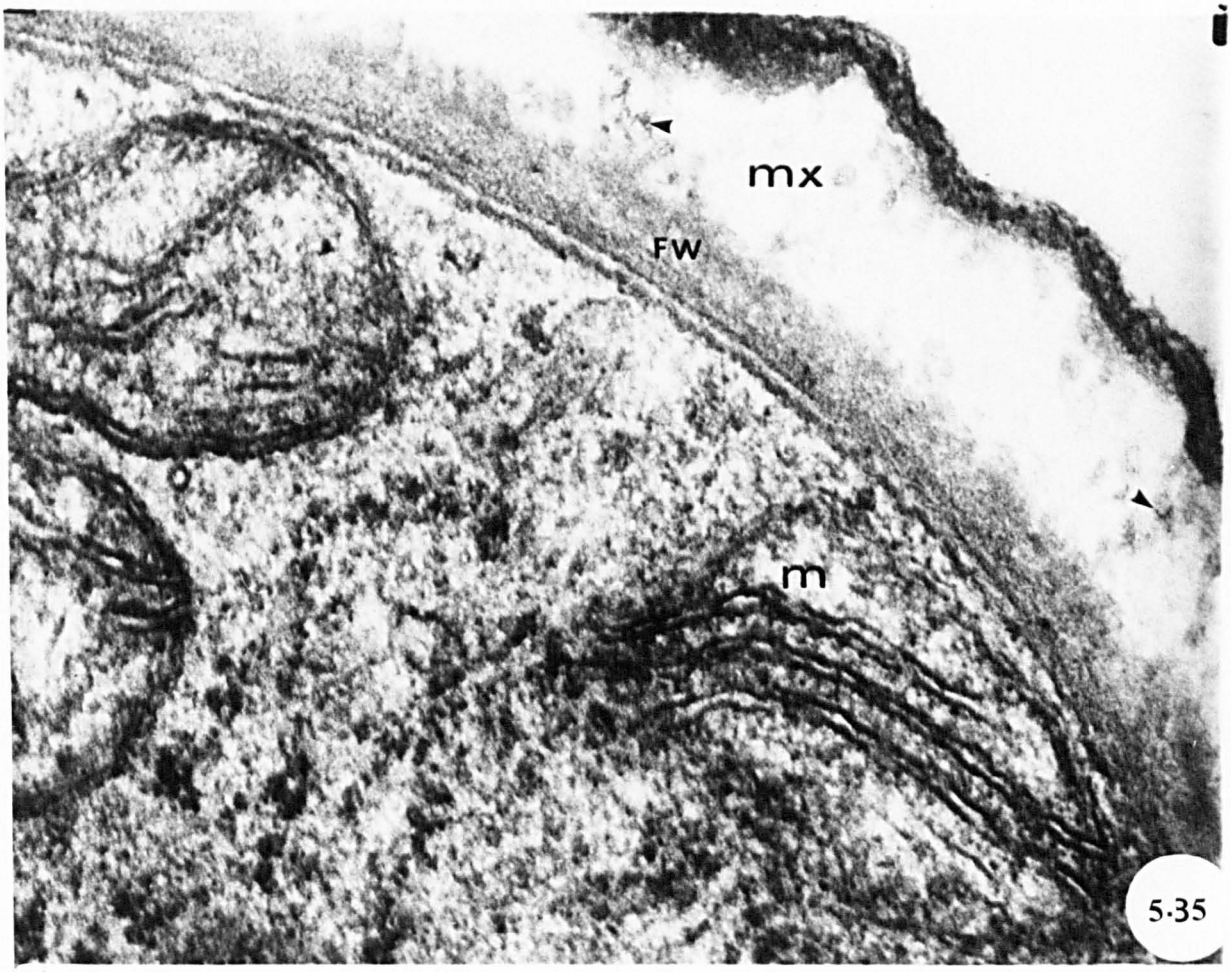

5.35

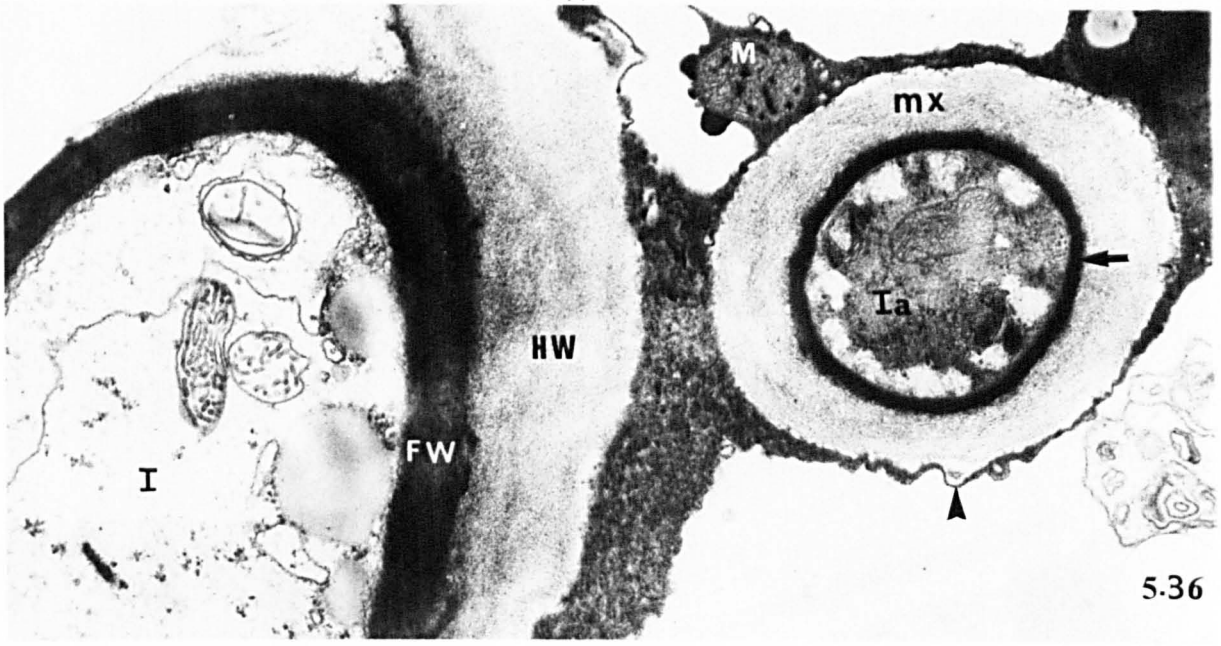

5.36

Figure 5.37

Intracellular hyphae in mesophyll cell showing vesicle-like structure enclosing membranous material (arrowhead) associated with invaginated host plasmalemma, several mitochondria and nucleus. Note host mitochondria adjacent to intracellular hypha.
x20000

Figure 5.38a

A septate intracellular hypha showing several vesicle-like structures with electron-dense material (arrowheads) associated with invaginated host plasmalemma.
x7500

Figure 5.38b

A higher magnification of part of the intracellular hypha (between arrows) shown in Figure 5.38a. The plasma membrane surrounding the intracellular hypha forms vesicle-like structure enclosing electron-dense material (arrow). Note host wall-like material deposited over fungal wall.
x75000

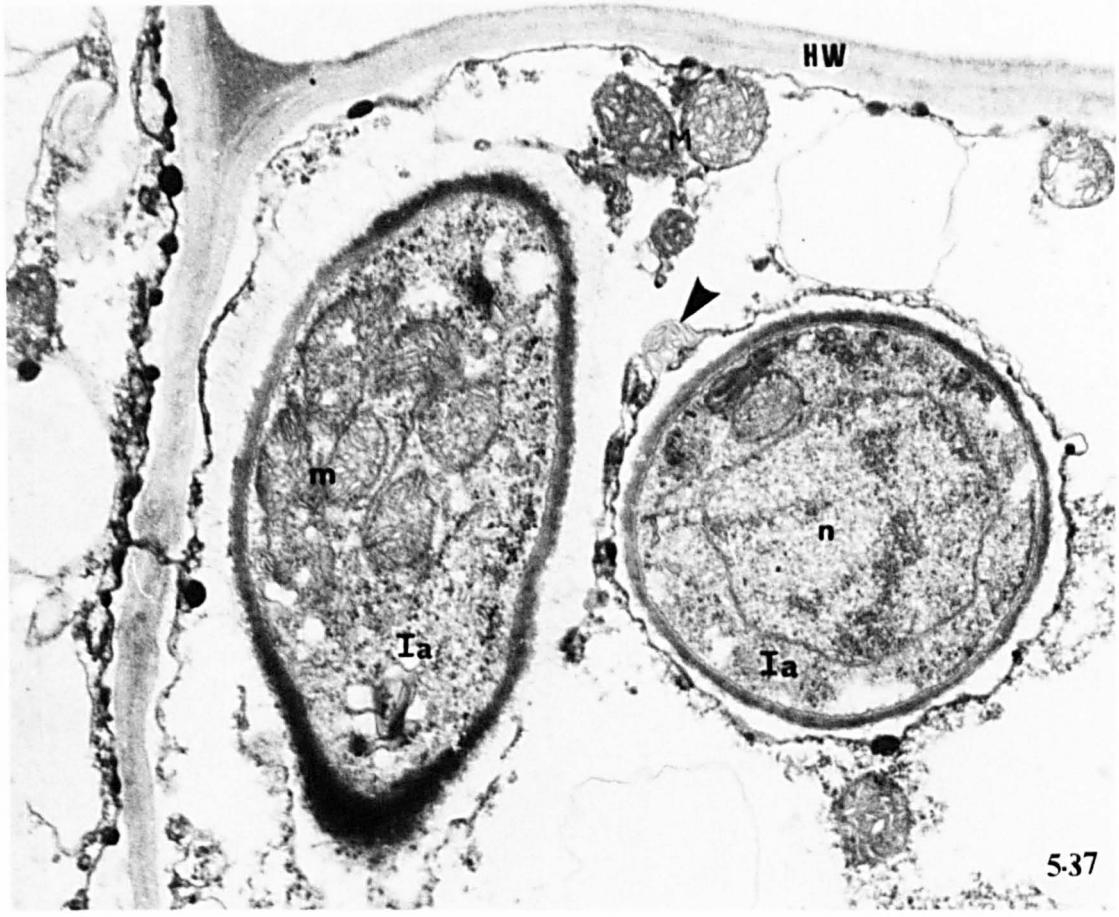

5-37

5-38a

5-38b

Figure 5.38c

Part of intracellular hypha showing small vesicles (small arrows) in the matrix region. Similar vesicles (large arrows) are present around intracellular hypha. Note fungal mitochondria and lipid drops.

x75000


L
Ta
m
mx
HW
5.38c

Figure 5.39

Association of haustorium with host nucleus. The intervening cytoplasm includes a crystal-containing microbody and mitochondria.

x18750

Figure 5.40

Part of haustorium body showing nucleus, vacuole and vesicle with membranous material (arrowhead). Note the close proximity of fungal nucleus and host nucleus. Host mitochondria lie between haustorium and host nucleus.

x15000

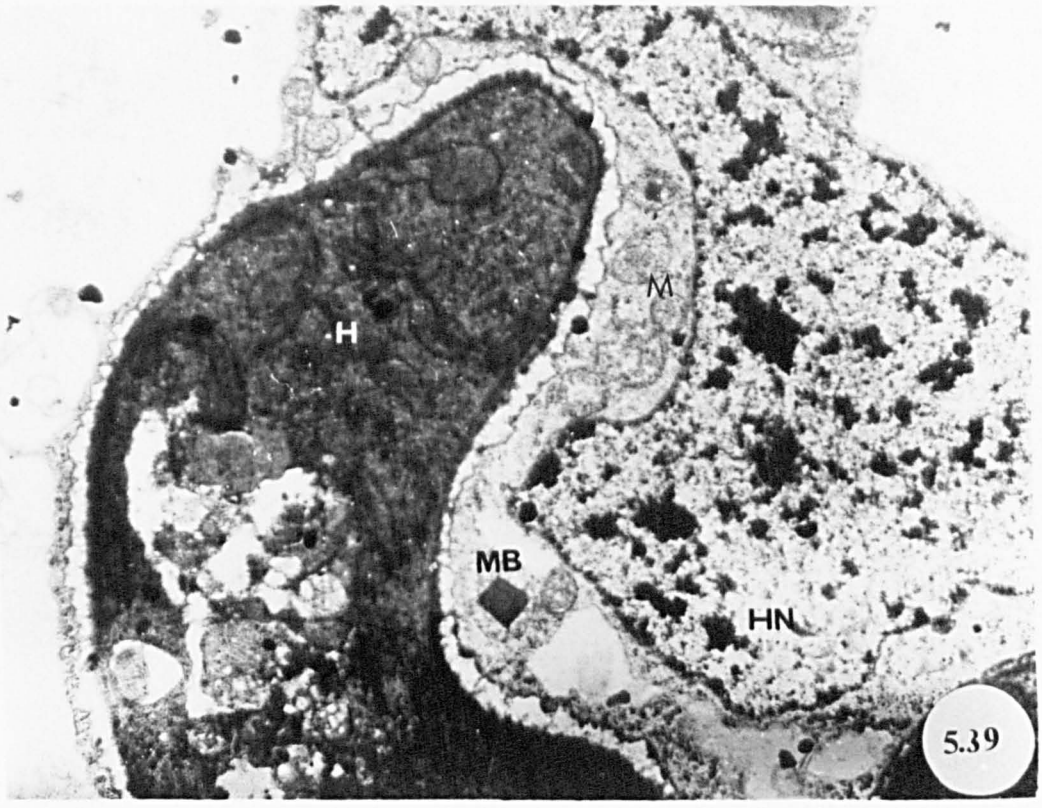

5.39

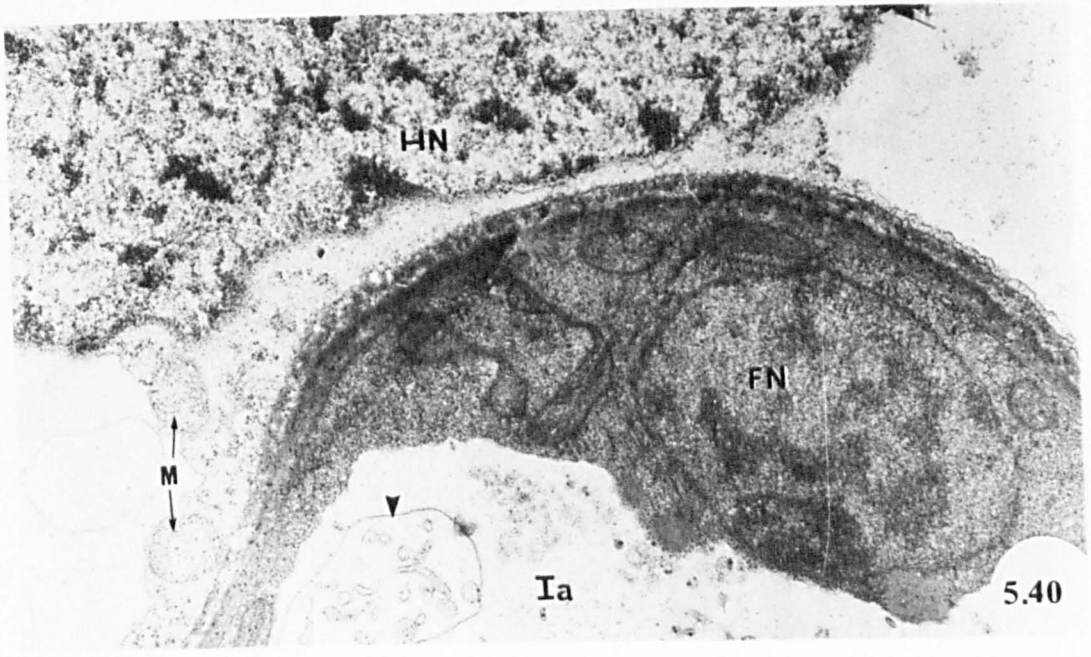

5.40

Figure 5.41

Transverse section of monokaryotic hypha surrounded by host wall-like material in phloem parenchyma cells. Some cristae of the mitochondria appear to be continuous with the endoplasmic reticulum (arrows). Note plasmodesmata.

x50000

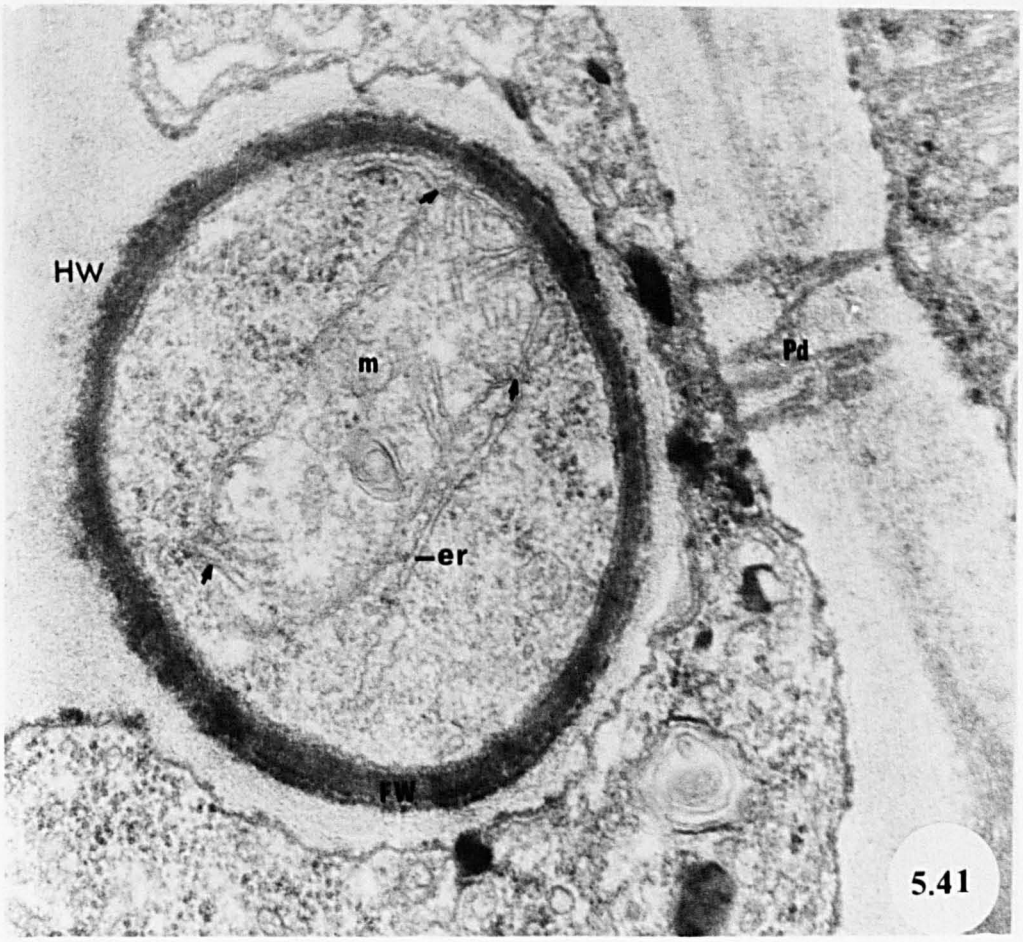
HW
m
Pd
er
FW
5.41

Figure 5.42

Diagrammatic representation of structural differences between haustorium (1, 2, 3) and intracellular hypha (4, 5, 6) of *P. poarum* (see text).

1, 4: General morphology of haustorium and intracellular hypha showing differentiation of neck, body and mother cell and relationship to host cell wall.

2, 5: Detail of neck region and mother cell at point of penetration. Note the localized thickening, collar-like region and neckband. Relative sizes of neck regions and other parts are indicated in 1 and 4.

3, 6: Matrix region containing electron-dense fibrils around haustorium wall and host wall-like material surrounded by less dense fibrils around intracellular hypha.

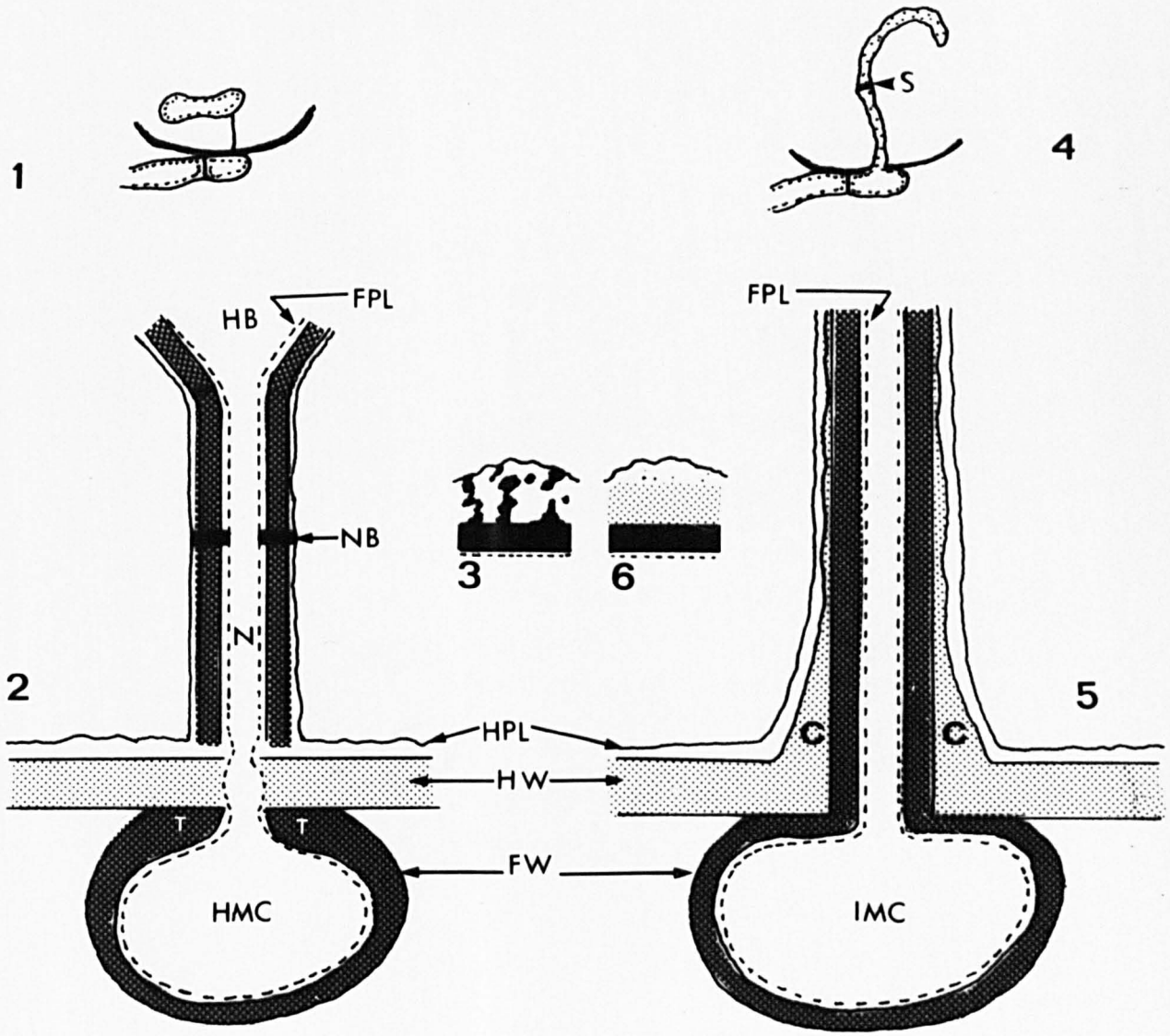
1
S
4
FPL
HB
FPL
NB
3
6
N
2
5
HPL
C
C
HW
T
T
FW
HMC
IMC

Figure 6.1 and 6.2

P. poarum on *Tussilago farfara*. Scale lines = 10 μm

Figure 6.1

Transverse section of minor vein of *Tussilago* leaf, showing infection of vascular tissue. Note the relative density of intracellular hyphae in parenchyma (arrows) of phloem and xylem and in bundle sheath, compared with distribution in mesophyll of intercellular and intracellular hyphae (semi-thin section of Epon-embedded tissue).

Figure 6.2

Longitudinal section of infected *Tussilago* leaf, showing intracellular hyphae (arrowheads) in phloem parenchyma, bundle sheath and mesophyll cells. No infection of non-living xylem elements is seen (semi-thin section of Epon-embedded tissue).

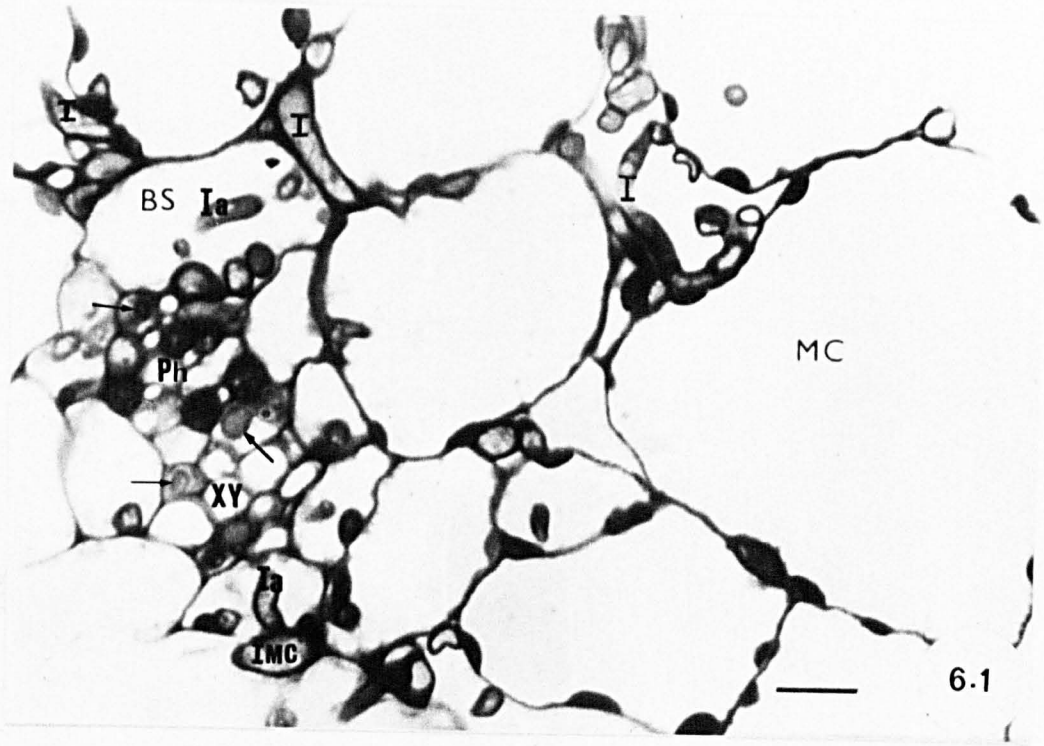

6.1

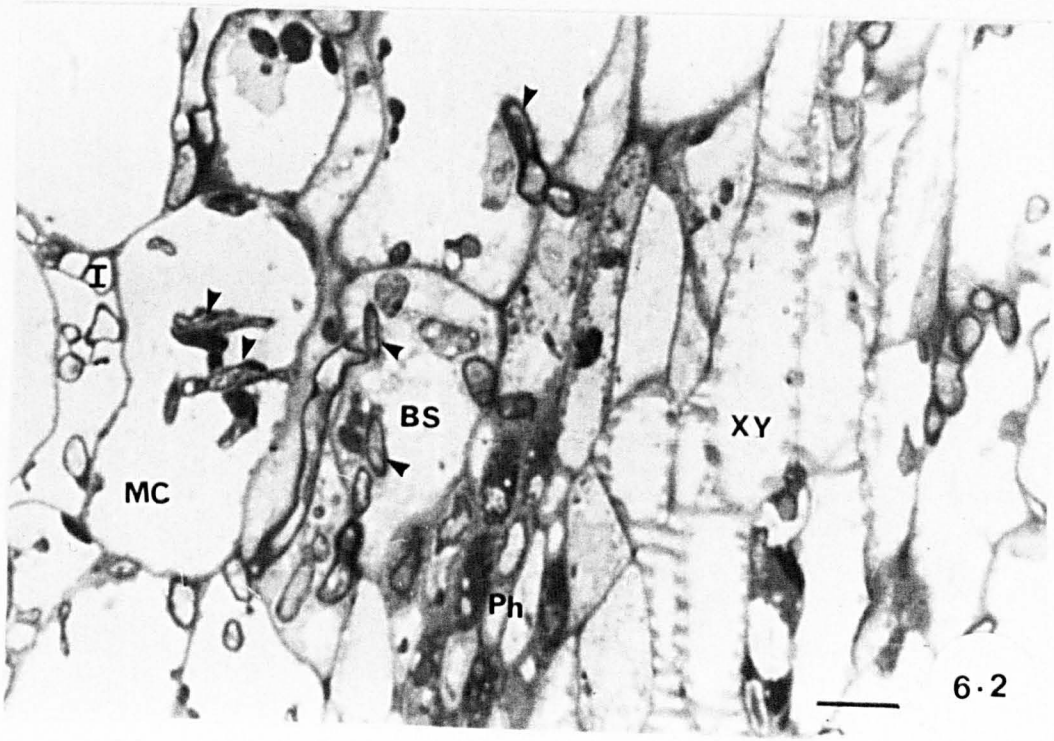

6·2

Figure 6.3 and 6.4

P. poarum on *Tussilago farfara*. Scale lines = 10 µm

Figure 6.3

Longitudinal section of *Tussilago* leaf tangential to minor vein, showing intracellular hyphae containing lipid drops (arrowheads) in bundle sheath cells.

Figure 6.4a

Semi-thin section of large vascular bundle of infected *Tussilago* leaf at later stage of infection showing invasion of non-living xylem element by intracellular hypha. Note intracellular hyphae in xylem parenchyma and bundle sheath cells.

Figure 6.4b

Serial section of Figure 6.4a showing penetration by intracellular hyphae (arrows) of phloem and xylem parenchyma, xylem tracheary element, and bundle sheath cells. No infection of sieve tubes is seen.

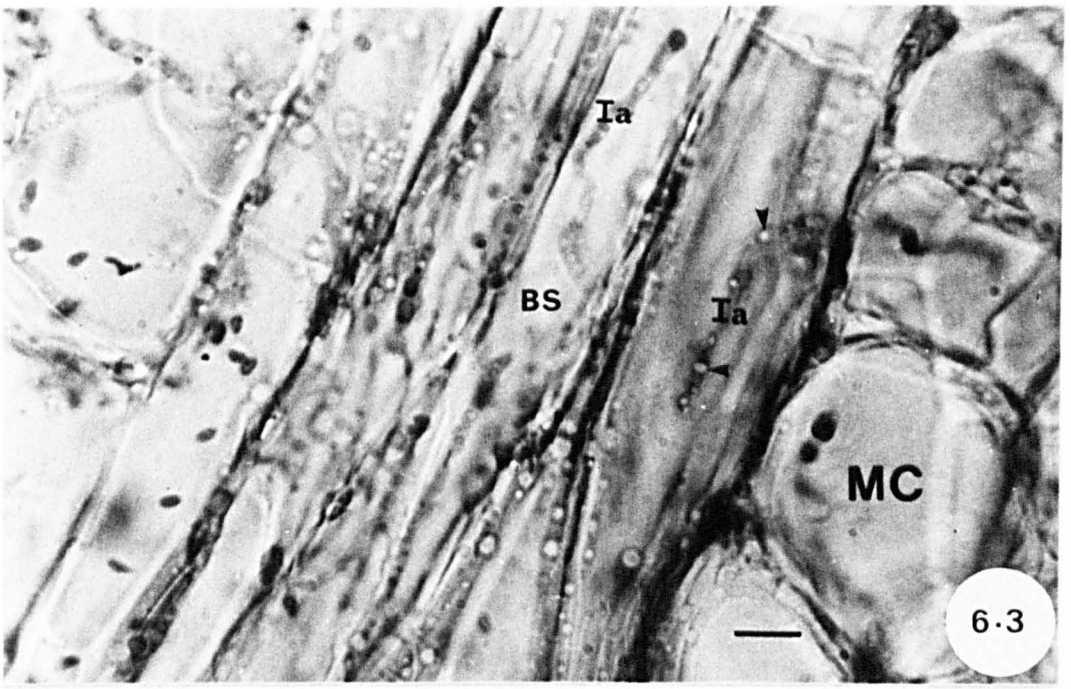

6.3

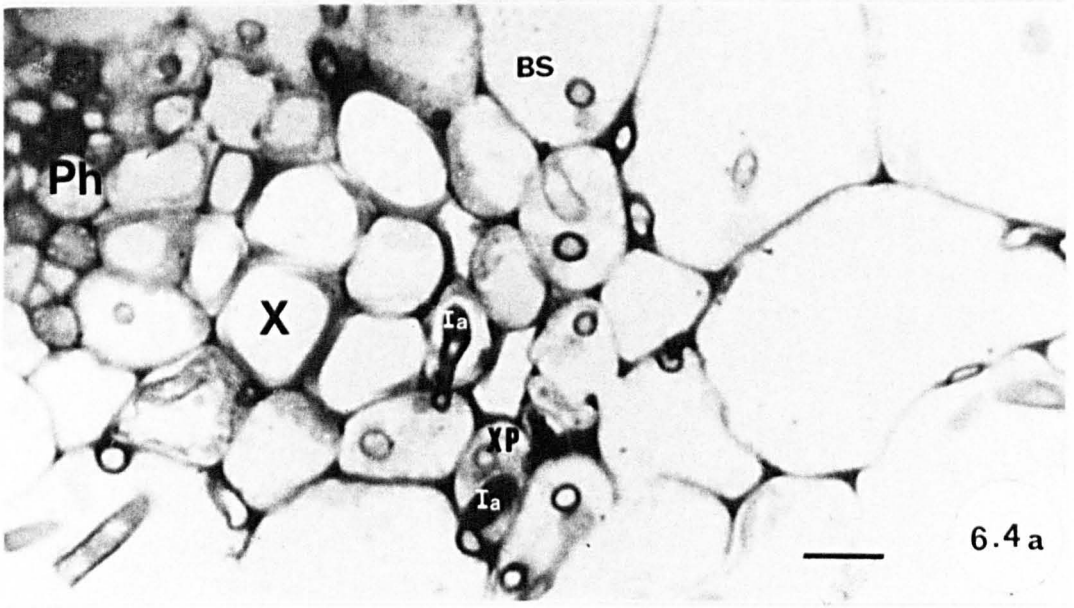

6.4a

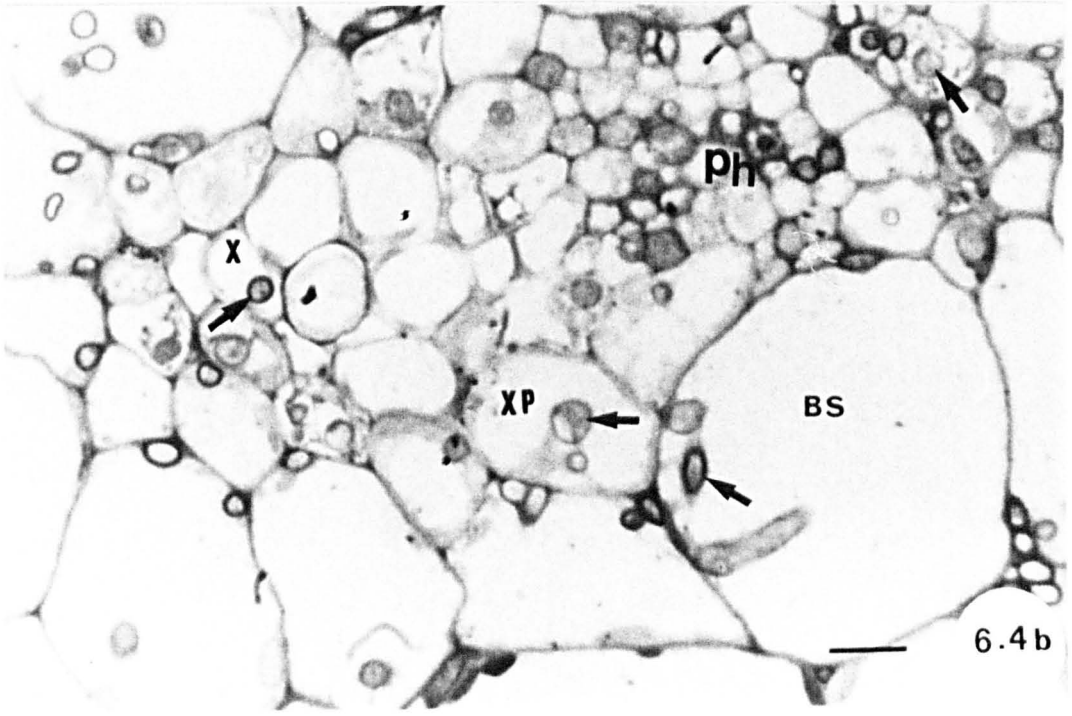

6.4b

Figure 6.5

Transverse section of vascular bundle of *Poa*, showing infections of bundle sheath by haustoria but no penetration of vascular tissue enclosed by the thickened endodermis. The arrow indicates a haustorium lying slightly out of the plane of focus of the section. Thickened fibres lie between the vascular bundle and epidermis.

Scale line = 10 μm

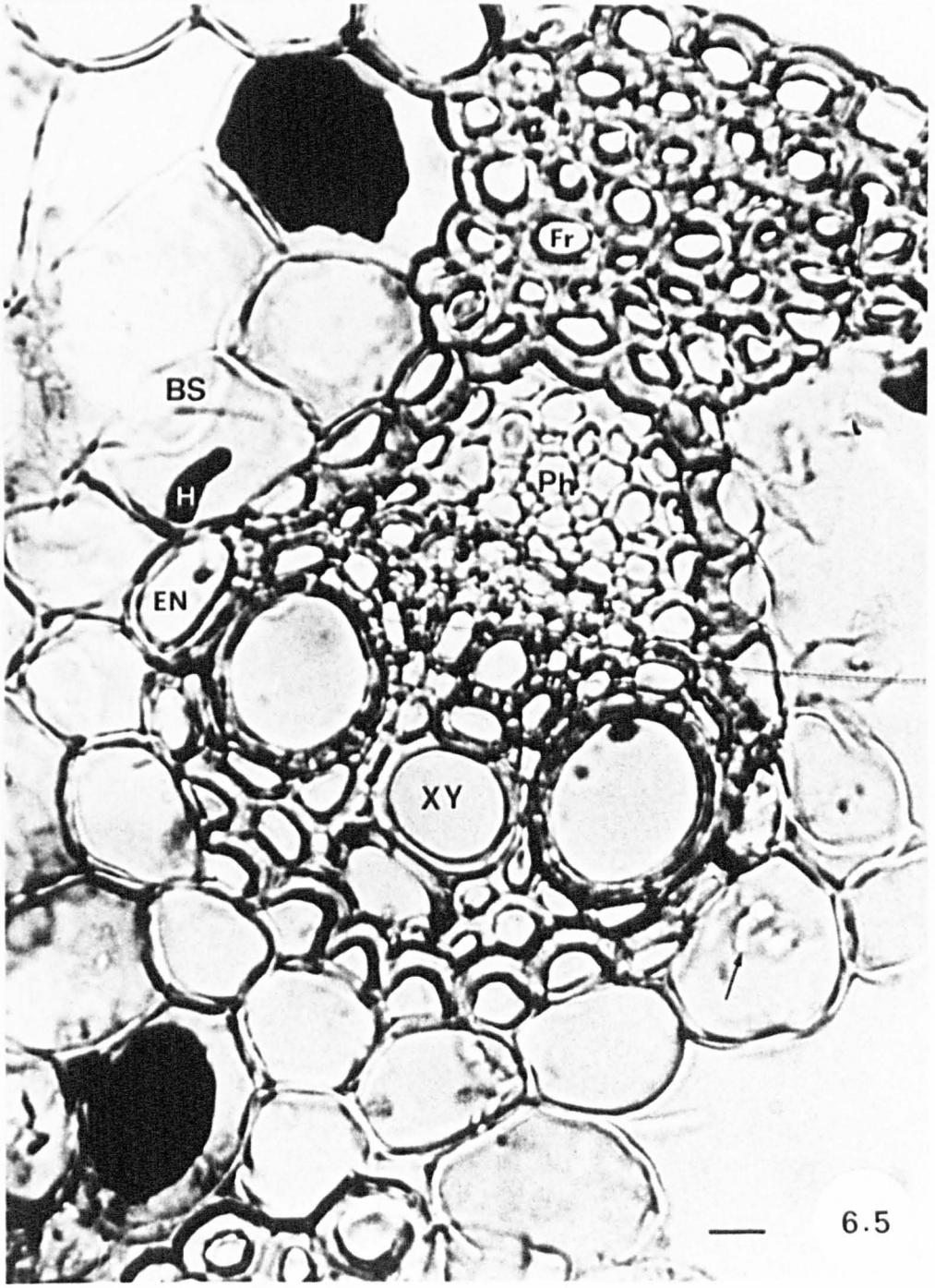

6.5

Figure 6.6

P. poarum infections on *Poa pratensis*.

Scale lines = 10 µm

a - longitudinal section of vascular strands of *Poa* leaf, showing haustorium in bundle sheath cell.

b - isolated bundle sheath cell containing two elongated haustoria.

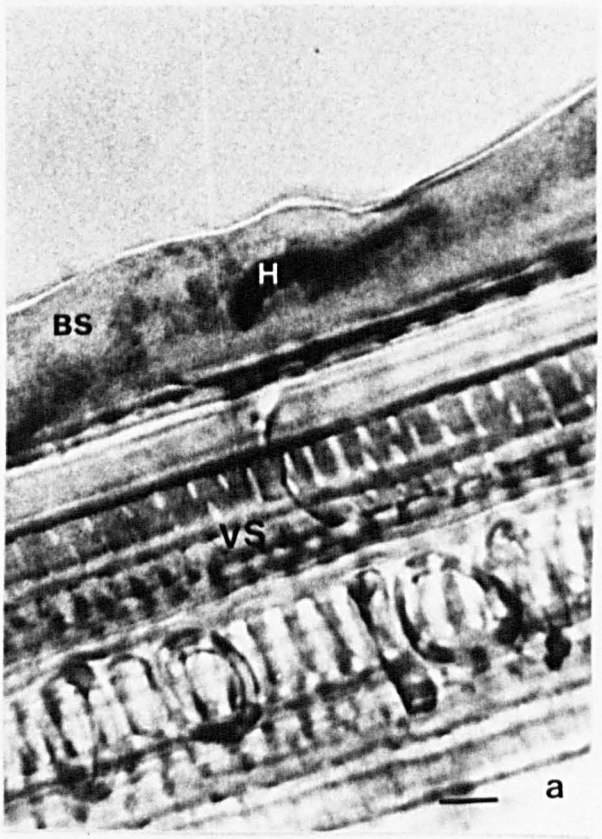
H
BS
VS
a

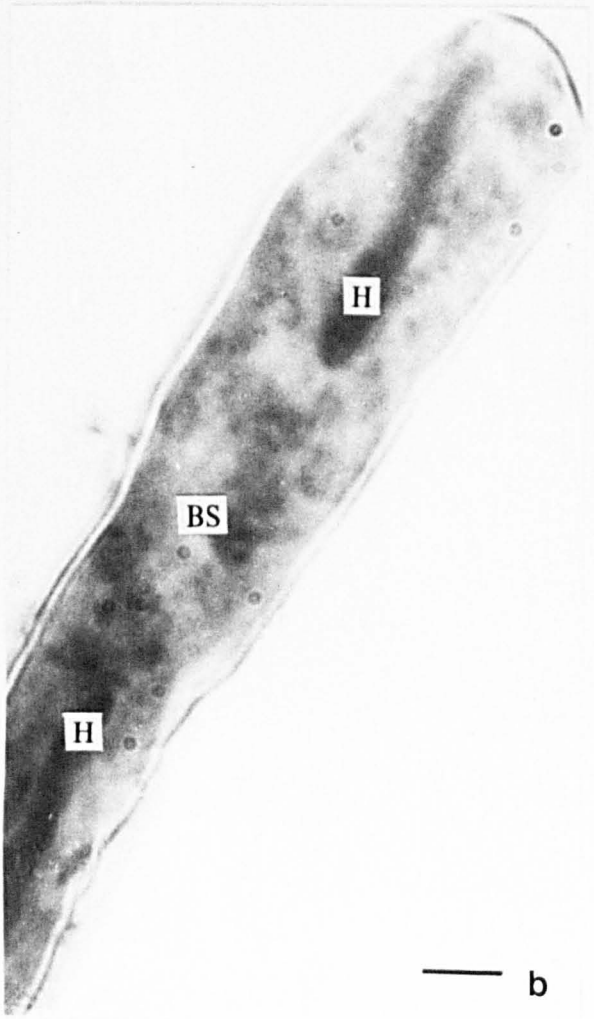
H
BS
H
b

Figure 6.7

Transverse section of small vascular bundle of *Tussilago* leaf at an early stage of infection by monokaryon of *Puccinia poarum*. Intercellular hyphae, in one of which the fungal nucleus can be seen, lie between mesophyll and bundle sheath cells. Intracellular hyphae occur in cells of mesophyll, bundle sheath, phloem parenchyma and xylem parenchyma but not in sieve tubes and tracheary elements. Intracellular hyphae are more frequent in bundle sheath cells than in the living cells associated with xylem or phloem.

x3000

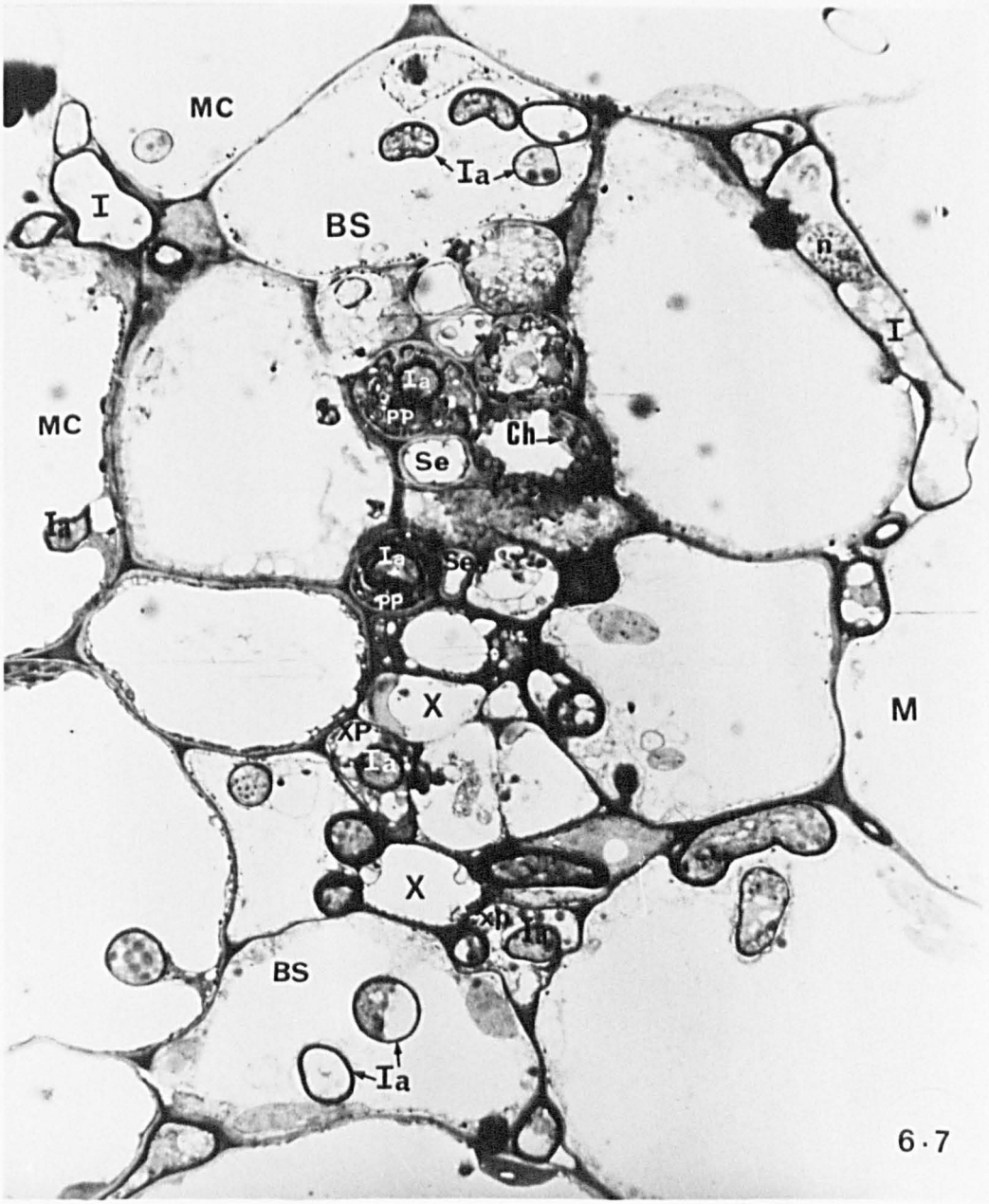
MC
Ia
I
BS
n
I
Ia
MC
PP
Ch
Se
Ia
Ia
Se
PP
X
M
XP
Ia
X
xh
Ph
BS
Ia
6·7

Figure 6.8

Transverse section of large vascular bundle of *Tussilago* leaf at an early stage of pycnial infection. Intracellular hyphae occur in bundle sheath, xylem parenchyma, phloem parenchyma and companion cells. The frequency of phloem transfer cells and the complexity of their wall proliferations appear less than in Figure 6.12. An ingrowth of host wall-like material occurs in advance of the penetrating fungus (arrow). Note nucleus with large nucleolus in xylem parenchyma cell.

x3750

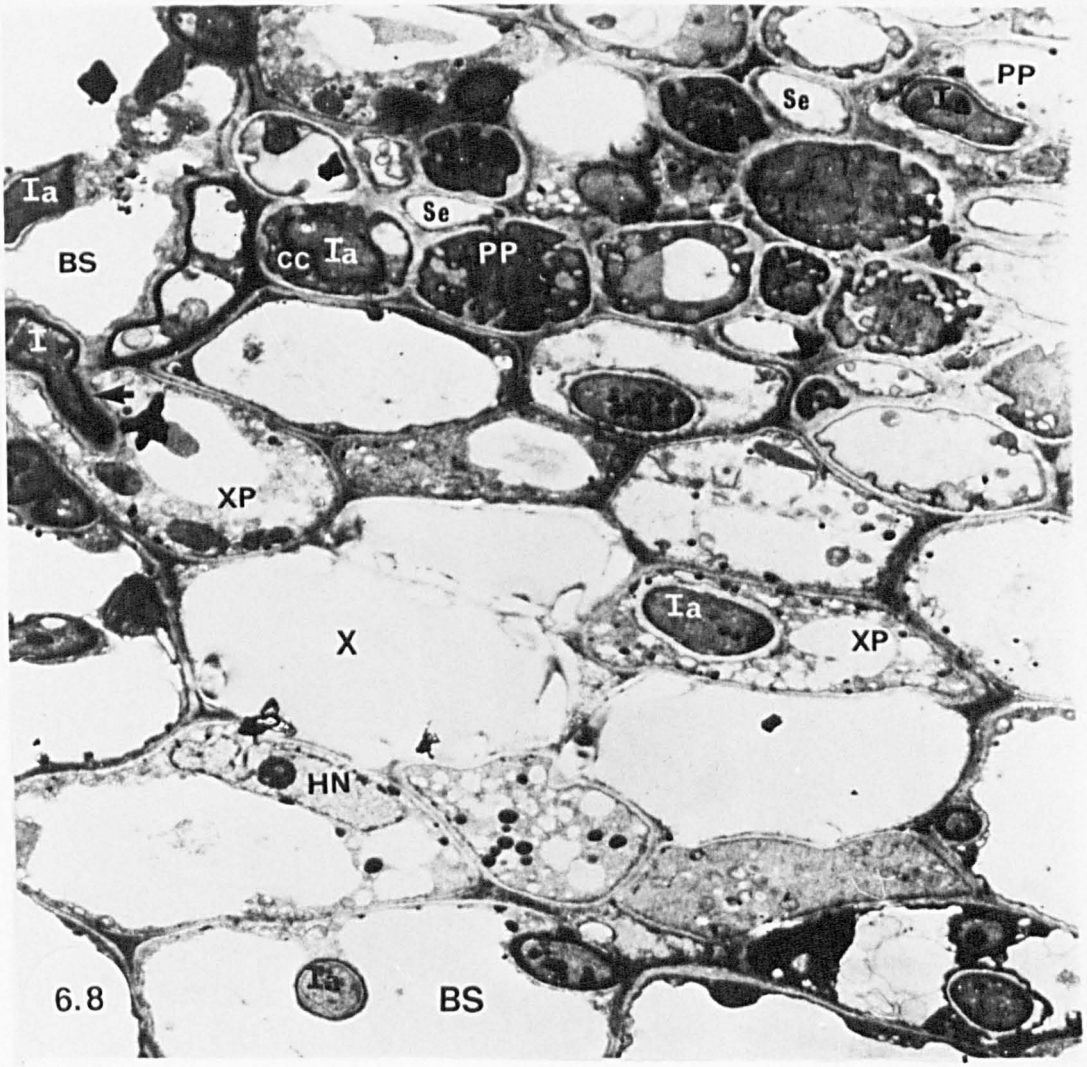
PP
Se
I
Ia
Se
BS
cc Ia
PP
I
XP
Ia
X
XP
HN
6.8
Ia
BS

Figure 6.9

Transverse section of vein of *Tussilago* at early aecial stage of infection with *P. poarum*. More extensive invasion of phloem parenchyma and xylem parenchyma has occurred. Cell walls of some intercellular and intracellular hyphae are thicker and more electron-dense than in Figure 6.7.

x3600

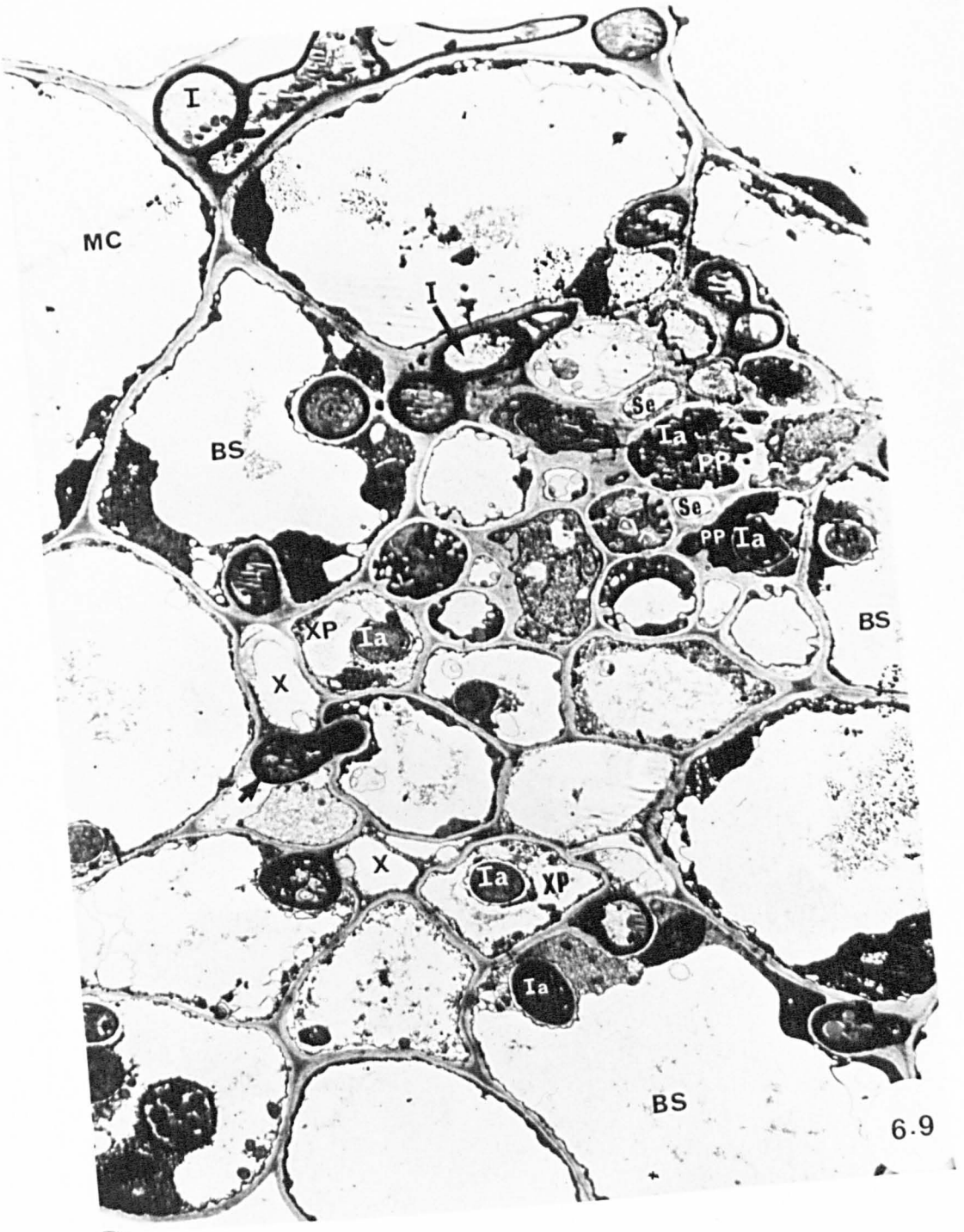

6.9

Figure 6.10

Part of transverse section of vascular bundle of *Tussilago* showing intracellular hyphae in bundle sheath cells, xylem parenchyma and companion cells. Transfer cells of phloem parenchyma show dense cytoplasm, wall ingrowths and large, lobed nucleus. No intervening space occurs between wall ingrowths and plasmalemma. Some hyphae lying adjacent to host cell wall are embedded in wall material similar in staining reaction to host cell wall. Inter- and intracellular hyphae of bundle sheath and xylem parenchyma contain lipid drops. A well-defined membrane surrounds intracellular hyphae.

Note plasmodesmata (arrowheads) in the phloem region.

x7500

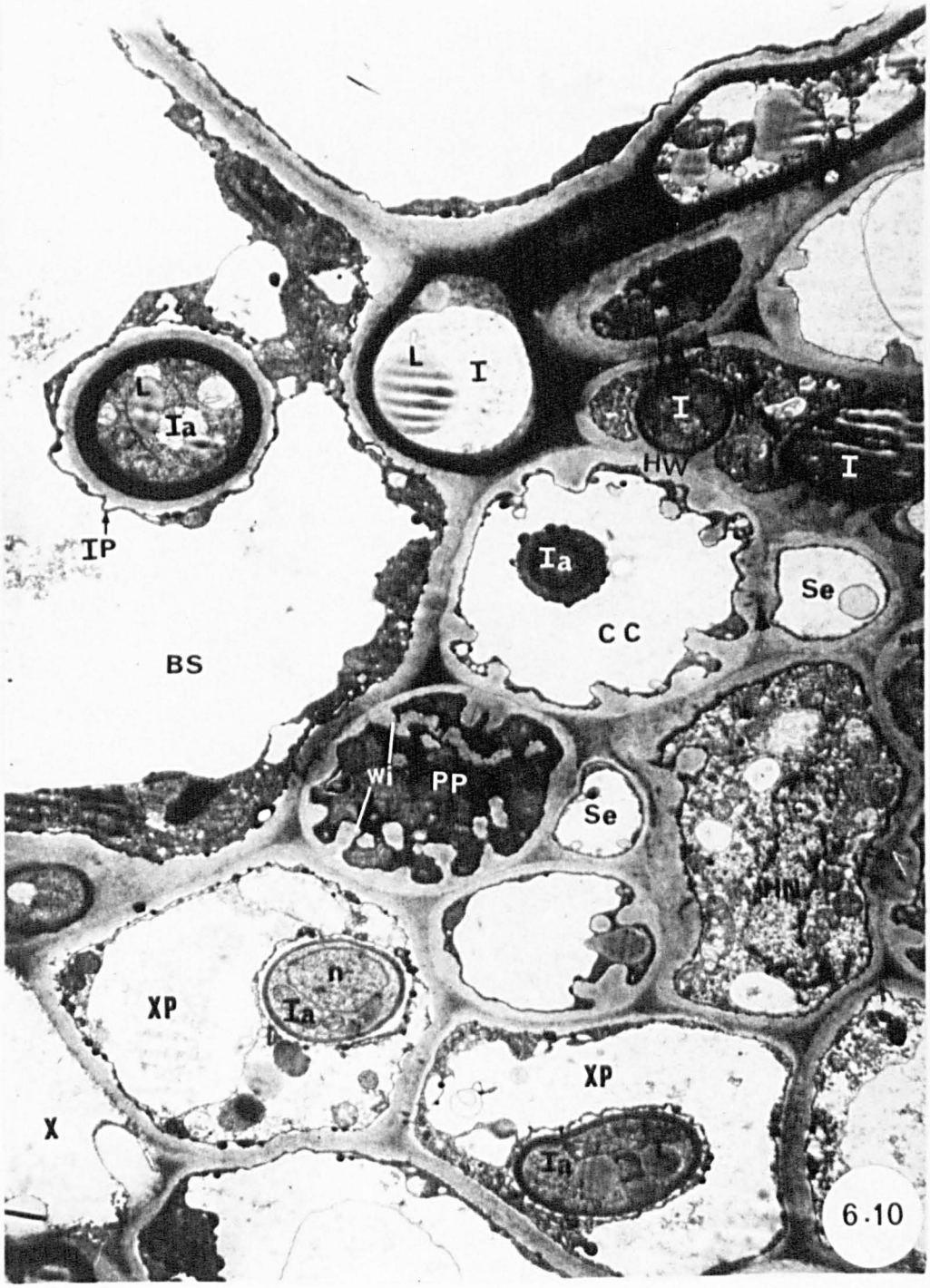
L
Ia
IP
L
I
I
HW
I
Ia
Se
CC
BS
wi
PP
Se
XP
n
Ia
XP
X
Ia
6.10

Figure 6.11

Part of phloem in infected leaf of *Tussilago* showing the invasion of phloem transfer cells by intracellular hyphae.
A lomasome-like structure (arrows) occurs between wall ingrowths and host plasmalemma.
Note the wall ingrowths (arrowheads) are closely attached to the plasmalemma without leaving an intervening space.
Note also the enlarged and lobed host nucleus.

x7500

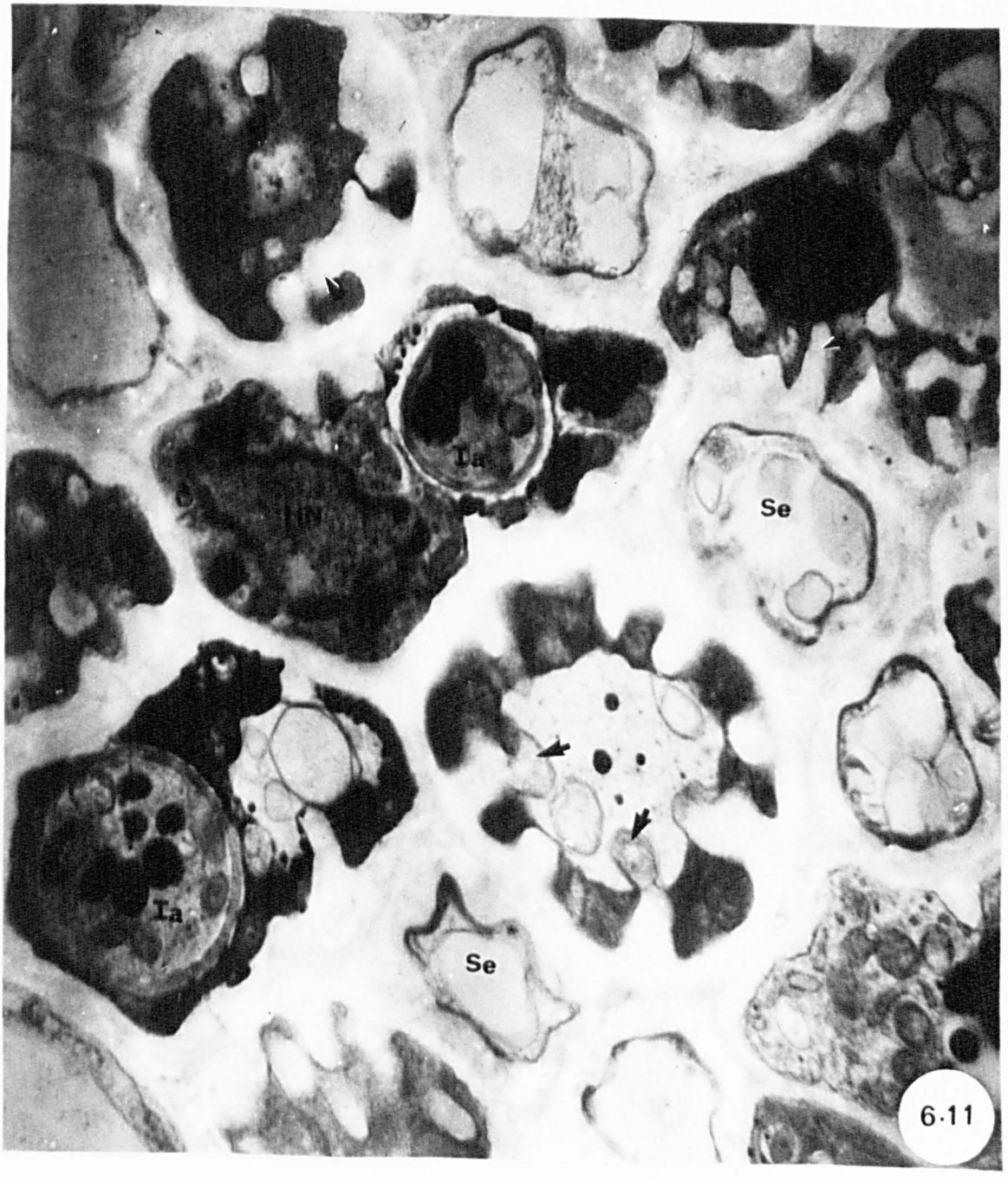
Ia
Se
Ia
Se
6·11

Figure 6.12

Part of phloem in healthy leaf of *Tussilago* showing phloem parenchyma and companion cells modified by the extensive development of wall ingrowths. In these transfer cells, an intervening space (arrows) is present between wall ingrowths and plasmalemma. Chloroplasts and many mitochondria are present in the vicinity of the wall ingrowths.
Note plasmodesmata (arrowhead) in the wall between sieve element and companion cell.

x10000


Wl
Wl
Ch
M
Se
M
6.12

Figure 6.13

Part of vascular bundle in infected leaf of *Tussilago*. The transfer cells of the infected phloem show lomasome-like structure (arrow) between plasmalemma and wall ingrowths. Note intercellular hyphae embedded in host wall and intracellular hypha in bundle sheath cell surrounded by host wall-like material (arrowhead).

x12500

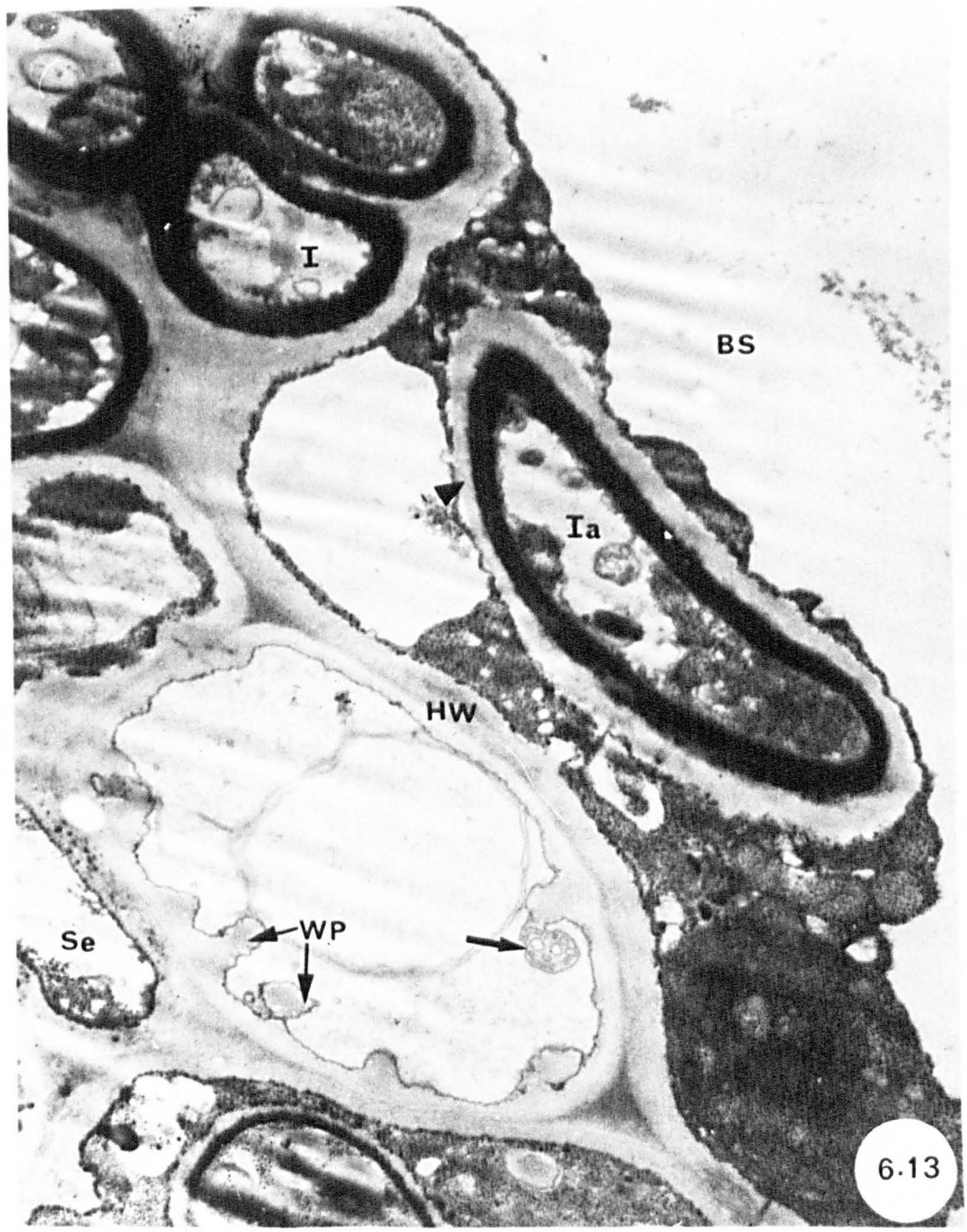
I
BS
Ia
HW
WP
Se
6.13

Figure 6.14

Part of healthy phloem of *Tussilago* showing transfer cells. Intervening space is seen between wall ingrowths and plasmalemma. Note dense cytoplasm and nuclei with nucleoli.

x7500

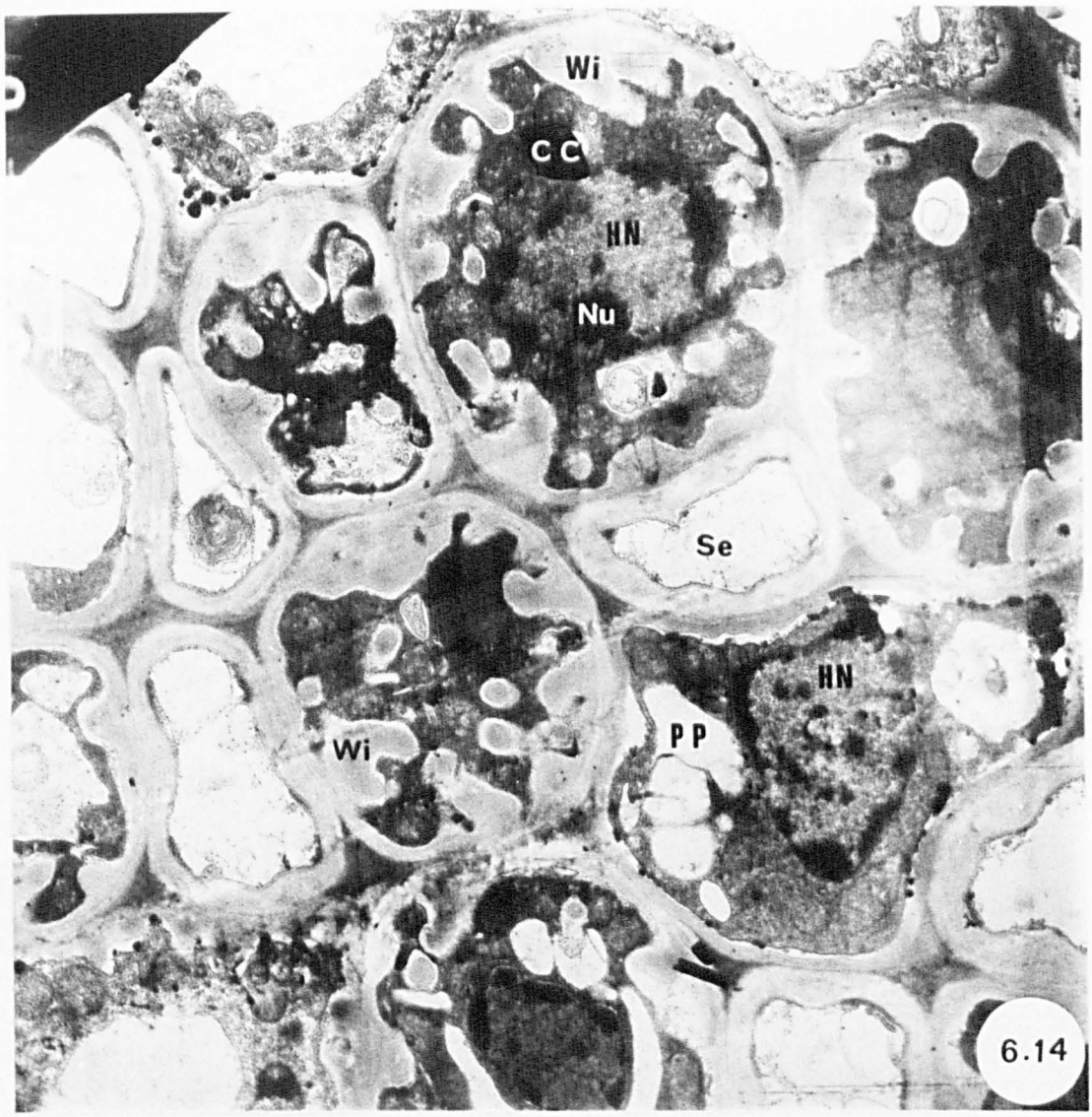
Wi
C C
HN
Nu
Se
HN
P P
Wi
6.14

Figure 6.15a

Part of vascular bundle of *Tussilago* leaf showing hyphae in xylem parenchyma and bundle sheath cells.
Note tracheary element with thickening (solid arrows) and evidence of breakdown of primary wall (open arrow).
Note also hyphae in bundle sheath, showing electron-dense wall layer enclosed by host cell wall.

x7500

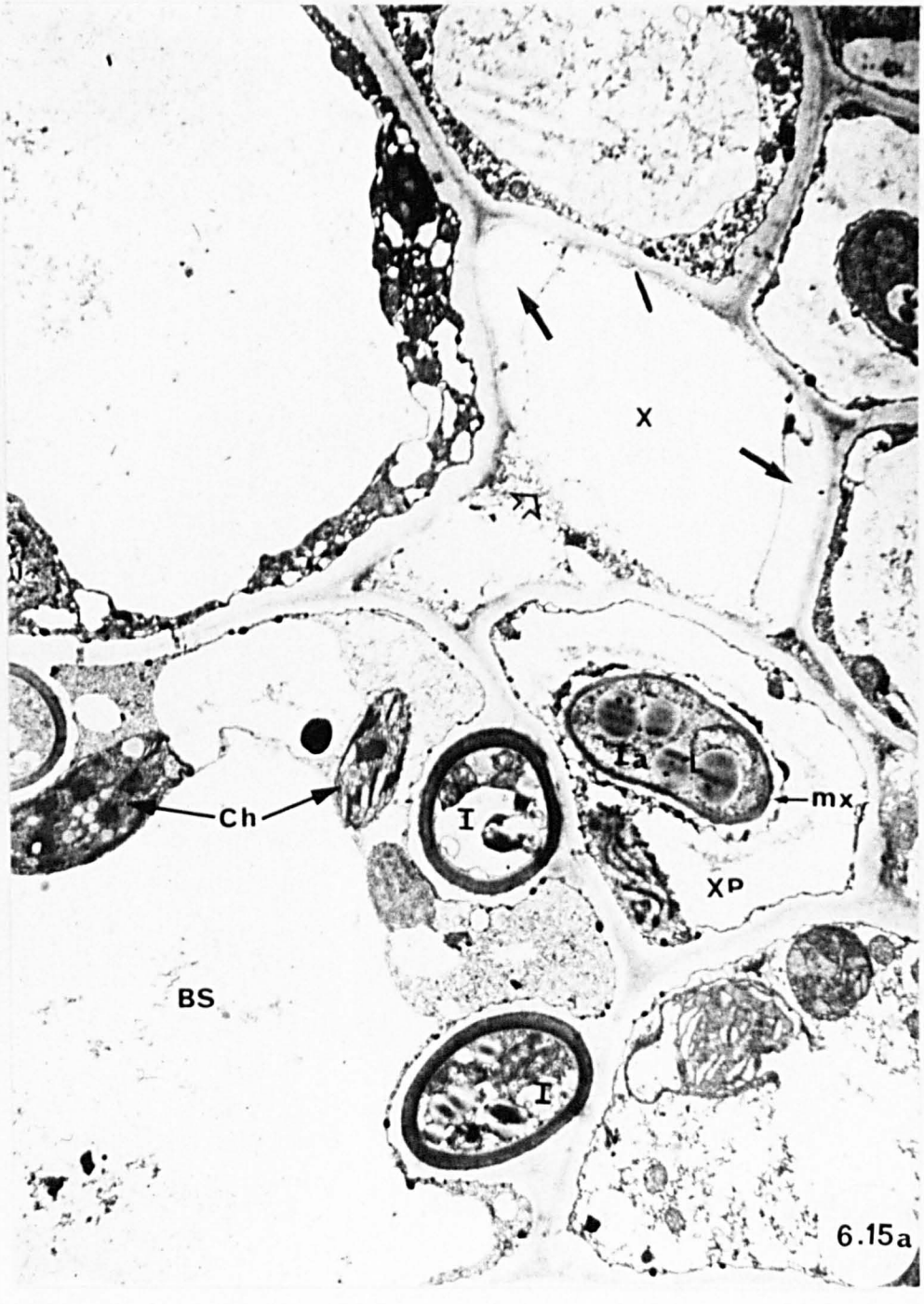
X
Ch
I
Ia
mx
XP
BS
I
6.15a

Figure 6.15b

Part of vascular bundle of *Tussilago* leaf showing invasion of xylem by intercellular and intracellular hyphae. Hyphae with thick, electron-dense walls lie in close contact with xylem elements and bundle sheath cells. Note tracheary element and evidence of breakdown of primary wall (arrow). Note also highly vacuolated xylem parenchyma cells and plasmodesmata (arrowheads) between them.

x7500

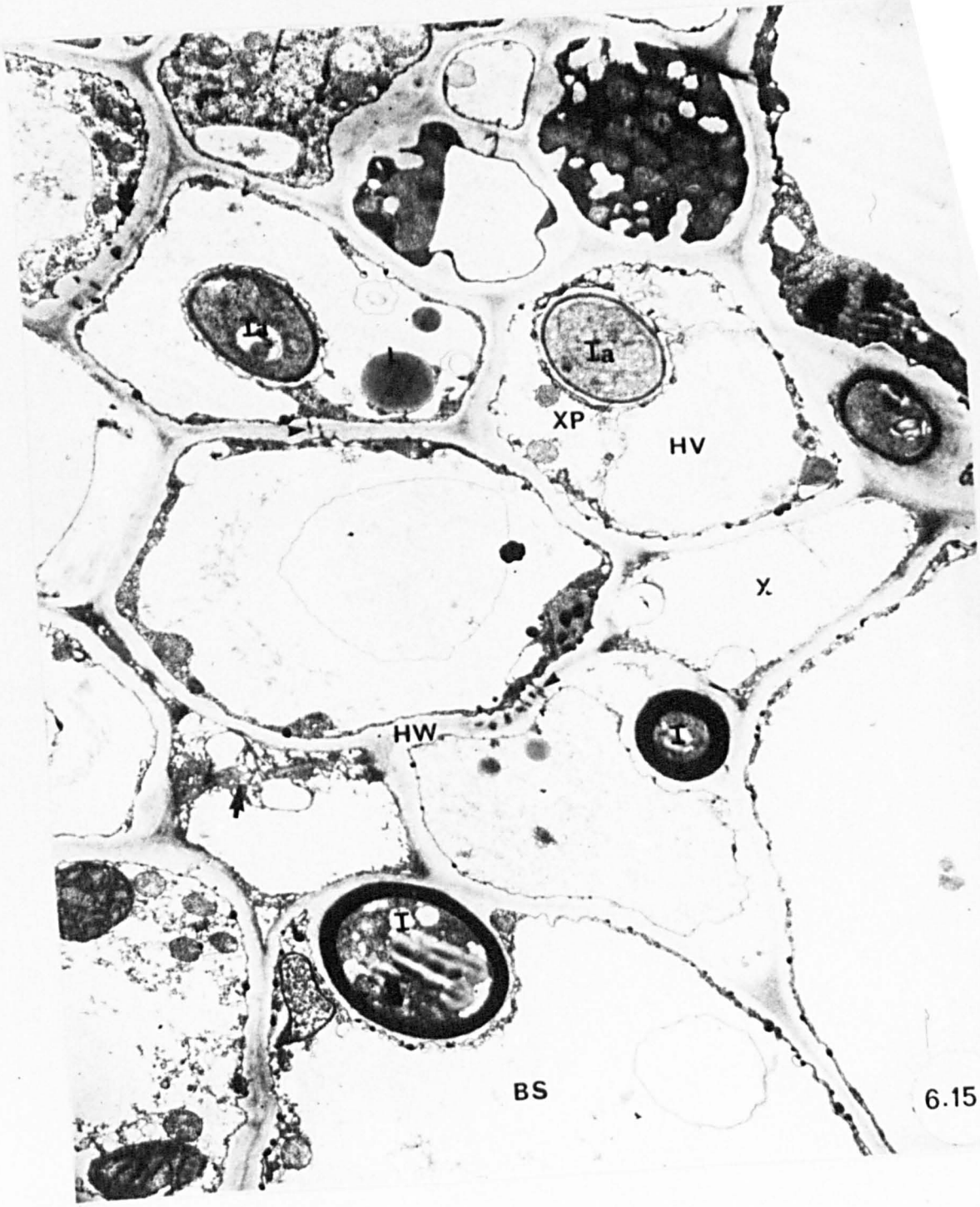
Ia
XP
HV
X
HW
I
I
BS
6.15b

Figure 6.16a

Fungal hypha growing between xylem vessel and xylem parenchyma of *Tussilago* leaf. Note only a thin layer of host wall (arrow) separating the hypha from the vessel lumen. Note also lipid droplets, mitochondria and glycogen-like deposits (arrowheads).

x22750

6·16 a

Figure 6.16b

Part of invaded vascular bundle of *Tussilago* leaf showing intracellular hypha in xylem parenchyma and hyphae projecting into the cell lumen of bundle sheath cell. Black glycogen-like particles (small arrows) are seen in fungal hyphae. Note the breakdown of walls of xylem elements (large arrow). Note also lipid droplets in both host and parasite.

x12500


X
I
L
HW
I
L
Ia
mx
L
L
BS
6.16b

Figure 6.17

Part of phloem in longitudinal section of healthy vascular bundle of *Tussilago* leaf showing phloem parenchyma containing nucleus with nucleolus. Note wall ingrowths (arrows) in phloem parenchyma and companion cells.

x10000

Figure 6.18

Part of infected phloem region of *Tussilago* leaf showing phloem parenchyma cells. No nucleolus is seen in the host nucleus. Note intracellular hypha and wall ingrowths.

x15000

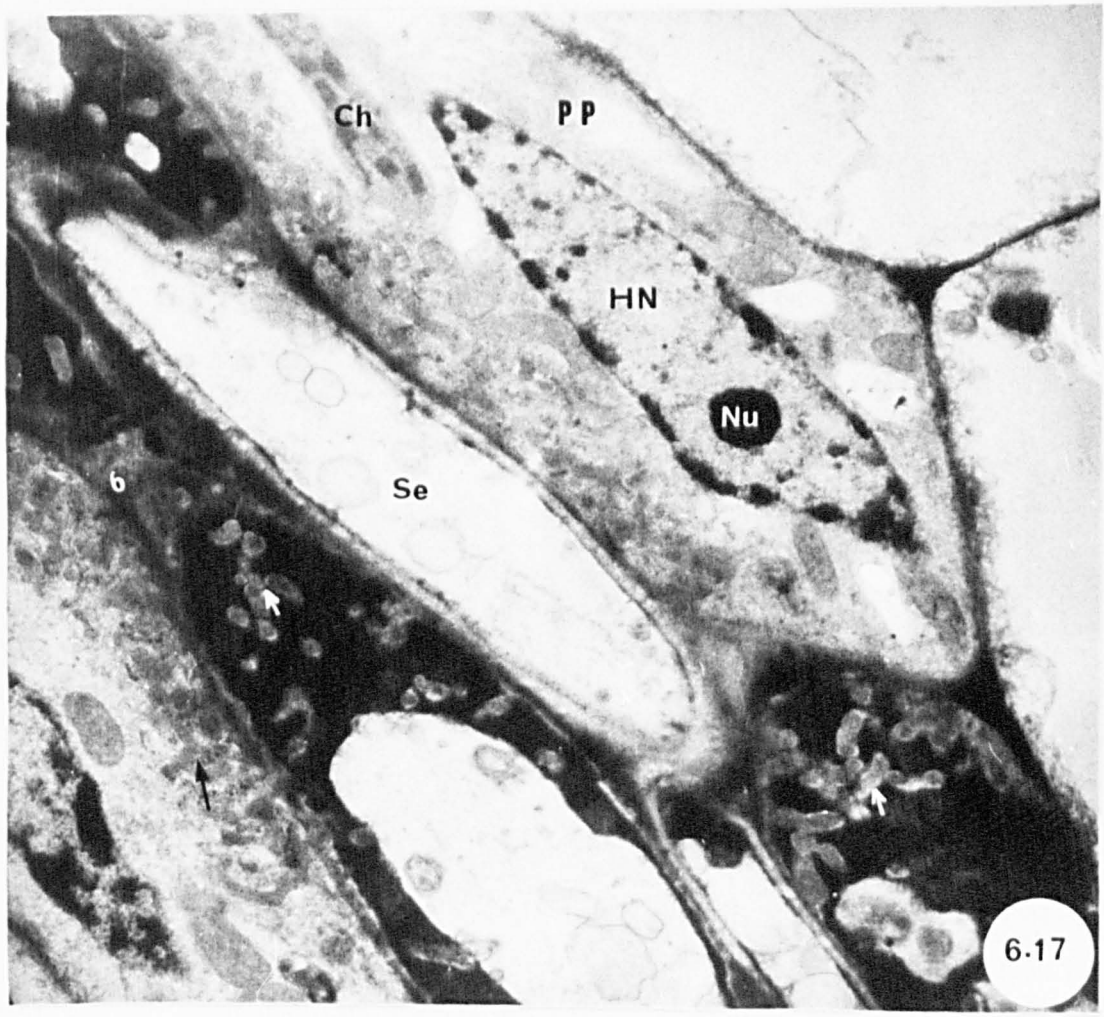

6.17

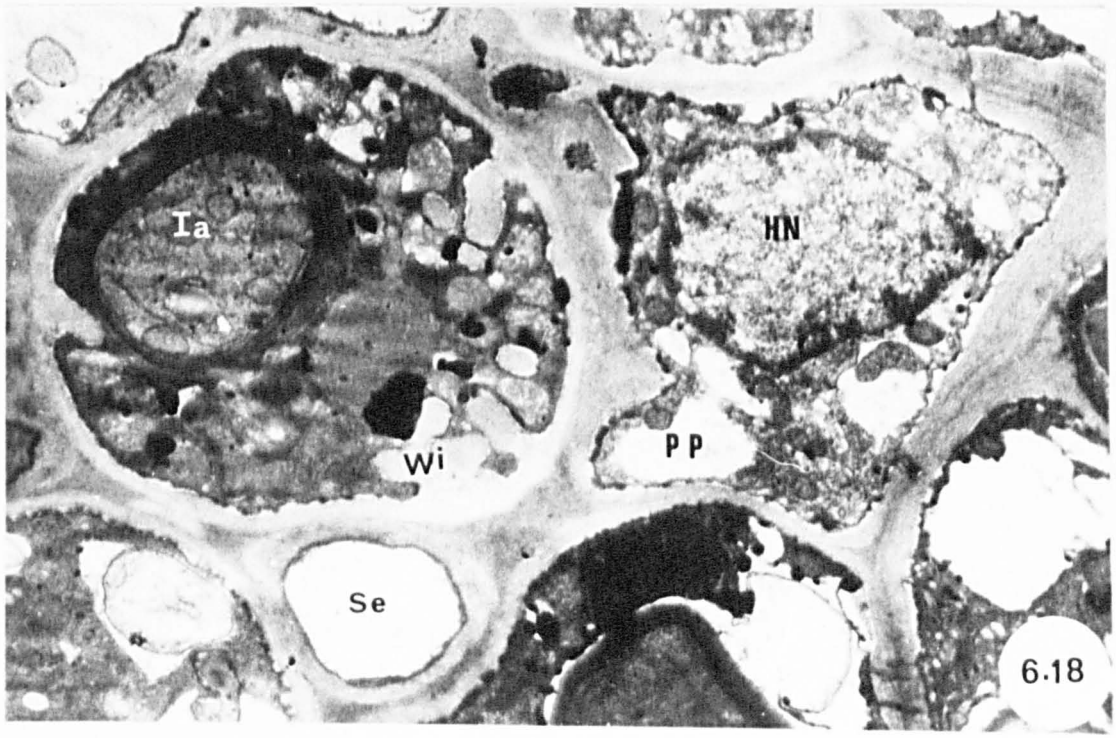

6.18

Figure 6.19a

Intracellular hypha in bundle sheath cell showing electron-dense wall layer, enclosed in a layer of material resembling host cell wall which partly occupies the matrix region, invaginated host plasma membrane and lipid drops.
Note the intercellular hypha lying adjacent to host cell wall.

x25000

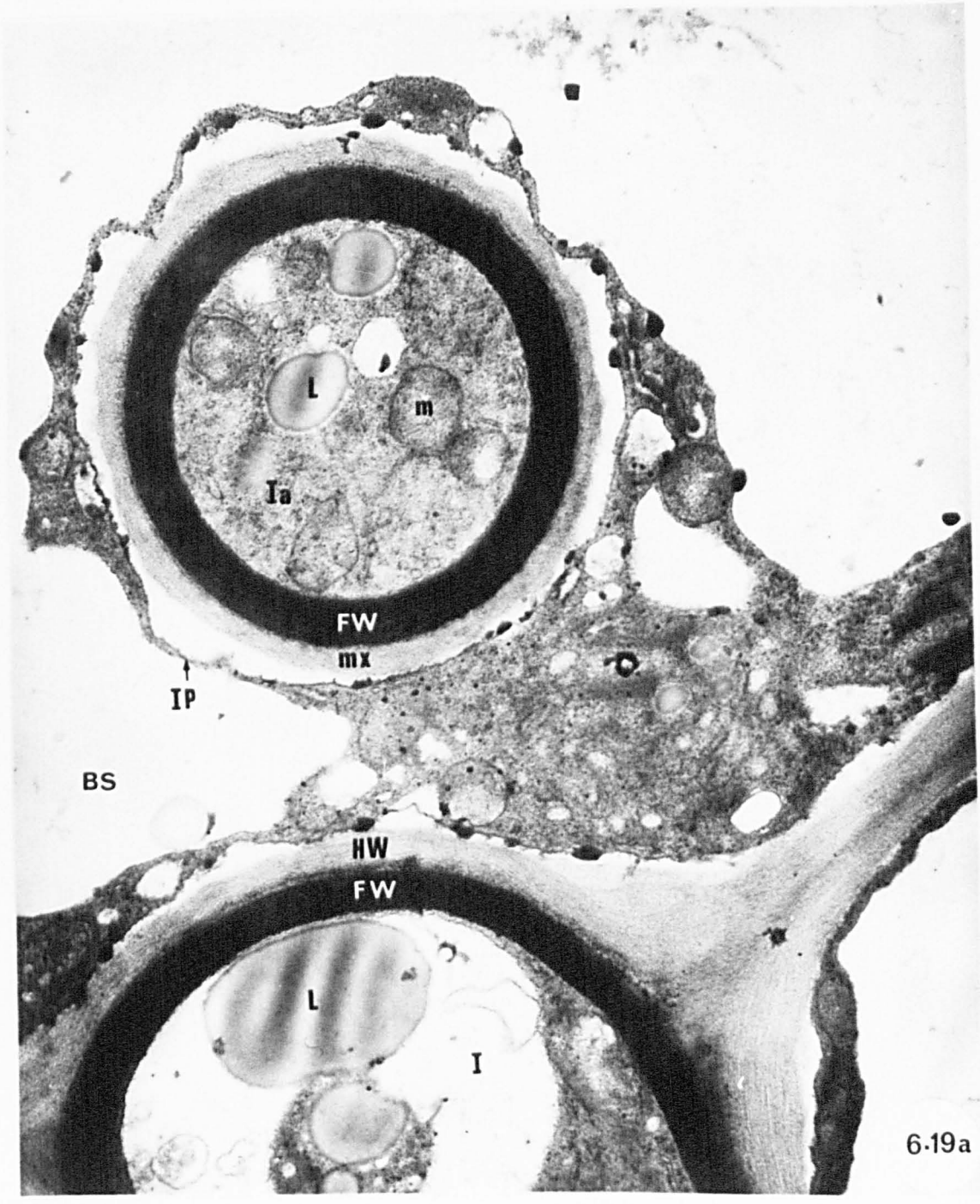

6·19a

Figure 6.19b

Intracellular hypha in phloem parenchyma cell and bundle sheath cell.

Note sieve tube, plasmodesmata, matrix and its bounding membrane, mitochondria and host nucleus. Fibrillar material appears to be present in expanded region of the matrix of intracellular hypha in phloem parenchyma (unlabelled arrows).

x18750

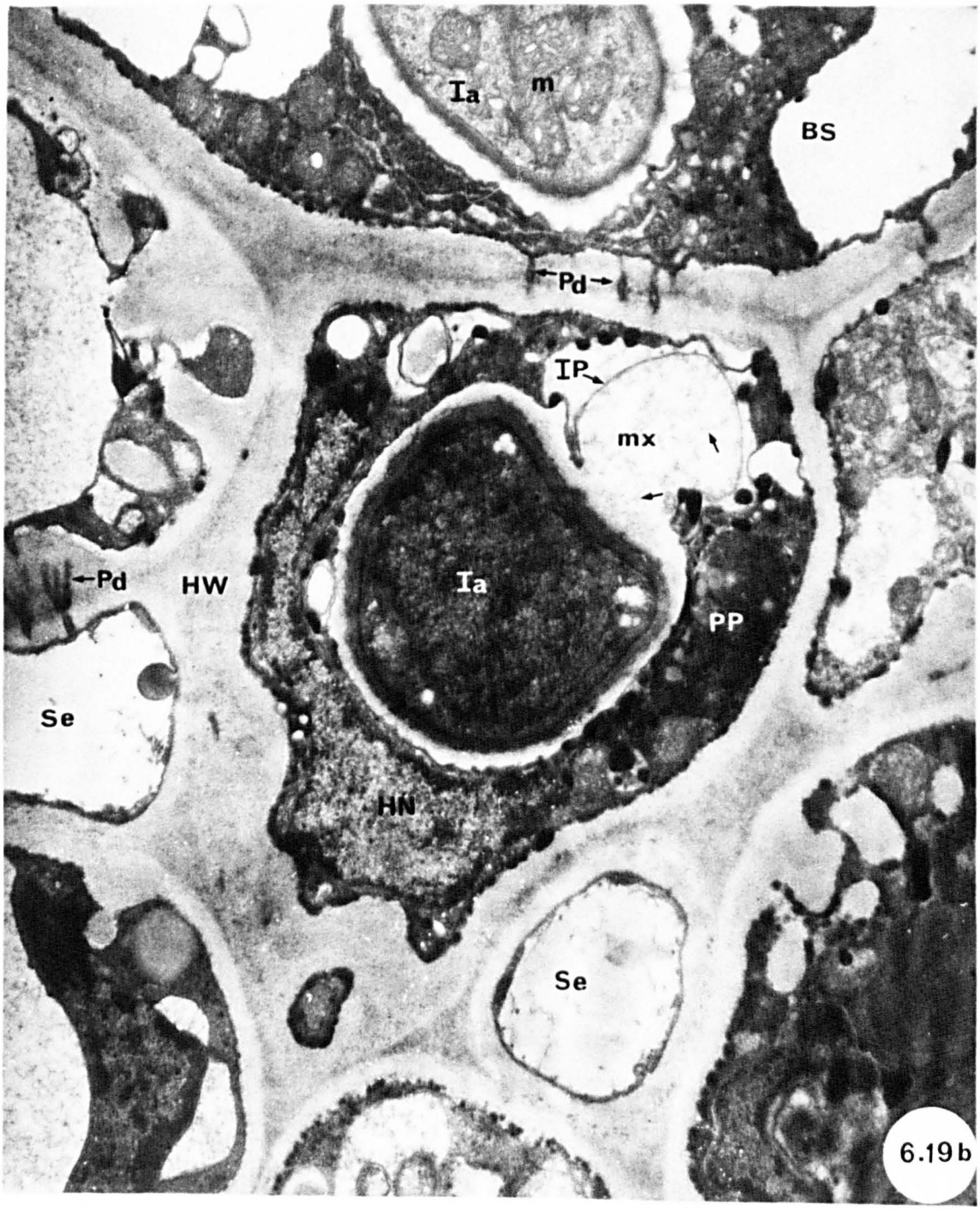
Ia
m
BS
Pd
IP
mx
Ia
Pd
HW
PP
Se
HN
Se
6.19b

Figure 6.20

Monokaryotic hypha lying adjacent to cell wall of bundle sheath cell. The hypha is embedded in wall material similar in staining reaction to host cell wall. Note thick, electron-dense fungal wall, mitochondria and fungal nucleus with its double membrane.

x50000

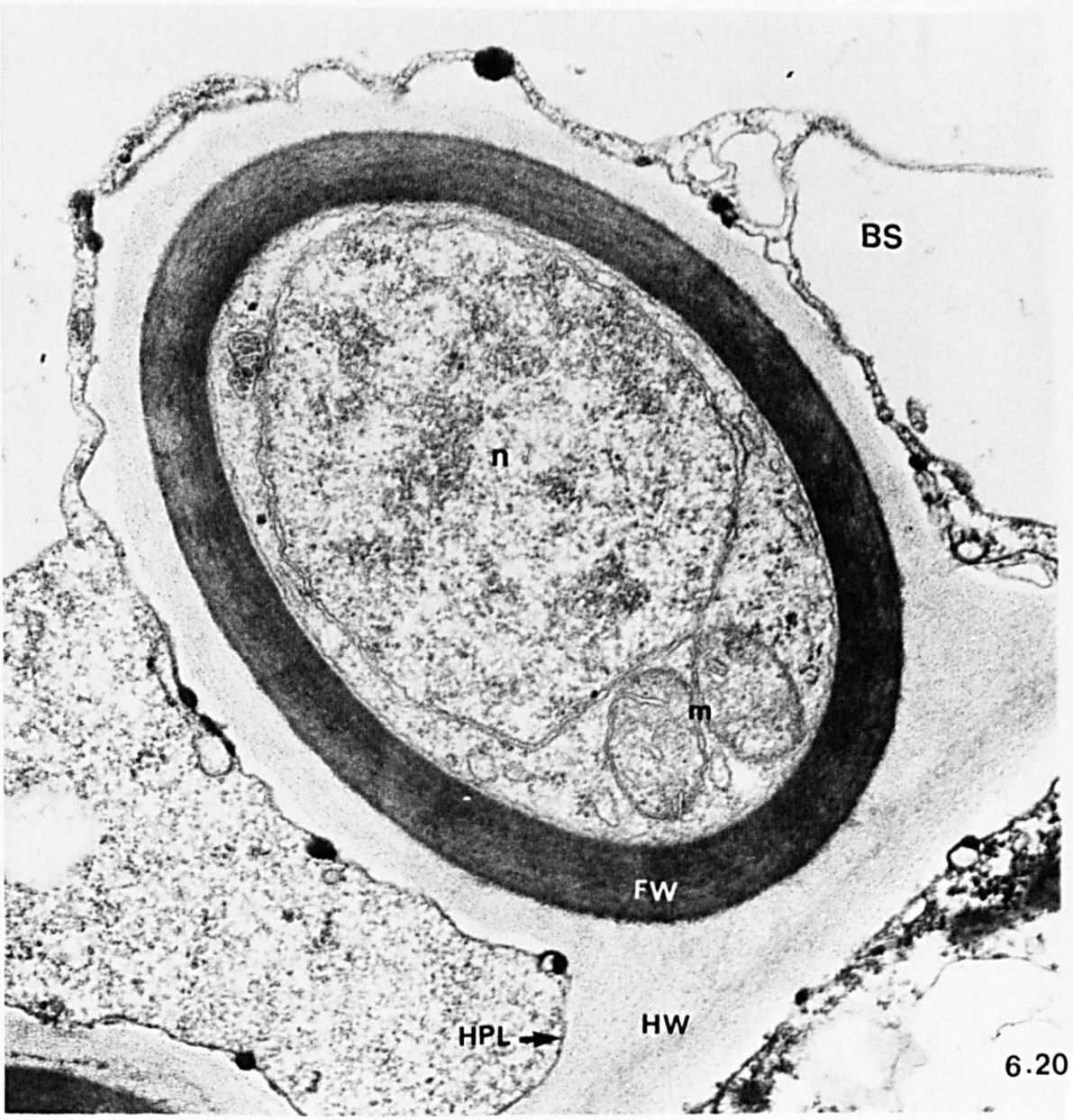

6.20

Figures 6.21-6.23

P. poarum on *Poa pratensis*. Scale lines = 10 μm

Figure 6.21

S.E.M. micrograph of vascular bundle of infected *Poa* leaf showing sectioned haustorium (arrow) in bundle sheath cell. No infection of endodermis, xylem and phloem is seen.

Figure 6.22

S.E.M. micrograph of vascular bundle of infected *Poa* leaf showing xylem elements, endodermis and bundle sheath cells. Note intercellular hyphae between bundle sheath cells and adjacent mesophyll cells.

Figure 6.23

S.E.M. micrograph of transverse section of infected *Poa* leaf showing telium with teliospores and vascular bundle. Note intercellular hyphae (arrows) between bundle sheath cells and adjacent mesophyll cells and haustorium in mesophyll cell.

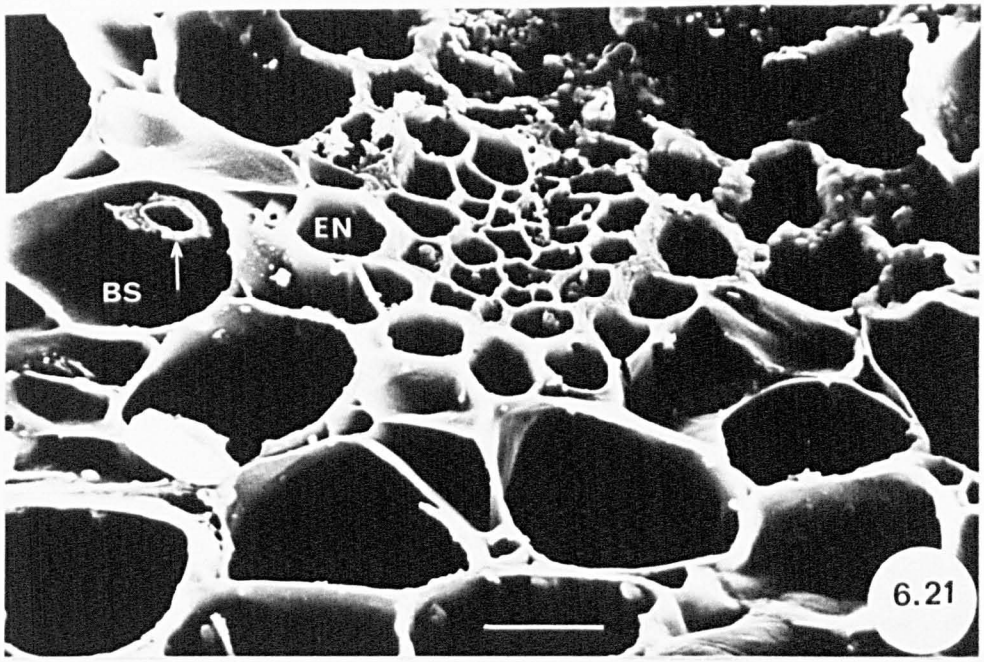
EN
BS
6.21

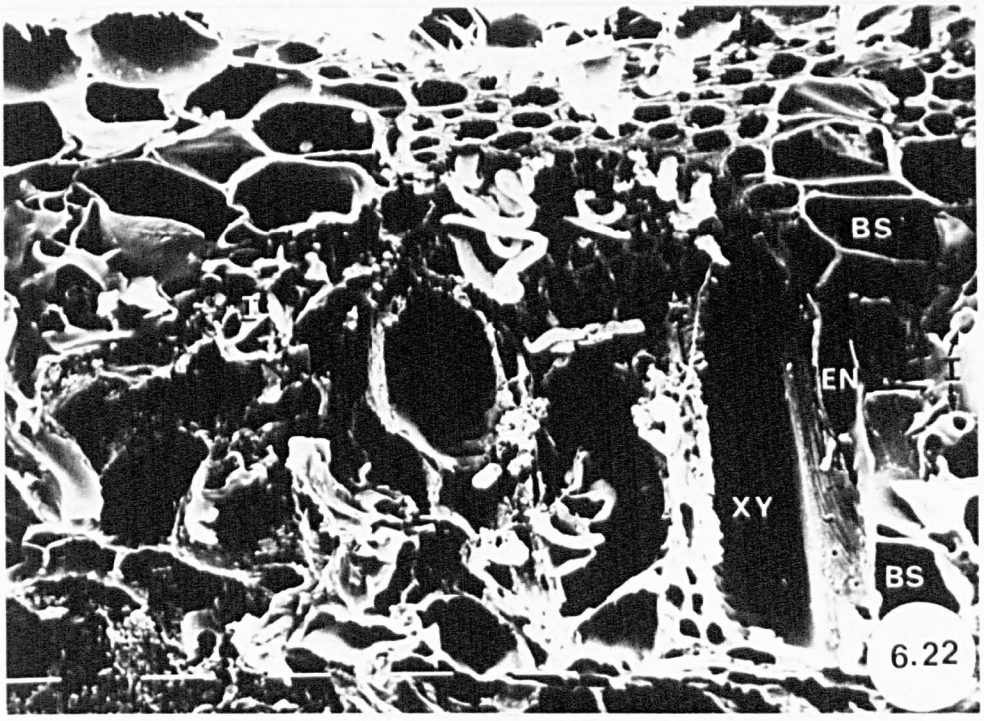
BS
EN
XY
BS
6.22

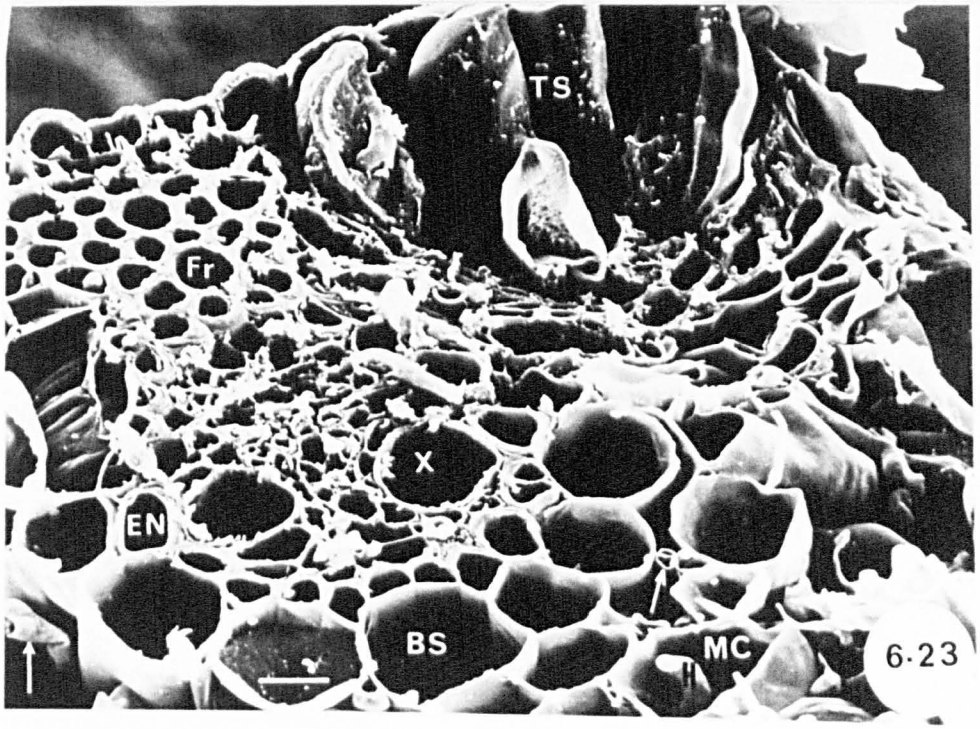
TS
Fr
X
EN
BS
MC
6·23

Figure 6.24

Part of transverse section of vascular bundle of healthy leaf of *Poa*. Note part of xylem tracheary elements, phloem parenchyma, companion cells and sieve tubes. Nucleus, mitochondria and lipid drops are shown. Some mature sieve tubes showed thick walls.

x7500

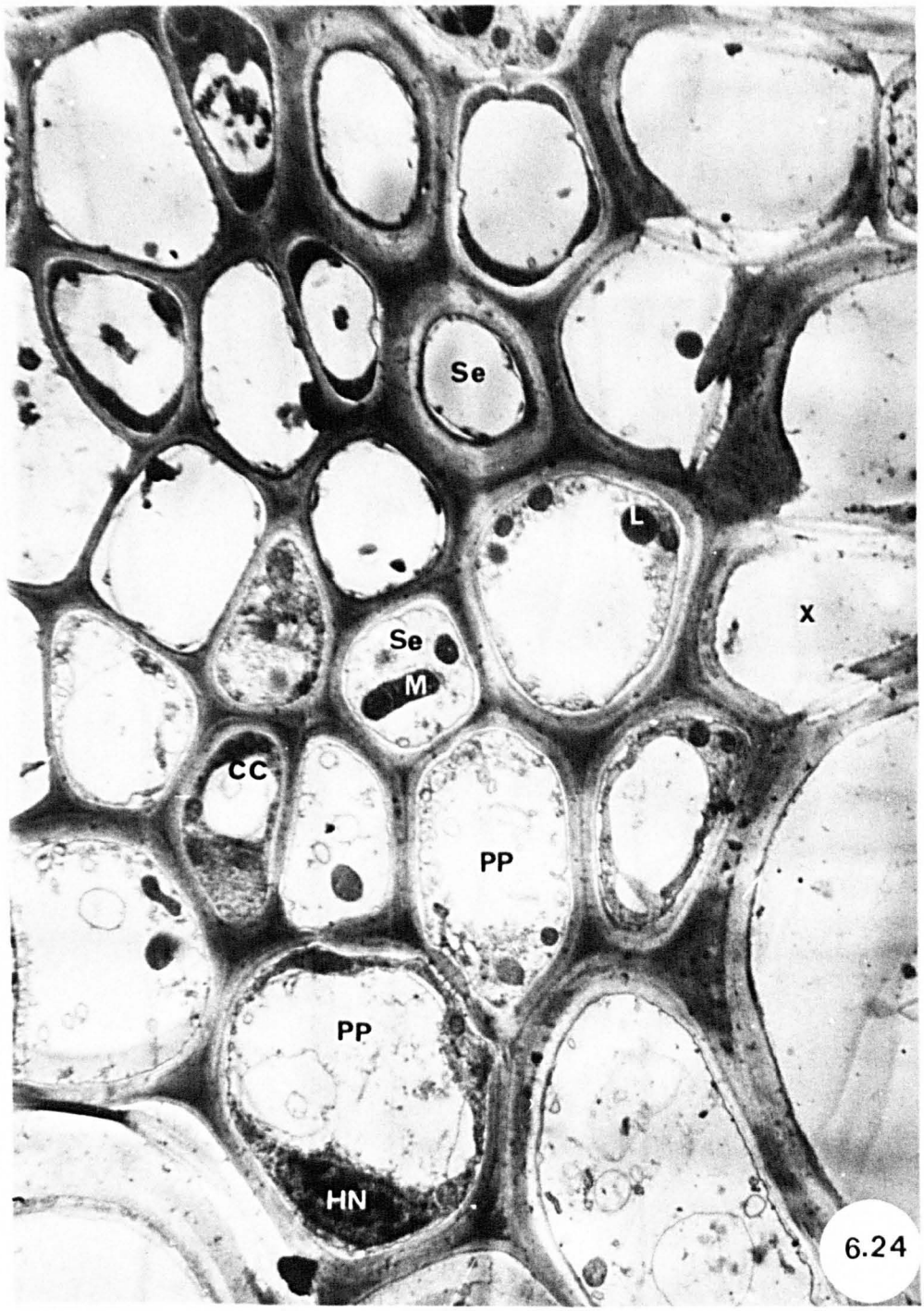
Se
L
X
Se
M
CC
PP
PP
HN
6.24

Figure 6.25a

Part of healthy phloem of *Poa* leaf showing phloem parenchyma cells. Note nucleus, mitochondria, plastid (arrowhead) and electron-dense body (large arrow). Note also plasmodesmata (small arrow).

x10000

Figure 6.25b

Part of healthy phloem of *Poa* leaf showing sieve tubes and companion cells. Note mitochondria plastid (arrowhead) and nucleus in companion cell. Unbranched plasmodesmata (arrow) are seen between companion cell and sieve tube.

x15000

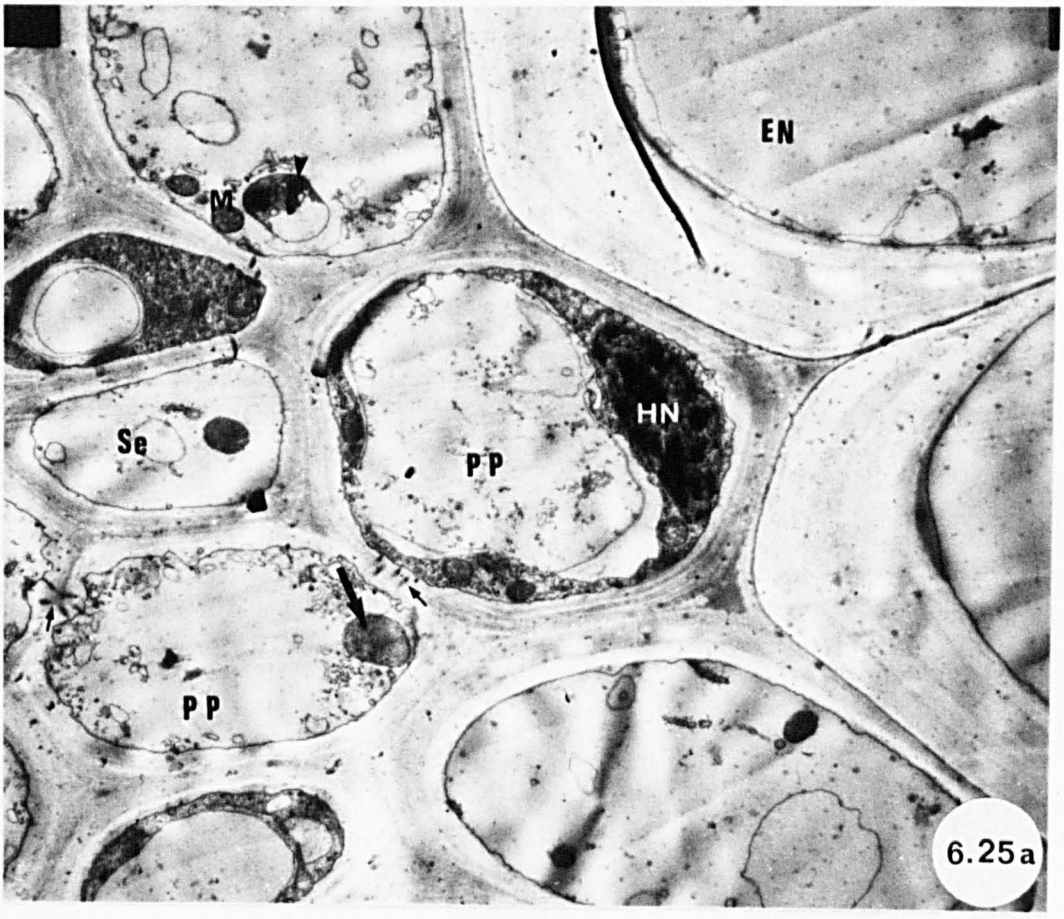
EN
M
Se
HN
PP
PP
6.25a

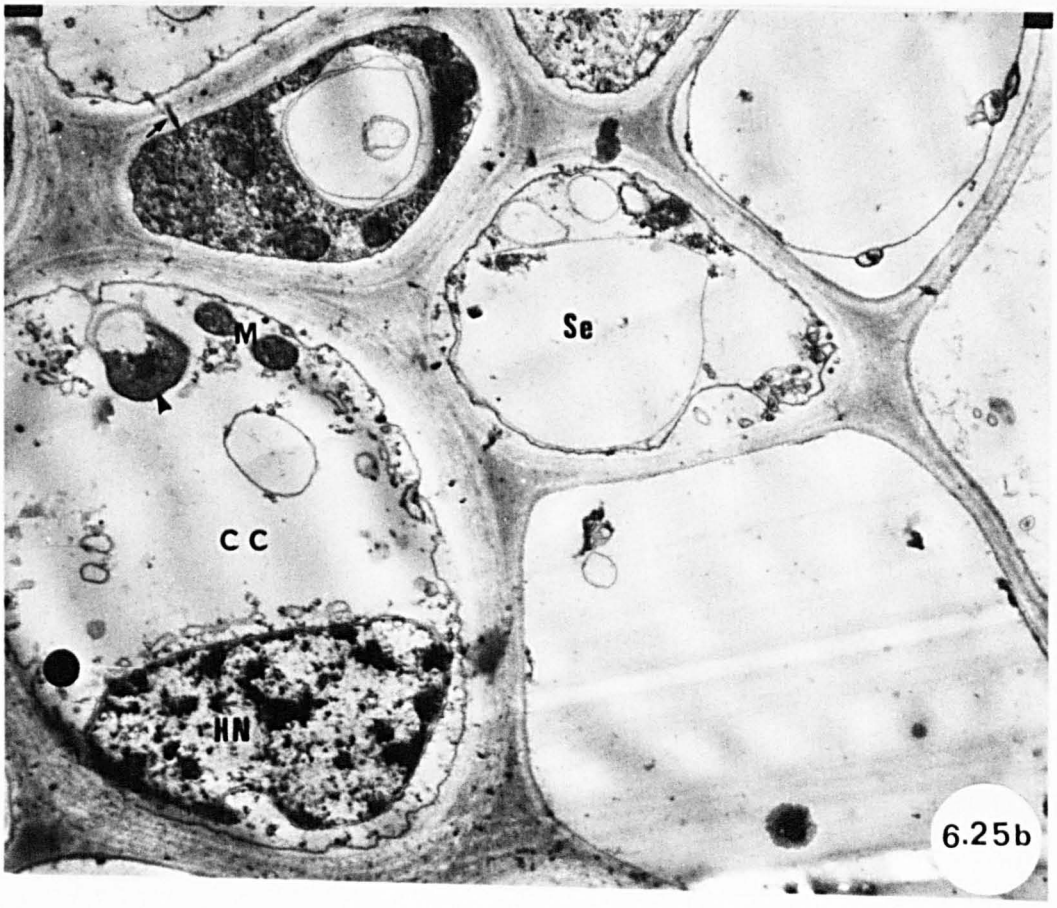
M
Se
CC
HN
6.25b

Figure 6.26

Phloem parenchyma cells of vascular bundle of infected *Poa* leaf showing dense cytoplasm, mitochondria, R.E.R. and free ribosomes (small arrows). Note electron-dense body with double-membrane (large arrow).

x40000


PP
M
RER
M
6.26

Figure 6.27

Part of healthy phloem of *Poa* leaf showing young and mature sieve tubes. Note mitochondria in sieve tubes.

x15000

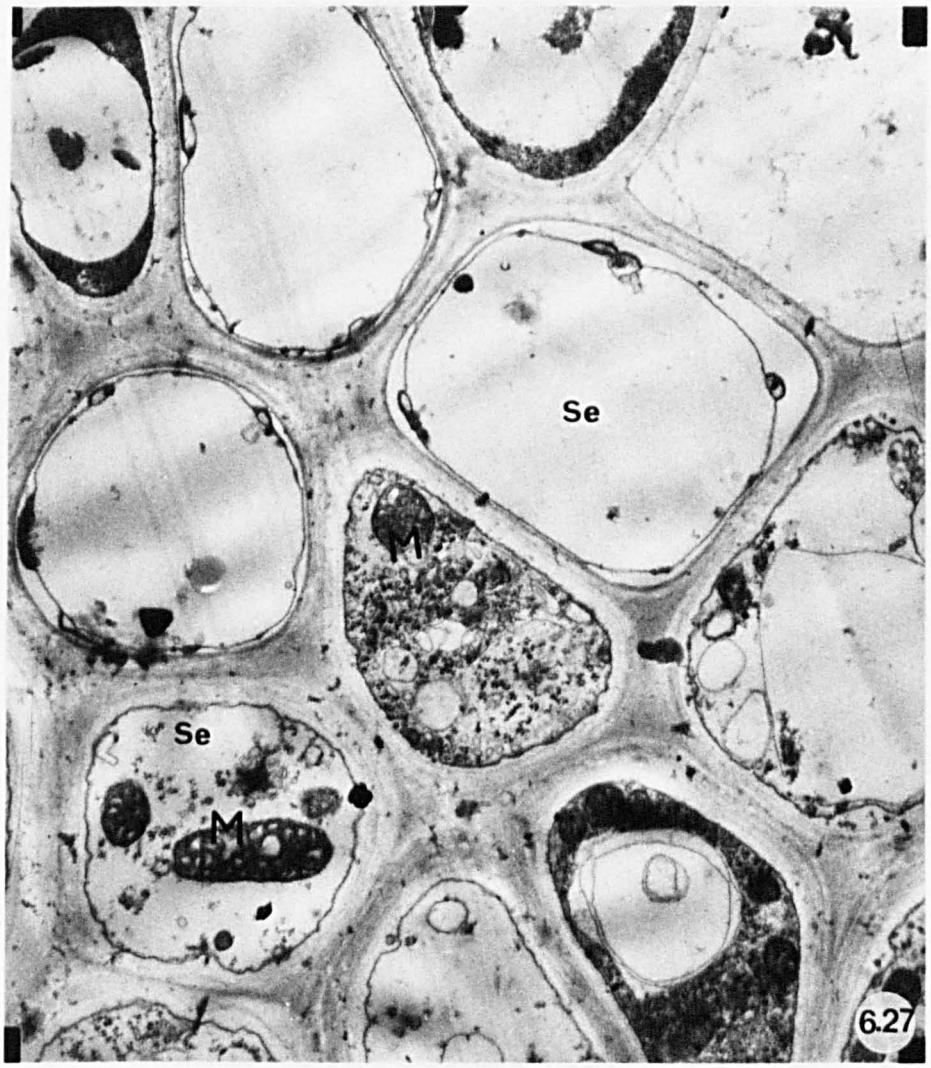
Se
M
Se
M
6.27

Figure 6.28

Plasmodesmata (arrows) connecting two adjacent sieve elements of healthy *Poa* leaf. Note electron-transparent areas around plasmodesmata which may be sites of callose deposition.
x50000

6.28

Figure 6.29a

Part of healthy xylem of *Poa* leaf showing many mitochondria and endoplasmic reticulum (arrowhead) in xylem parenchyma cell.

x7500

Figure 6.29b

Part of healthy vascular bundle of *Poa* leaf showing nuclei in living cells of xylem and phloem. Note the balanced ratio of heterochromatin and euchromatin in nucleus of xylem parenchyma.

x7500

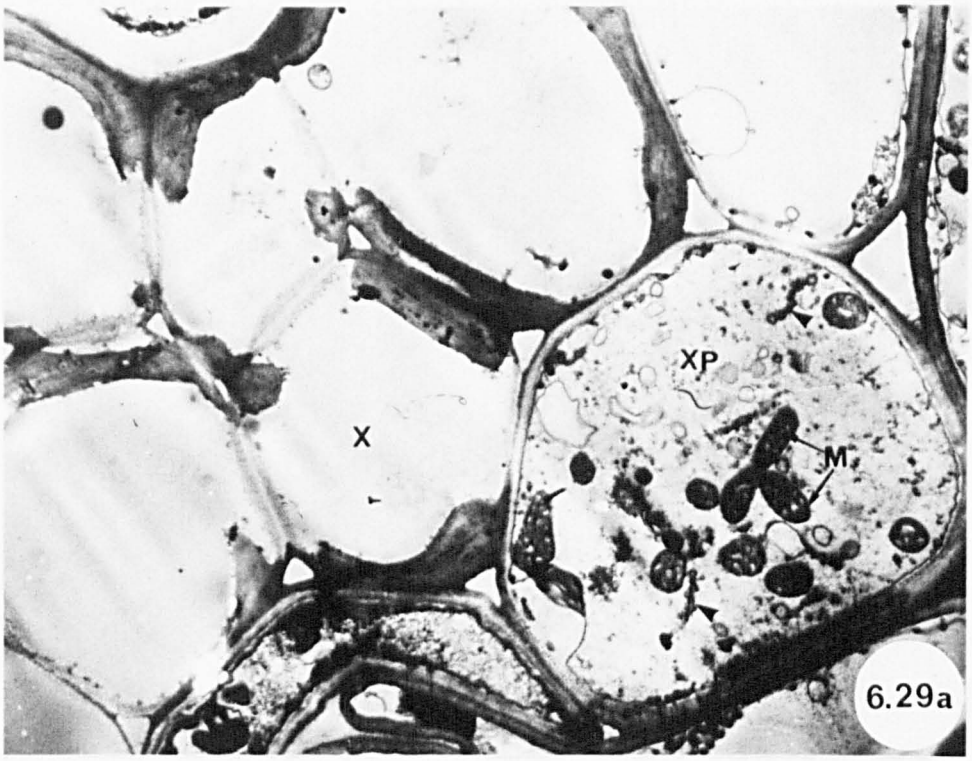

6.29a

6.29b

Figure 6.30

Xylem parenchyma cell from healthy vascular bundle of *Poa* leaf, showing nucleus with its double bounding membrane. Note the balanced ratio of heterochromatin and euchromatin and the thickening of the walls of xylem elements (arrows).

x375000

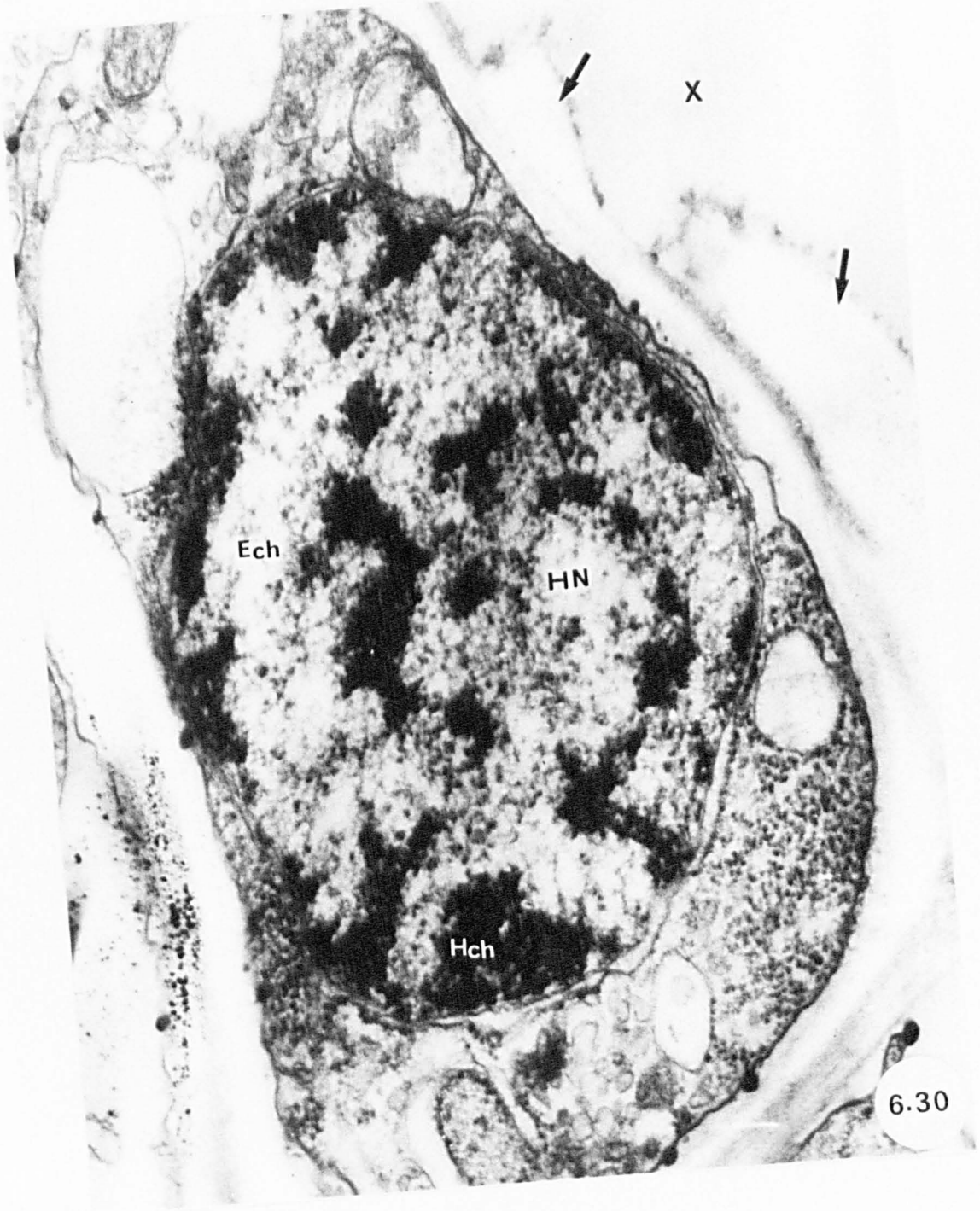
X
Ech
HN
Hch
6.30

Figure 6.31

Part of xylem region of vascular bundle from infected *Poa* leaf showing xylem elements with lignified thickenings and remnants of the cellulosic primary walls (arrows). Note xylem parenchyma containing nucleus and mitochondria as well as unidentified membrane-bound body (small arrow).

x18750

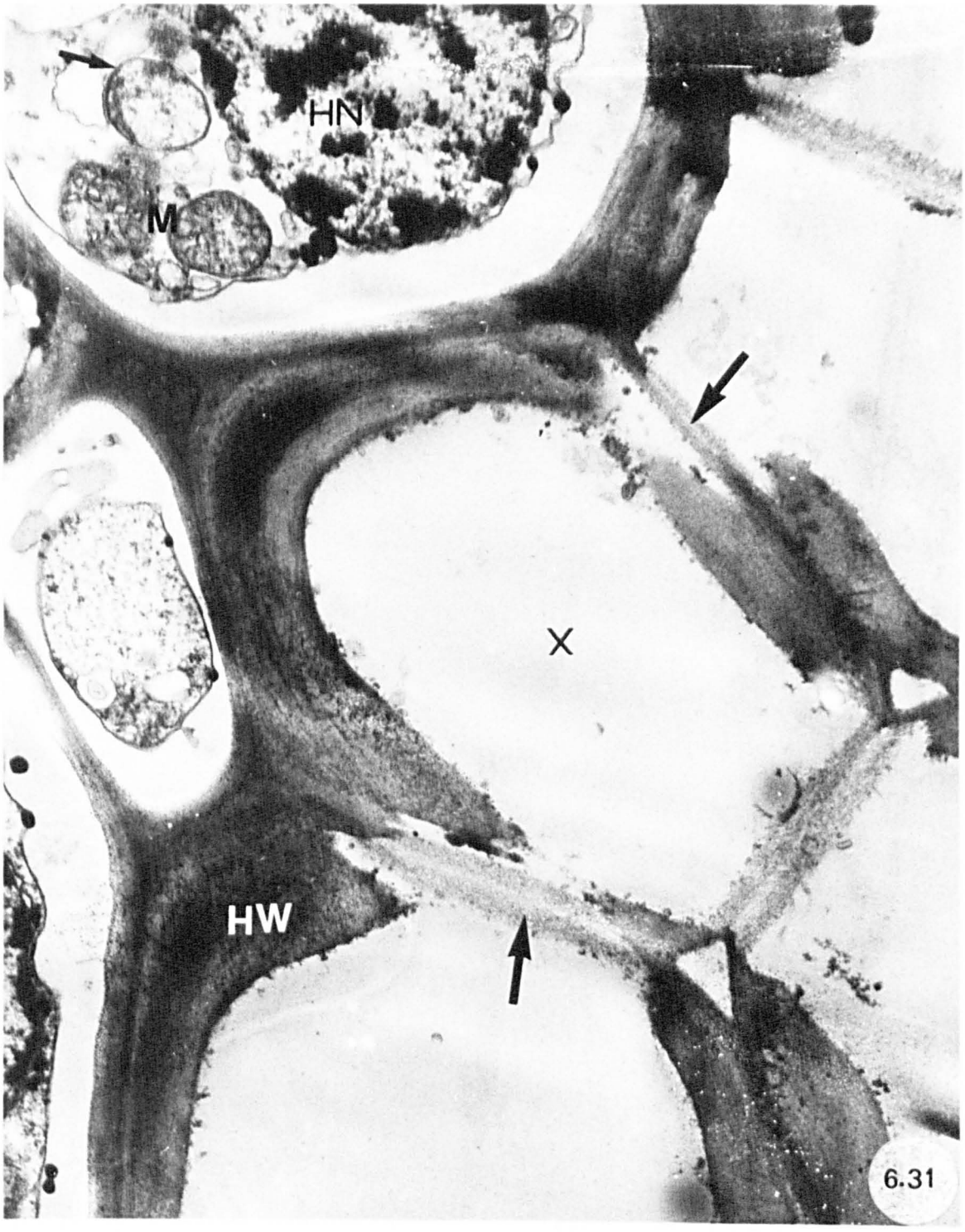
HN
M
X
HW
6.31

Figure 6.32

Part of endodermal cell of healthy *Poa* leaf showing heavily thickened wall and crystal-containing microbody.

x37500

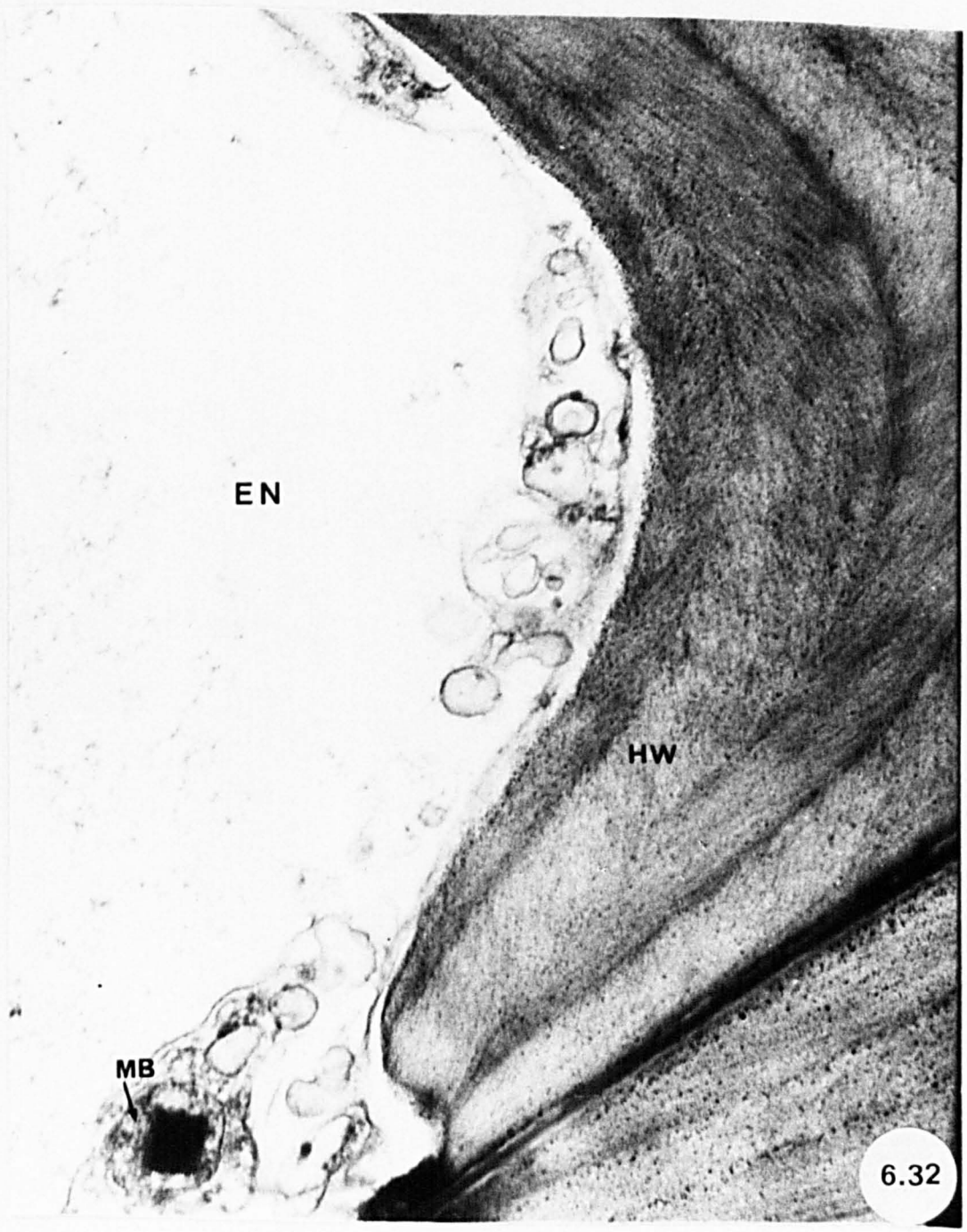

6.32

Figure 6.33

Part of healthy vascular bundle of *Poa* leaf showing thick-walled endodermal cells and bundle sheath cells. Note chloroplasts in bundle sheath cell. Starch grains can be seen in chloroplast.

x6000

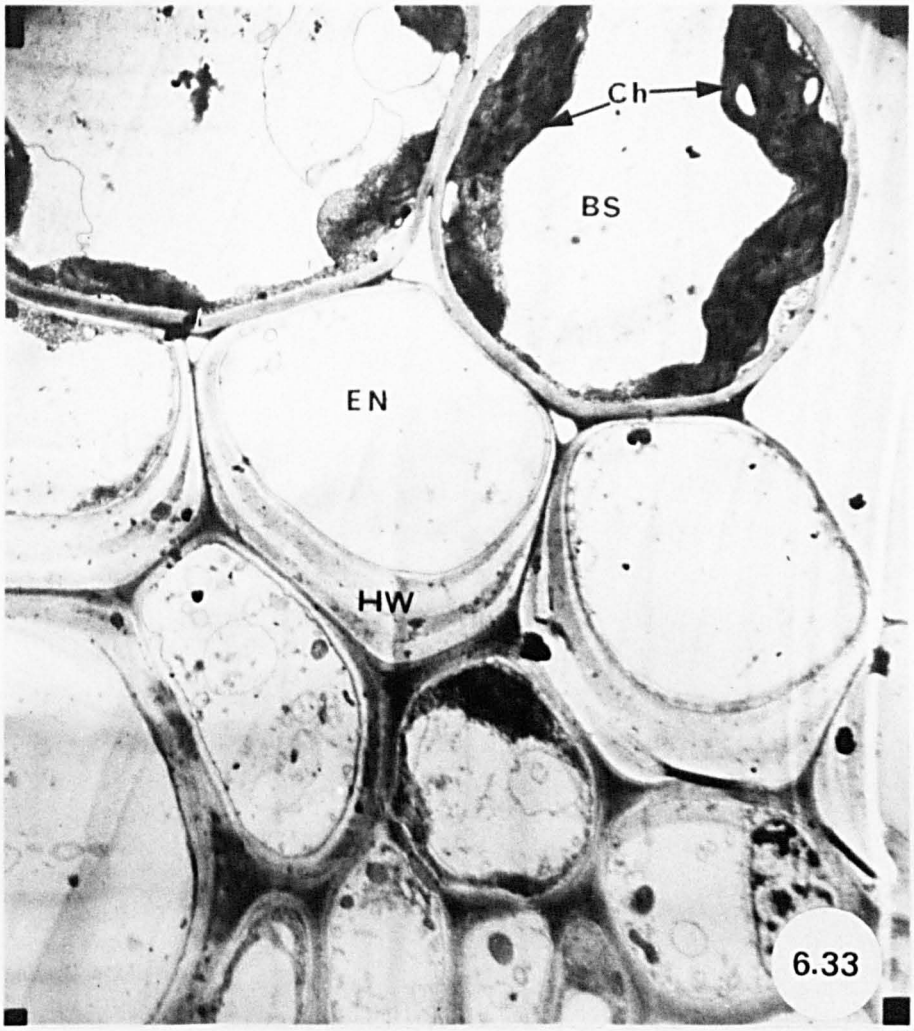
Ch
BS
EN
HW
6.33

Figures 7.1 and 7.4

P. poarum on *Tussilago* leaf.

Figures 7.2 and 7.3

P. poarum on *Poa* leaf.

Scale lines = 10 µm

Figure 7.1

Mesophyll cells and intercellular hyphae adjacent to pycnium. The host cells adjacent to pycnium are smaller in size than those further away. Note intracellular hypha (arrow) in host cell.

Figure 7.2

Close association of host cell nucleus and haustorium in epidermal cell of *Poa*. Note the haustorial neck (arrow).

Figure 7.3a

Healthy mesophyll cell of Poa with normal nucleus.

Figure 7.3b

Infected mesophyll cells of *Poa* showing enlarged nuclei, compared with that in Figure 7.3a. Note fungal haustorium (arrowhead).

Figure 7.4a

Healthy mesophyll cell of *Tussilago* showing chloroplasts adjacent to host cell wall.

Figure 7.4b

Infected *Tussilago* mesophyll cell showing reduced numbers of chloroplast (compared with those in Figure 7.4a), intercellular and intracellular hyphae. Note close association of chloroplasts and intracellular hyphae (arrowhead). Septate intracellular hyphae are clearly seen.

7.1

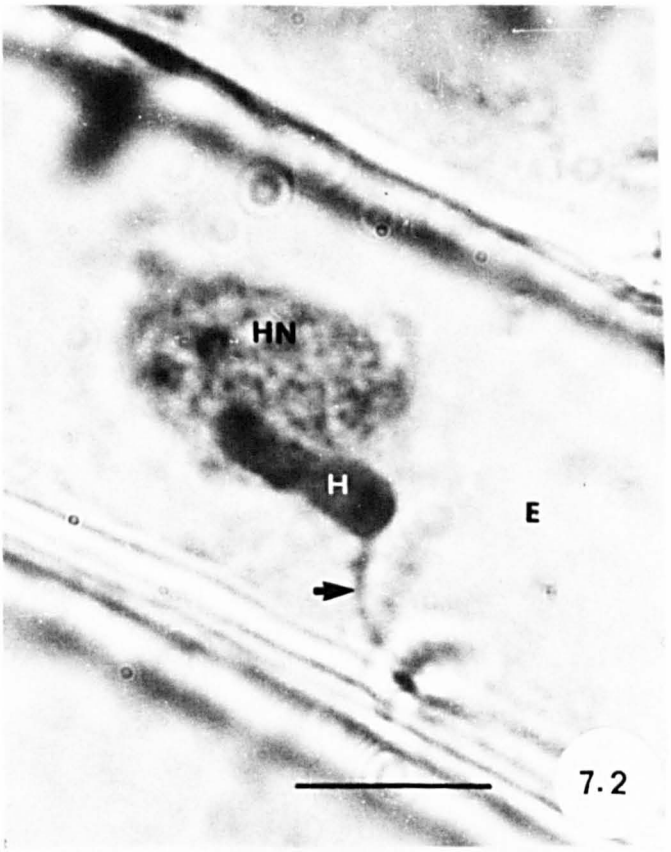

7.2

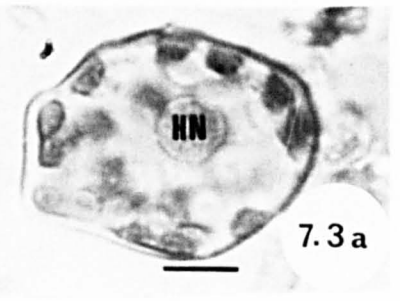

7.3a

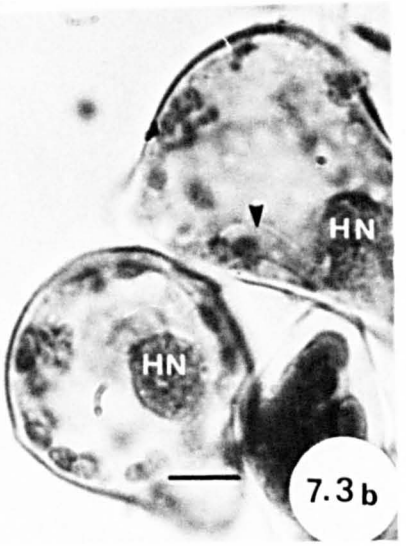

7.3b

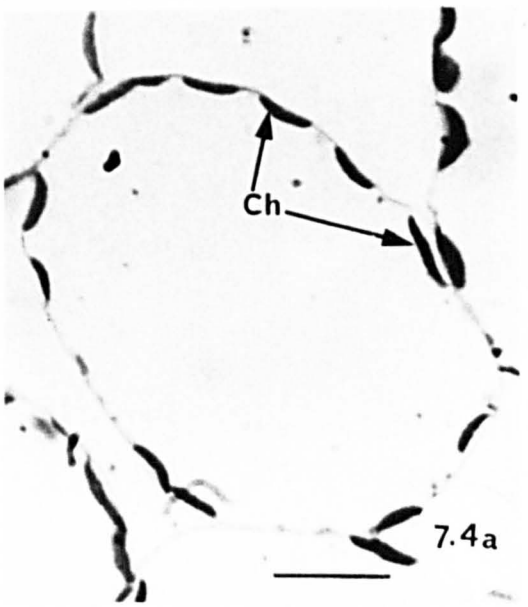

7.4a

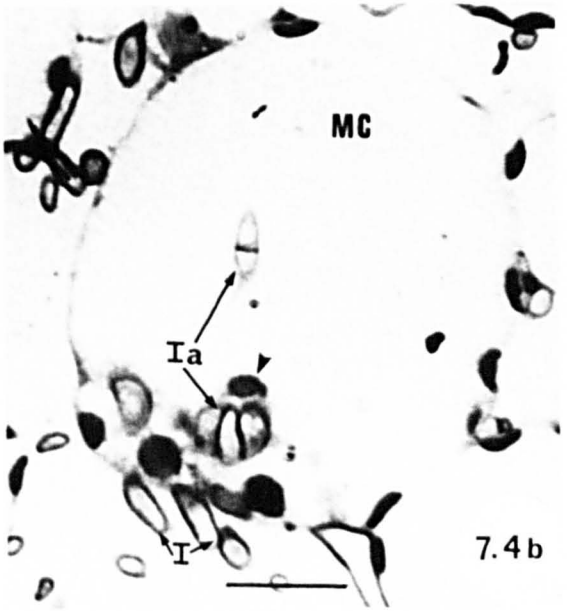

7.4b

Figures 7.5a-f

Freezing microtome section of *Tussilago* mesophyll cells.

Scale lines = 10 μm

Left column (Figures 7.5a,c and e) shows mesophyll cells from uninfected leaves of *Tussilago* taken at 3-day intervals, in which the chloroplast numbers increase progressively.

Right column (Figures 7.5b,d and f) shows infected mesophyll cells of *Tussilago* leaves at successive early stages of pycnial development, comparable to those in the left column. Note the chloroplast numbers are decreased with age. Note also the association of chloroplasts and intracellular hyphae.

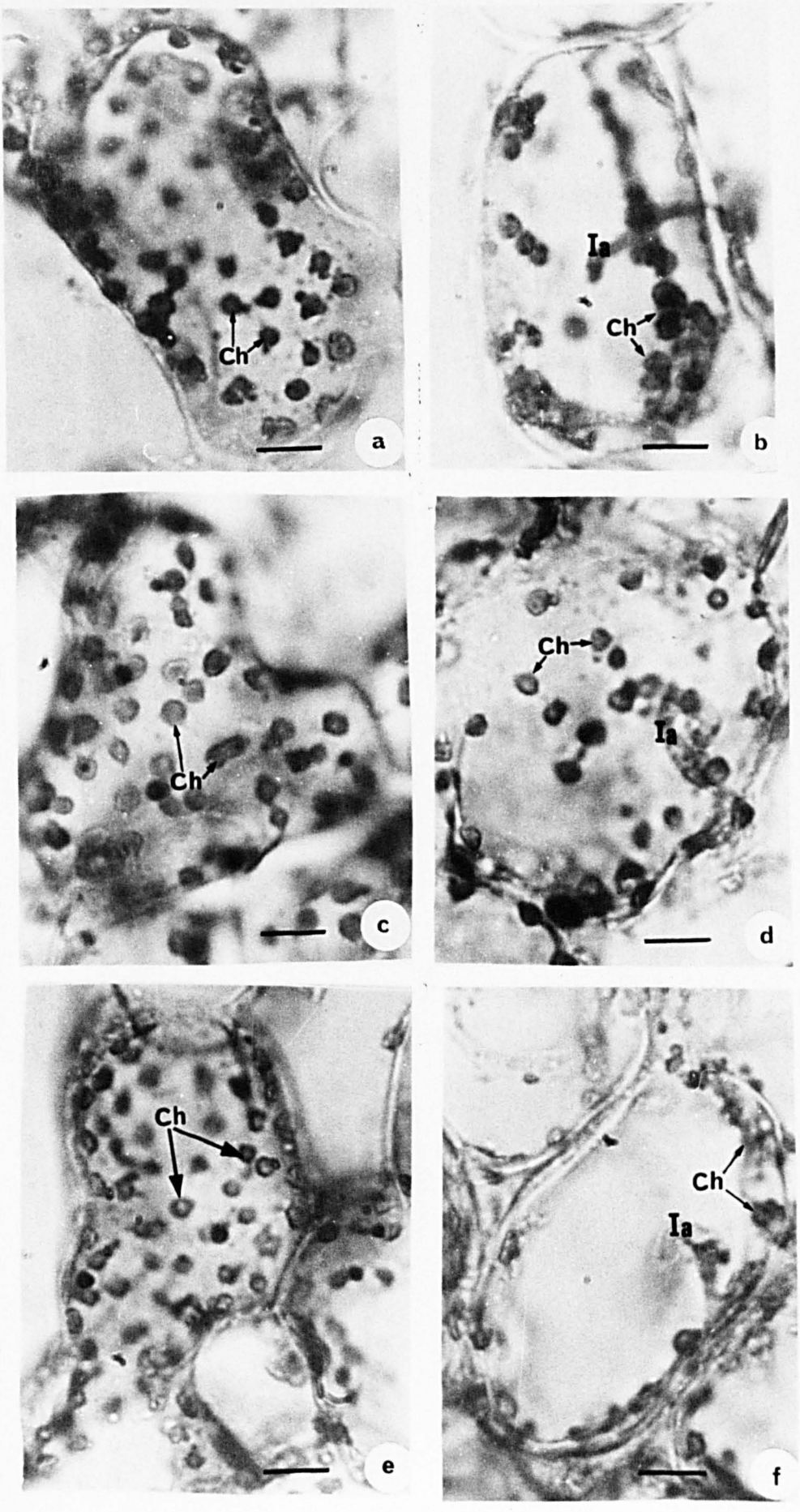
Ch
a
Ia
Ch
b
Ch
c
Ch
Ia
d
Ch
e
Ch
Ia
f

Figure 7.6a and b

Uninfected and infected *Tussilago* mesophyll cells.

Figure 7.7a, b and c

Infected and uninfected *Poa* mesophyll cells.

Scale lines = 10 μm

Figure 7.6a

Chloroplasts with starch grains in old uninfected mesophyll cells of *Tussilago*.

Figure 7.6b

Infected mesophyll cells of *Tussilago* showing chloroplasts with few starch grains. These cells contain fewer chloroplasts, compared with those in Figure 7.6a. Note intercellular hyphae and septate intracellular hypha (arrowhead).

Figure 7.7a

Infected mesophyll cells of *Poa* showing reduced number of chloroplasts (see comparable uninfected cells in Figure 7.7b). Note close association between host nucleus and fungal haustorium. Intercellular hyphae are seen.

Figure 7.7b

Uninfected mesophyll cells of *Poa* showing higher number of chloroplasts, compared to those in Figure 7.7a.

Figure 7.7c

Older healthy mesophyll cells of *Poa*, compared to those in Figure 7.7b showing increased numbers of chloroplasts.

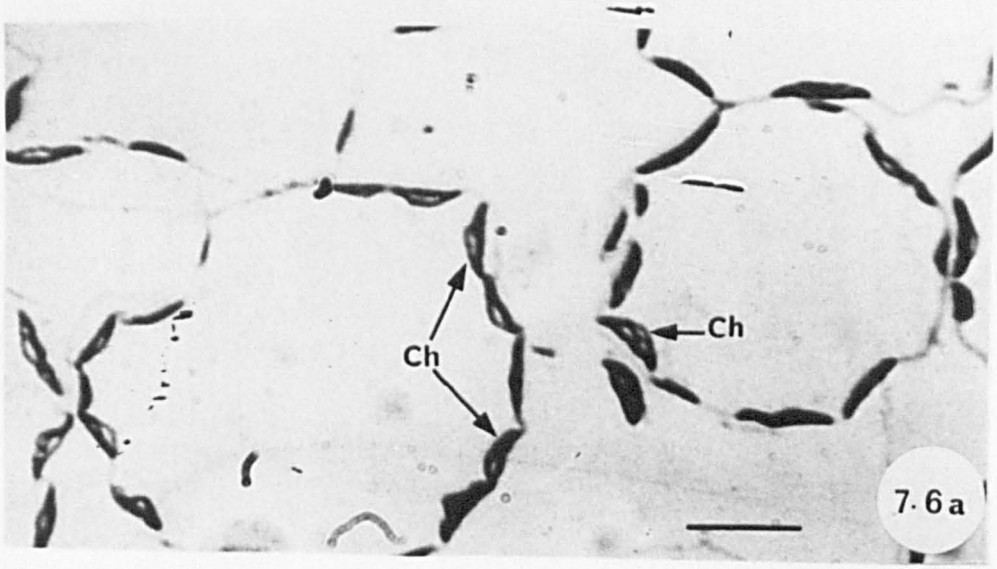

7.6a

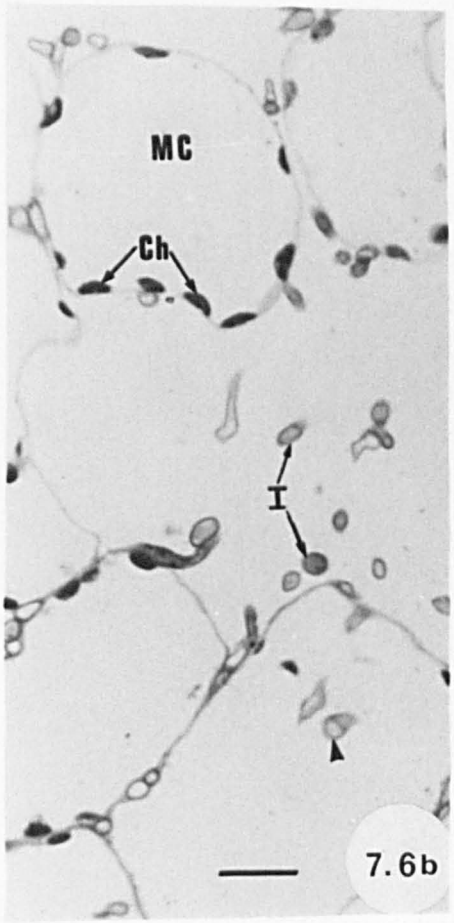

7.6b

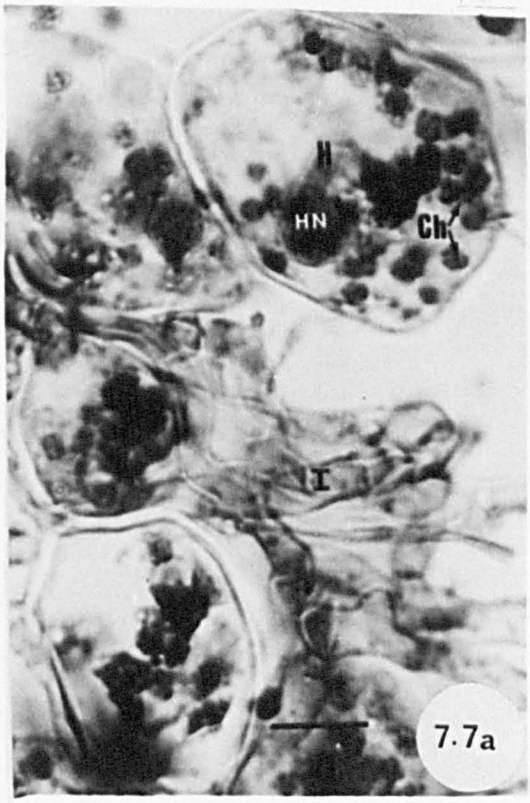

7.7a

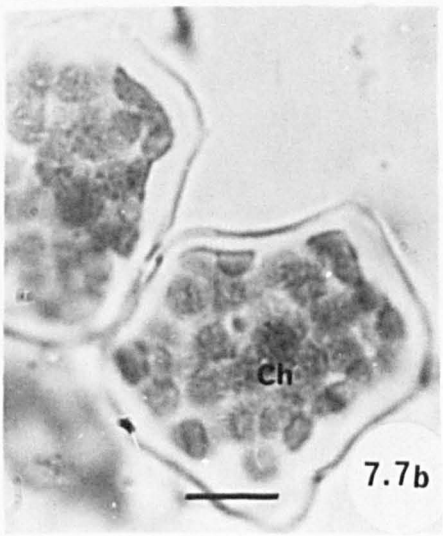

7.7b

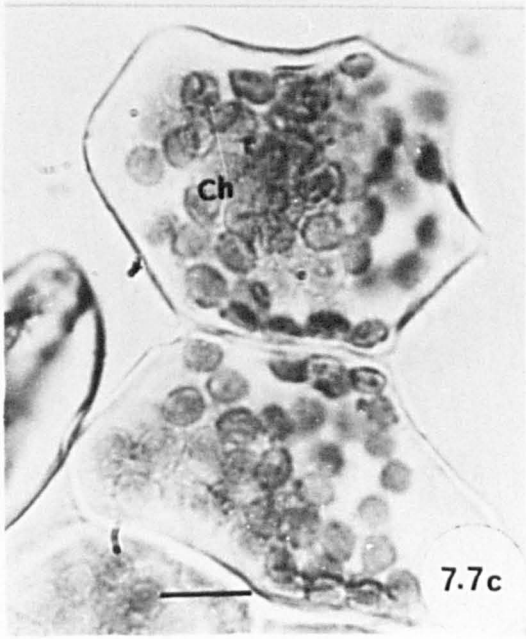

7.7c

Figure 7.8a

Uninfected mesophyll cell of *Tussilago* showing nucleus, chloroplast and crystal-containing microbody. Note heterochromatin (arrows) in the periphery of the nucleus and euchromatin. The double membrane of the nucleus can also be seen.

x25000

Figure 7.8b

Uninfected mesophyll cell of *Tussilago* showing nucleus lying adjacent to chloroplasts. Note euchromatin, heterochromatin (arrows) and nucleolus (arrowheads). See Figure 7.10a.

x15000

Figure 7.8c

Uninfected mesophyll cell of *Tussilago* showing nucleus with nucleolus and heterochromatin (arrows) in the periphery of the nucleus.

x8000

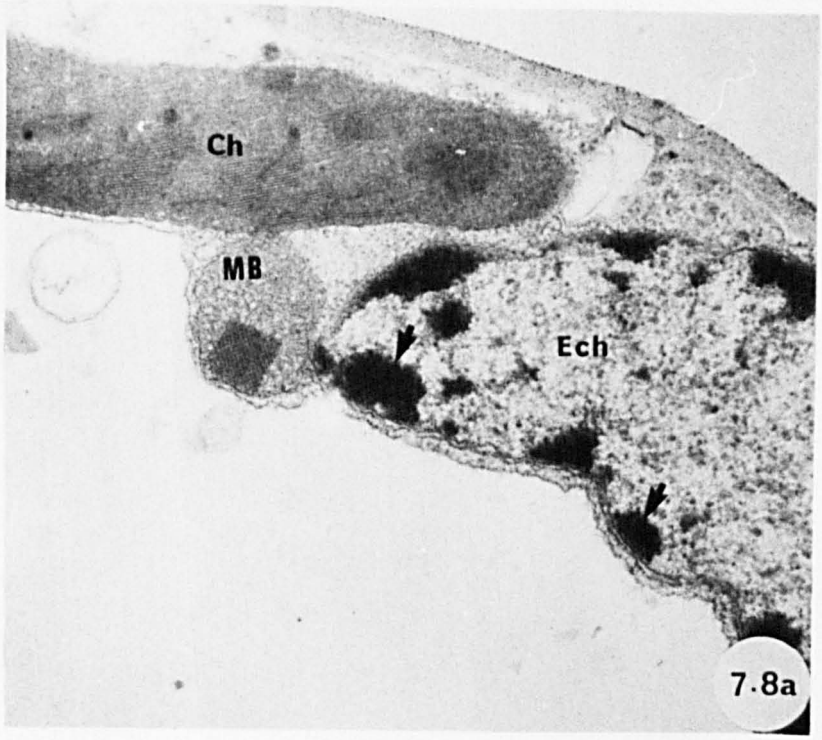

7·8a

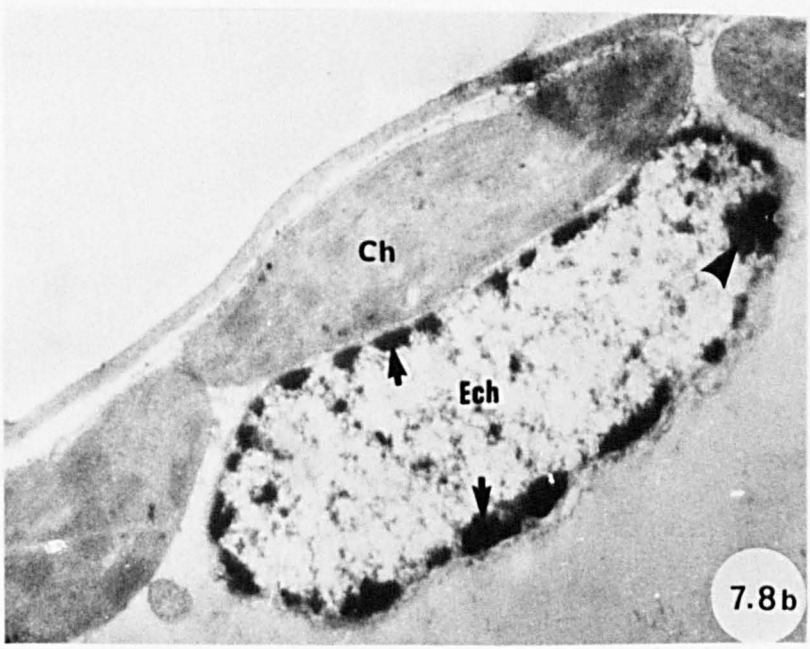

7.8b

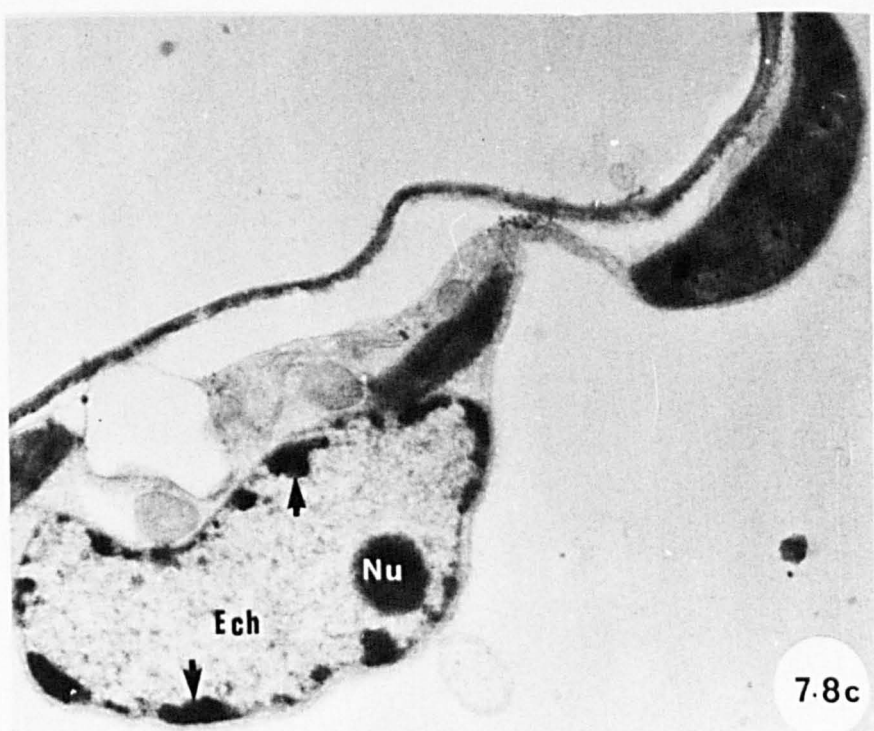

7·8c

Figure 7.9

Infected mesophyll cell of *Tussilago* at later stage of pycnial-aecial infection showing elongated host nucleus (see Figure 7.8b) associated with fungal intracellular hypha. Note very small clumps of heterochromatin (arrows) and euchromatin with increased electron density.

x10000

Figure 7.10a

Nucleus of infected mesophyll cell of *Tussilago* at early stage of pycnial-aecial development showing heterochromatin in the periphery of the nucleus and nucleolus associated with electron-dense material (arrowhead). Note intracellular hypha.

x15000

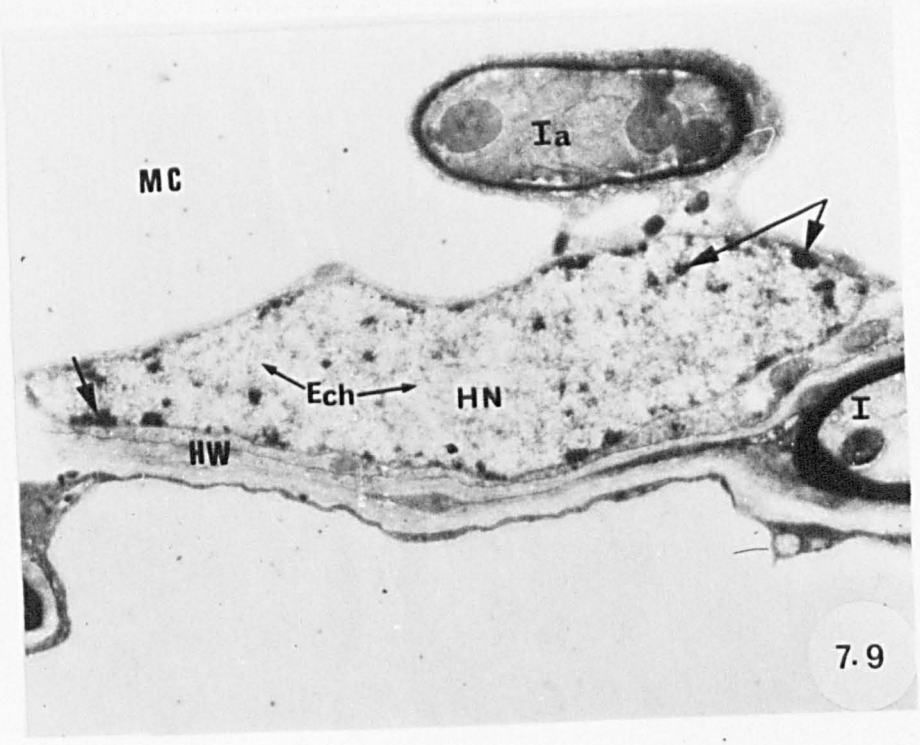

7.9

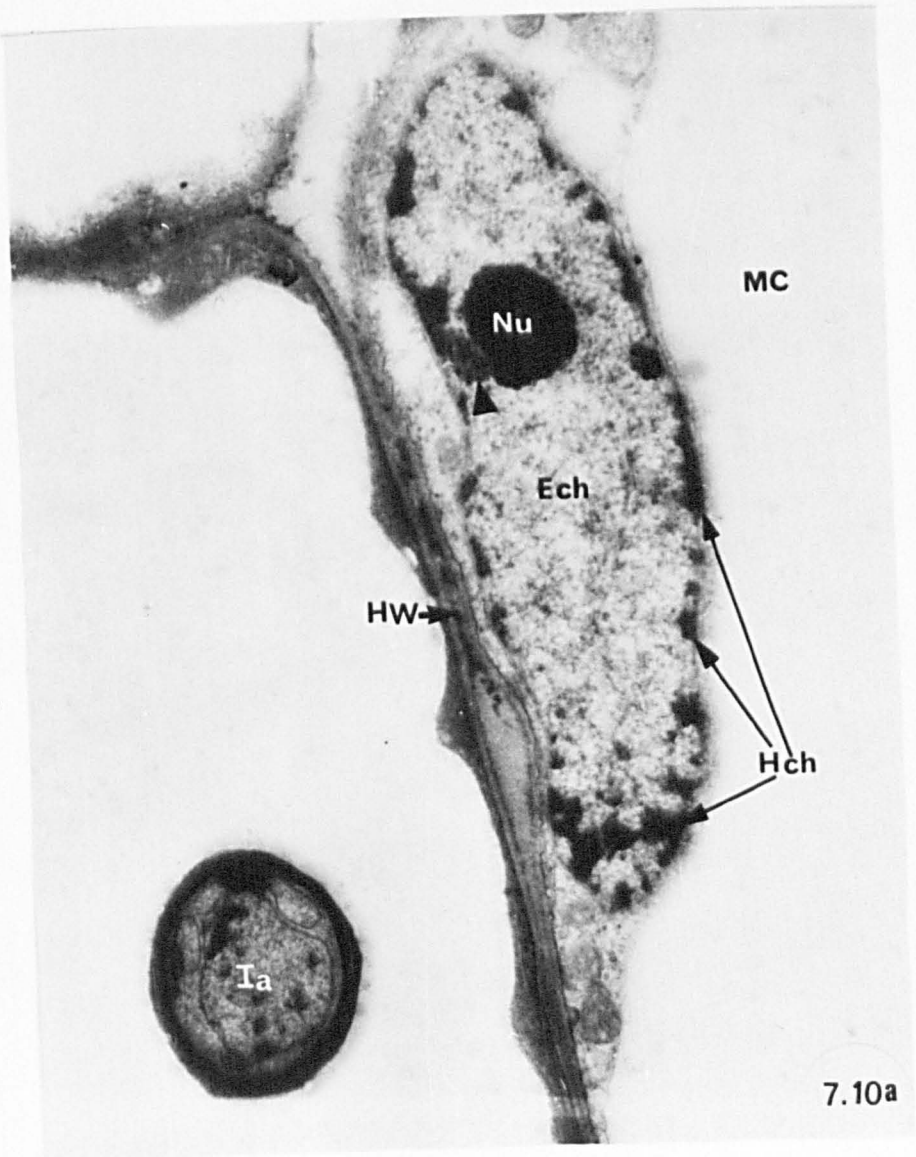

7.10a

Figure 7.10b

Infected mesophyll cell of *Tussilago* at later stage of infection showing nucleus with nucleolus. Heterochromatin (arrowheads) is in the form of very small clumps in the periphery of the nucleus and its amount appears less than that of euchromatin. Note intracellular hypha with lipid droplets.

x18750

Figure 7.11

Infected mesophyll cell of *Tussilago* at later stage of pycnial-aecial development showing host nucleus with nucleolus, heterochromatin (arrows) in the periphery of nucleus. Less amount of heterochromatin than euchromatin is seen. Note nucleolus associated with electron-dense material (arrowhead) similar to that seen in Figure 7.10a and double membrane of nucleus (open arrow). Note also intercellular hypha.

x25000

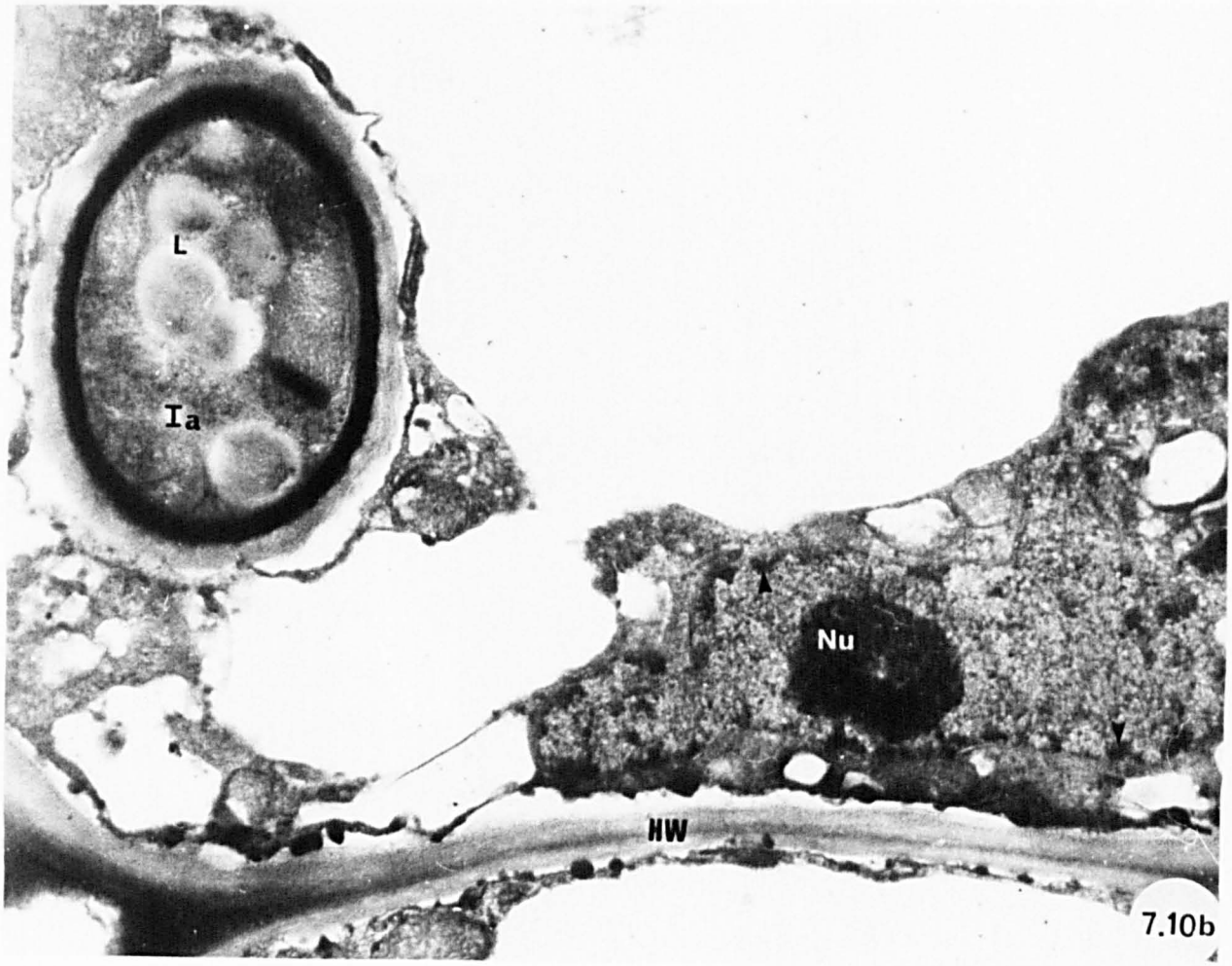

7.10b

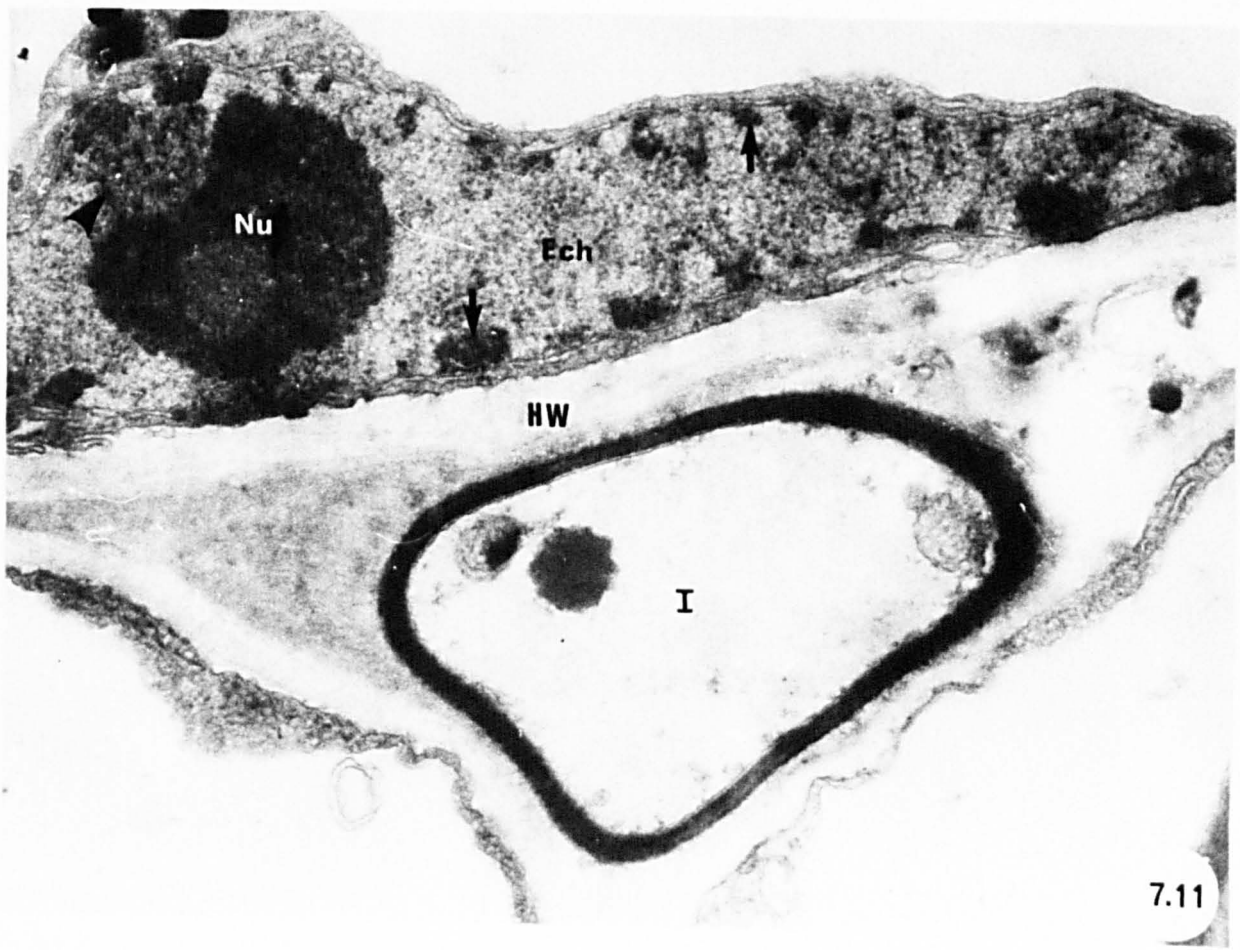

7.11

Figure 7.12a

Uninfected mesophyll cell of *Poa* showing chloroplasts and oval nucleus. Note large amount of heterochromatin (arrows) and euchromatin (arrow) in the nucleus, well-developed membrane system of chloroplast and lipid droplet.

x12500

Figure 7.12b

Uninfected mesophyll cell of *Poa* showing chloroplasts, microbody and nucleus with nucleolus. Note heterochromatin, euchromatin and host vacuole.

x12500

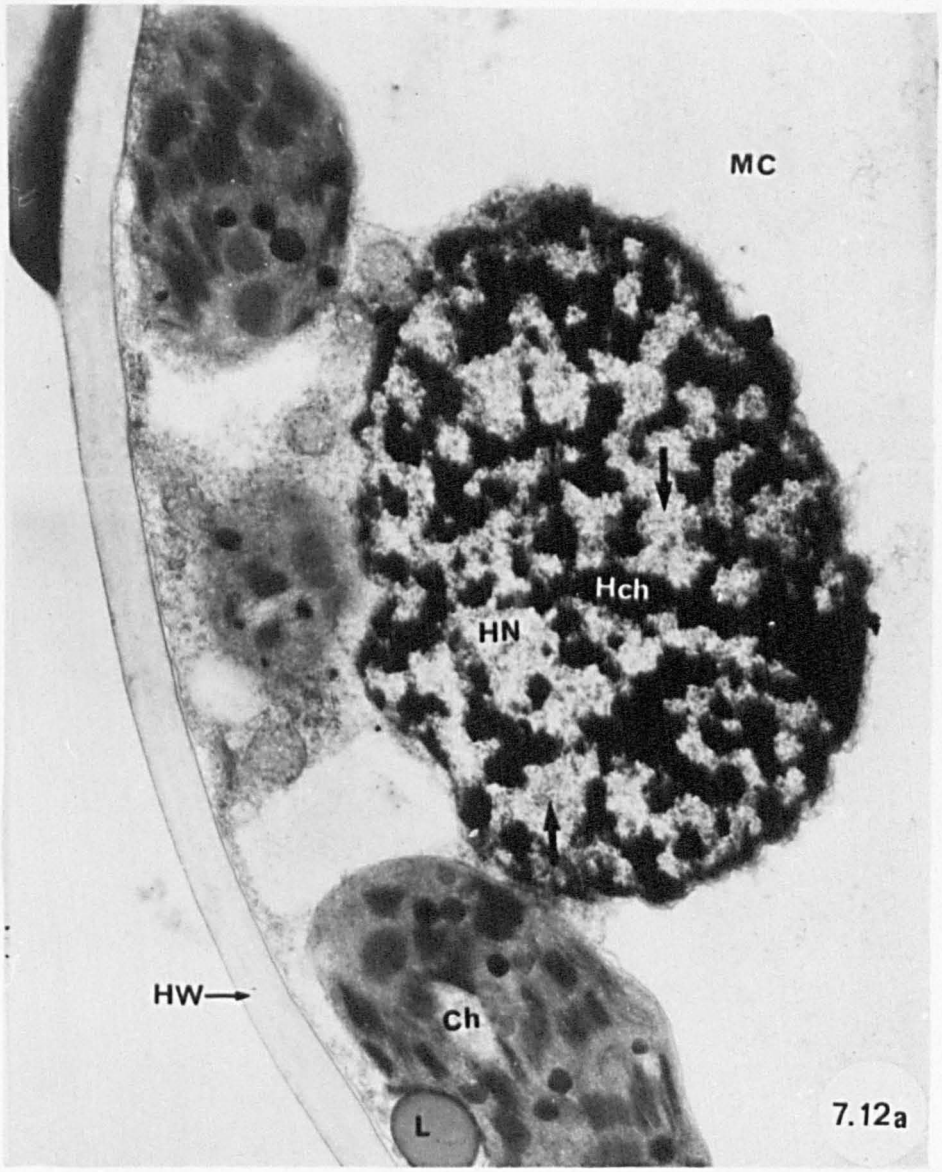

7.12a

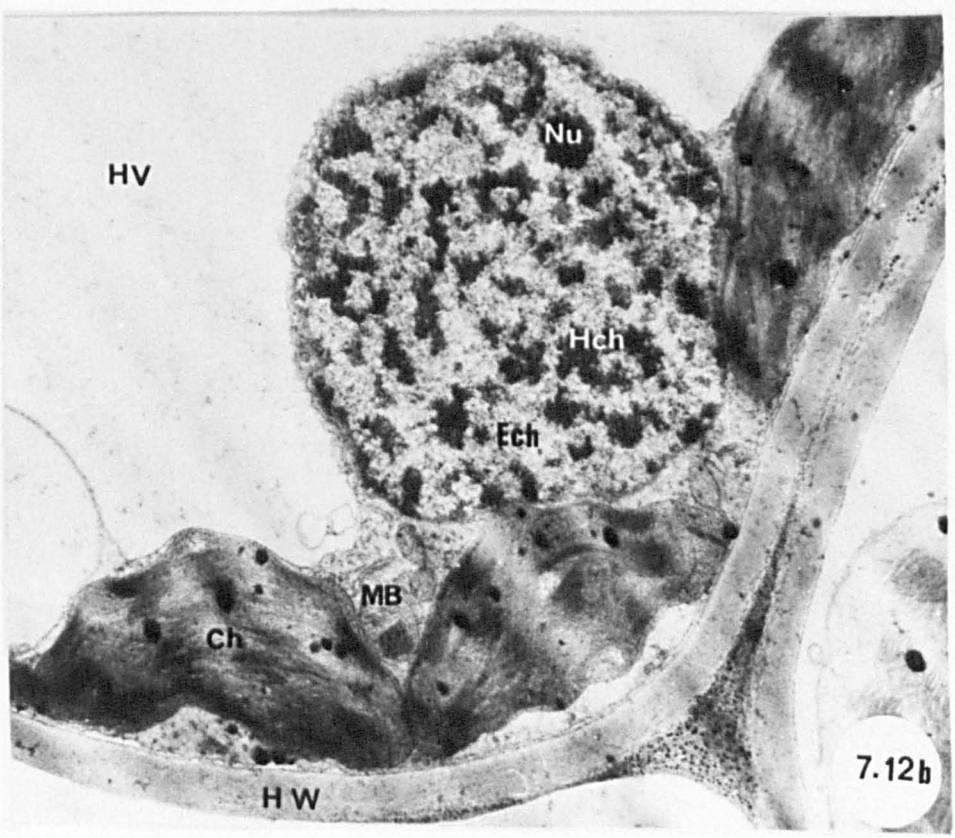

7.12b

Figure 7.12c

Enlarged nucleus of uninfected mesophyll cell of *Poa* showing nucleolus, euchromatin, heterochromatin and double unit nuclear membrane (arrowhead). Note mitochondria and chloroplast.

x22500

Figure 7.13

Old healthy mesophyll cell of *Poa* showing chloroplasts with starch grains and nucleus with nucleolus. Note the balanced ratio of euchromatin and heterochromatin.

x10000

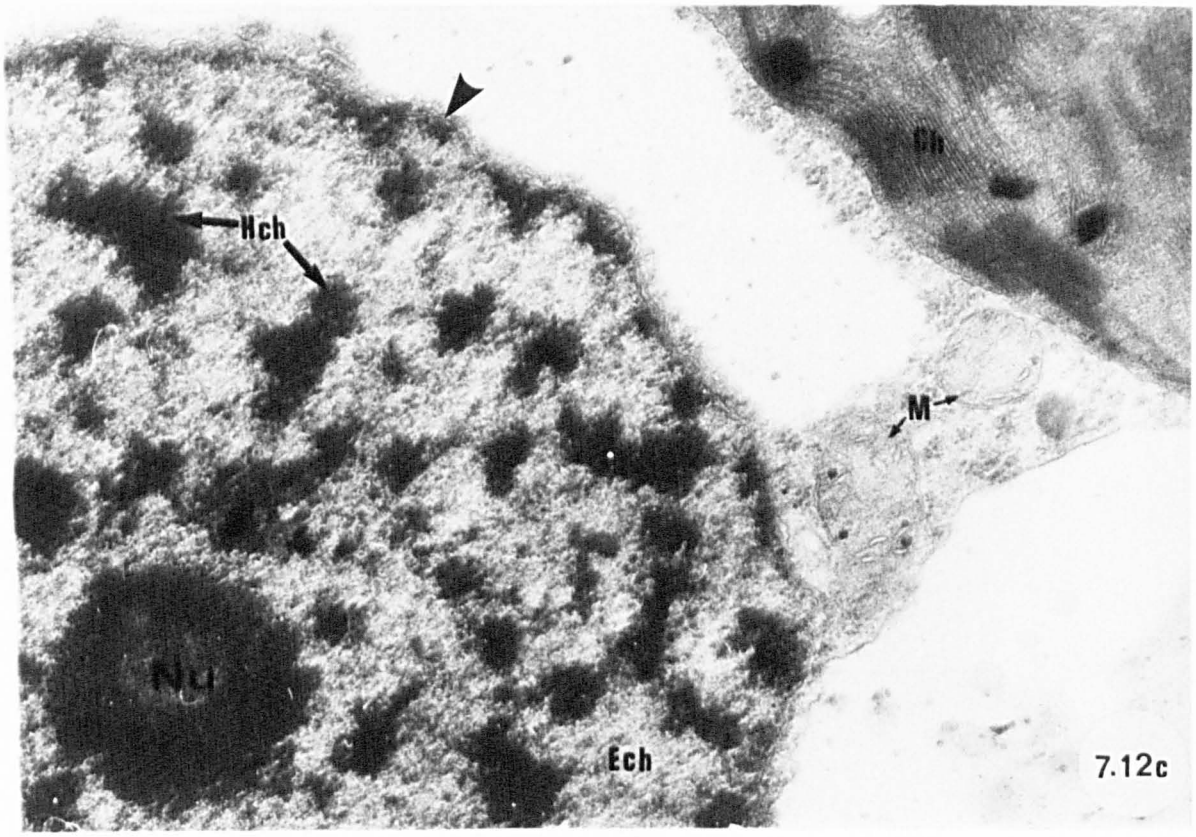

7.12c

7.13

Figure 7.14a

Infected *Poa* mesophyll cell at early stage of uredial infection showing fungal haustorium closely associated with host nucleus. More euchromatin (unlabelled arrows) than heterochromatin is seen in host nucleus. Note chloroplasts with starch grains and osmiophilic globules.

x14000

Figure 7.14b

Infected *Poa* mesophyll cell at early stage of uredial infection showing lobed host nucleus closely associated with fungal haustorium. Note nucleolus, euchromatin (unlabelled arrows) and heterochromatin in host nucleus. Note fungal nucleus in one section of haustorium.

x15000

7.14a

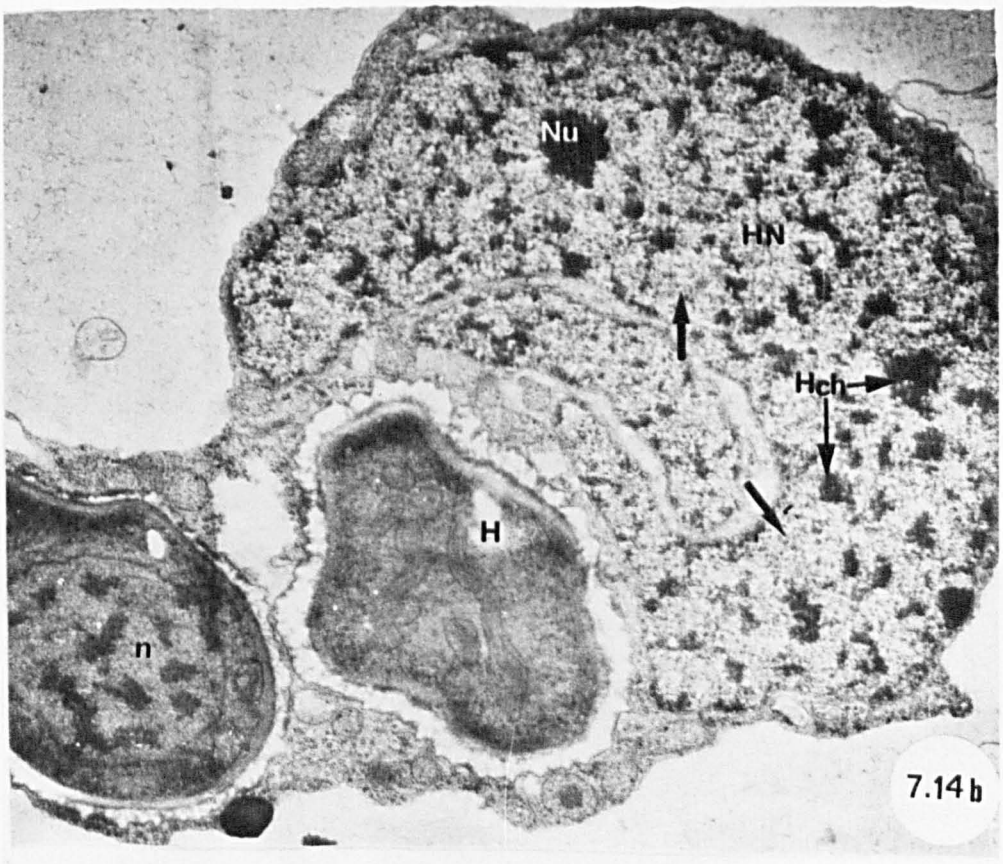

7.14b

Figure 7.15

Infected mesophyll cell of *Poa* at later stage of infection showing host nucleus invaginated by fungal haustorium. Note host mitochondria between haustorium and host nucleus. Note also chloroplast and microbody.

x16800

Figure 7.16a

Haustorium in transverse section completely surrounded by host nucleus from which it is separated by a narrow region of cytoplasm containing mitochondria.

x15000

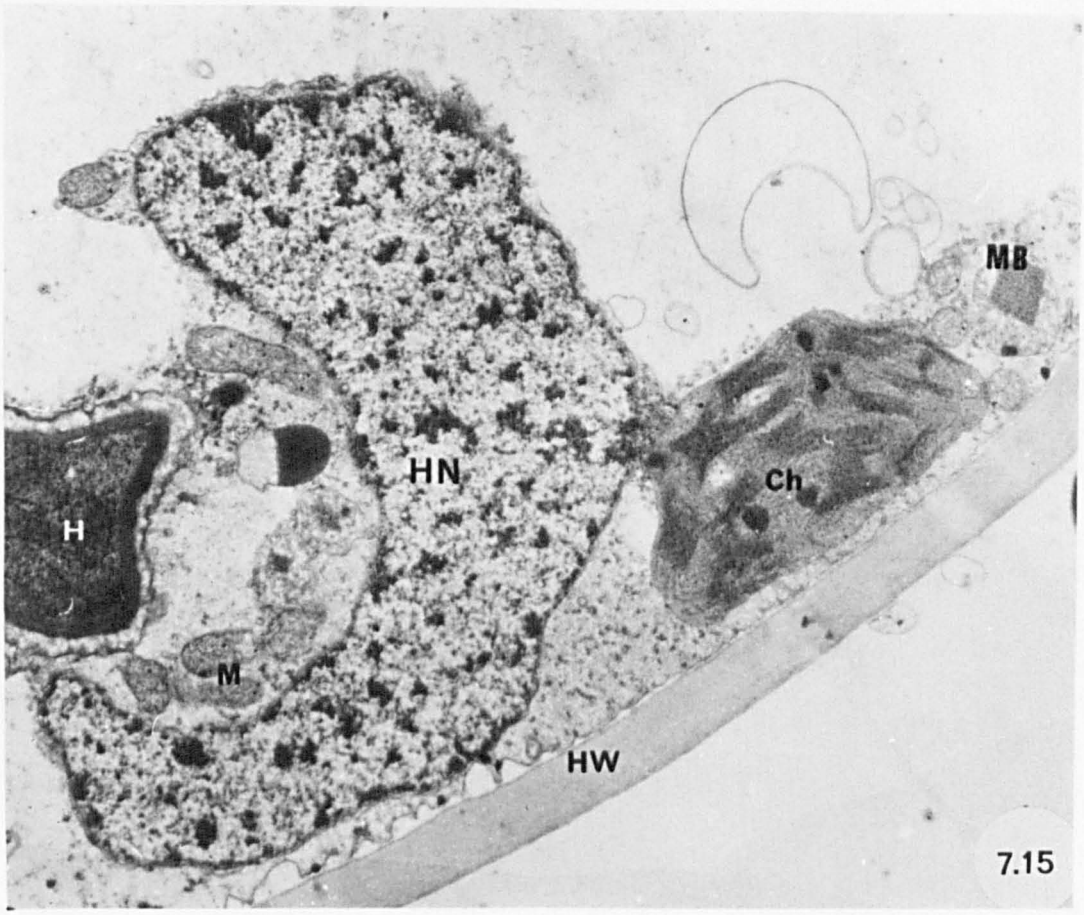

7.15

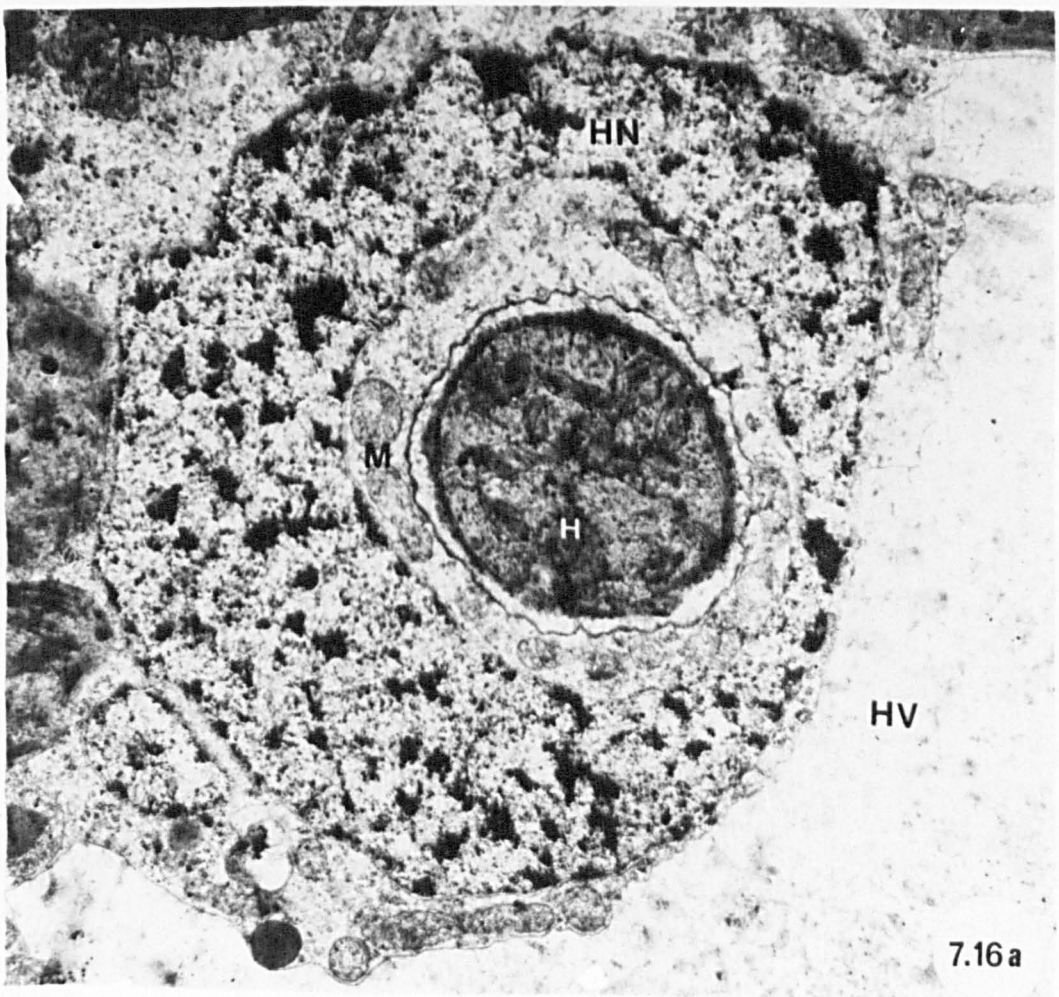

7.16 a

Figure 7.16b

Enlargement of Figure 7.16a. The film of cytoplasm between the haustorium and host nucleus includes mitochondria. No points of contact between nuclear membrane and extrahaustorial membrane are seen. Note many mitochondria in fungal haustorium. Note also the increased amount and density of euchromatin in nucleus.

x25000

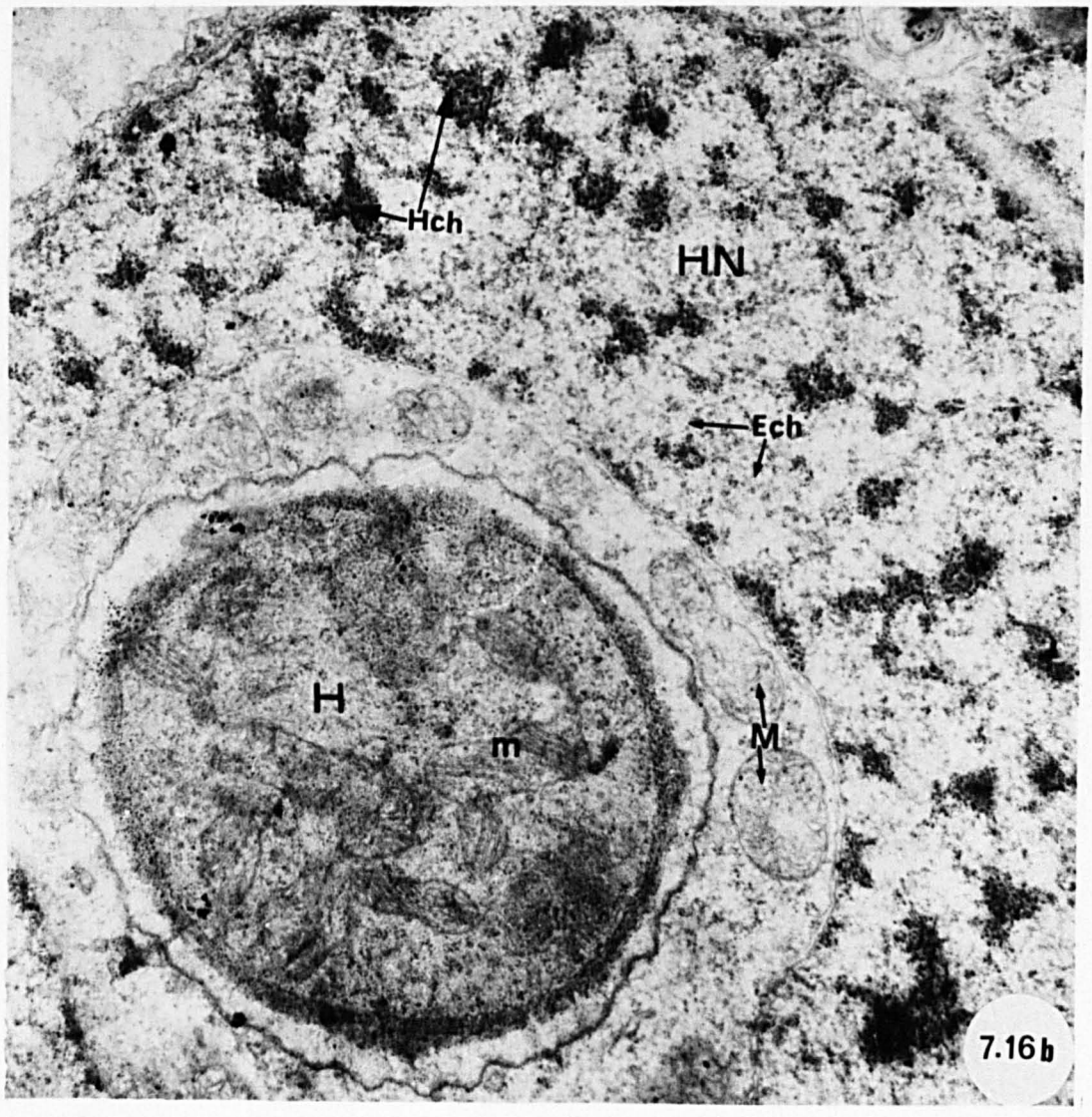
Hch
HN
Ech
H
m
M
7.16b

Figure 7.17

Association of haustorium with host nucleus at later stage of uredial development in *Poa*. Note the increased amount and electron-density of euchromatin (arrows). Note host mitochondria between the haustorium and host nucleus, extrahaustorial membrane (arrowhead) and fungal plasmalemma (open arrows).

x25000

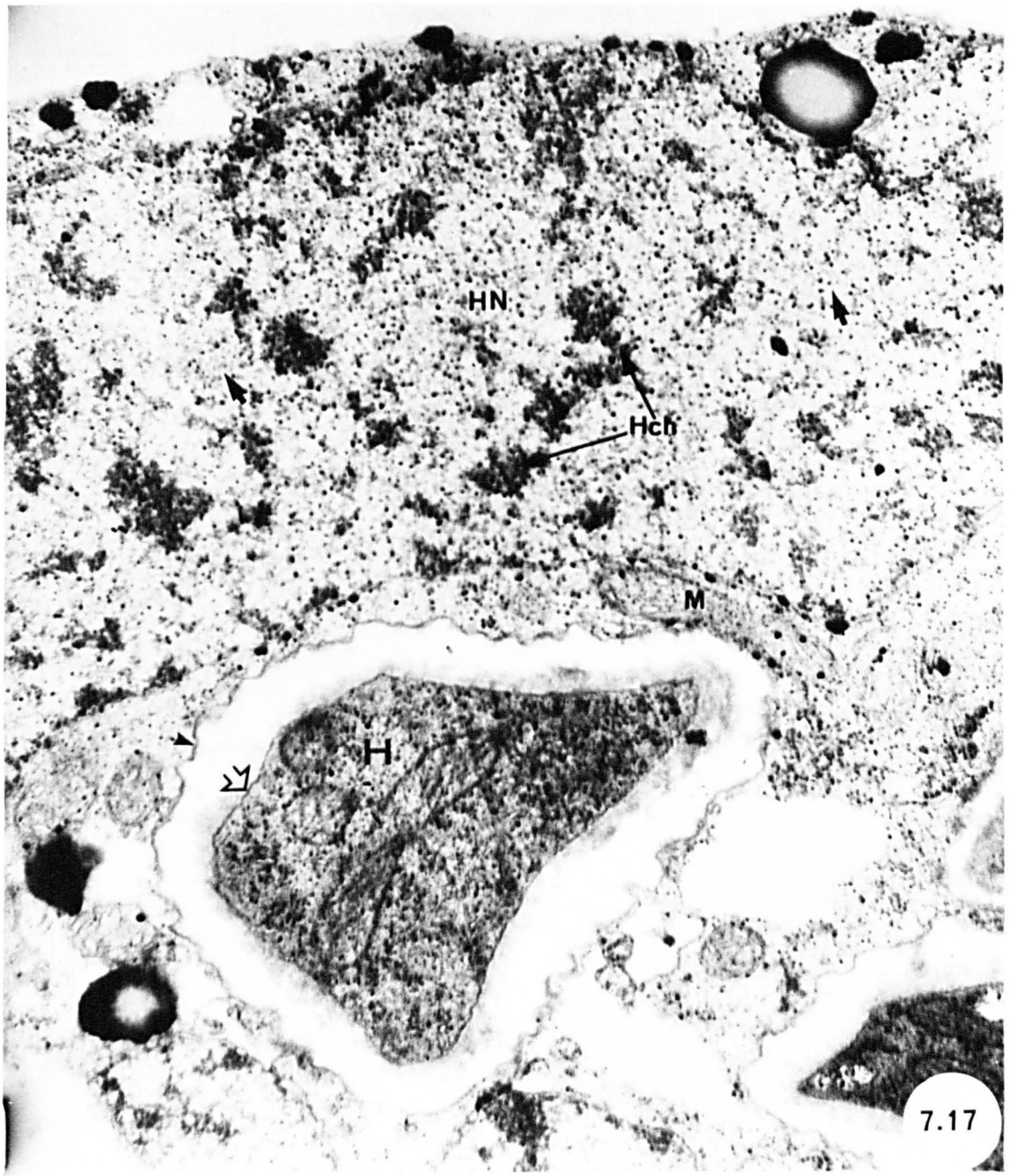
HN
Hch
M
H
7.17

Figure 7.18

Tussilago chloroplast in uninfected mesophyll cell showing well-developed membrane system of grana and intergranal lamellae, chloroplast bounding membranes and few osmiophilic globules.

x37500

7.18

Figure 7.19

Tussilago chloroplast in infected mesophyll cell at early stage of pycnial-aecial infection showing elongation of intergranal lamellae, reduced number and size of grana, increased number and size of osmiophilic globules and the appearance of starch grains.

x50000

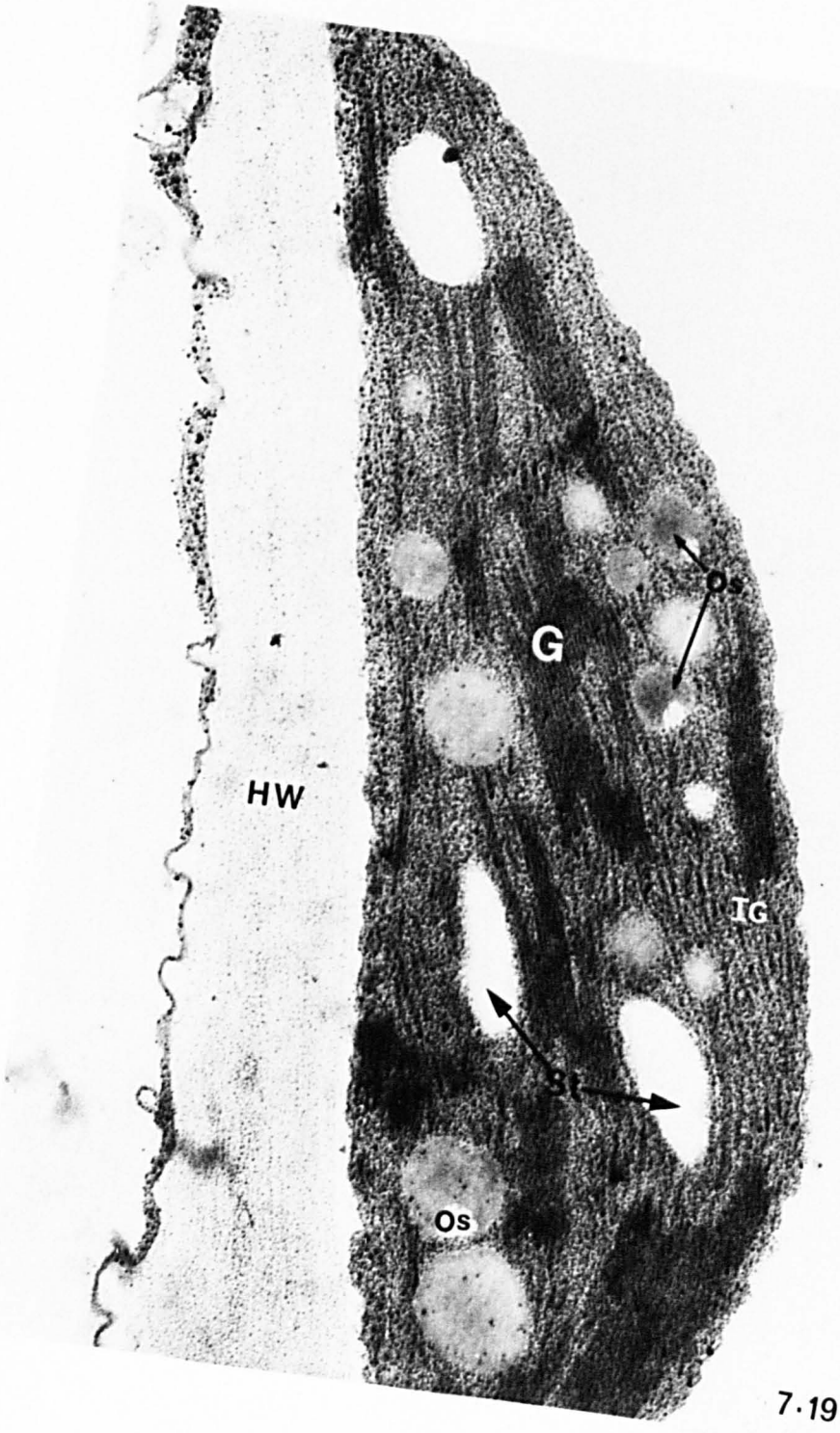

7·19

Figure 7.20a

Association of *Tussilago* chloroplast and fungal intracellular hyphae at later stages of pycnial-aecial infection. Note the breakdown of the chloroplast envelope (open arrow), fungal nucleus, mitochondria and lipid drop.

x12500

Figure 7.20b

Infected mesophyll cell of *Tussilago* at later stages of infection showing degenerated chloroplast. Note the disappearance of internal membranes and osmiophilic globules. Mitochondria and lipid drops are seen in intracellular hypha.

x30000


n
m
Ia
Ch
L
m
HW
7.20a

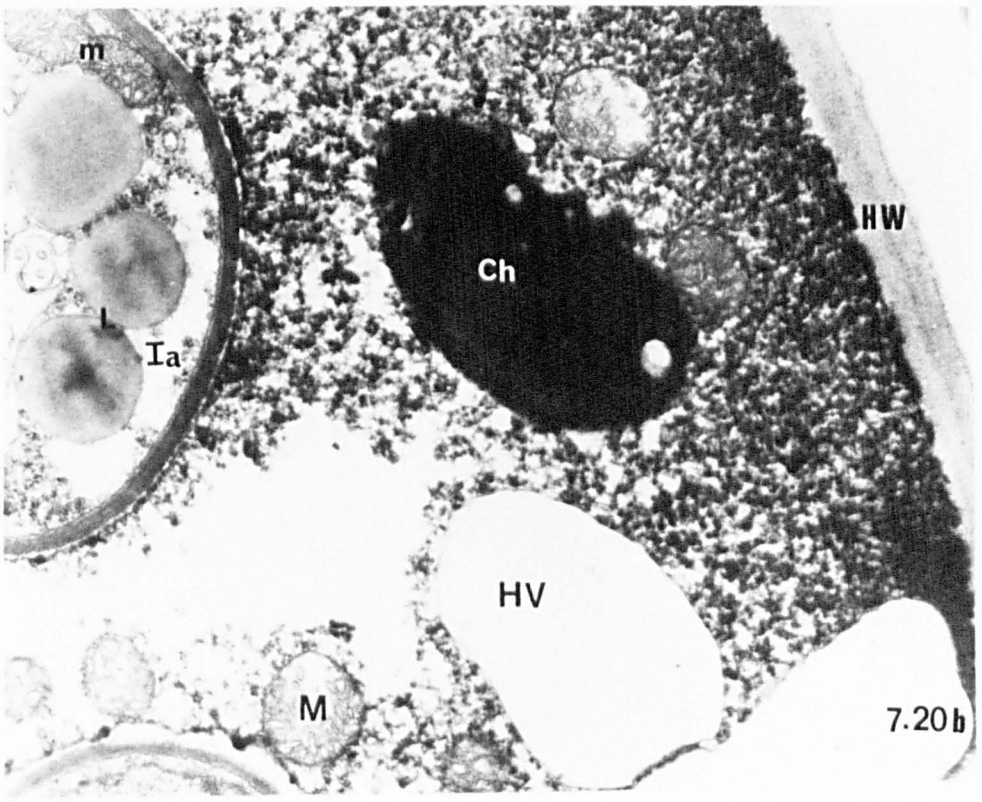
m
HW
Ch
L
Ia
HV
M
7.20b

Figure 7.20c

Degeneration of *Tussilago* chloroplasts at later stage of pycnial-aecial infection. Degradation of starch grains and osmiophilic globules and the breakdown of the chloroplast membranes are seen (unlabelled arrows). Some chloroplasts show few starch grains and osmiophilic globules. Note inter- and intracellular hyphae, host plasmalemma (arrowhead) and mitochondria.
x3750

Figure 7.20d

Part of infected mesophyll cell of *Tussilago* showing degenerated chloroplast. Note breakdown of chloroplast envelope (arrow) and degradation of starch grains and osmiophilic globules. Note vesiculated mitochondria and intracellular hyphae.
x12500

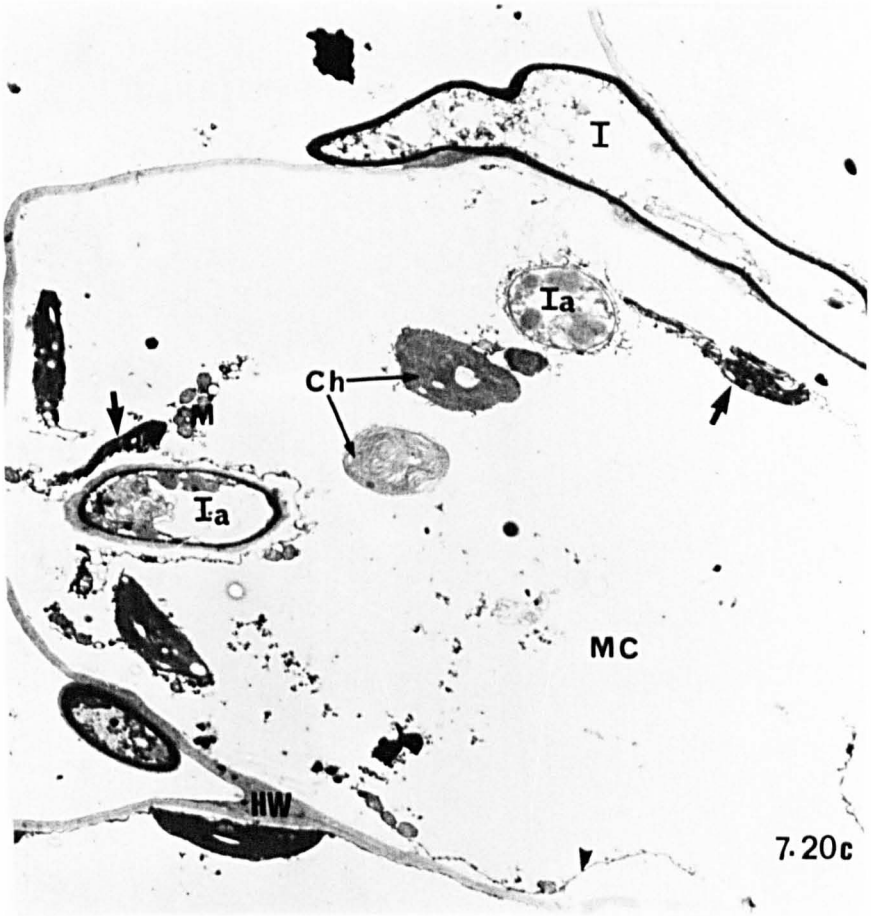

7.20c

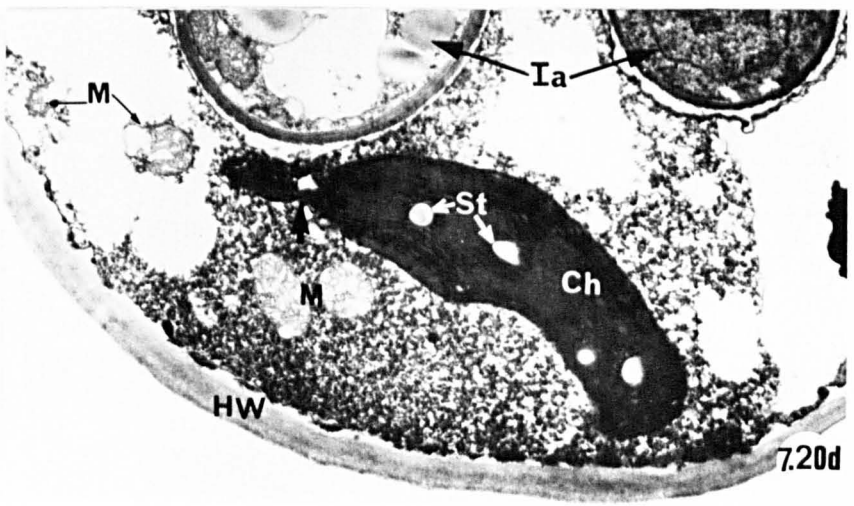

7.20d

Figure 7.21

Electron micrograph showing *Tussilago* chloroplast in close proximity to fungal intracellular hypha.

x30000

Figure 7.22a

Chloroplasts of aged healthy mesophyll cells of *Tussilago* showing well-developed membrane system of grana and intergranal lamellae. Note each chloroplast contains one large starch grain.

x25000

Figure 7.22b

Chloroplast of aged healthy mesophyll cell of *Tussilago* with three large starch grains and well-developed grana and intergranal lamellae.

x25000

7.21

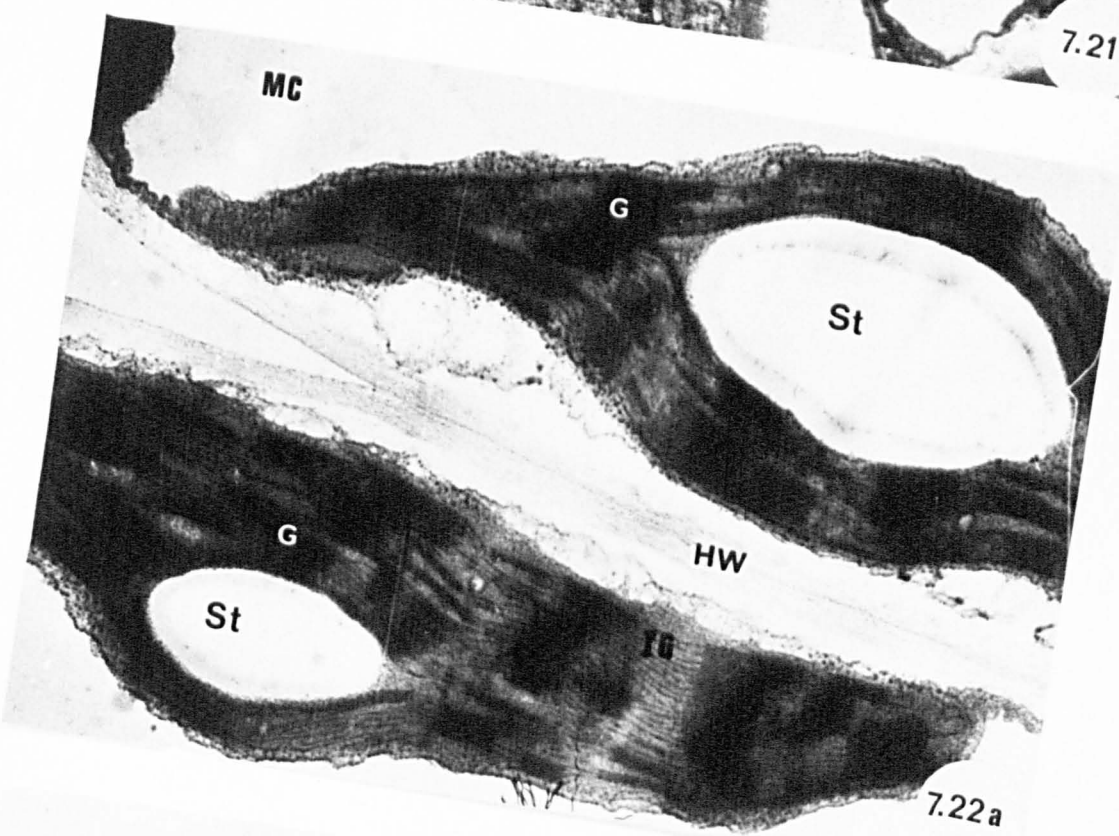

7.22a

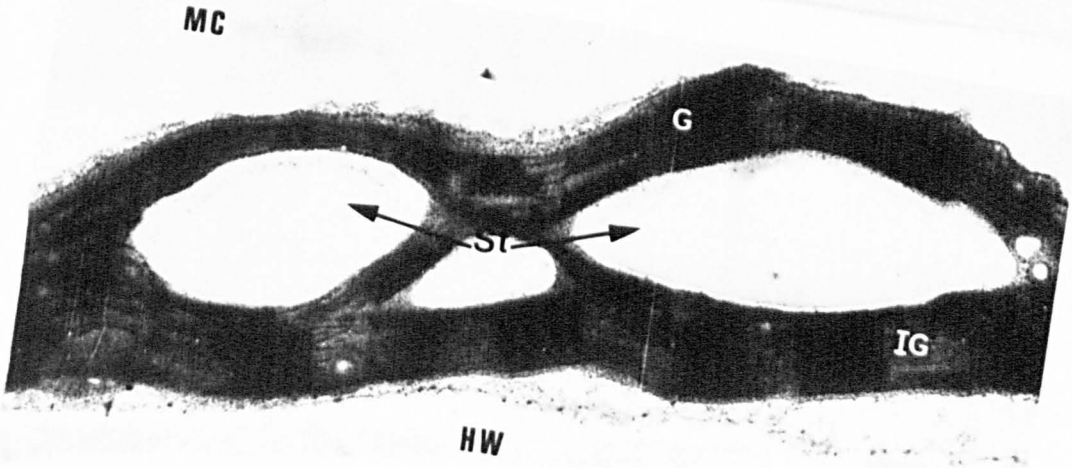

7.22b

Figure 7.23

Chloroplast of uninfected *Poa* mesophyll cell showing well-developed grana, intergranal lamellae (arrowheads) and bounding membranes. Note osmiophilic globules.

x35000

Figure 7.24

Chloroplasts of aged healthy mesophyll cells of *Poa* showing well-developed membrane structure and starch grains.

x6250

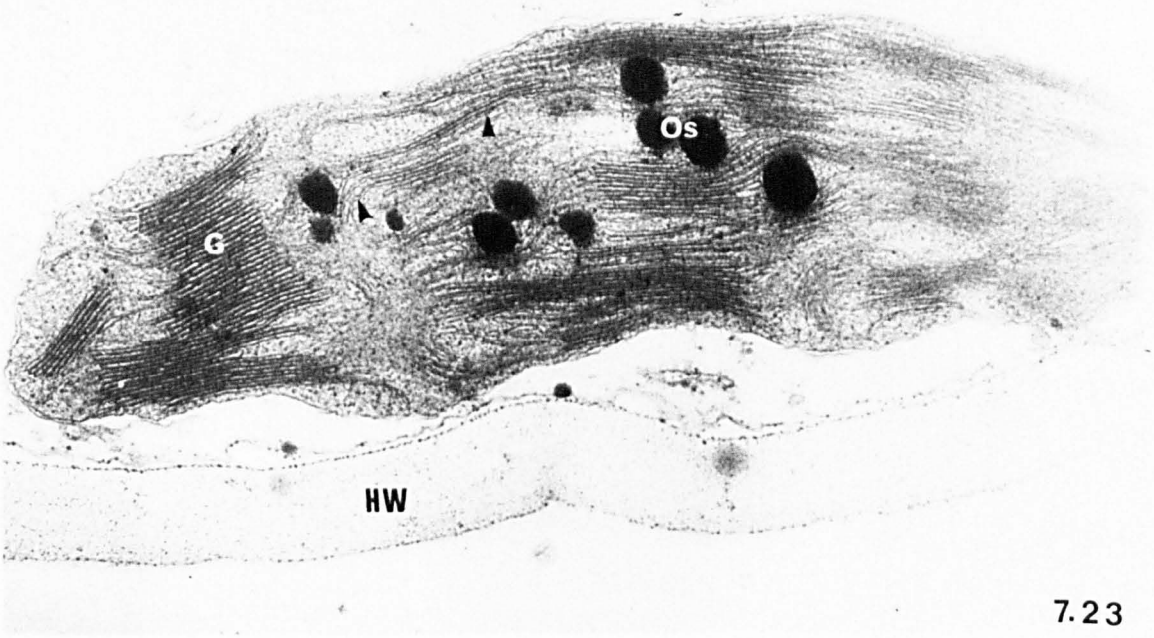

7.23

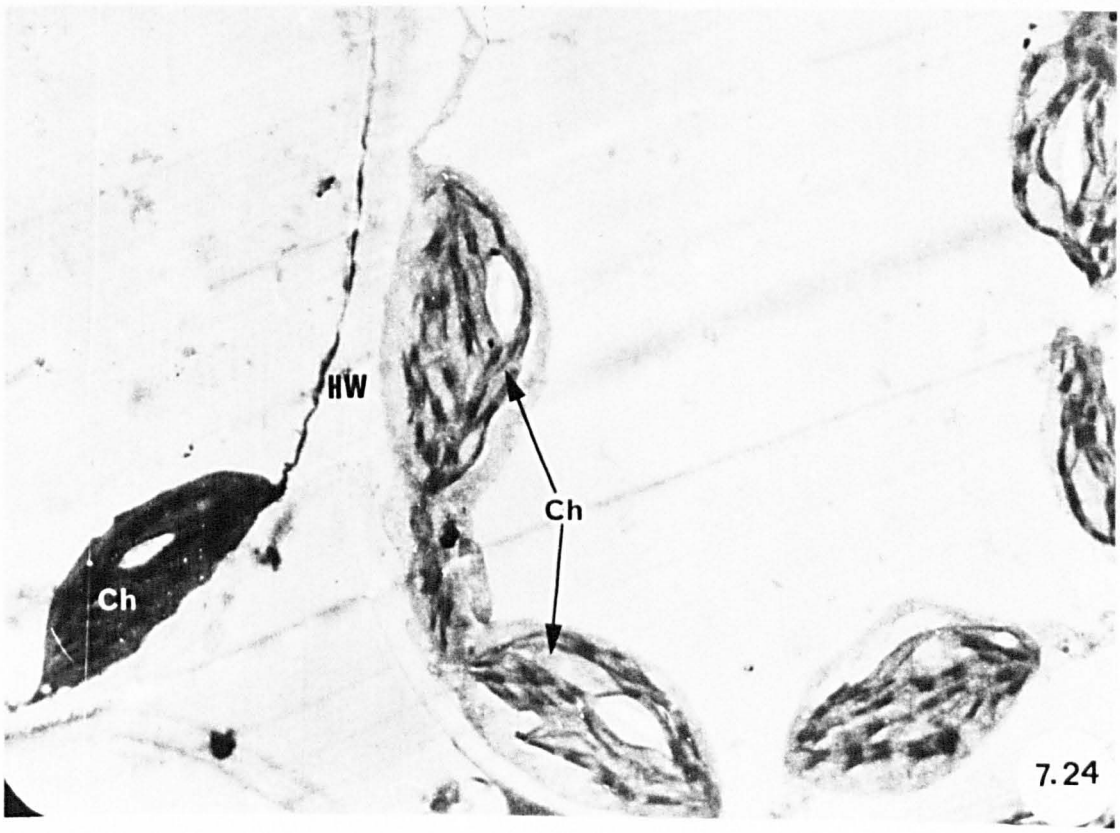

7.24

Figure 7.25

Chloroplasts of aged healthy mesophyll cell of *Poa* showing vesiculated areas (arrows) and starch grain.

x10000

Figure 7.26

Infected *Poa* mesophyll cell at early stage of uredial and telial development showing chloroplasts with well-developed membrane structure. Note osmiophilic globules and starch grains. Note also intercellular hypha.

x10000

Figure 7.27

Infected *Poa* mesophyll cell at early stage of uredial-telial infection showing increased number of osmiophilic globules and the appearance of starch grains. Note intercellular hypha.

x15000


Ch
St
HW
7.25

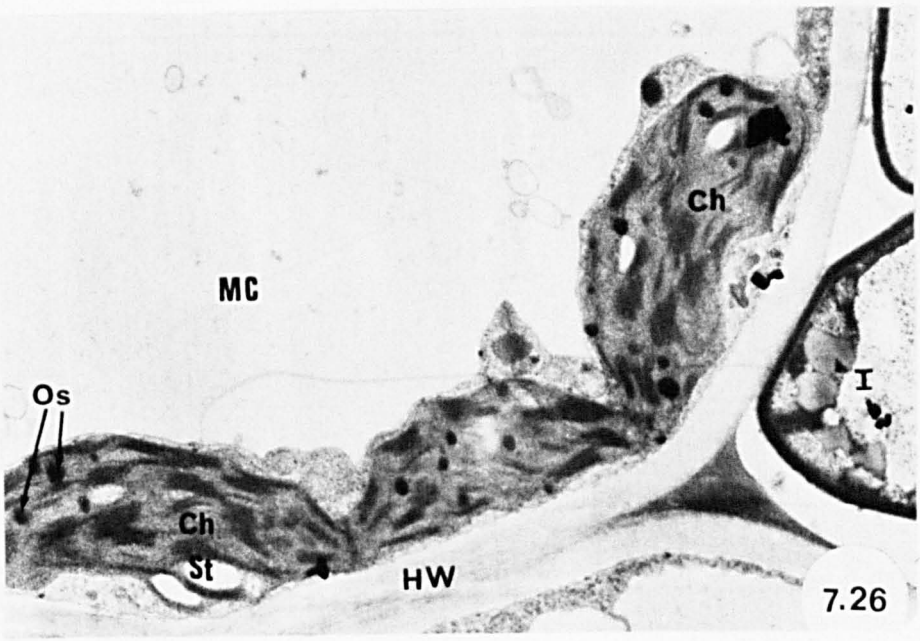
Ch
MC
Os
I
Ch
St
HW
7.26

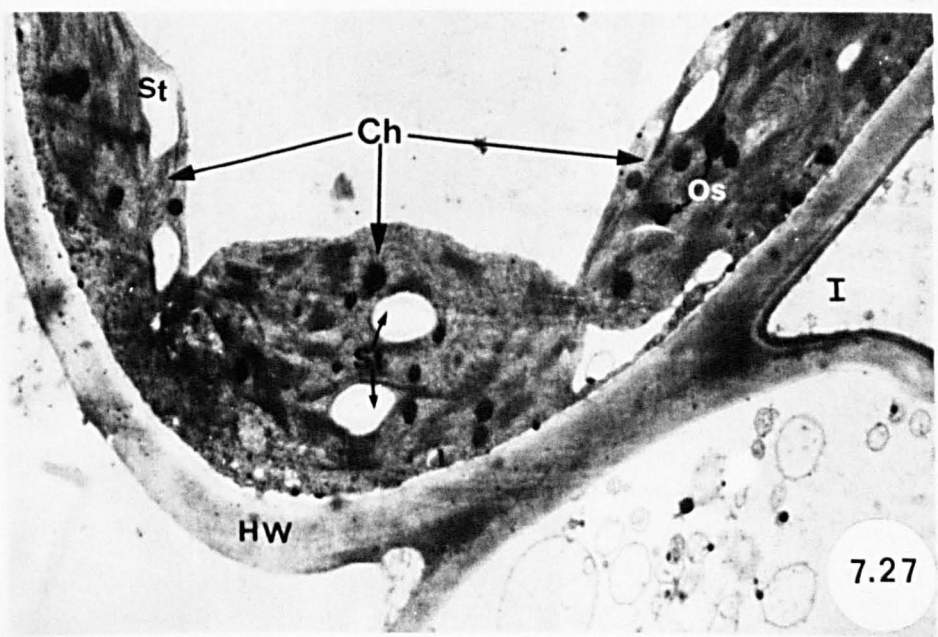
St
Ch
Os
I
St
HW
7.27

Figure 7.28a

Infected *Poa* mesophyll cell at later stage of uredial and telial development showing chloroplasts with relatively normal membrane structure. Note starch grains and many osmiophilic globules. Note intercellular hypha.

x15000

Figure 7.28b

Chloroplasts of infected *Poa* mesophyll cell showing many osmiophilic globules and several starch grains. Note haustorium.

x12500

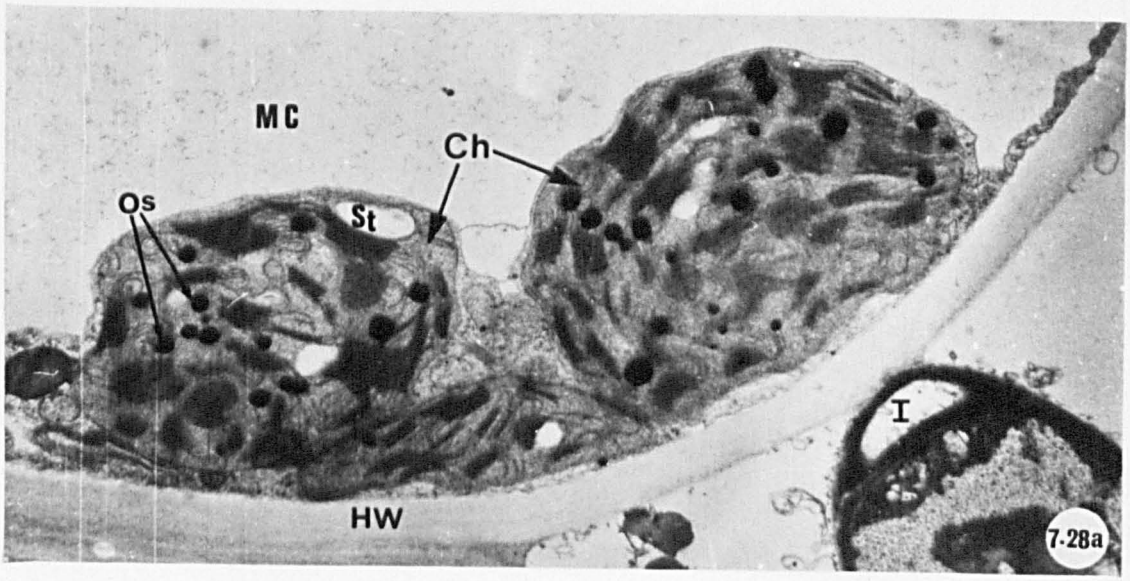
MC
Ch
Os
St
I
HW
7.28a


H
Ch
MC
Ch
Os
St
HW
7.28b

Figure 7.29

Chloroplast of infected mesophyll cell of *Poa* at early stage of uredial infection showing peripheral vesicle (solid arrow). Note grana, intergranal lamellae (open arrow) and osmiophilic globules.

x37500

Figure 7.30

Infected *Poa* mesophyll cell showing chloroplast with swollen grana and intergranal lamellae. Note crystal-containing microbody.

x37500

Figure 7.31

Chloroplast of infected *Tussilago* mesophyll cell at early stage of pycnial infection showing swelling of grana (arrows) and intergranal lamellae (arrowhead). Note intracellular hypha.

x30000

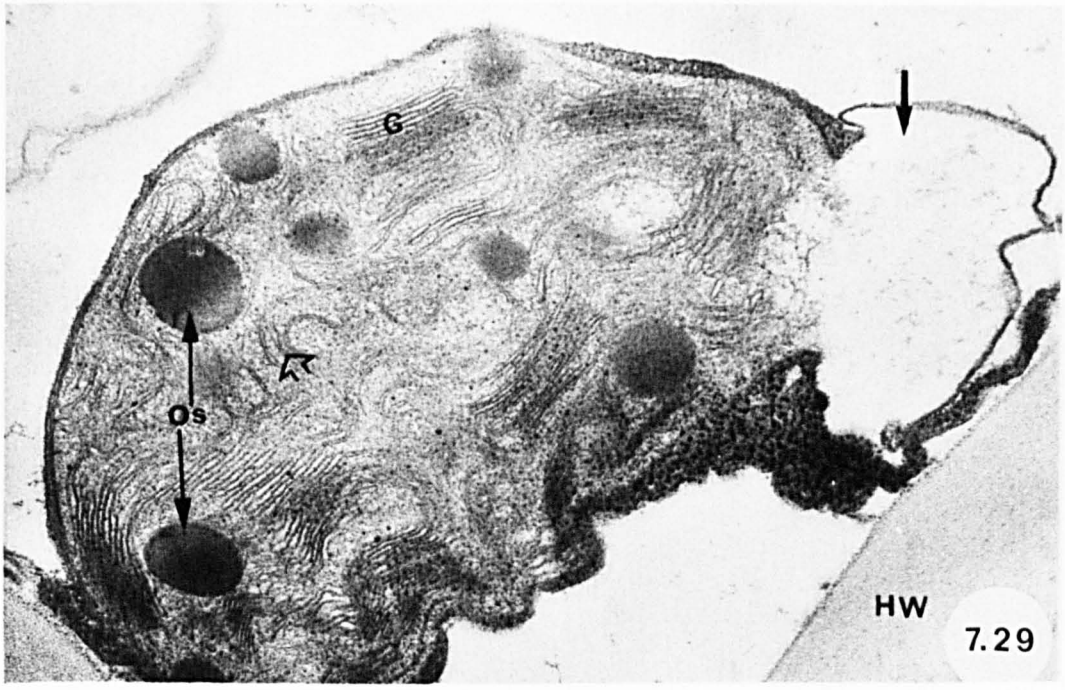

7.29

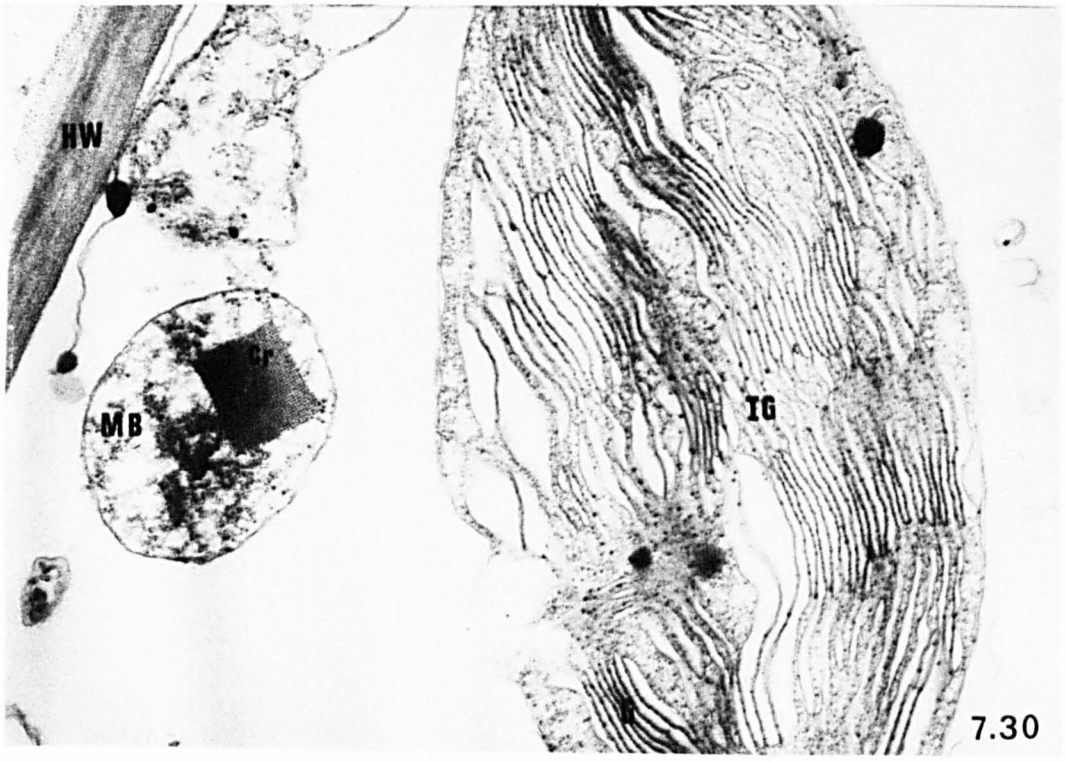

7.30

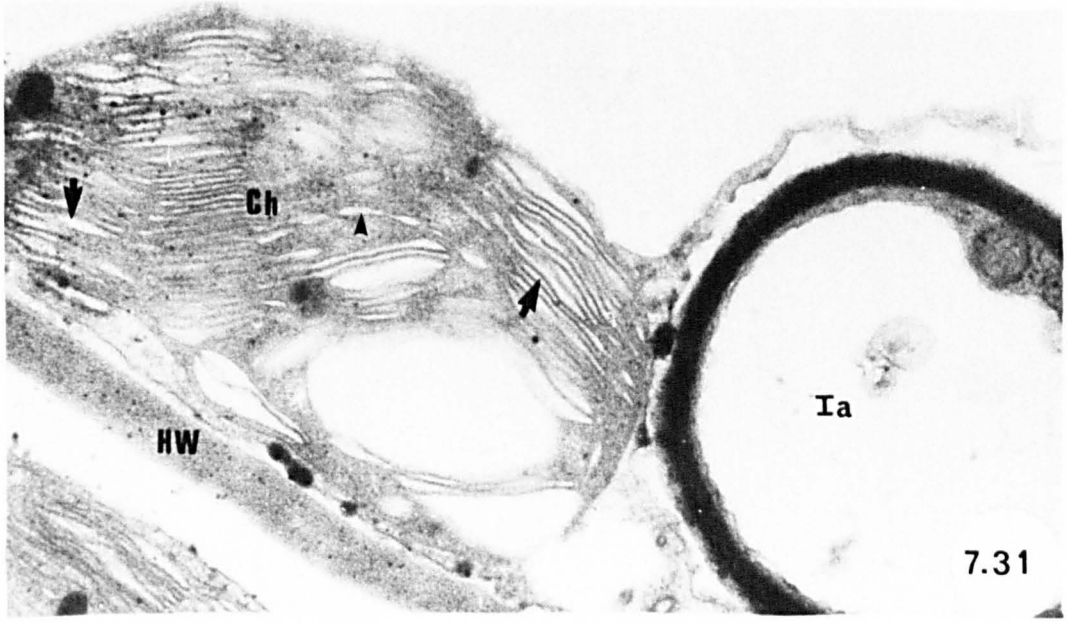

7.31

Figure 7.32a

Infected *Tussilago* mesophyll cell showing crystal-containing microbodies close to host nucleus and mitochondria.

x10000

Figure 7.32b

Magnified microbody of infected *Tussilago* mesophyll cell showing large crystal and the surrounding granular material.

x120000

Figure 7.32c

Crystal-containing microbody of infected *Tussilago* mesophyll cell adjacent to host cell wall. The microbody is surrounded by a single membrane.

x37500

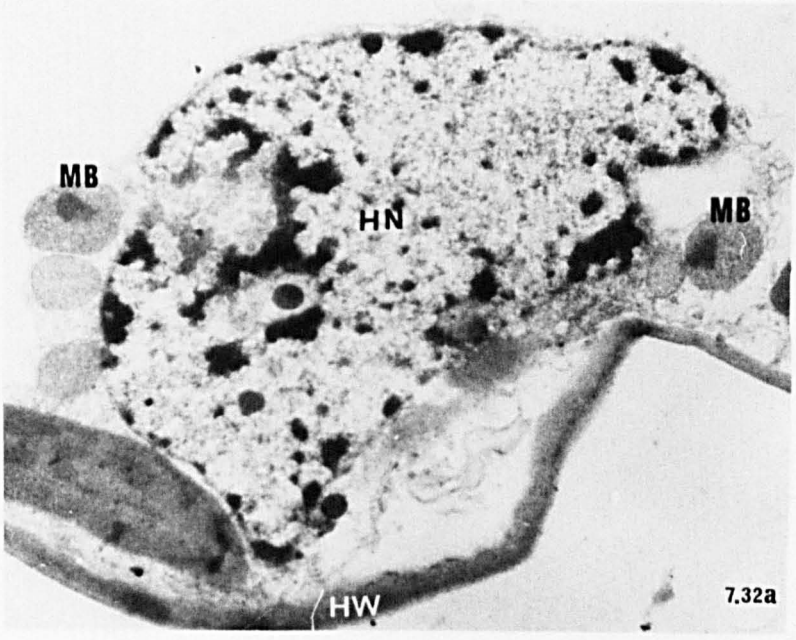
MB
HN
MB
HW
7.32a

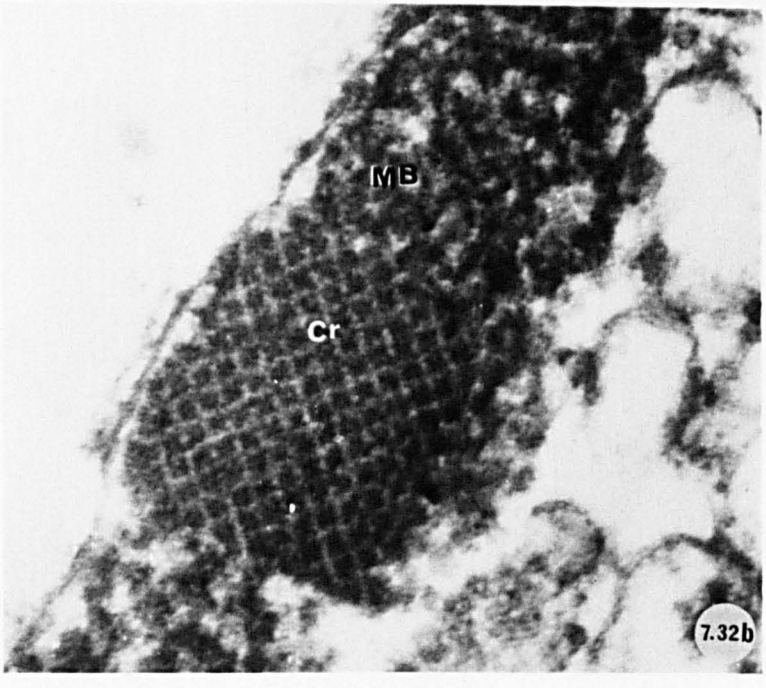
MB
Cr
7.32b

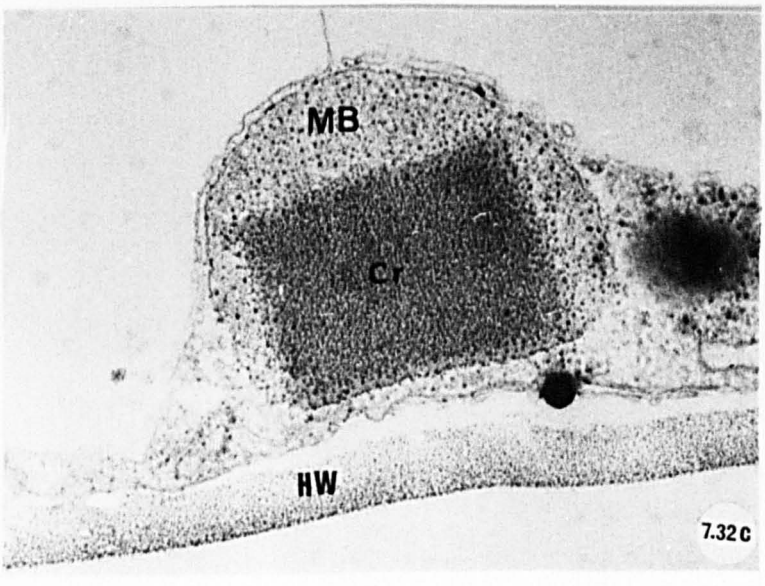
MB
Cr
HW
7.32c

Figure 7.33

Association of crystal-containing microbodies and cell wall of uninfected *Tussilago* mesophyll cell. Note each microbody is bounded by a single membrane.

x37500

Figure 7.34

Aged uninfected mesophyll cell of *Tussilago* showing microbodies in close association with chloroplasts and mitochondria. Note traces of crystal in microbodies (arrowhead).

x15000

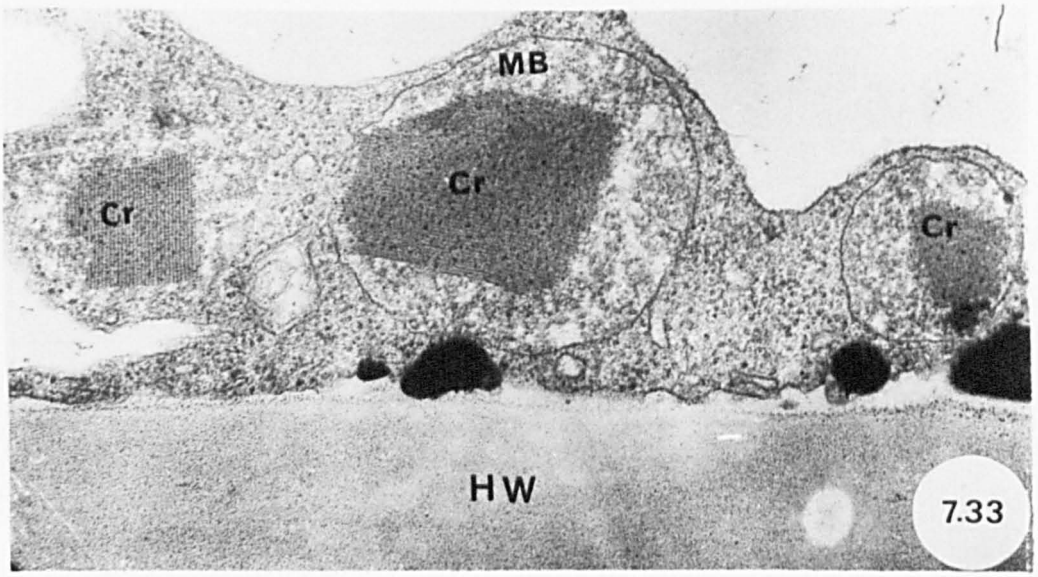

7.33

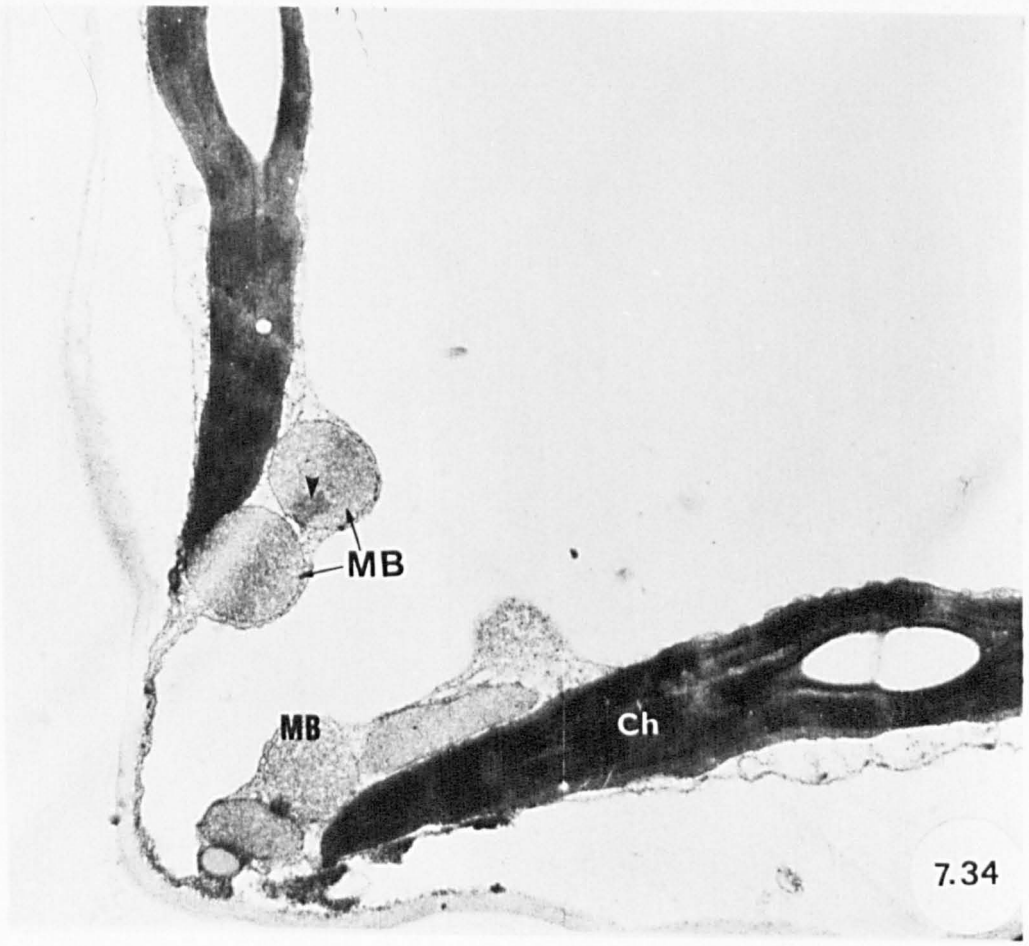

7.34

Figure 7.35a

Crystal containing microbody in uninfected *Poa* mesophyll cell showing fibrillar units (arrowheads). Note chloroplast and lipid drop.

x75000

Figure 7.35b

Crystal-containing microbody in uninfected *Poa* mesophyll cell showing several fibrillar units (arrows) and granular material. The single bounding membrane of the microbody is closely appressed to the outer membrane of the chloroplast.

x40000

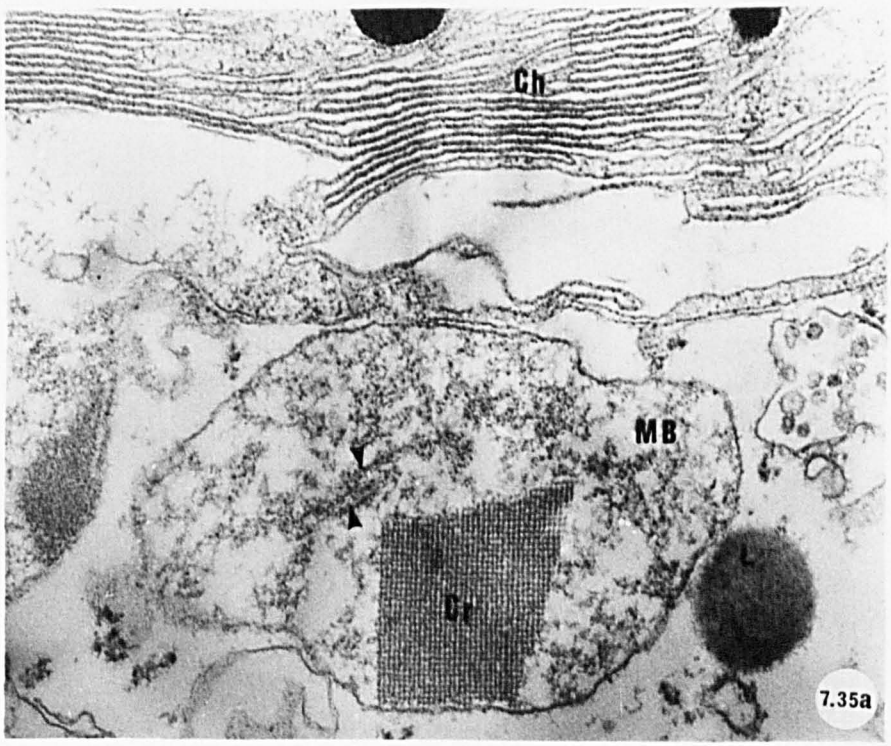
Ch
MB
Cr
L
7.35a

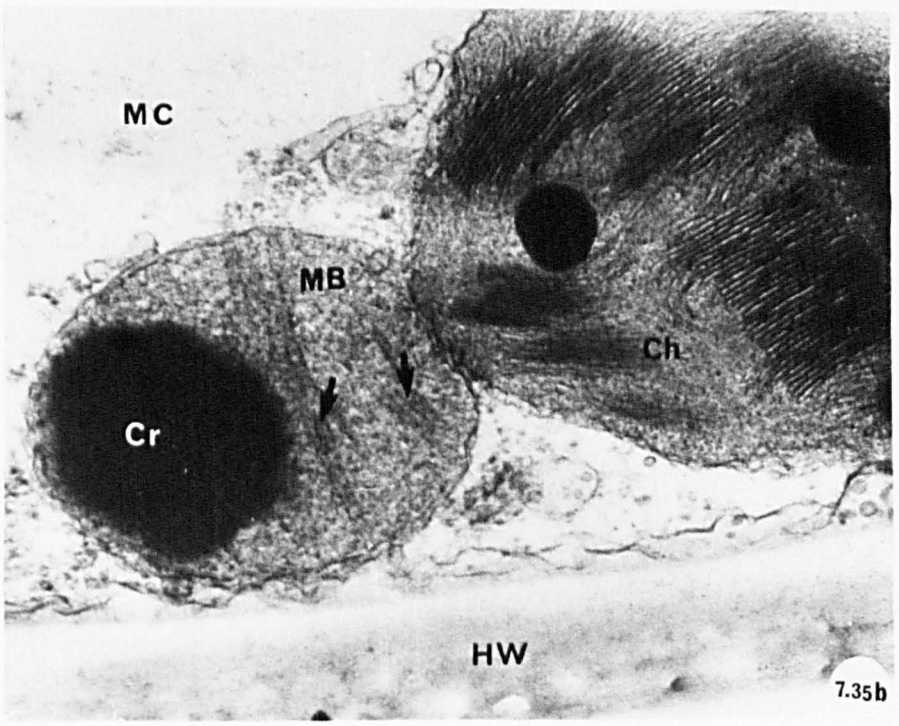
MC
MB
Ch
Cr
HW
7.35b

Figure 7.35c

Uninfected mesophyll cell of *Poa* showing microbody closely associated with chloroplast and mitochondria. Less granular material is seen in the microbody, compared with that in Figure 7.35b (see also variation in size and shape of crystal in Figure 7.35a, b and c). Note endoplasmic reticulum closely appressed to nuclear membrane.

x37500

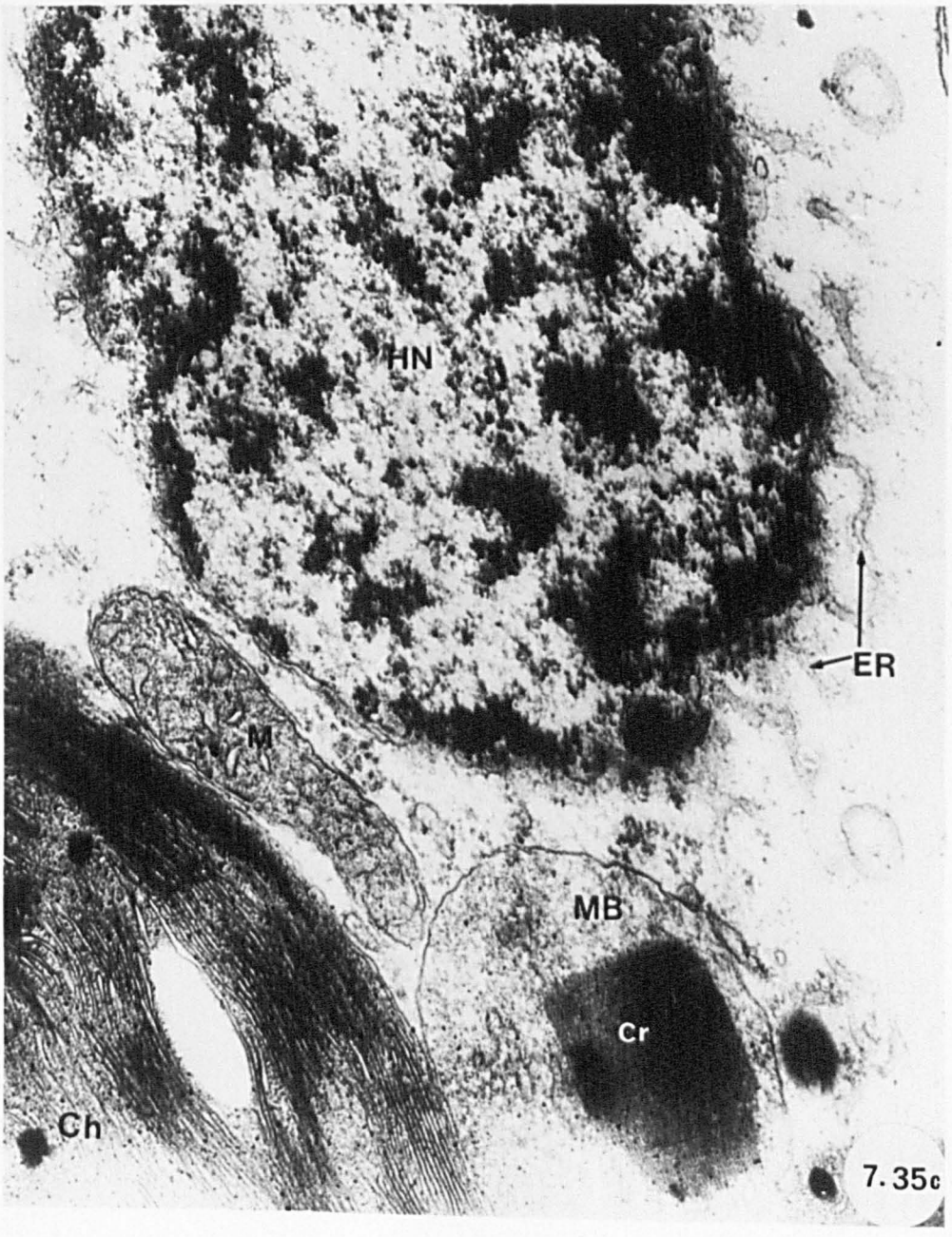
HN
ER
M
MB
Cr
Ch
7.35c

Figure 7.36

Association of crystal-containing microbody and chloroplast in infected *Poa* mesophyll cell. The single bounding membrane of microbody is closely appressed to the chloroplast envelope.

x75000

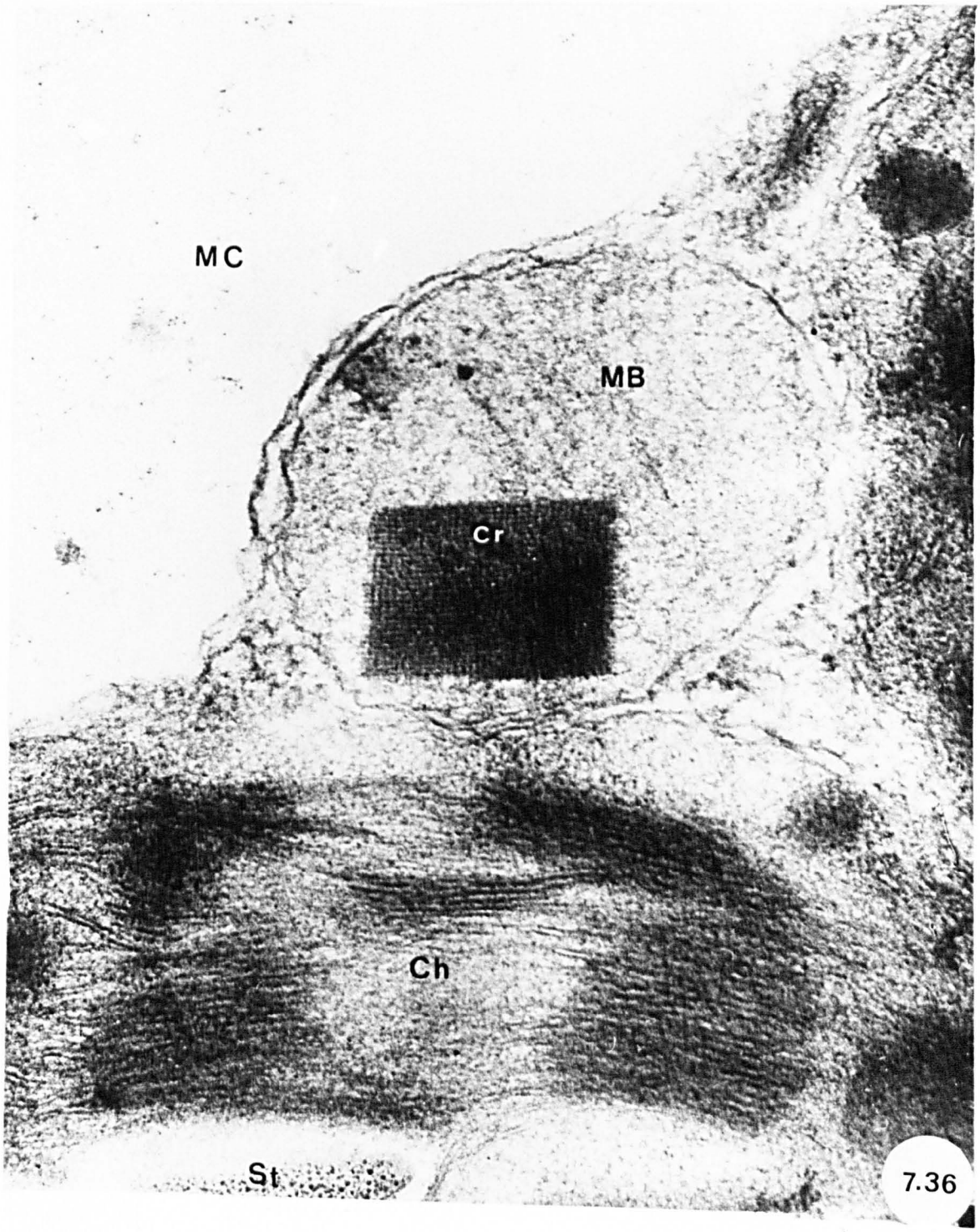

7.36

Figure 7.37

Association of crystal-containing microbody and mitochondrion in infected *Poa* mesophyll cell.

x50000

Figure 7.38

Association of crystal-containing microbodies and nucleus in infected *Poa* mesophyll cell. Variations in the size and morphology of crystals and the amount of granular material are seen (see also Figures 7.36 and 7.37).

x75000

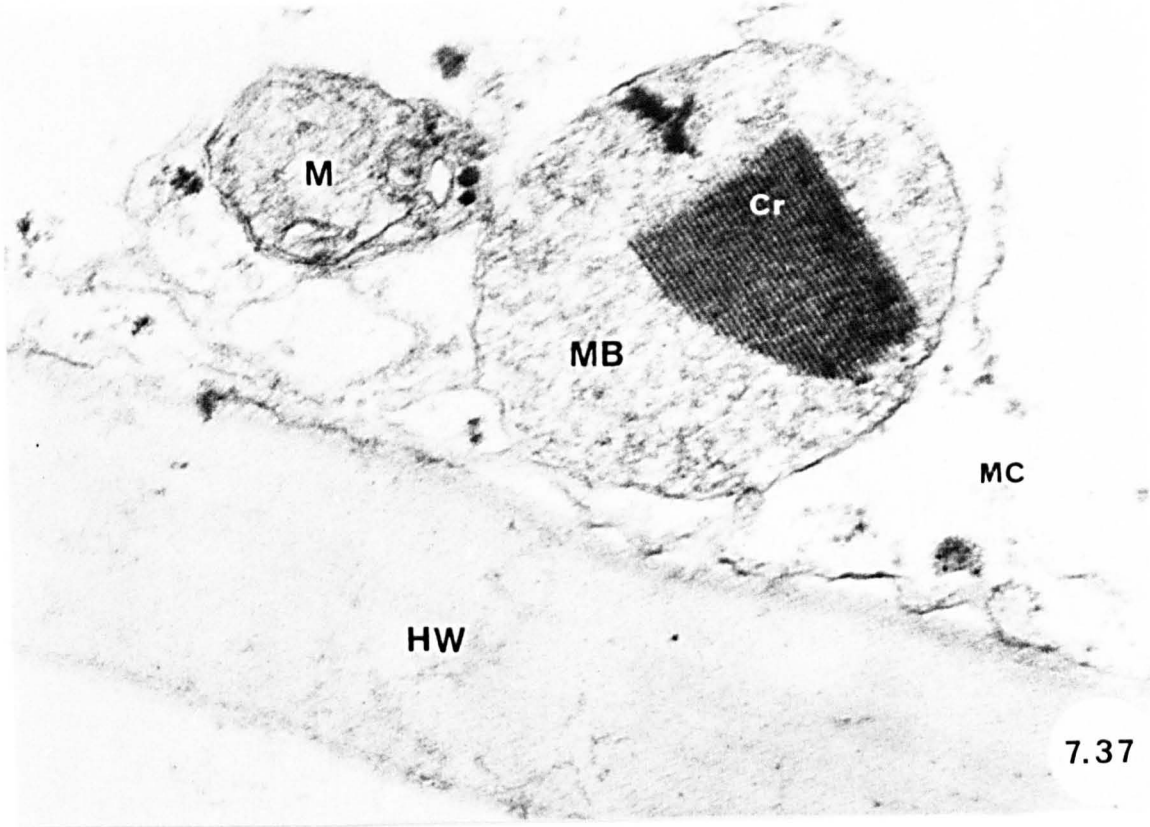

7.37

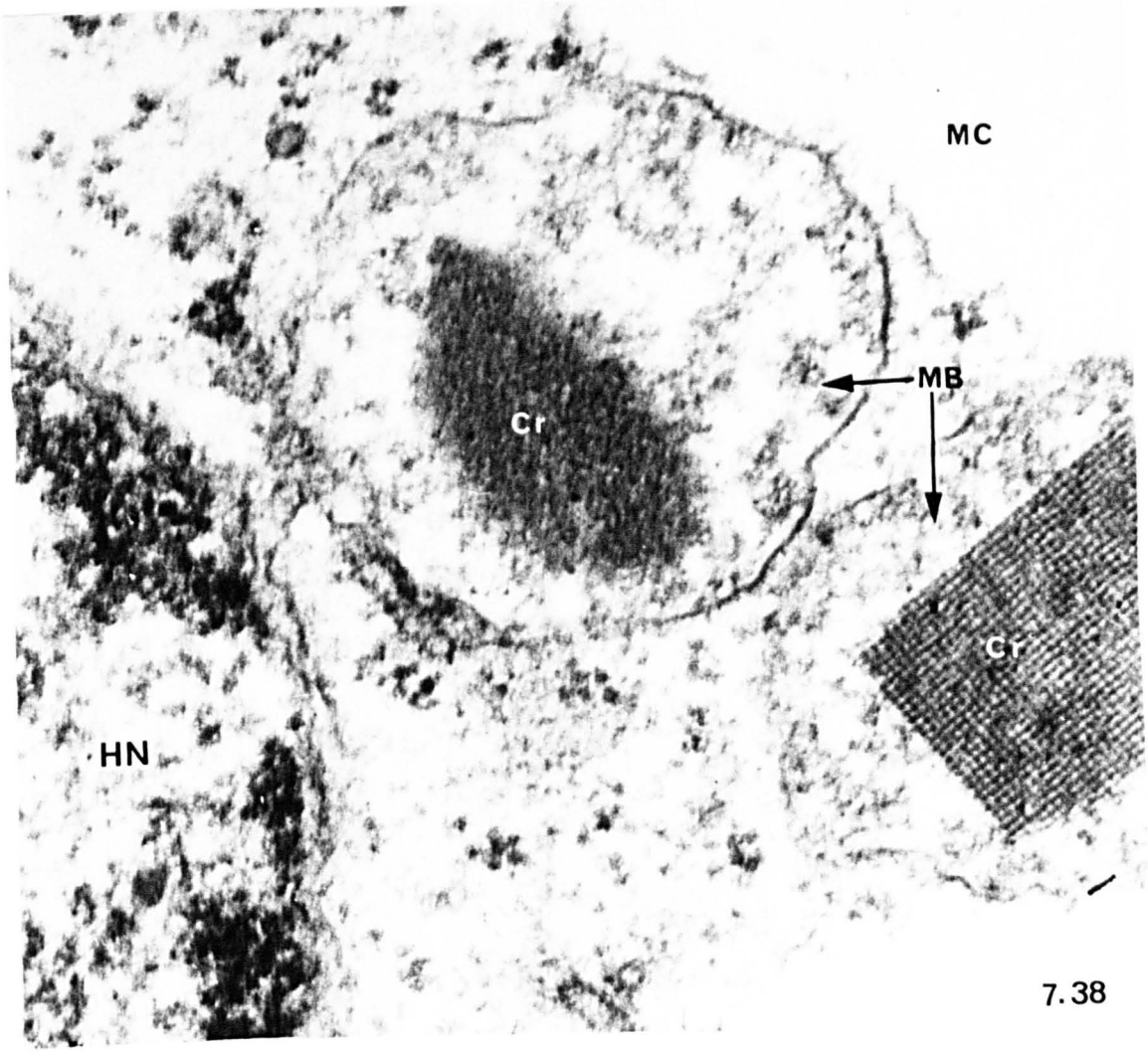

7.38

Figure 7.39

Infected *Poa* mesophyll cell at early stage of uredial infection showing several crystal-containing microbodies associated with host chloroplasts and nucleus. Note fungal cells showing nucleus and lipid droplets.

x10000

Figure 7.40

Infected *Poa* mesophyll cell at later stage of uredial infection showing crystal-containing microbodies in close association with chloroplasts. Note intercellular hypha.

x15000

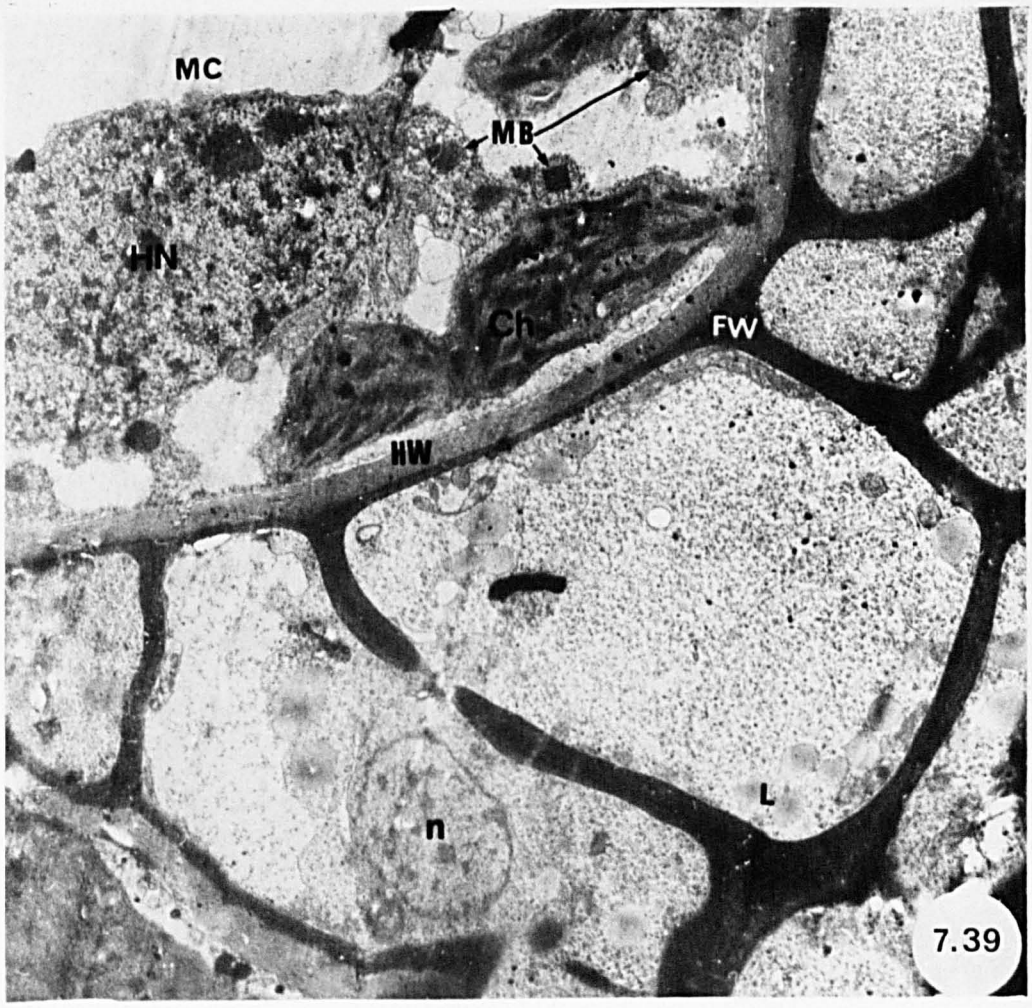

7.39

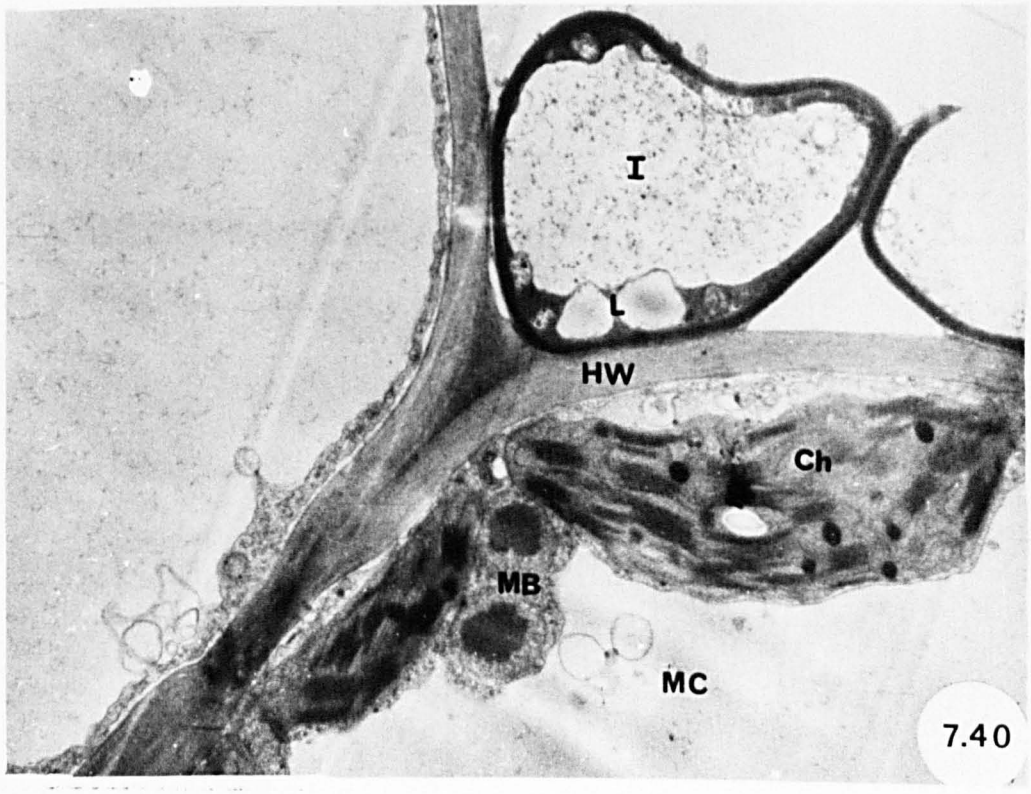

7.40

Figure 7.41

Two crystal-containing microbodies closely appressed to chloroplast of infected *Poa* mesophyll cell at later stage of uredial infection. Note variation in the size of crystals (arrowheads) and the single bounding membrane of microbody.

x75000

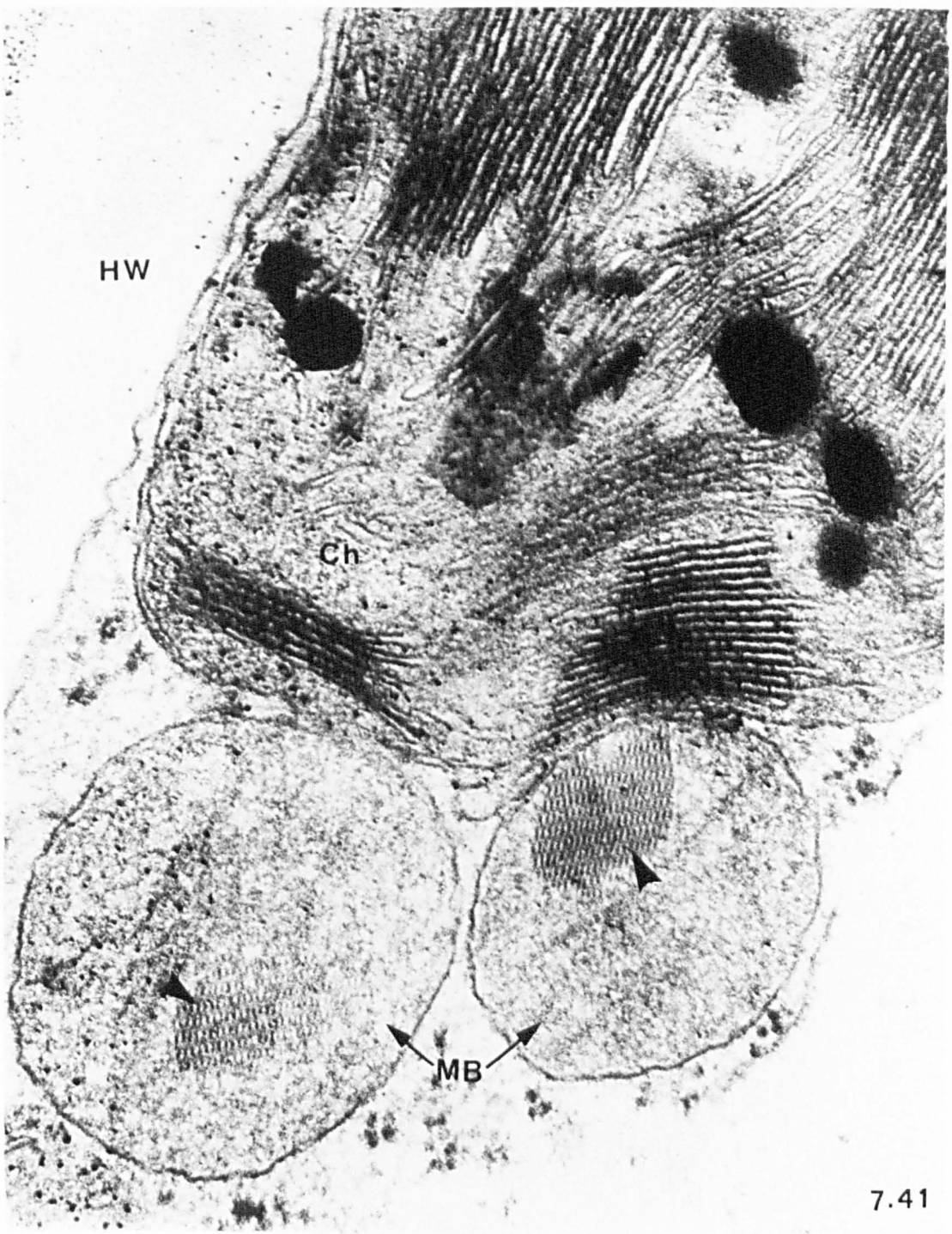

7.41

Figure 7.42

Infected mesophyll cell of *Tussilago* at later stage of pycnial-aecial infection showing vesiculated mitochondria. Note intracellular hypha.

x37500

Figure 7.43

Golgi body associated with cell wall of uninfected *Poa* mesophyll cell.

x100000

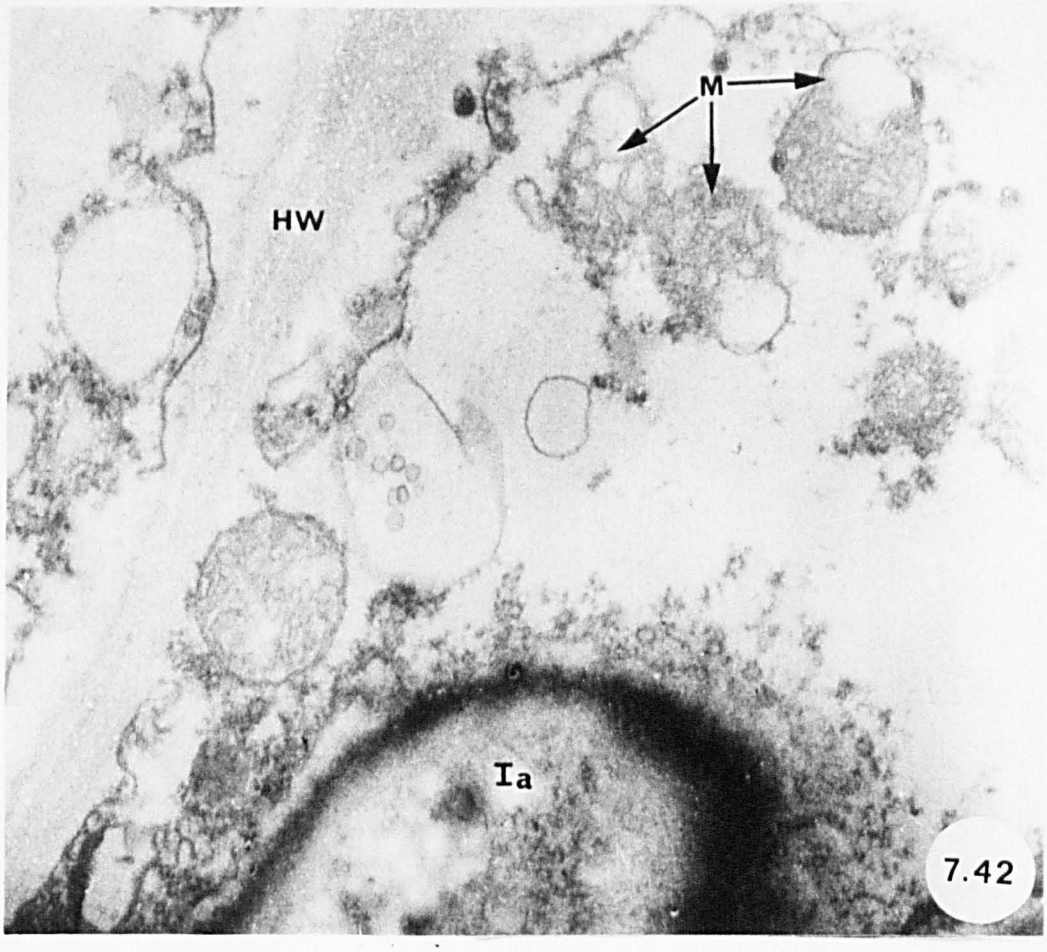
M
HW
Ia
7.42


g
HW
7.43

Figure 7.44a

Infected mesophyll cell of *Poa* at early stage of uredial infection showing Golgi body in close association with chloroplast.

x50000

Figure 7.44b

Infected mesophyll cell of *Poa* at later stage of uredial infection showing increased number of Golgi bodies.

x50000

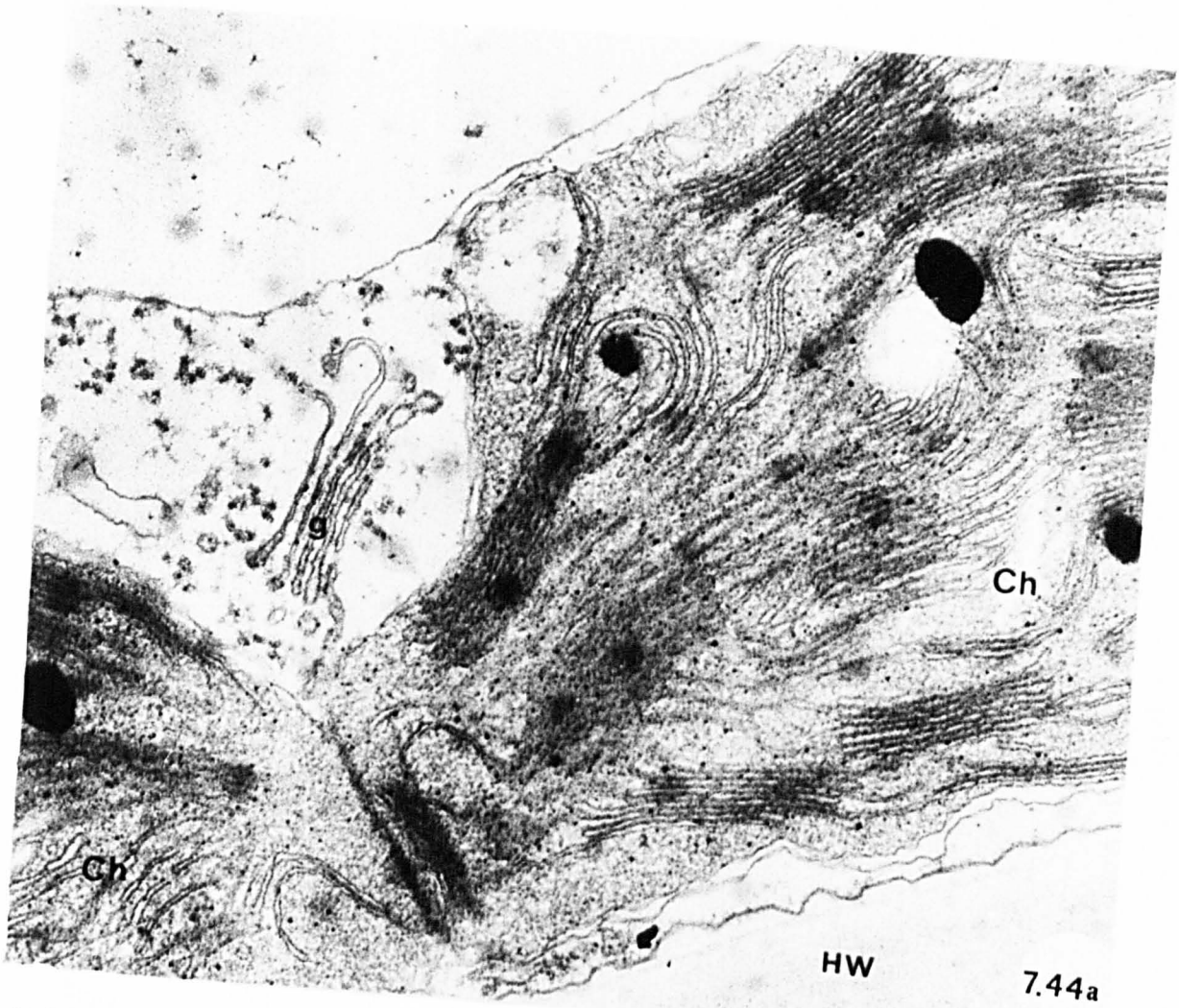

7.44a

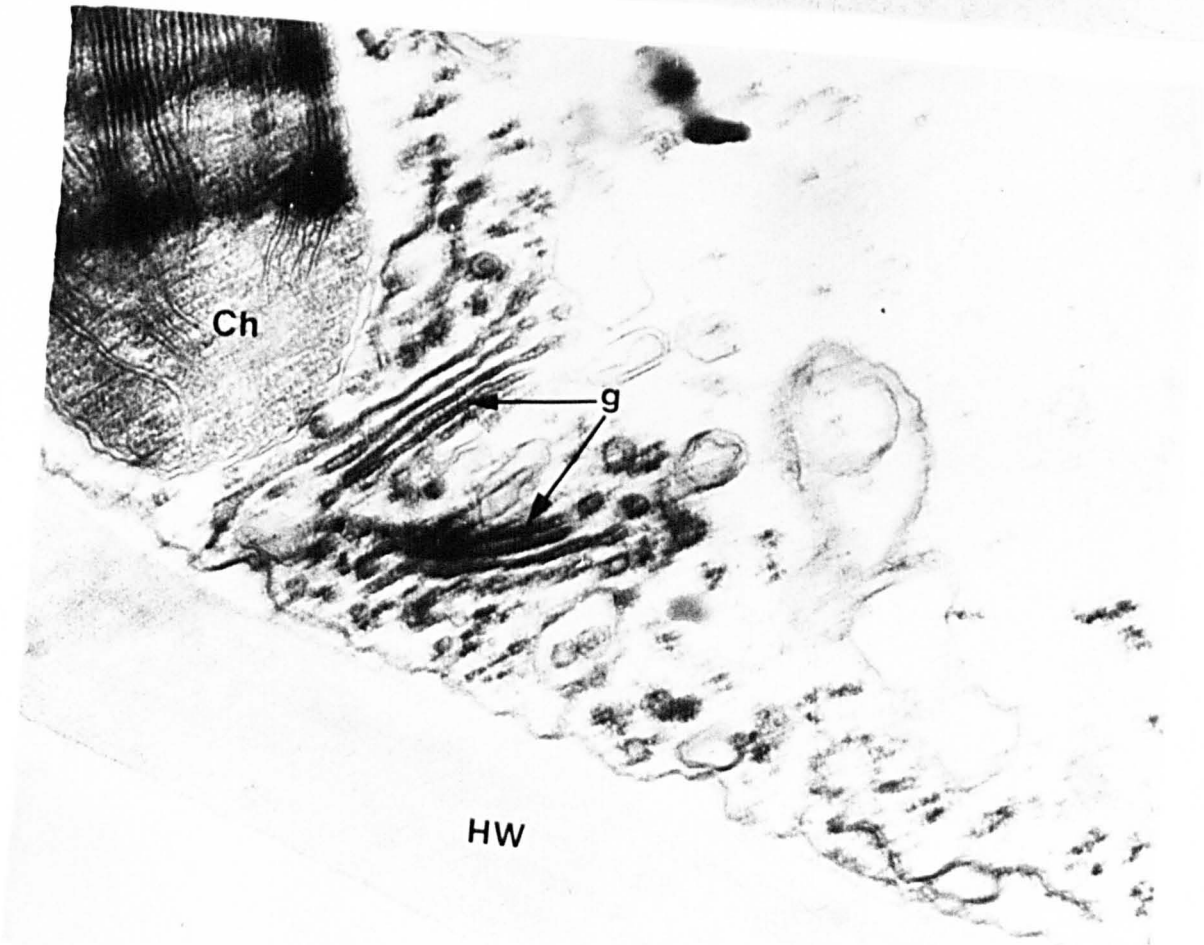

7.44b

Figure 7.45a

Infected mesophyll cell of *Poa* at later stage of uredial infection showing association of Golgi body with host chloroplast and mitochondria. Note rough endoplasmic reticulum.

x40000

Figure 7.45b

Association of Golgi body and crystal-containing microbody in infected mesophyll cell of *Poa* at later stage of infection.

x75000

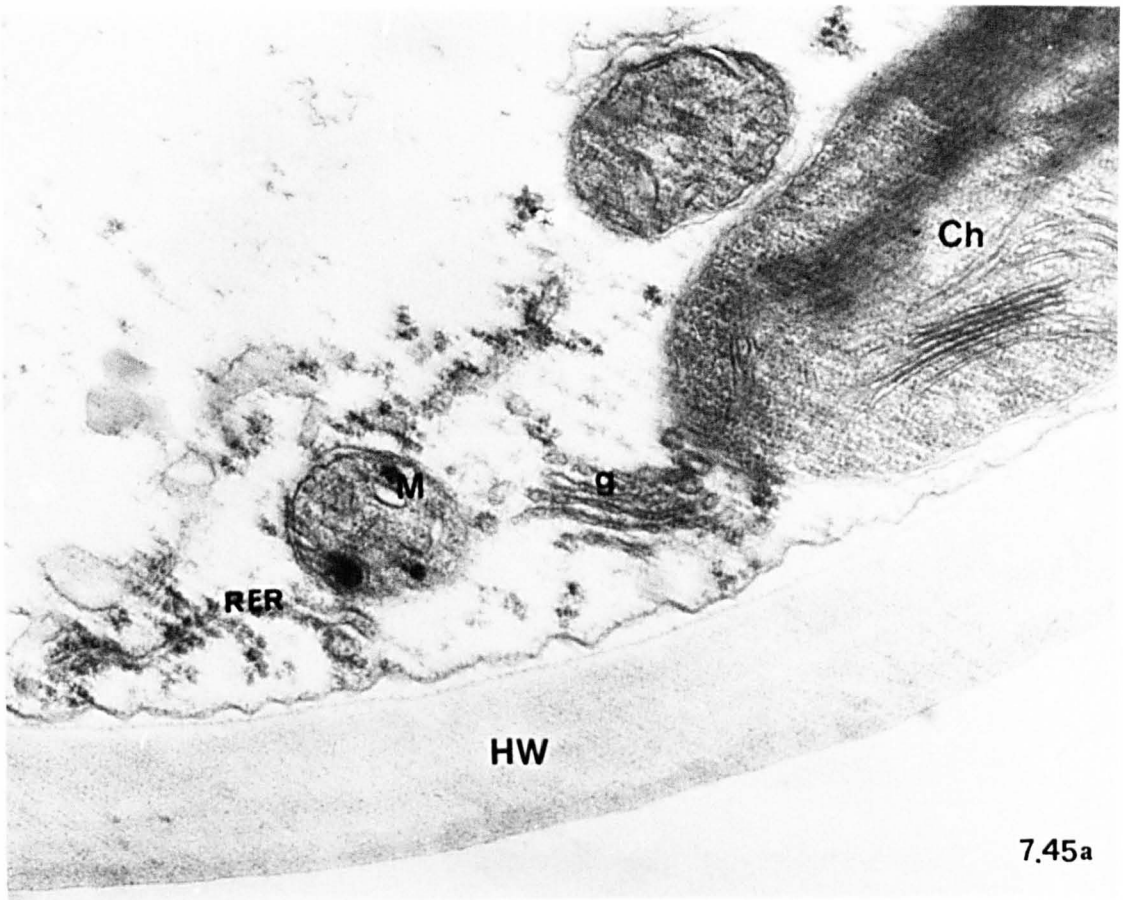

7.45a

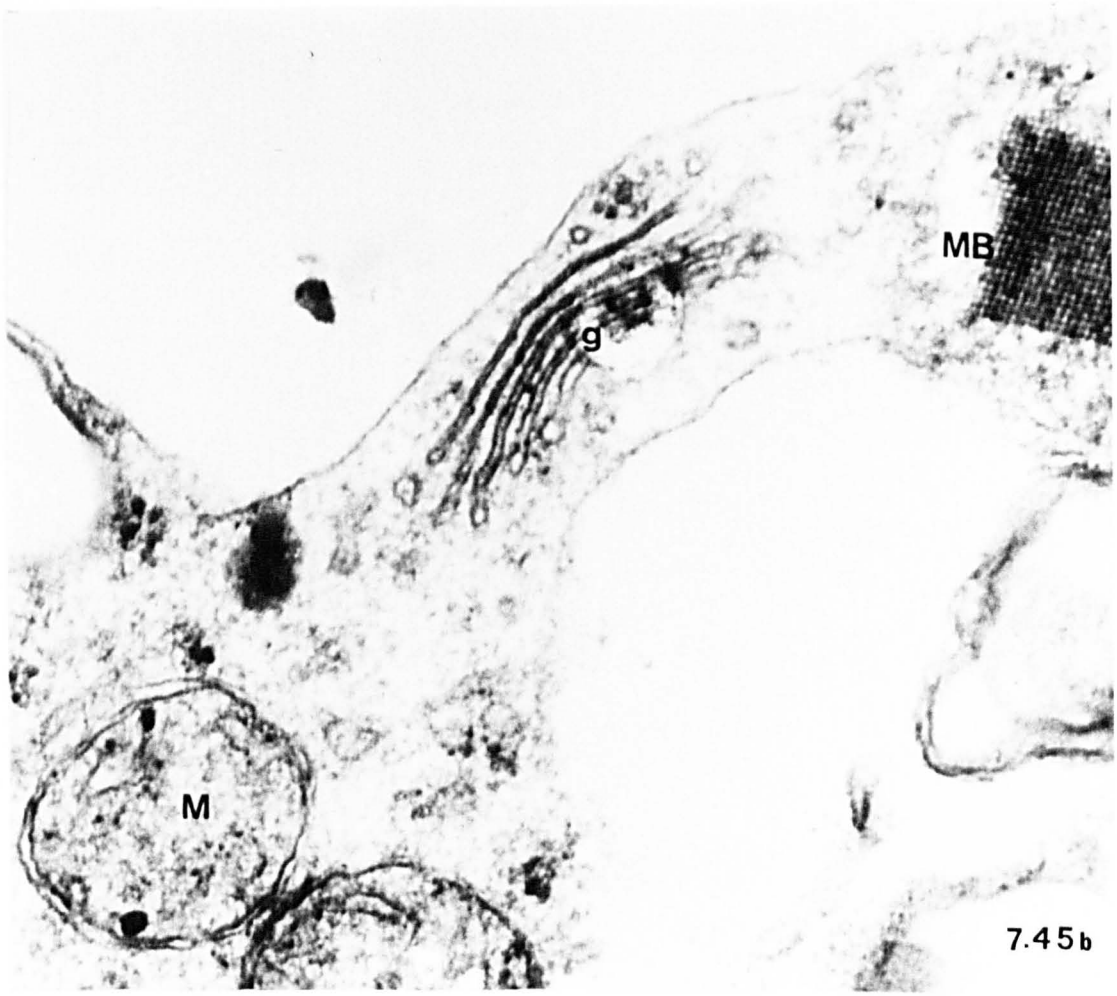

7.45b

Figure 7.46

Association of rough endoplasmic reticulum and chloroplast of *Poa* mesophyll cell at later stage of uredial infection.

x50000

Figure 7.47

Infected *Tussilago* mesophyll cell showing numerous vesicles containing granular material (arrowheads), close to host cell wall. These vesicles are bounded by host plasma membrane which appears fused with the tonoplast (unlabelled arrow). Note the close contact of the bounding plasma membrane and mitochondria.

x50000

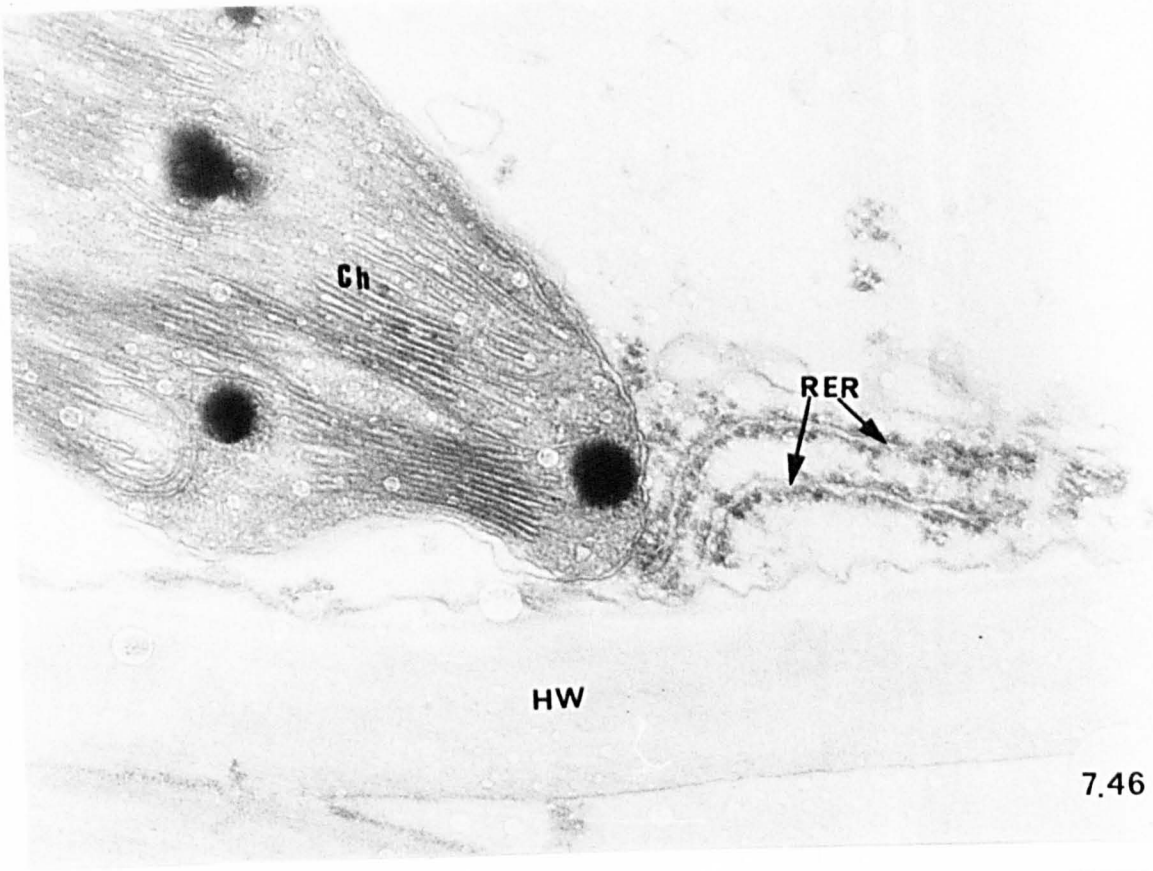

7.46

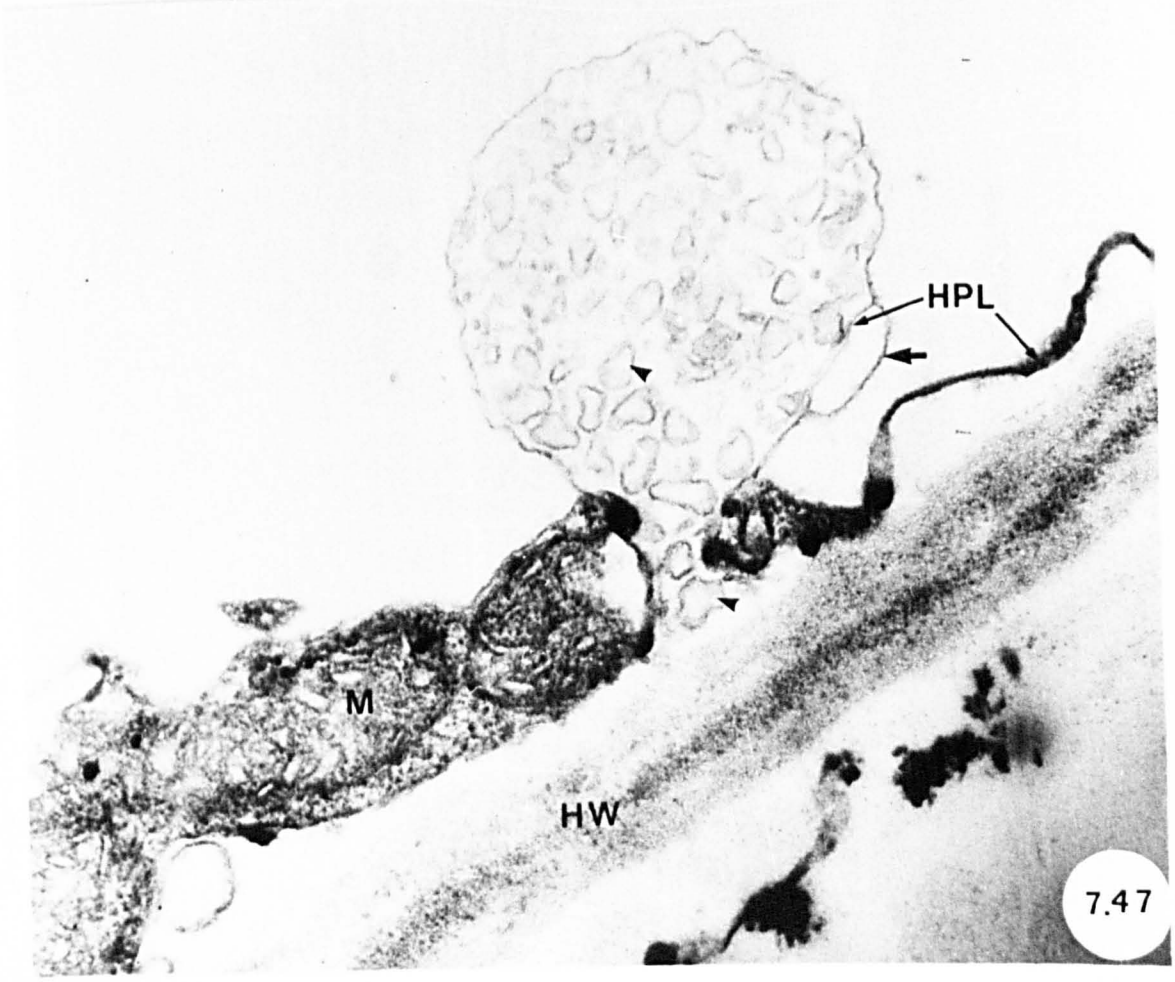

7.47

Figure 8.1

Feeding of the excised portions of infected leaves of *Tussilago* (A) and *Poa* (B) with ^{3}H-glycerol. Each leaf segment includes infected and uninfected parts with veins passing through them. The positions of tissue samples are indicated in C and D. The injured areas (i.e. the cut edges) of the leaves are not sampled.

■ Sample from uninfected part

□ Sample from infected part

Tussilago farfara

Poa pratensis

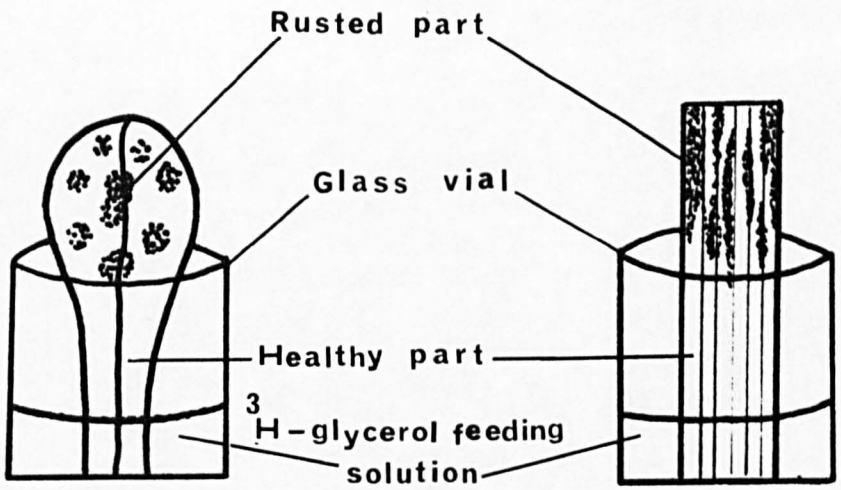

A

B

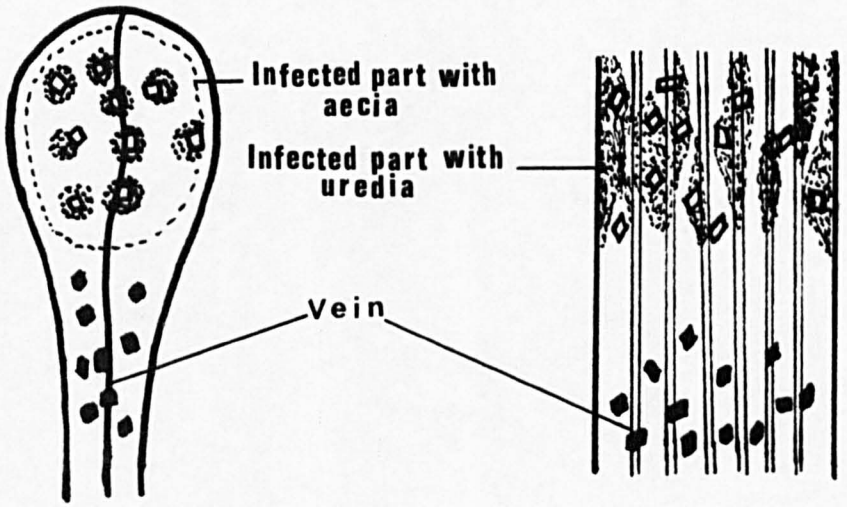

C

D

Figures 8.2 and 8.3

Autoradiographs of portions of infected leaves after uptake of 200 µCi tritiated glycerol. Note the accumulation of radioactivity in areas colonised by the fungus (arrows) and in host leaf veins (arrowheads). Brackets indicate infected regions. Scale lines = 0.5 cm

Figure 8.2

Infected *Tussilago* leaf.

Figure 8.3

Infected *Poa* leaf.

Figures 8.4 to 8.26 show microautoradiographs of tissue from portions of leaves similar to those in Figures 8.2 and 8.3. Silver grains lie in a slightly different plane of focus to that of the underlying tissue, appearing as white dots when photographed with incident light and black when only transmitted light is used.

Figures 8.4-8.6

Distribution of label in T.S. *Tussilago* leaf. Scale lines = 10 µm

Figure 8.4

Uninfected *Tussilago* leaf tissue, showing radioactivity in vascular bundle, particularly the phloem region. In mesophyll cells silver grains lie mainly over the peripheral cytoplasm.

Figure 8.5

Infected leaf tissue, showing labelling of vascular tissue, mesophyll cells, intercellular hyphae, some intracellular hyphae and host cell walls. Note hypha in xylem tracheary element (unlabelled arrow).

Figure 8.6a

Infected tissue showing accumulation of radioactivity in phloem region of vascular bundle. Note label around the penetrating hypha (arrow) in bundle sheath cell.

Figure 8.6b

Enlarged bundle sheath cell from Figure 8.6a, showing silver grains around intracellular hypha, apparently in matrix region, in labelled intercellular hypha (arrowhead) and around intracellular hypha-mother cell (arrow).

8.2

8.3

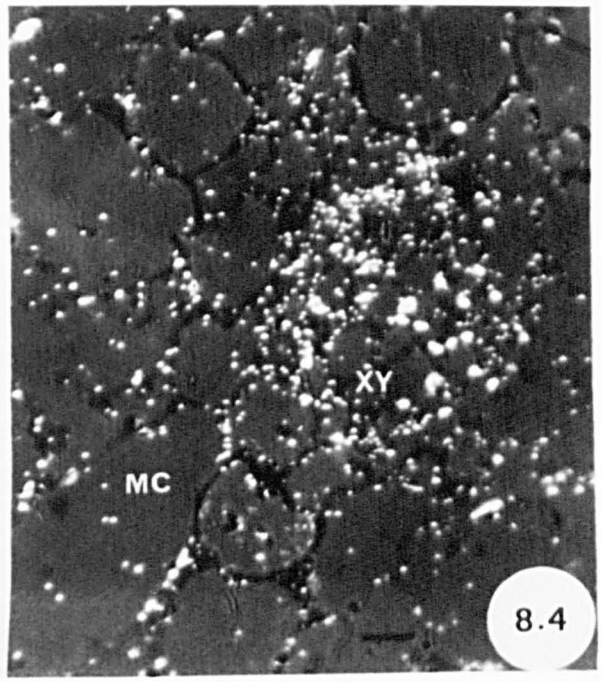

8.4

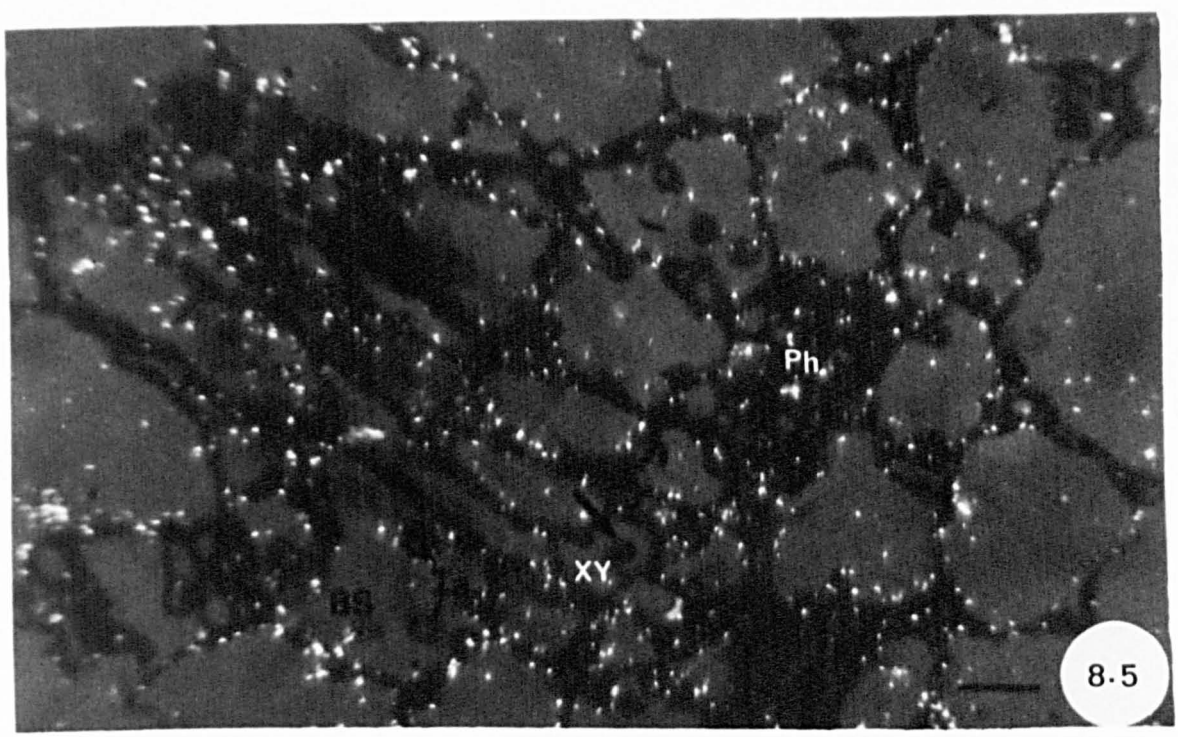

8.5

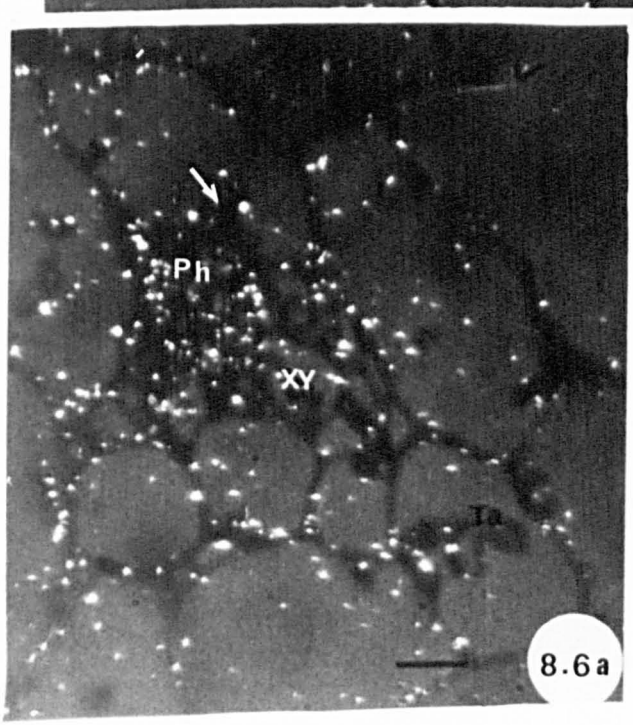

8.6a

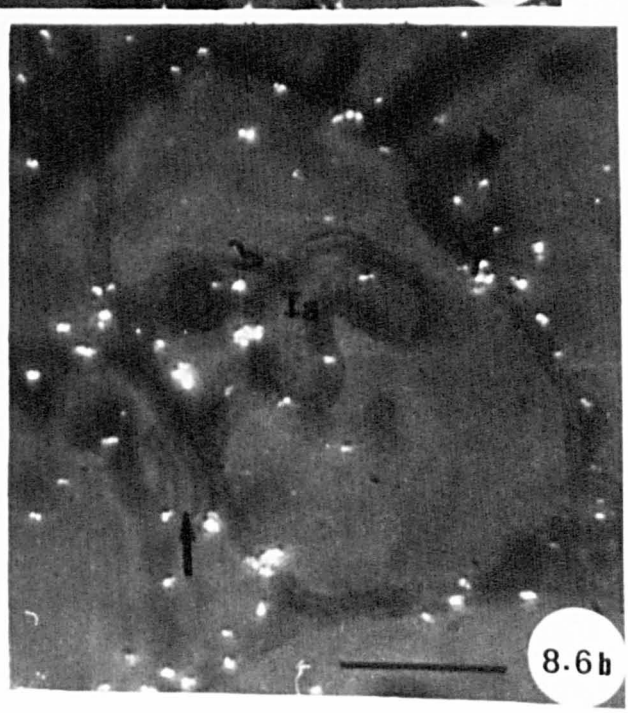

8.6b

Figures 8.7 and 8.8

Distribution of radioactivity in *Tussilago* leaf. Scale lines = 10 μm

Figure 8.7

Microautoradiographic demonstration of the accumulation of ^{3}H-glycerol in the vascular bundle of infected *Tussilago* leaf. Silver grains are seen over phloem and xylem regions and bundle sheath cells. Note the labelling of host cell walls and fungal intercellular and intracellular hypha (arrowhead).

Figure 8.8a

Microautoradiograph of uninfected *Tussilago* mesophyll cells showing silver grains over the thin peripheral layer of cytoplasm, particularly over the chloroplasts (arrowheads).

Figures 8.8b and 8.8c

Microautoradiographs of mesophyll cell of uninfected *Tussilago* leaf showing silver grains over chloroplasts (arrowheads).

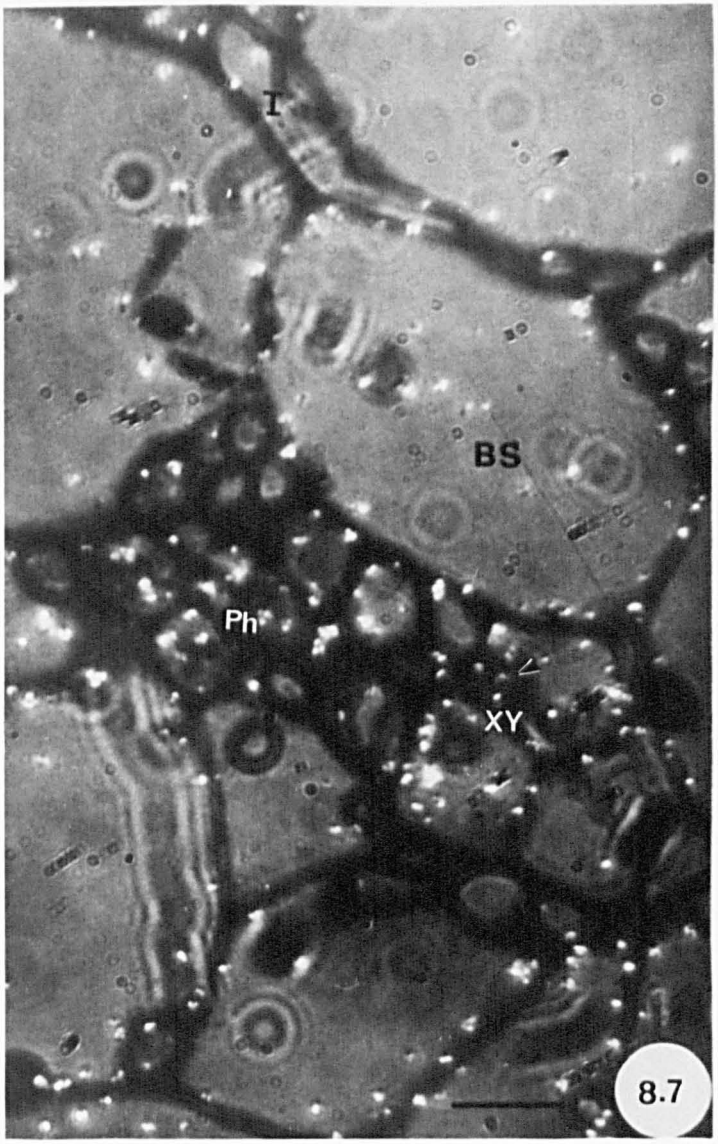
I
BS
Ph
XY
8.7

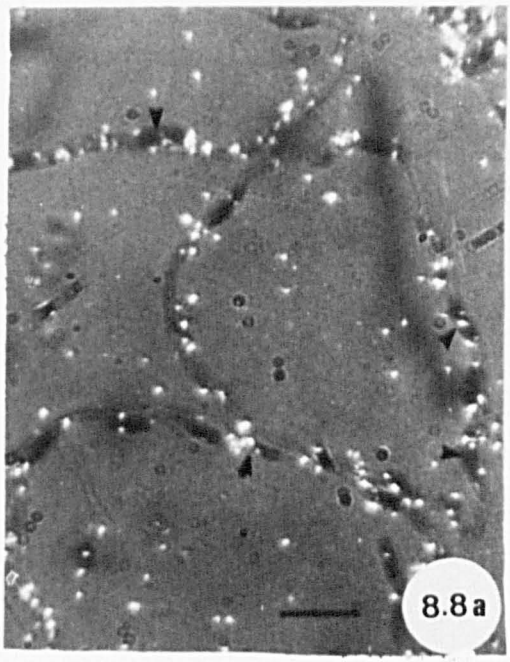
8.8a

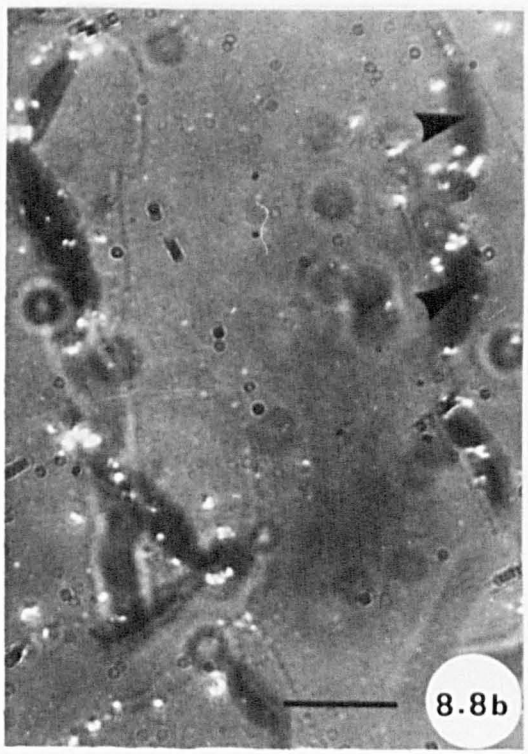
8.8b

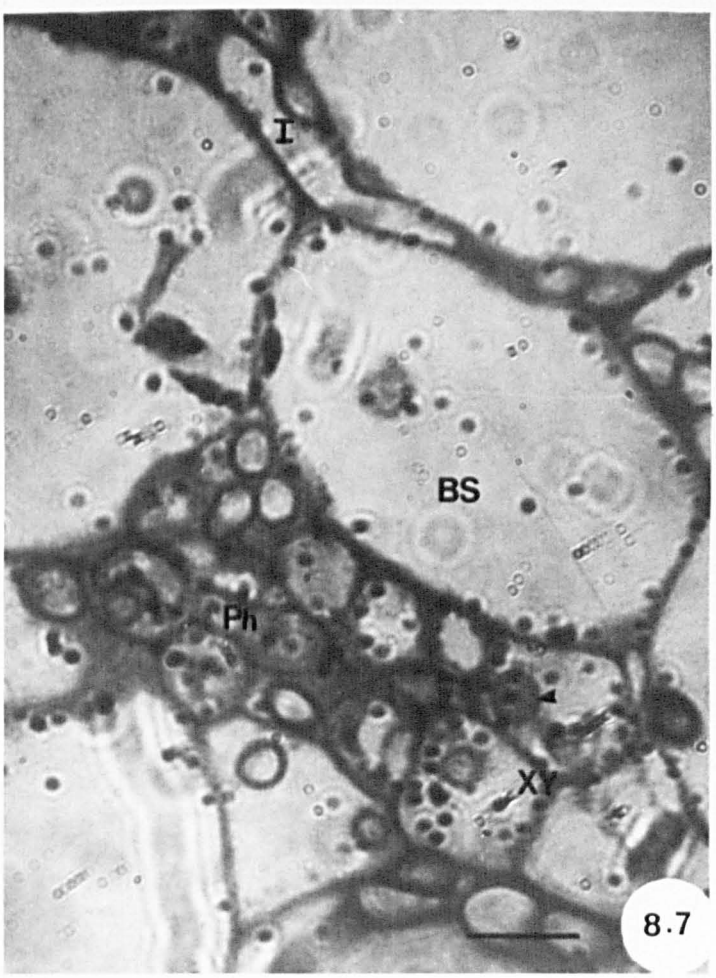
I
BS
Ph
XY
8.7

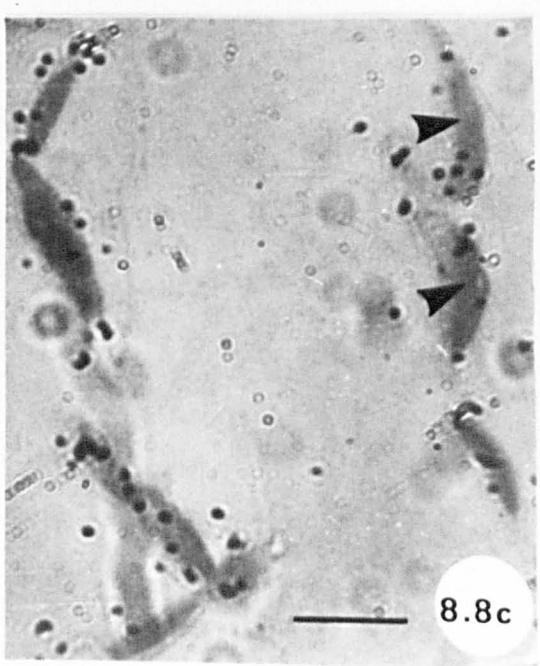
8.8c

Figures 8.9 and 8.10

Distribution of radioactivity in fungal inter- and intracellular structures of monokaryon in *Tussilago*. Scale lines = 10 µm

Figure 8.9

Microautoradiograph showing silver grains over intercellular hyphae in intercellular spaces of *Tussilago* mesophyll tissue and in intracellular hyphae in mesophyll cells. Note labelling of host peripheral cytoplasm and host cell walls.

Figure 8.10

Microautoradiograph of infected *Tussilago* mesophyll cell showing radioactivity in intercellular hypha and in/or around intracellular hyphae in mesophyll cell (arrowheads).

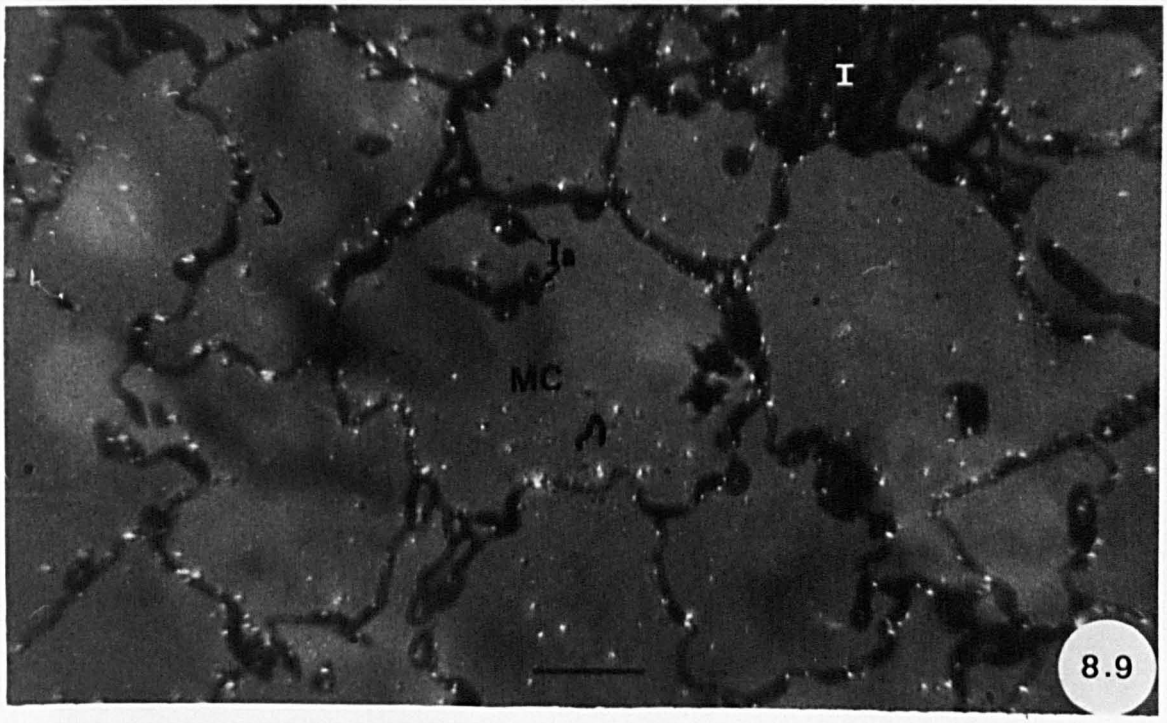

8.9

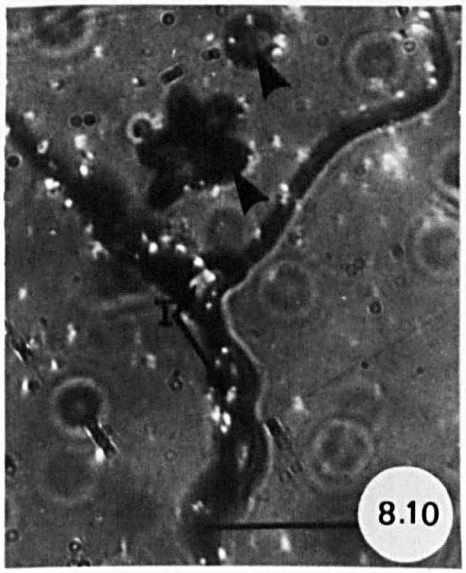

8.10

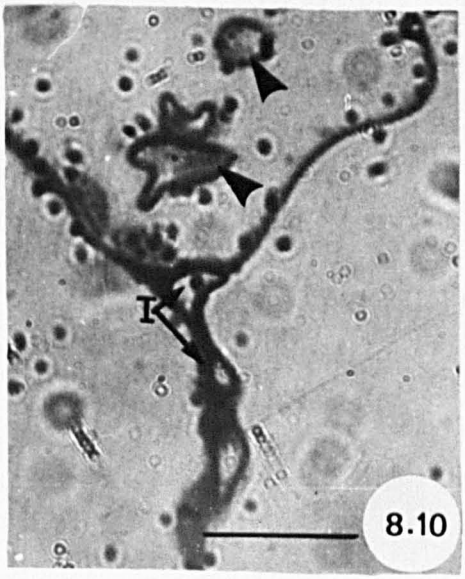

8.10

Figures 8.11 and 8.12

Distribution of radioactivity in *Poa* leaf. Scale lines = 10 μm

Figure 8.11

Microautoradiograph of uninfected *Poa* leaf showing accumulation of radioactivity in phloem and xylem regions, bundle sheath and mesophyll cells. Note dense labelling of phloem and the labelling of peripheral cytoplasm.

Figure 8.12

Microautoradiograph of infected *Poa* leaf showing densely labelled vascular strand and mesophyll cells. Note labelled intercellular hyphae (arrows). No label is seen in the non-living cell enclosing the vascular strand (arrowheads).

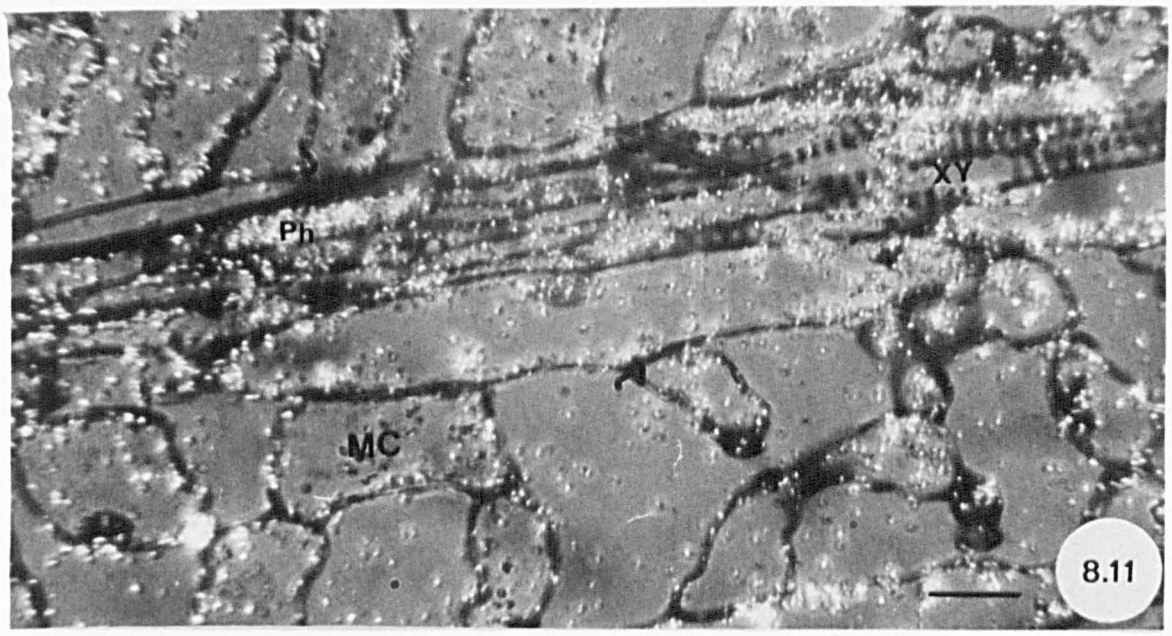
XY
Ph
MC
8.11

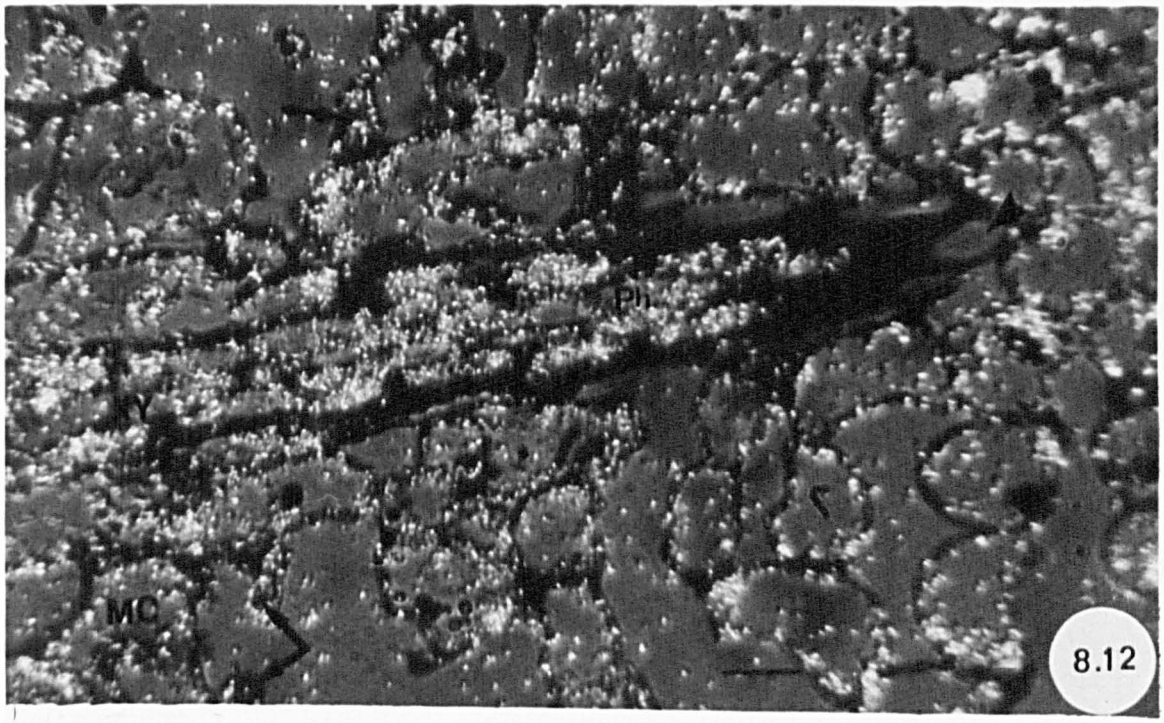
Ph
Y
MC
8.12

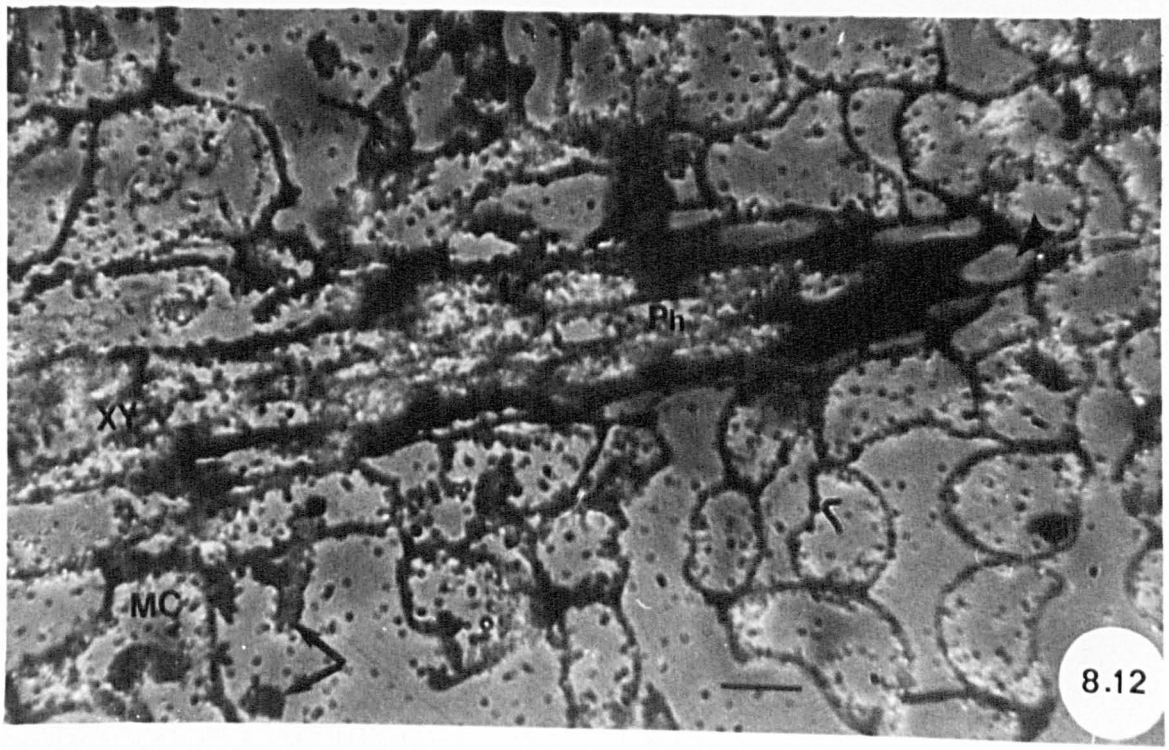
Ph
XY
MC
8.12

Figures 8.13-8.15

Distribution of label in fungal structures of monokaryon in *Tussilago* leaf. Scale lines = 10 μm

Figure 8.13a

Microautoradiograph of obliquely sectioned aecion of *P. poarum* showing densely labelled fungal stroma, aeciospores, peridial cells. Note also the densely labelled fungal tissue (open arrow) surrounding aecium. Silver grains are particularly associated with fungal cell walls and also occur between aeciospores.

Figure 8.13b

Enlarged portion of Figure 8.13a with lower proportion of incident light. Silver grains lie over and between aeciospores, over peridial cell walls and the fungal tissue (unlabelled arrow) surrounding aecium.

Figure 8.14

L.S. aceium of *P. poarum* in *Tussilago* showing radioactivity in fungal stroma, hymenium and aeciospores.

Figure 8.15

Tangential section of an aecial peridium showing heavily labelled peridial cell walls (see similar section of aecial peridium in Figure 3.34).

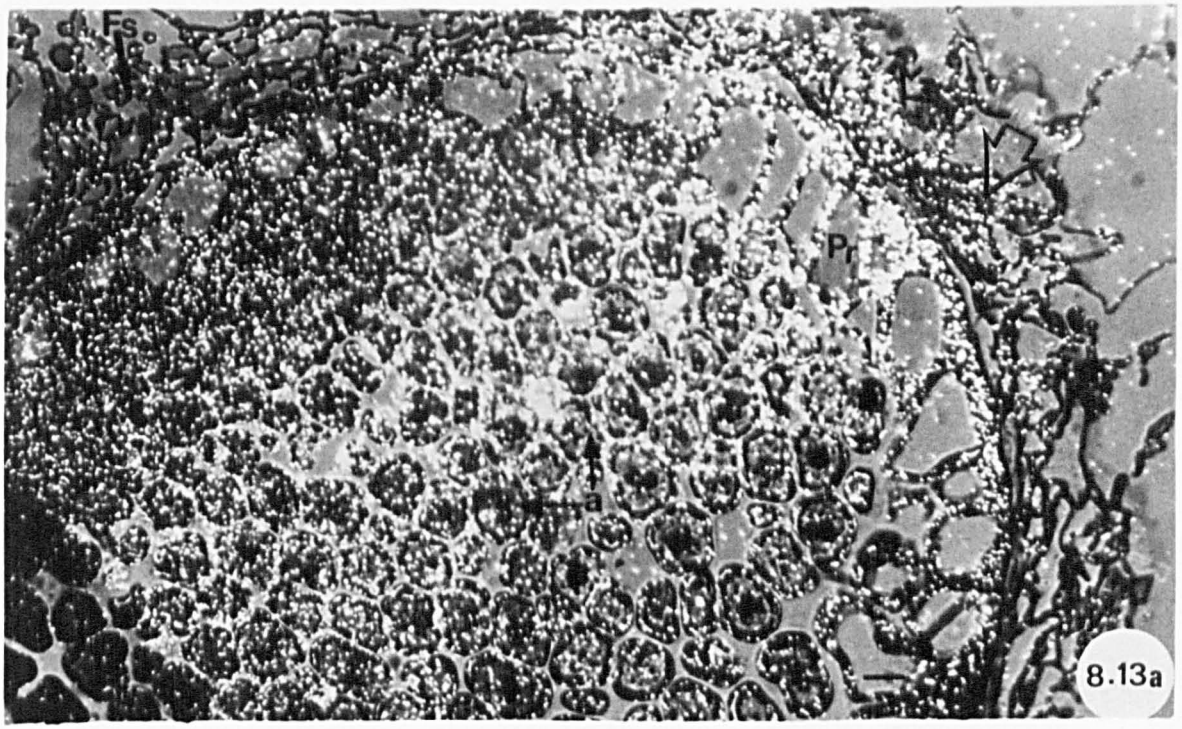

8.13a

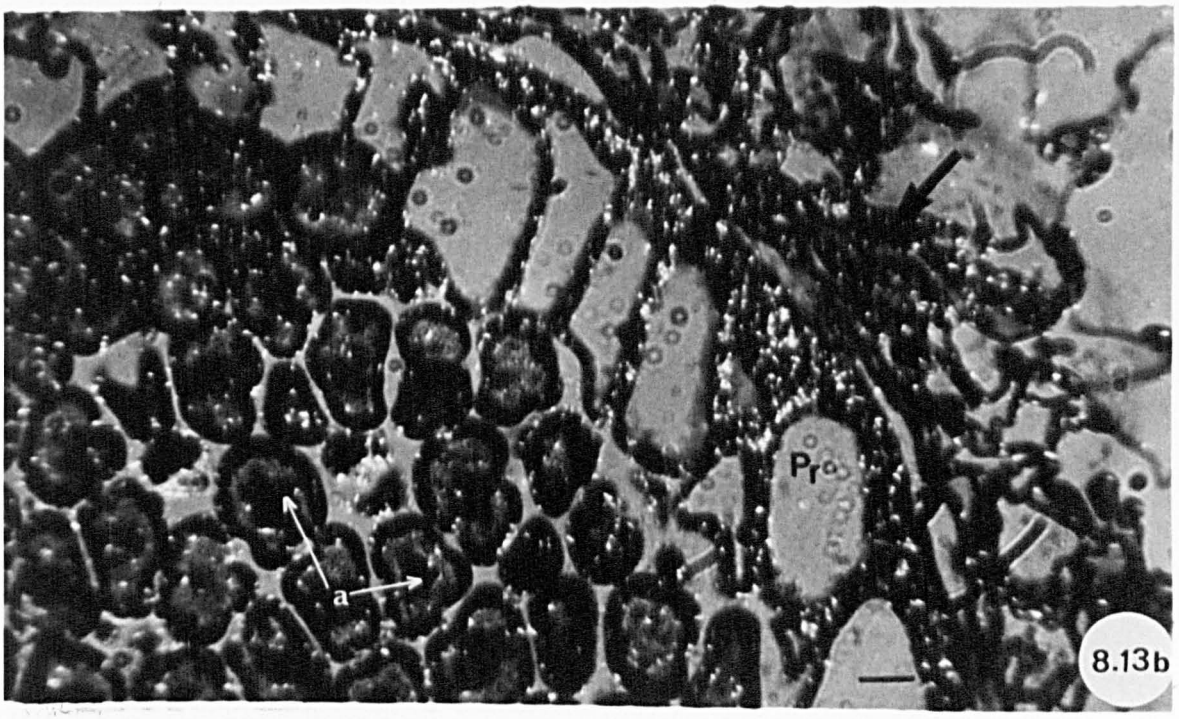

8.13b

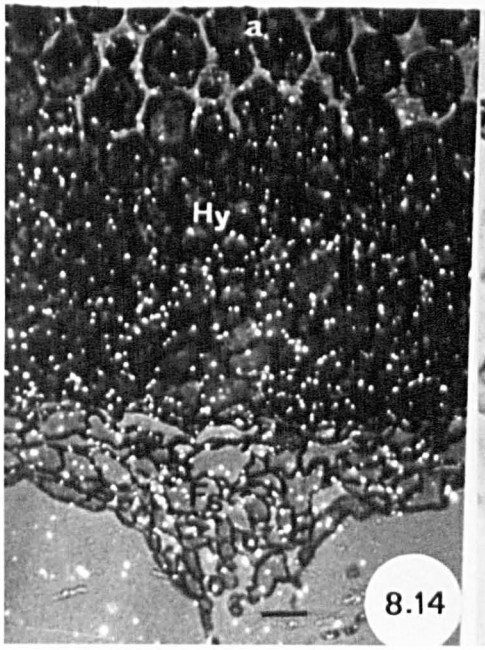

8.14

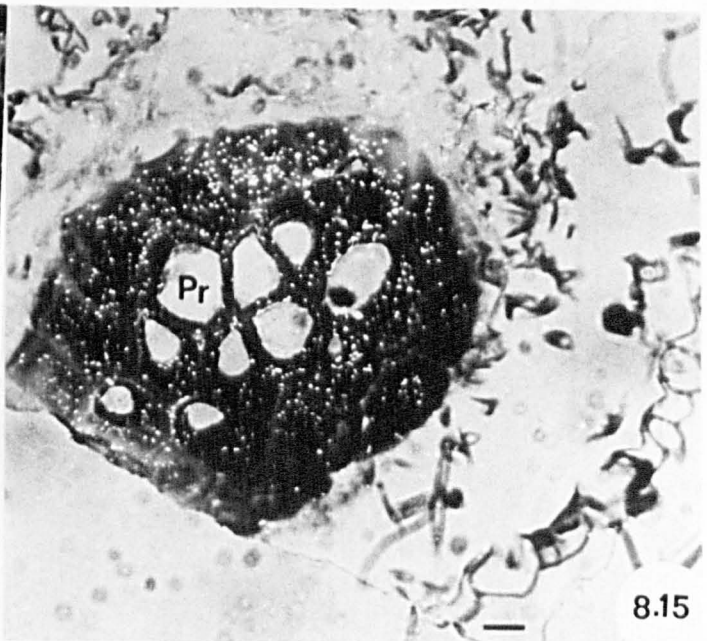

8.15

Figures 8.16 and 8.17

L.S. aecium of *P. poarum* in *Tussilago* leaf. Scale lines = 5 μm

Figure 8.16

Microautoradiographs showing a gradient of increasing density of silver grains from fungal stroma to hymenium to aeciospores. Note silver grains between aeciospores.

Figure 8.17

Enlargement of Figure 8.16 showing labelled aeciosporophores and aeciospore initials. Note association of silver grains with septa separating aeciosporophores and spore initials. Note also the lack of silver grains over the wall thickenings (arrowheads) at the upper end of hymenial cells.

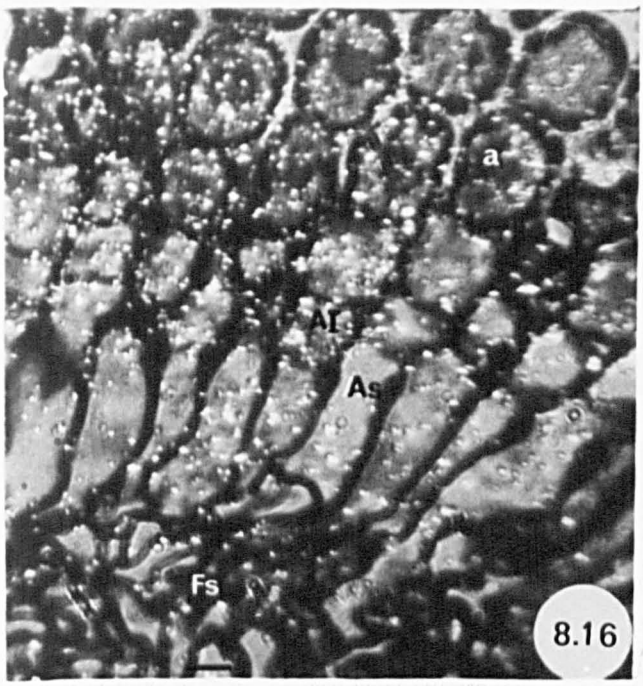
a
AI
As
Fs
8.16

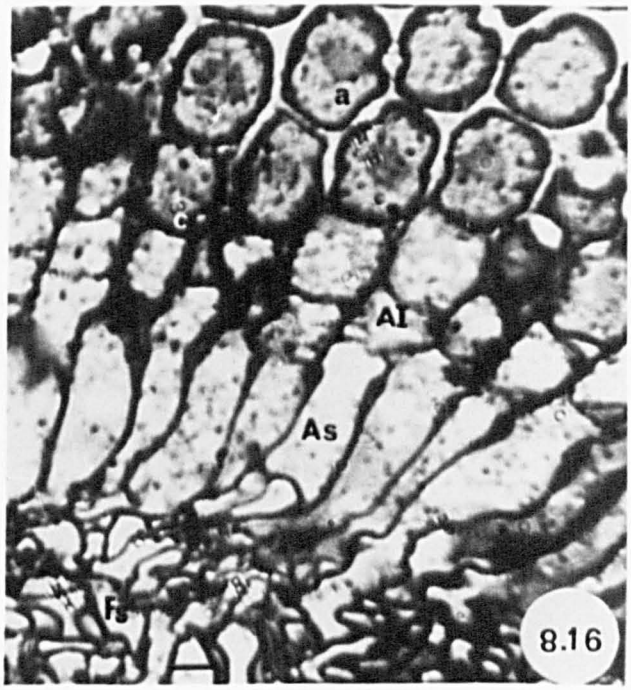
a
c
AI
As
Fs
8.16

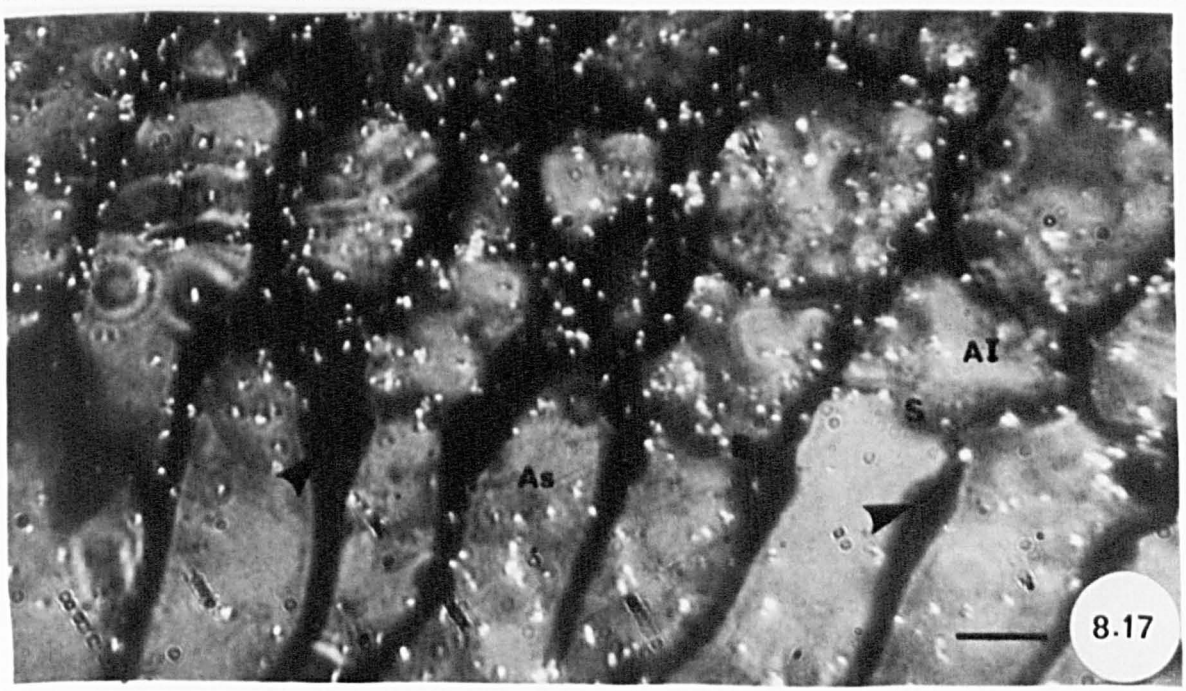
AI
S
As
8.17

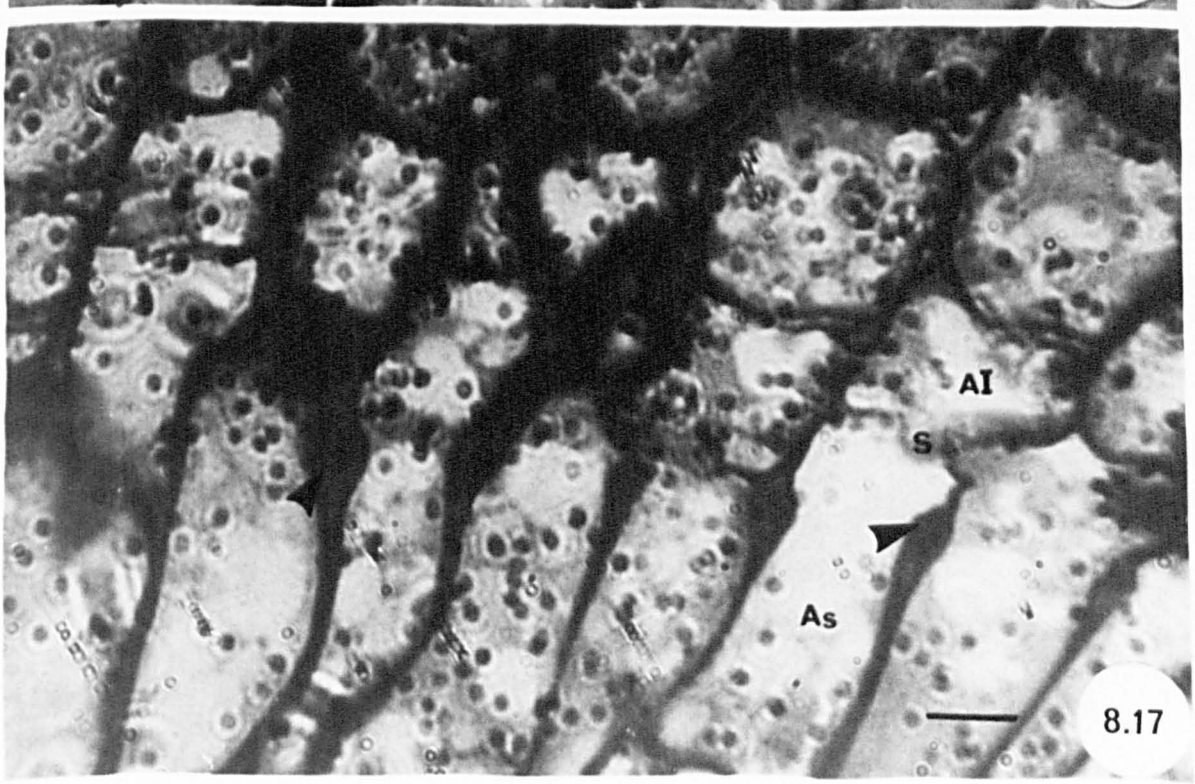
AI
S
As
8.17

Figures 8.18-8.20

Distribution of radioactivity in *Poa* leaf. Scale lines = 10 µm

Figure 8.18

Microautoradiograph of uninfected mesophyll tissue of *Poa* showing radioactivity over nuclei, chloroplasts (arrowheads), cell walls and peripheral cytoplasm.

Figure 8.19

Microautoradiograph of uninfected mesophyll of *Poa* in the vicinity of uredial infection showing radioactivity over the vascular strand and mesophyll cells. Note labelled cell nucleus (arrows) and high concentration of radioactivity in lipid drop in mesophyll cell (arrowhead).

Figure 8.20

Microautoradiograph of infected *Poa* mesophyll tissue showing heavily labelled haustorium, closely associated with host nucleus. Label is also present around host nucleus and over intercellular hyphae.

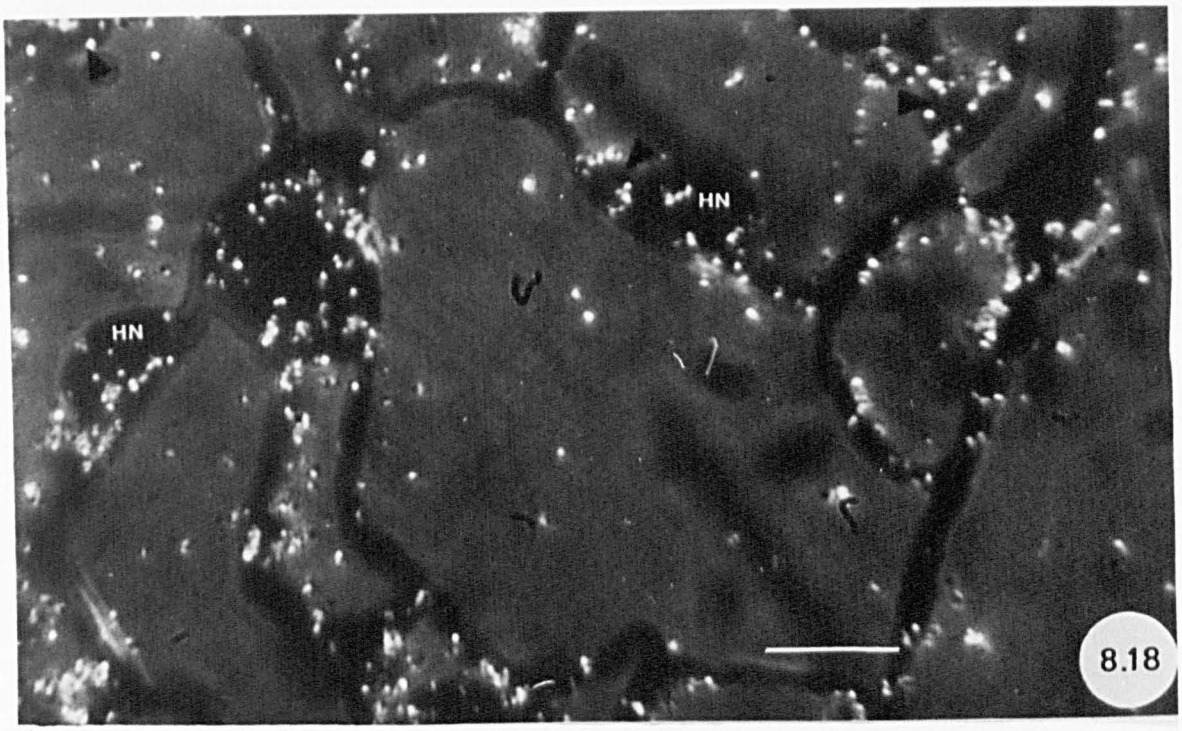

8.18

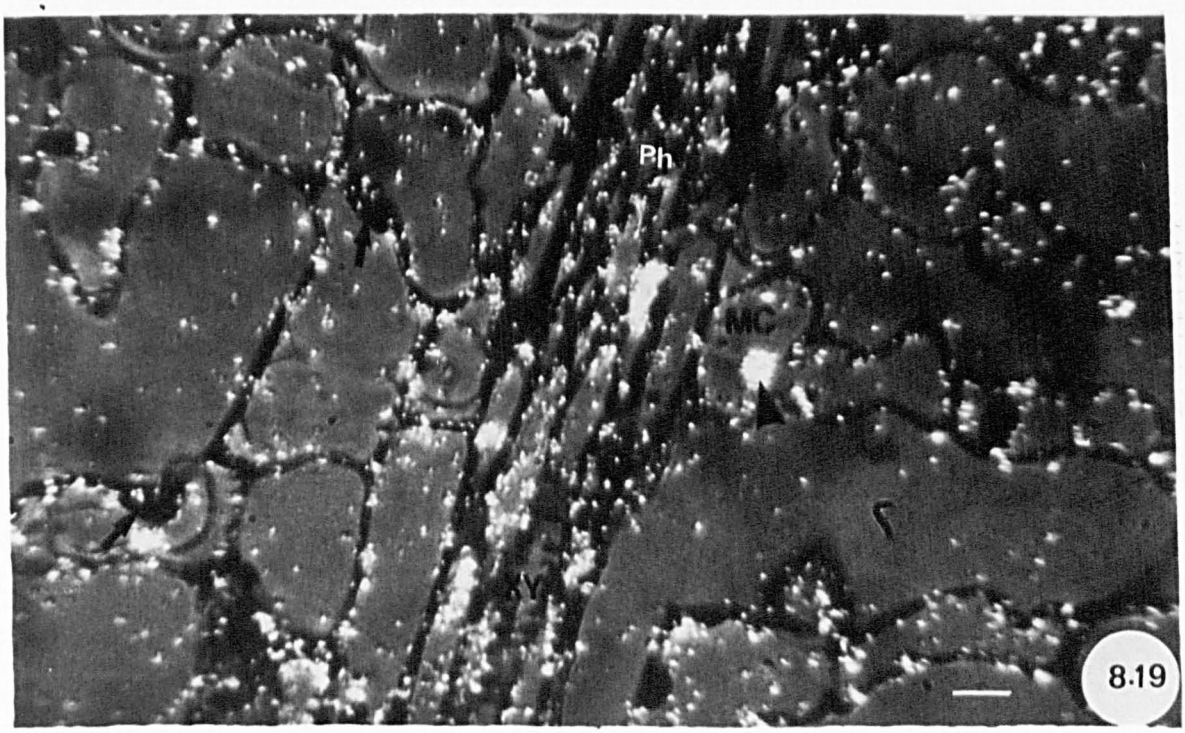

8.19

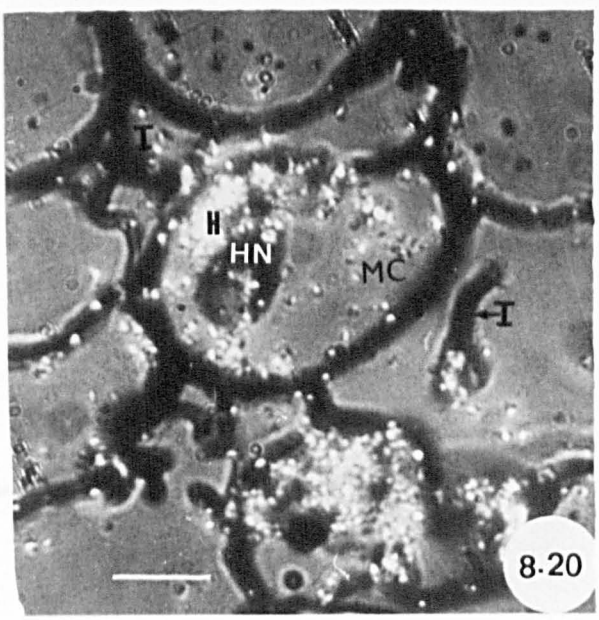

8.20

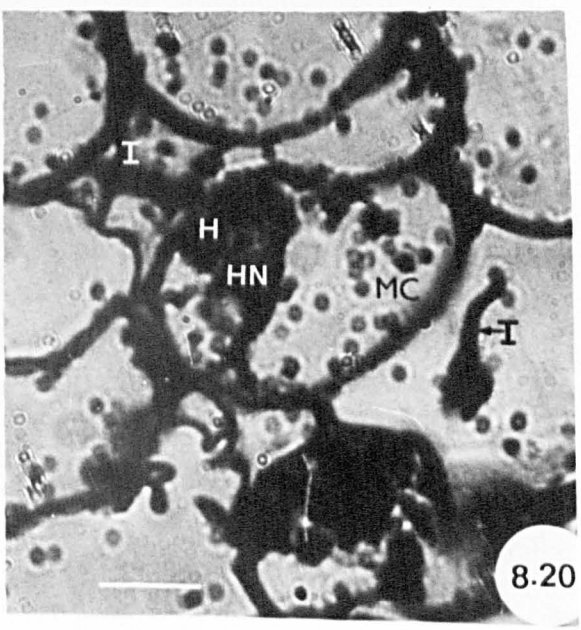

8.20

Figures 8.21 and 8.22

Distribution of radioactivity in infected *Poa* leaf. Scale lines = 10 µm

Figure 8.21a

Microautoradiograph showing radioactivity over host nucleus, host cell wall and fungal inter- and intracellular structures of the dikaryon.

Figure 8.21b

Microautoradiograph showing heavily labelled infected mesophyll cell. Silver grains are present over intercellular hyphae, in and around haustorium and in the peripheral host cytoplasm. Note heavily labelled cytoplasm between host nucleus and haustorium (arrow).

Figure 8.22a

Microautoradiograph of infected *Poa* mesophyll tissue. The greatest density of silver grains is found over mesophyll cells containing haustoria (labelled cells). Chloroplasts, host cytoplasm and intercellular hyphae have also accumulated radioactivity.

Figure 8.22b

Enlargement of the framed area from Figure 8.22a, showing radioactivity of chloroplasts and intercellular hyphae.

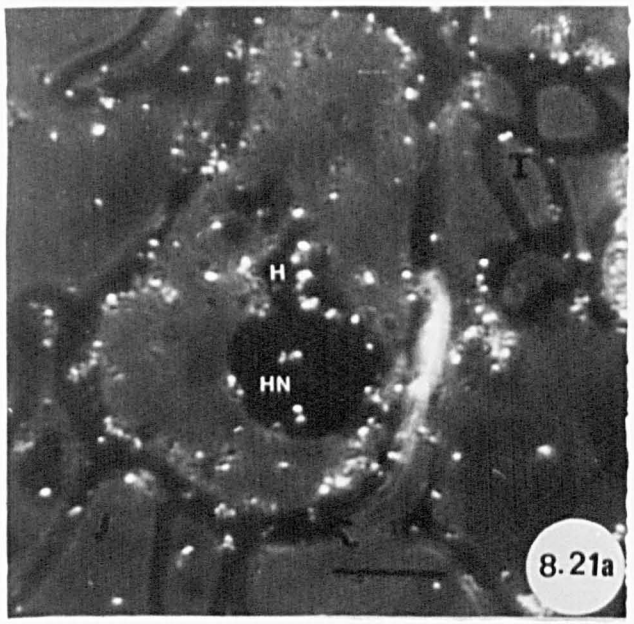

8.21a

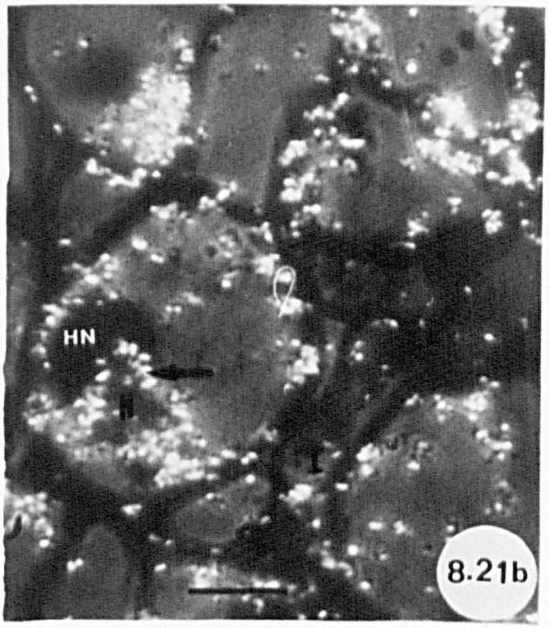

8.21b

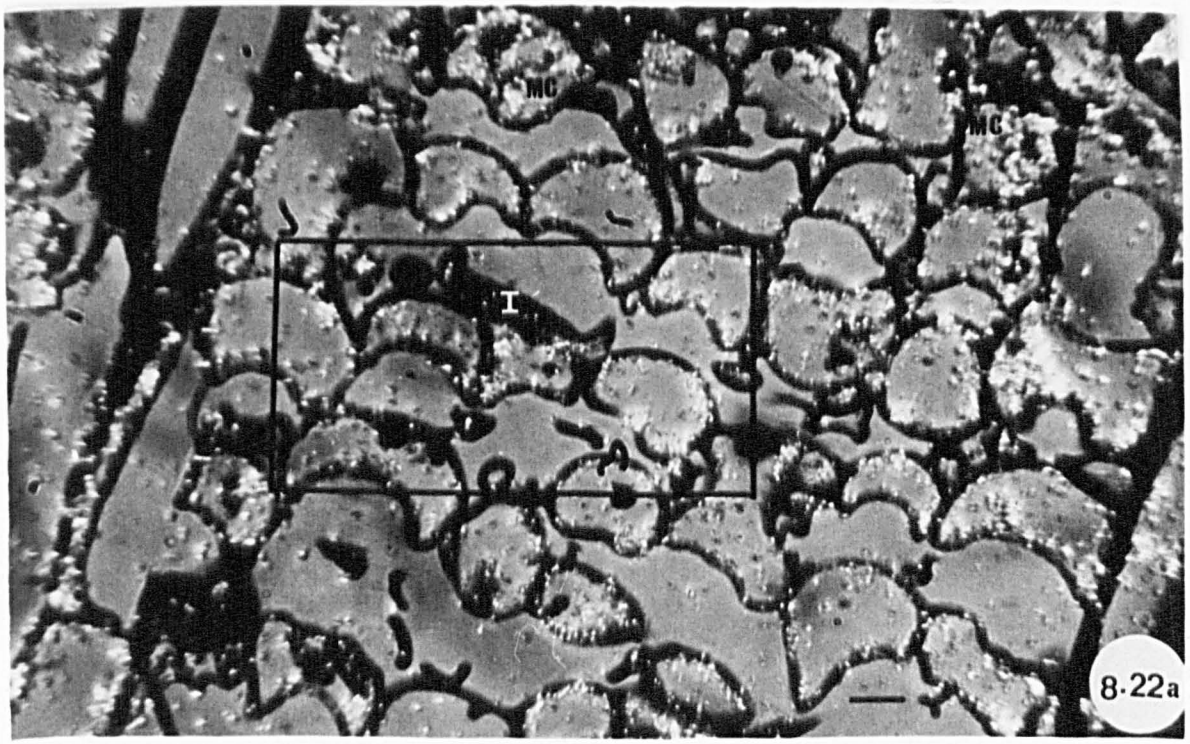

8.22a

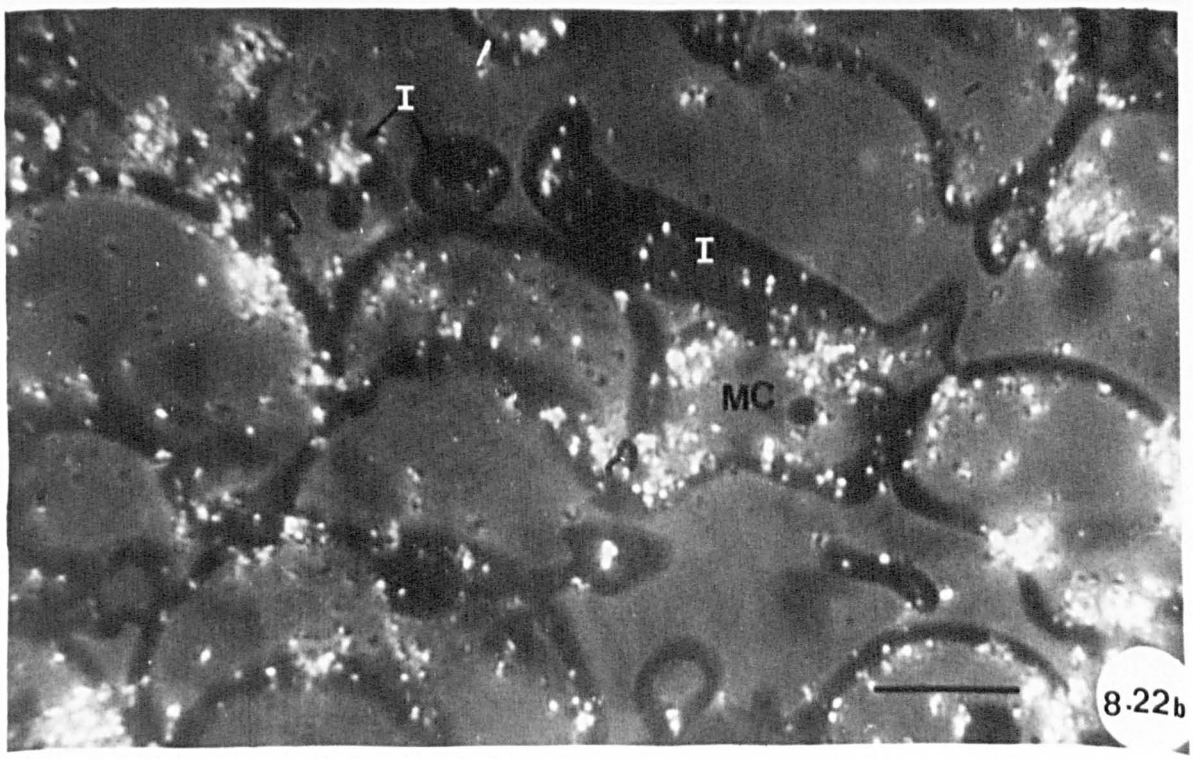

8.22b

Figure 8.23

Microautoradiographs of a section cut longitudinally through *Poa* epidermis in a plane parallel to leaf surface, at the margin of a developing urediosorus, showing narrow zones (arrows) of densely labelled fungal cells, penetrating between adjacent epidermal cells. Note heavily labelled urediosorus and dense deposits of silver grains over host nuclei in epidermal cells (arrowheads).

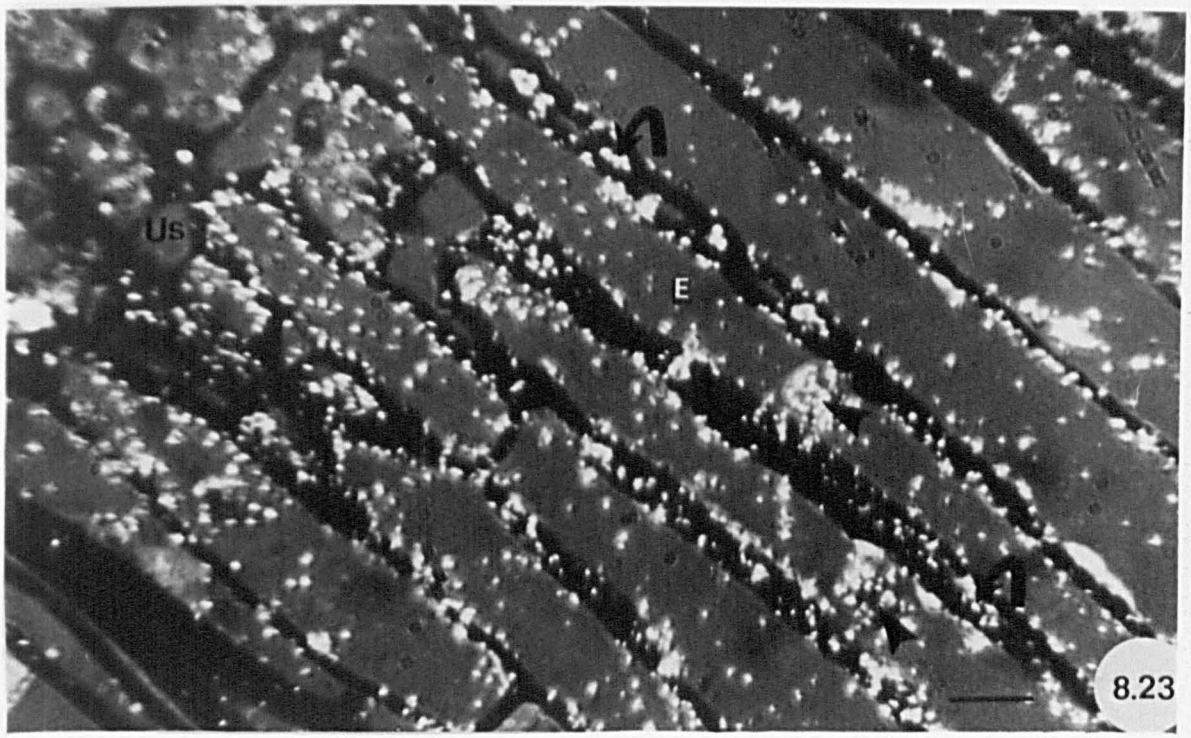
Us
E
8.23

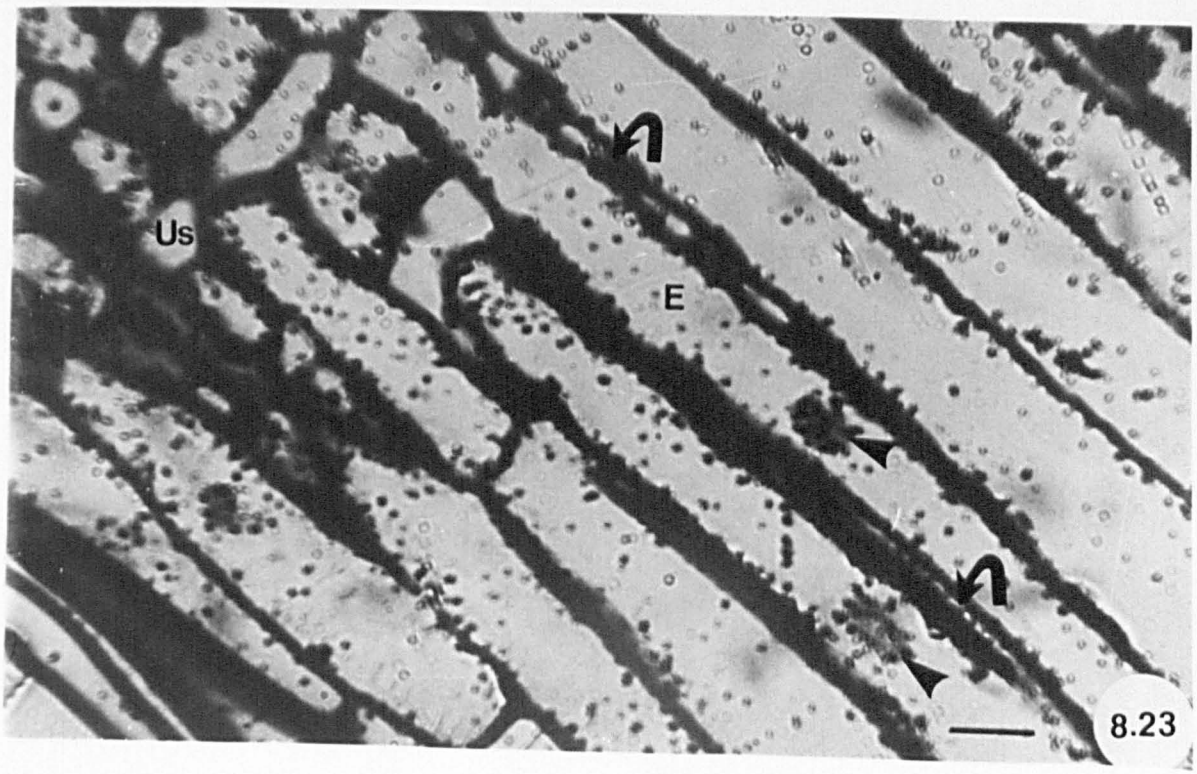
Us
E
8.23

Figure 8.24

Enlarged portion from Figure 8.23 showing heavily labelled fungal cells of a developing urediosorus. Note dense labelling of host epidermal cells.

Scale lines = 10 µm

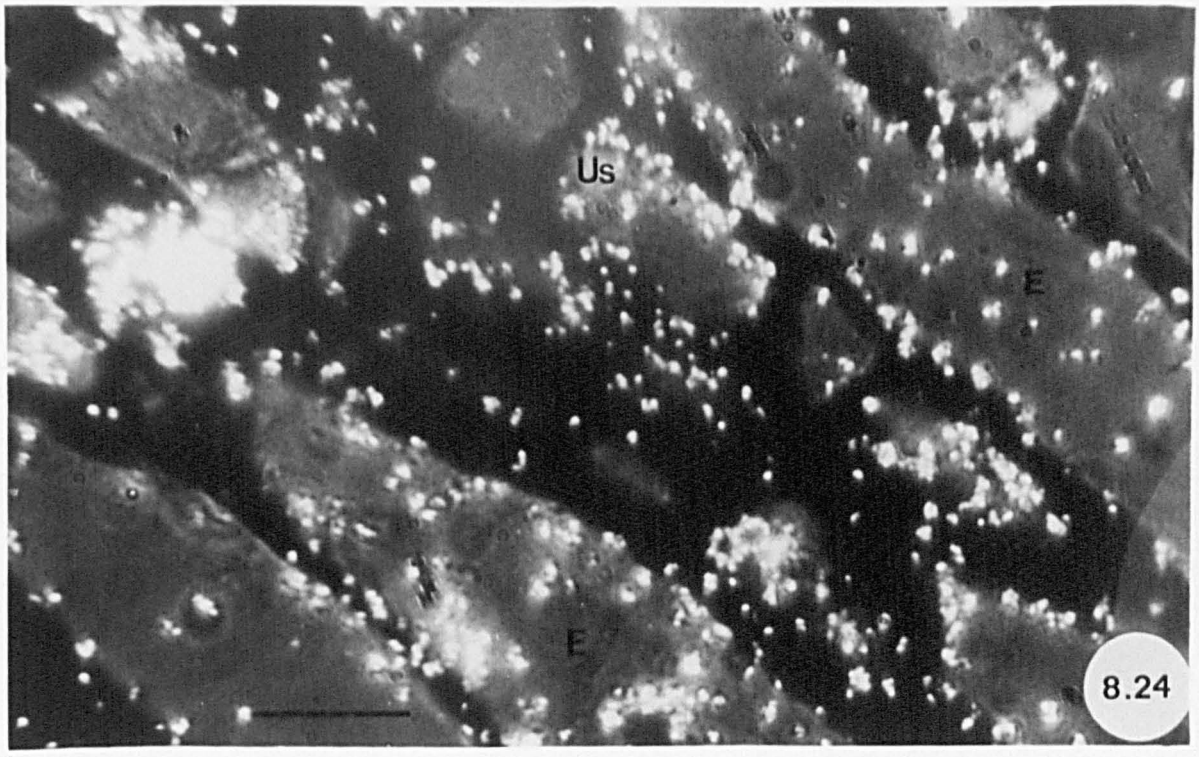
Us
E
E
8.24

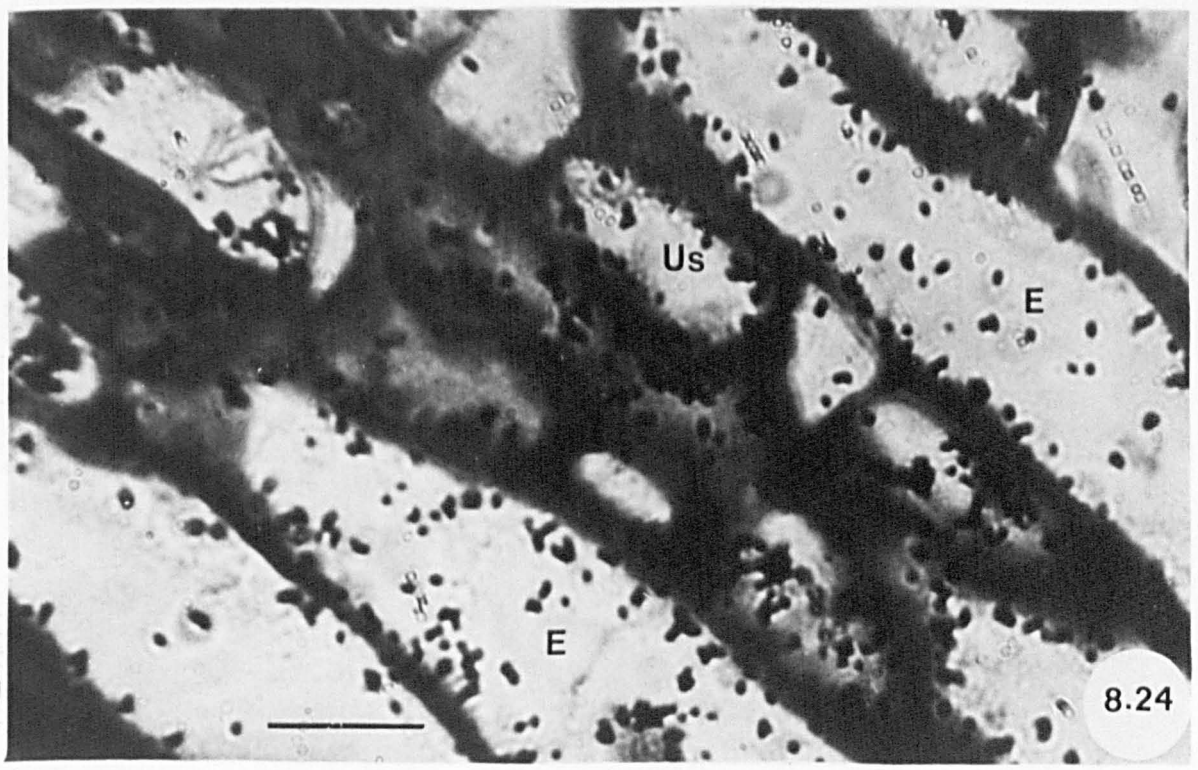
Us
E
E
8.24

Figure 8.25

Distribution of radioactivity in urediosorus of *P. poarum* in *Poa* leaf. Scale lines = 10 µm

Figure 8.25a

Microautoradiograph of developing urediosorus showing highly labelled urediospores, uredial peridium and associated fungal structures.

Figure 8.25b

Enlargement of Figure 8.25a showing radioactivity in urediospores and surrounding fungal structures.

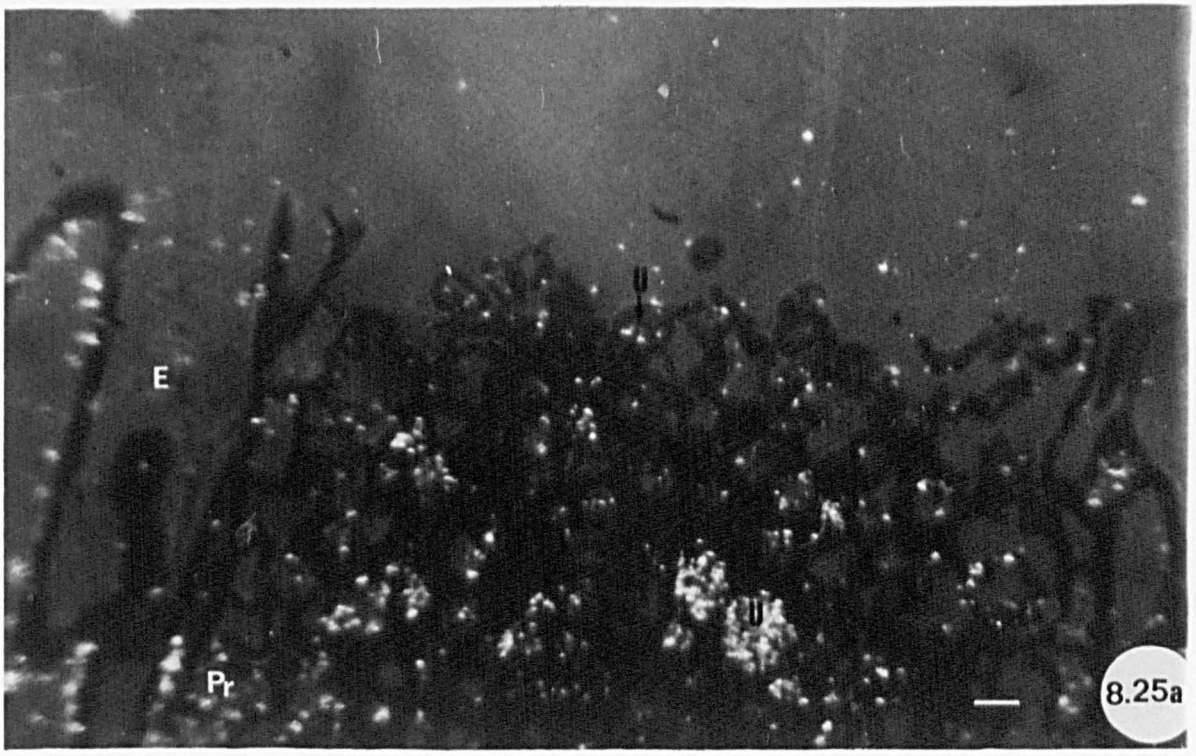

8.25a

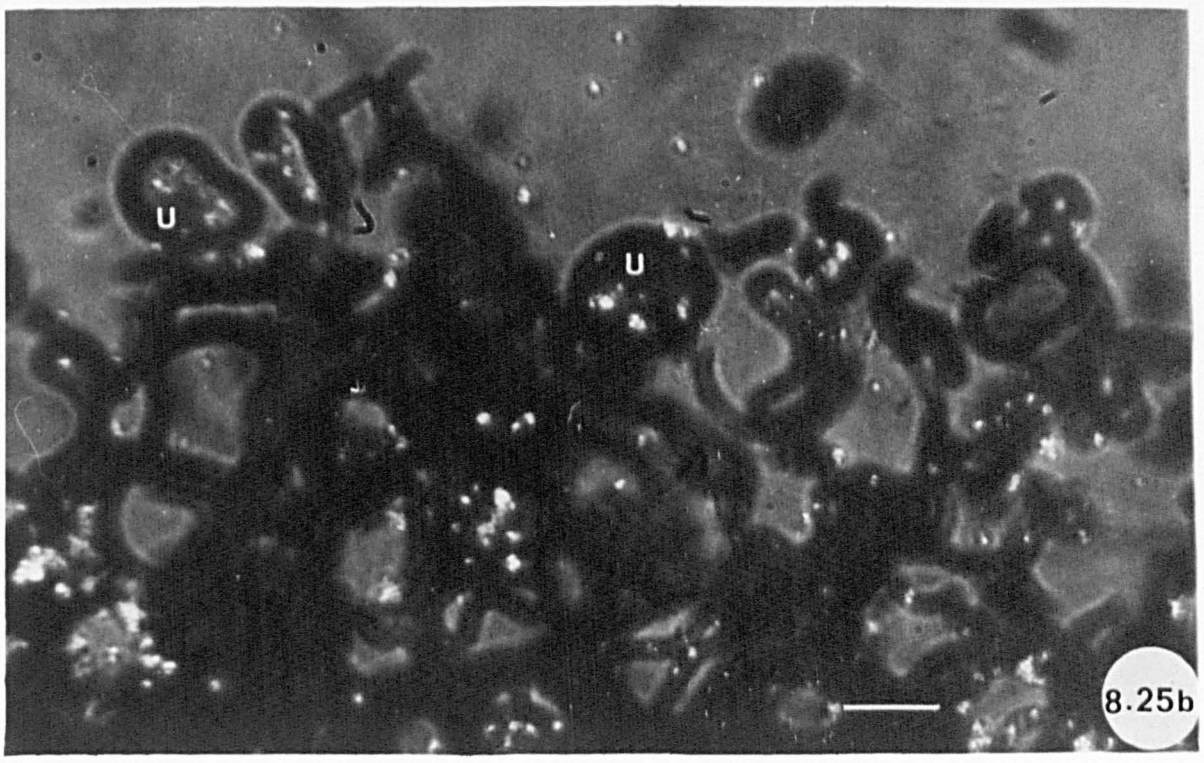

8.25b

Figure 8.26

Distribution of label in urediosorus of *P. poarum* in *Poa*.
Scale lines = 20 µm

Figure 8.26a and b

Microautoradiographs of more mature region of uredium, compared with that in Figure 8.23, showing high concentration of radioactivity in urediospores and to lesser extent in closely associated fungal structures. Note little label in mature uredial peridium and paraphyses.

Figure 8.26c and d

Enlargement of Figures 8.26a showing strongly labelled urediospores and little label in closely associated fungal structures. Note paraphyses.

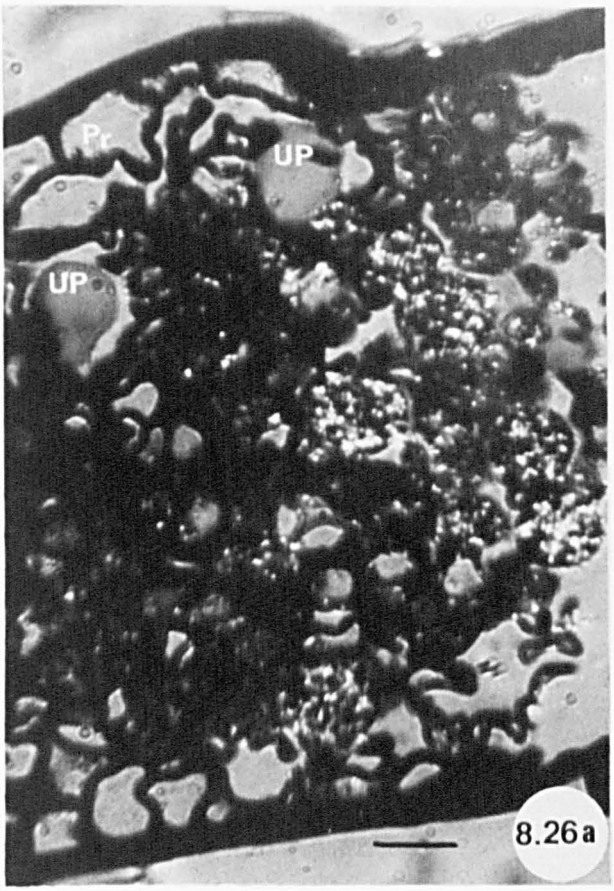

8.26a

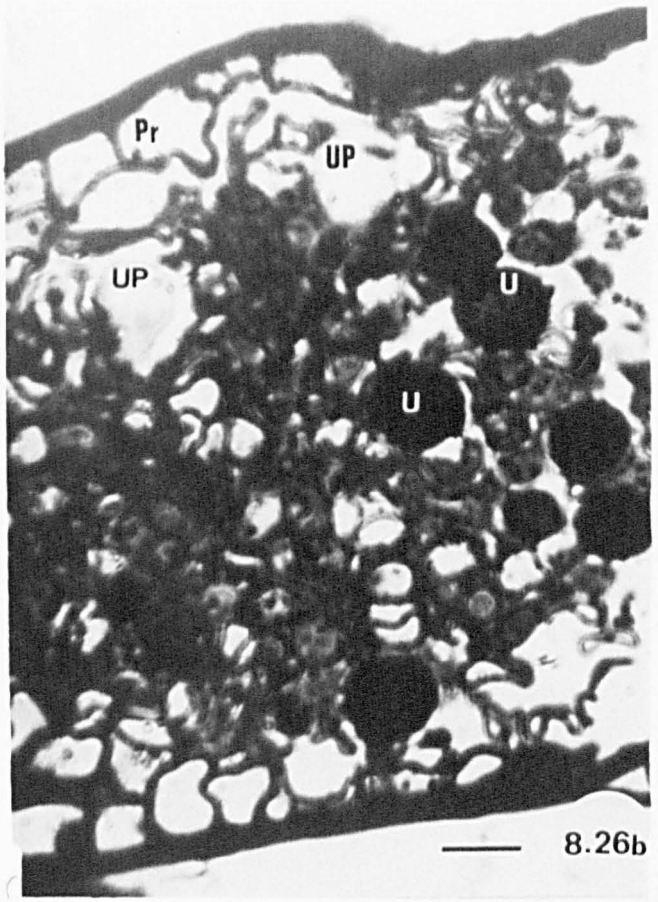

8.26b

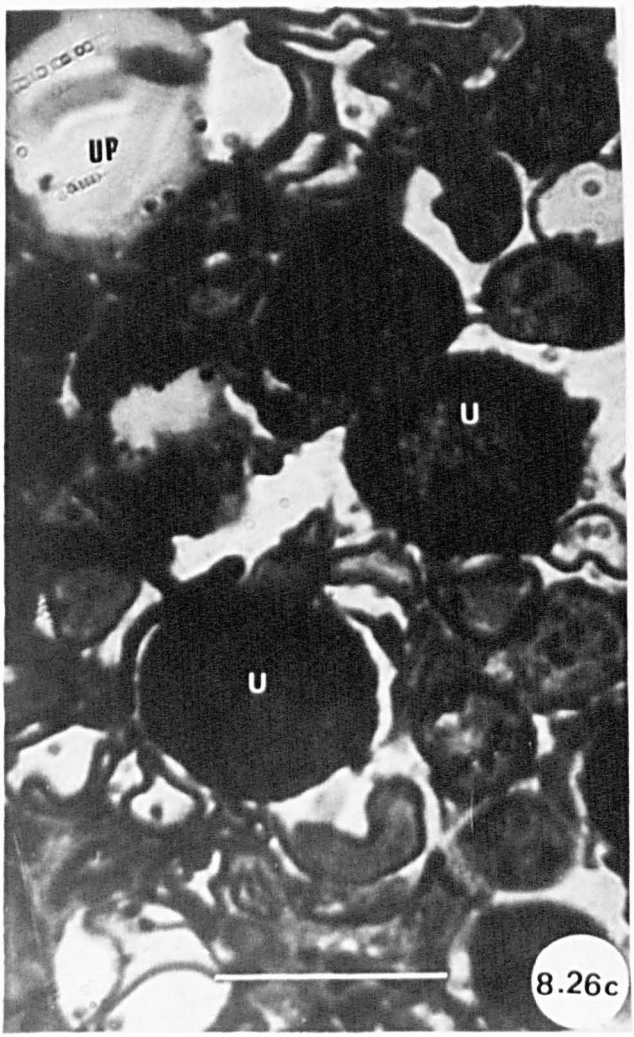

8.26c

8.26d